DINITROGEN AND ORGANOMETALLIC CHEMISTRY OF TRIMETHYLSILYL-SUBSTITUTED TRIAMIDOAMINE COMPLEXES OF MOLYBDENUM

by

MYRA BRIGID O'DONOGHUE

B.Sc. (First Class Honors)
University College Cork
(July 1988)

Submitted to the Department of Chemistry
in Partial Fulfillment of the Requirements
for the Degree of

DOCTOR OF PHILOSOPHY
at the
MASSACHUSETTS INSTITUTE OF TECHNOLOGY
June 1998

Signature of Author _____
Department of Chemistry
May 19, 1998

Certified by _____
Richard R. Schrock
Thesis Supervisor

Accepted by _____
Dietmar Seyferth
Chairman, Departmental Committee on Graduate Students

This doctoral thesis has been examined by a Committee of the Department of Chemistry as follows:

Professor Christopher C. Cummins_____
Chairman

Professor Richard R. Schrock_____
Thesis Supervisor

Professor Daniel G. Nocera_____

To Mum and Dad,
for your unwavering belief in me.

Brevity is the soul of wit.

William Shakespeare

DINITROGEN AND ORGANOMETALLIC CHEMISTRY OF TRIMETHYLSILYL-SUBSTITUTED TRIAMIDOAMINE COMPLEXES OF MOLYBDENUM

by

MYRA BRIGID O'DONOGHUE

Submitted to the Department of Chemistry on May 19, 1998
in Partial Fulfillment of the Requirements
for the Degree of Doctor of Philosophy in Chemistry

ABSTRACT

{[N_3N]Mo-N=N}$_2$Mg(THF)$_2$, isolated from the reduction of [N_3N]MoCl by magnesium powder under dinitrogen, serves as an entry into the dinitrogen chemistry of molybdenum complexes containing the TMS-TREN ligand. {[N_3N]Mo-N=N}$_2$Mg(THF)$_2$ is smoothly oxidized by $ZnCl_2$ to yield paramagnetic [N_3N]Mo(N_2), an X-ray study of which shows it to be a terminal dinitrogen complex. Heating toluene solutions of [N_3N]Mo(N_2) under dinitrogen affords the homobimetallic dinitrogen complex [N_3N]Mo-N=N-Mo[N_3N]. The stepwise reduction and functionalization of dinitrogen is achieved and examples of diazenido, hydrazido and nitrido complexes are isolated. {[N_3N]Mo-N=N}$_2$Mg(THF)$_2$ reacts with transition metal halides such as $FeCl_2$, VCl_4(DME) and $ZrCl_4$(THF)$_2$ to give heterometallic dinitrogen complexes. The highlight of this research is the isolation of the iron-molybdenum dinitrogen complex, {[N_3N]Mo-N=N}$_3$Fe, which contains iron in a trigonal planar coordination environment. Magnetic susceptibility and Mössbauer studies unequivocally demonstrate that {[N_3N]Mo-N=N}$_3$Fe is best formulated in the solid state as a high-spin Fe(III) complex. Addition of dimethylphosphinoethane (DMPE) to solutions of {[N_3N]Mo-N=N}$_3$Fe yields the tetrahedral Fe(II) complex {[N_3N]Mo-N=N}$_2$Fe(DMPE). Organometallic complexes such as [N_3N]Mo(CO), [N_3N]Mo(CN^{t}Bu), [N_3N]Mo(CNAr) and [N_3N]Mo(C_2H_4) are synthesized by ligand exchange reactions employing [N_3N]Mo(N_2) and the appropriate ligand. [N_3N]Mo(CO) is reduced by magnesium power in the presence of TMSCl to yield the oxycarbyne complex [N_3N]MoCOTMS. Although [N_3N]Mo(CNAr) is thermally stable, [N_3N]Mo(CN^{t}Bu) readily loses a ^{t}Bu radical to form the cyanide complex [N_3N]MoCN. Reduction of [N_3N]MoCl in the absence of a donor ligand affords the cyclometallated product [bitN_3N]Mo.

Five coordinate tungsten oxo alkylidene complexes of the general type (ArO)$_2$W(O)(CH^{t}Bu)(PR_3) (Ar = 2,6-$Ph_2C_6H_3$) are synthesized by reaction of Ta(CH^{t}Bu)(PR_3)$_2X_3$ (X = Cl, Br) with W(O)(O^{t}Bu)$_4$. ^{1}H NMR spectroscopy reveals that only the *syn* rotamer is present in solution and PPh_2Me is labile on the NMR time scale. These complexes are potent catalysts for the ROMP of norbornadienes, yielding polymers that are highly cis and isotactic. The living nature of the polymerization has been demonstrated for (ArO)$_2$W(O)(CH^{t}Bu)(PMe_3).

Thesis Supervisor: Professor Richard R. Schrock

TABLE OF CONTENTS

LIST OF FIGURES

LIST OF TABLES

LIST OF SCHEMES

LIST OF X-RAY STRUCTURES

ABBREVIATIONS USED IN THE TEXT

Ar	aryl
ax	axial
br	broad
calcd	calculated
C_α	carbon bound to metal
C_β	carbon bound to C_α
$C_{\beta,\ ax}$	carbon bound to N_{ax}
C_{ipso}	carbon in the ipso position of an aromatic ring
Cp	C_5H_5
Cp'	C_5H_4Me
Cp*	C_5Me_5
15-crown-5	1, 4, 7, 10, 13-pentaoxacyclopentadecane
d	doublet
DCMNBD	2,3-dicarbomethoxynorbornadiene
DME	1,2-dimethoxyethane
DMPE	dimethylphosphinoethane
DPPO	diphenylphenoxide
Bu	butyl
^tBu	tertiary butyl
eq	equatorial
Et	ethyl
$[Et_3Si\text{-}N_3N]$	$[(Et_3SiNCH_2CH_2)_3N]^{3-}$
eV	electron volts
FcOTF	ferrocenium triflate
GPC	gel permeation chromatography
h	hours
H_α	hydrogen (proton) bound to C_α
Hz	Hertz
IR	Infrared
$^nJ_{AB}$	A-B coupling constant through n bonds
m	multiplet
Me	methyl
$[Me\text{-}N_3N]^{3-}$	$[N(CH_2CH_2NTMS)_2(CH_2CH_2NMe)]^{3-}$
min	minutes

M_n	number average molecular weight
M_w	weight average molecular weight
$[N_2NNMe_2]^{2-}$	$[N(CH_2CH_2NTMS)_2(CH_2CH_2NMe_2)]^{2-}$
$[N_3N]^{3-}$	$[(Me_3SiNCH_2CH_2)_3N]^{3-}$
$[N_3N_F]^{3-}$	$[(C_6F_5NCH_2CH_2)_3N]^{3-}$
N_α	nitrogen bound to metal
N_β	nitrogen bound to N_α
na	not available
NBDF6	2,3-bis(trifluoromethyl)norbornadiene
NMR	nuclear magnetic resonance
Np	neopentyl
OTf	O_3SCF_3, triflate, trifluoromethanesulfonate
PDI	polydispersity index (M_w/M_n)
Ph	phenyl
ppm	parts per million
Pr	propyl
^iPr	isopropyl
py	pyridine
q	quartet
ROMP	ring-opening metathesis polymerization
r.t.	room temperature
s	singlet
SQUID	superconducting quantum interference device
t	triplet
THF	tetrahydrofuran
tol	toluene
TMS	trimethylsilyl, Me_3Si
TMS-TREN	$[(Me_3SiNCH_2CH_2)_3N]^{3-}$
TREN	2, 2', 2" - triaminotriethylamine, $N(CH_2CH_2NH_2)_3$
UV	ultraviolet
VT	variable temperature
χ_m	molar magnetic susceptibility
δ	chemical shift in parts per million
$\Delta\nu_{1/2}$	peak width at half-height
ε	extinction coefficient at wavelength of maximum optical absorption
λ_{max}	wavelength of maximum optical absorption

ν	frequency
μ	magnetic moment
μ_B	Bohr magneton
μ_{eff}	effective magnetic moment

CHAPTER 1

Derivatization of Dinitrogen in Trimethylsilyl-Substituted Triamidoamine Complexes of Molybdenum

A portion of the material covered in this chapter has appeared in print:

Mösch-Zanetti, N. C., Schrock, R. R., Davis, W. M., Wanninger, K., Seidel, S. W., O'Donoghue M. B. *J. Am. Chem. Soc.* **1997**, *119*, 11037.

O'Donoghue, M. B., Zanetti, N. C., Davis, W. M., Schrock, R. R. *J. Am. Chem. Soc.* **1997**, *119*, 2753.

INTRODUCTION

Dinitrogen is the most abundant component of the Earth's atmosphere and is chemically rather inert. N_2 has a high bond dissociation energy (225 kcal/mol), high ionization potential (15.058 eV) and negative electron affinity (-1.8 eV).[1] The industrial synthesis of ammonia from its elements is achieved by the Haber-Bosch process in which dinitrogen is reduced at high temperatures and pressures in the presence of an iron catalyst, and millions of tons of ammonia are produced in this manner every year (equation 1). In contrast, nitrogenase enzymes found in bacteria in the roots of legumous plants achieve the same conversion at ambient temperatures and pressures (equation 2).

$$N_2 + 3\,H_2 \xrightarrow[\text{Fe catalyst}]{\text{350-650 °C, 200-400 atm}} 2\,NH_3 \qquad (1)$$

$$N_2 + 8\,H^+ + 8\,e^- \xrightarrow{\text{nitrogenase}} 2\,NH_3 + H_2 \qquad (2)$$

Three types of nitrogenases are now known, containing Fe/Mo, V/Fe and Fe centers.[2,3] The crystal structure of the FeMo cofactor of nitrogenase isolated from *Azotobacter vinelandii* has been refined to 2.2 Å resolution and provides tantalizing clues as to how dinitrogen might be activated and reduced in biological systems.[4] Salient features include the presence of two cubane fragments, Fe_4S_3 and Fe_3MoS_3, bridged by inorganic sulfurs, molybdenum in an octahedral environment, and six trigonally-coordinated iron atoms. It is not immediately obvious from the structure if or how dinitrogen could be activated at the apparently coordinatively-saturated molybdenum center, but it must be noted that the enzyme is in a resting state and the exact mechanism by which dinitrogen is bound and reduced by nitrogenase is unknown.

A common thread linking the industrial synthesis of ammonia and biological N_2 fixation is the presence of transition metals. The challenge to the inorganic chemist has been the reduction and functionalization of dinitrogen to ammonia utilizing well-defined transition metal complexes.

References begin on page 65

Work in this area was initiated by the discovery of the first dinitrogen complex $[Ru(NH_3)_5(N_2)]^+$ by Allen and Senoff in 1965.[5] Ironically, the dinitrogen ligand in this complex is derived from hydrazine and not free dinitrogen. Nevertheless, isolation of this complex provided the first unequivocal evidence for the activation of dinitrogen by discrete transition metal complexes. In the following three decades numerous other transition metal dinitrogen complexes have been isolated and characterized and examples of stable N_2 complexes exist for all metals from Group 4 through to Group 10 with the exception of palladium and platinum.[6] Extensive work on the functionalization of dinitrogen in low oxidation state complexes of type $M(N_2)_2L_4$ (M = Mo, W; L = phosphine) has been carried out by the groups of Chatt, Leigh and Hidai and several comprehensive reviews of this chemistry have appeared.[6-8] Protonation of these complexes by strong acids leads to the isolation of diazenido, hydrazido and hydrazidium complexes and in the presence of excess acid ammonia is produced. C-N bond formation has been extensively studied in $M(N_2)_2(P\text{-}P)_2$ complexes (M = Mo, W; P-P = chelating diphosphine) and the synthesis of organonitrogen compounds such as pyrrole and pyridine has been demonstrated.[9] However, in general the fate of the metal-containing species has not be determined. Earlier work in the Schrock group centered on high oxidation complexes of Mo and W containing the Cp^*MMe_3 core and the catalytic reduction of hydrazine to ammonia has been documented in these systems.[10-12] More recently, two unprecedented reactions of dinitrogen have been discovered; Cummins has shown that homolytic cleavage of the N-N triple bond can be achieved by the three-coordinate molybdenum complex $Mo[N(R)Ar]_3$ (R = $C(CD_3)_2CH_3$, Ar = 3,5-$C_6H_3Me_2$) to yield $NMo[N(R)Ar]_3$[13,14] and Fryzuk has observed the first reaction of dihydrogen with bound dinitrogen.[15]

Current work in our group has focused on the synthesis of transition metal complexes containing triamidoamine ligands and an evaluation of their chemistry in the context of dinitrogen reduction. In particular we are interested in exploring the chemistry of complexes of the type MN_2R_x (x = 0-4) and MNR (x = 0-3) as well as multimetallic dinitrogen complexes so as to delineate what factors are of fundamental importance to the activation and reduction of dinitrogen.

References begin on page 65

Ligands of the type $[(RNCH_2CH_2)_3N]^{3-}$ can bind to a variety of main group elements[16,17] and transition metals in oxidation state 3+ or higher. When R is a sterically bulky group such as trimethylsilyl, opportunities to study rarely observed complexes and decomposition pathways have arisen. Examples include preparation of a tantalum phosphinidene complex,[18] preparation of molybdenum and tungsten phosphido and arsenido complexes,[19] and a demonstration that certain molybdenum and tungsten alkyl complexes decompose via α elimination as much as six orders of magnitude faster than via β elimination.[20,21]

Triamidoamine ligands usually bind to transition metals in a tetradentate manner thus creating a sterically-protected, three-fold symmetric pocket in which to bind small molecules. We have been interested in exploiting the sterically-protected apical site and the orbital arrangement in this pocket to bind and activate dinitrogen. The orbitals available to bind ligands such as dinitrogen consist of a σ orbital (approximately d_z2) and two degenerate π orbitals (approximately d_{xz} and d_{yz}). When these orbitals are compared with those that dinitrogen utilizes to bind "end-on" to a metal center, namely, the orbital containing the lone pair and the pair of degenerate π^* orbitals, it appears that triamidoamine complexes are well-suited to bind dinitrogen, assuming the metal and dinitrogen orbitals are matched in terms of energy. This appears to be the case and we recently showed that $[N_3N_F]MoCl$ could be reduced with sodium under dinitrogen by two electrons to give the sodium "diazenido" complex, $[N_3N_F]Mo\text{-}N{=}N\text{-}Na(ether)_x$, and by one electron to give the homobimetallic complex, $[N_3N_F]Mo\text{-}N{=}N\text{-}Mo[N_3N_F]$ ($[N_3N_F]^{3-} = [(C_6F_5NCH_2CH_2)_3N]^{3-}$).[22] Furthermore, it proved feasible to isolate a neutral Re(III) complex, $[N_3N_F]Re(N_2)$.[23]

Although much is unknown about the mechanism of the binding and reduction of N_2 in biological systems, it has been long recognized that transition metals such as molybdenum are essential elements for activity. It is also accepted that the coordination of dinitrogen to a metal center is a prerequisite for reduction and further transformation. A survey of the literature suggests that in seeking to prepare well-defined transition metal dinitrogen complexes, the selection of reductant and reducible precursor is all-important. However, the subtleties that govern such choices are difficult to rationalize and studies of new systems require the investigator to explore all

References begin on page 65

avenues in search of a potential entry into dinitrogen chemistry. Prior to this work a synthetically-useful entry into the dinitrogen chemistry of silylated triamidoamine complexes was lacking. $\{[(^tBuMe_2SiNCH_2CH_2)_3N]Mo\}_2(\mu\text{-}N_2)$ was the singular example of a dinitrogen complex in these systems, having been isolated in <10% yield from the reaction of $MoCl_3(THF)_3$ with Li_3N_3N.[24] Spurred on by the results obtained with $[N_3N_F]$Mo complexes, we initiated a study of the related $[N_3N]$Mo complexes and the chemistry described in this chapter charts our progress toward the derivatization of dinitrogen at a single metal center culminating with N-N bond cleavage and is summarized in Scheme 1.1. With the exception of two, all of the complexes reported are diamagnetic and so are easily characterized by standard spectroscopic methods. Five X-ray crystallography structures are reported including the first example of a hydrazido complex in TREN-based systems. In particular, X-ray crystallography proved to be a useful tool in delineating the course of reactions in which the TMS-TREN ligand has become involved in the chemistry. The susceptibility of the $[N_3N]^{3-}$ ligand toward degradation via Si-N bond cleavage has been documented by the isolation of several complexes in which a TMS group has been replaced by one or more methyl groups. Although this type of reactivity was not fully anticipated and in general is undesired, it has given rise to new types of diamido/bisdonor complexes that may be of use in future research.

References begin on page 65

Scheme 1.1. Derivatization of dinitrogen in $[N_3N]Mo$ complexes.

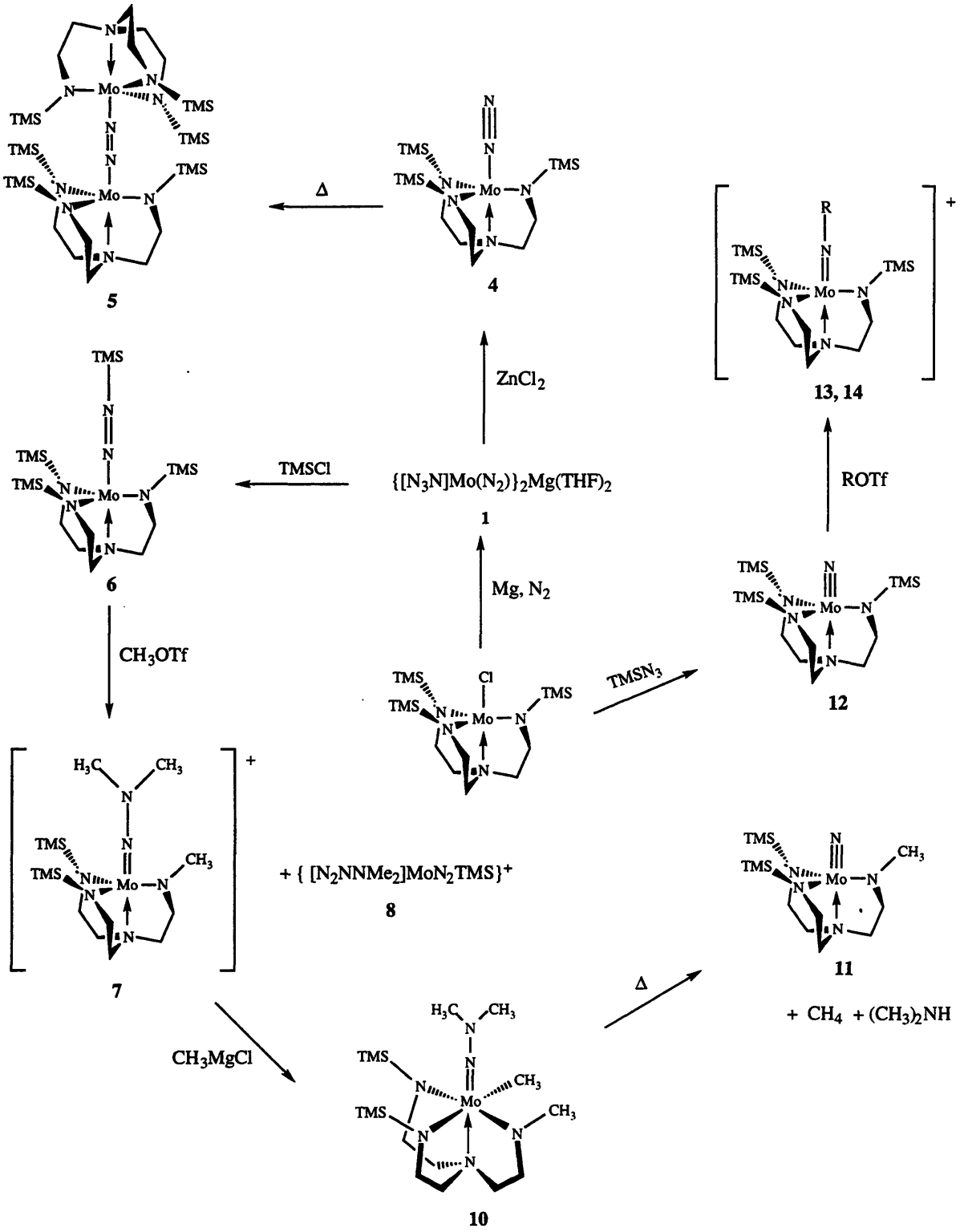

RESULTS

Activation of Dinitrogen

A solution of $[N_3N]MoCl$ in THF is reduced cleanly by magnesium powder under dinitrogen to give a mixture of two diamagnetic products in a ratio of 1:3, according to their respective TMS resonances in ^1H NMR spectra. Efforts to separate these products via fractional crystallization were unsuccessful. However, addition of 1,4-dioxane to a toluene solution of the mixture allows one of the products to be isolated in high yield (90%) as an orange crystalline solid. The ^1H NMR spectrum of this product, $\{[N_3N]Mo\text{-}N{=}N\}_2Mg(THF)_2$ (**1**; equation 3), consists of a single TMS resonance and a pair of triplets for the methylene protons on the ligand backbone characteristic of compounds in which the $[N_3N]Mo$ portion of the molecule is C_3-symmetric. The ^1H NMR spectrum also shows there to be one molecule of THF present per $[N_3N]Mo$ unit. If the

$$2\,[N_3N]MoCl \xrightarrow[1,4\text{-dioxane}]{Mg,\ THF,\ N_2} \underset{\mathbf{1}}{\{[N_3N]Mo\text{-}N{=}N\}_2Mg(THF)_2} + MgCl_2(dioxane) \qquad (3)$$

reduction of $[N_3N]MoCl$ is carried out under $^{15}N_2$, the ^{15}N NMR spectrum of the product in C_6D_6 consists of a pair of doublets at 377.0 and 304.4 ppm (J_{NN} = 12 Hz) corresponding to N_α and N_β of $\mathbf{1}\text{-}^{15}N_2$ respectively.[25] The IR spectrum of **1** has a strong broad stretch at 1719 cm^{-1} that shifts to 1662 cm^{-1} in $\mathbf{1}\text{-}^{15}N_2$. IR and ^{15}N NMR data for selected complexes reported in this chapter are summarized in Table 1.1. The second diamagnetic product present in approximately 25% yield before the addition of dioxane is proposed to be $\{[N_3N]Mo\text{-}N{=}N\}MgCl(THF)_2$ (**1a**), and the yield of **1** is believed to be raised to 90% (isolated) as a consequence of a Schlenk-like equilibrium that yields $MgCl_2(dioxane)$ (equation 4). Further support for this suggestion comes from the observation that addition of TMSCl to a mixture of **1** and **1a** yields $[N_3N]MoN_2TMS$ (see below) as the sole product in high yield.

$$2\,\underset{\mathbf{1a}}{\{[N_3N]Mo\text{-}N{=}N\}MgCl(THF)_2} \xrightarrow{1,4\text{-dioxane}} \mathbf{1} + MgCl_2(dioxane) \qquad (4)$$

References begin on page 65

Table 1.1. IR and ^{15}N NMR data for selected complexes.

Complex	$\nu_{^{14}N^{14}N}$	$\nu_{^{15}N^{15}N}$	δN_α	δN_β
1	1719[a]	1662[a]	377.0[b]	304.4
4	1934[c]	1870[c]		
6	1714[a]	1654[a]	356.9[b]	238.1
7			374.8[a]	157.2
8			361.5[a]	244.3
9	1640[d]	1577[d]	374.6[b]	239.5
10			354.9[a]	142.0
11	1002[d]	977[d]	866.1[b]	

[a]in THF, [b]in C_6D_6, [c]in pentane, [d]in Nujol.

One equivalent of magnesium powder is required for complete reduction of $[N_3N]MoCl$ but the reaction is unaffected by the presence of excess magnesium powder. The reaction is solvent dependent and reduction only occurs in the presence of THF. The sodium analog of **1**, $\{[N_3N]Mo\text{-}N{=}N\}[Na(15\text{-crown-}5)]$ (**2**) is accessed via reduction of $[N_3N]MoCl$ with two equivalents of sodium naphthalenide followed by addition of one equivalent of 15-crown-5. Orange, diamagnetic **2** is isolated in 65% yield and the IR spectrum of **2** in Nujol exhibits a strong N-N stretch at 1791 cm^{-1}. For comparison, the IR spectrum of the related complex $\{[N_3N_F]Mo\text{-}N{=}N\}[Na(15\text{-crown-}5)]$ has an N-N stretch at 1848 cm^{-1}.[22] It should be noted that the choice of magnesium as a reductant has several advantages over sodium naphthalenide in that it is readily available, does not require preactivation and can easily be separated from the desired product. $[N_3N]MoOTf$[21] is not a viable starting material for entry into dinitrogen chemistry; reduction of $[N_3N]MoOTf$ by magnesium yields the known dimeric complex, $\{(TMSNCH_2CH_2)_2N(CH_2CH_2N)Mo\}_2$[26] (**3**) via formal loss of TMSOTf (equation 5). This

reaction is illustrative of the importance of one's choice of precursor complex in gaining access to the dinitrogen chemistry of $[N_3N]Mo$ complexes.

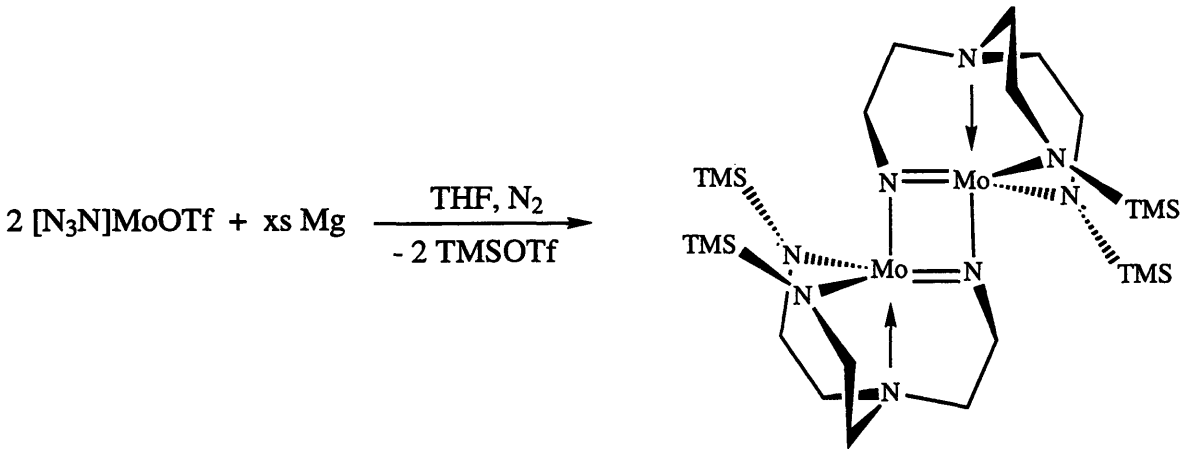

3

(5)

A toluene-d_8 solution of **1** shows no signs of decomposition upon being heated to 82 °C under dinitrogen for 24 h. Furthermore, a solution of **1** stored at room temperature under dinitrogen remains unchanged over a period of two weeks (according to ^1H NMR spectroscopy). However, **1** apparently decomposes rapidly in the solid state when exposed to high vacuum as evidenced by a color change from bright orange to dark brown. We speculate that loss of THF is the first step in this decomposition although no products of the reaction have been identified.

Crystals of **1** suitable for an X-ray study were grown from saturated diethyl ether solutions at -20 °C; a half a molecule of diethyl ether was found in the unit cell. Crystallographic data and collection and refinement parameters are given in Table 1.2. The molecular structure of **1** along with the atom-labeling scheme is shown in Figure 1.1, while pertinent bond lengths and bond angles are listed in Table 1.3. Table 1.4 summarizes selected metrical parameters for all of the crystallographically-characterized complexes reported in this chapter. **1** is comprised of two $\{[N_3N]Mo(N_2)\}^-$ units bound to pseudo-tetrahedral magnesium, the coordination sphere being completed by two molecules of THF. The N-Mg-N bond angle opens to 134.7° in order to

References begin on page 65

accommodate the sterically bulky $\{[N_3N]Mo(N_2)\}^-$ "ligands"; the Mo-N-N-Mg linkages are essentially linear. The N-N bond lengths (1.164(13) and 1.195(13) Å) are indicative of some reduction of the dinitrogen ligands in **1** compared with free dinitrogen (1.098 Å[27]) and are consistent with formulation of **1** as a diazenido complex of Mo(IV). We have found that the twisting of a given TMS group out of the N_{ax}-M-N_{eq} plane and the resulting decrease in the N_{ax}-M-N_{eq}-Si dihedral angle are useful measures of the degree of steric strain in the pocket in $[N_3N]$ complexes. For example, in $[N_3N]$Mo(cyclohexyl)[21] this angle was found to range from 129° to 136° as a consequence of the steric interaction between the cyclohexyl ring and the TMS groups of the ligand. In the case of **1**, this angle is found to average to 173.7°, consistent with there being little steric pressure in the pocket. Examples of Mg^{2+} salts of diazenido complexes have been crystallographically-characterized including $\{(PMe_3)_3Co(N_2)\}_2Mg(THF)_4$[28] which contains magnesium in a pseudo-octahedral environment.

Figure 1.1. A view of the structure of $\{[N_3N]Mo\text{-}N{=}N\}_2Mg(THF)_2$ (**1**).

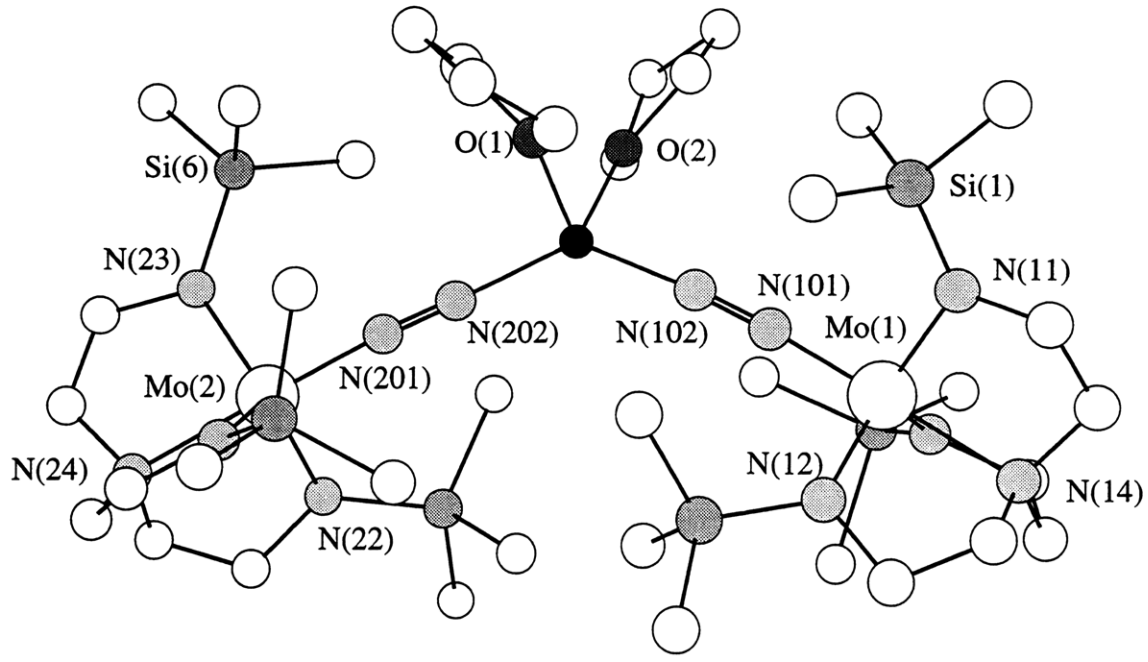

Table 1.2. Crystallographic data, collection parameters and refinement parameters for **1** and **4**.

	1	**4**
Empirical Formula	$C_{40}H_{98}MgMo_2N_{12}O_{2.50}Si_6$	$C_{15}H_{39}MoN_6Si_3$
Formula Weight	1172.03	483.73
Diffractometer	SMART/CCD	SMART/CCD
Crystal Dimensions (mm)	0.33 x 0.26 x 0.20	0.46 x 0.12 x 0.12
Crystal System	Triclinic	Orthorhombic
Space Group	$P\bar{1}$	Pbca
a (Å)	10.1540(2)	17.0164(2)
b (Å)	16.4300(3)	16.9922(3)
c (Å)	19.8388(5)	34.251
α (°)	89.4350(10)	90
β (°)	84.1230(10)	90
γ (°)	82.19	90
V (Å^3), Z	3261.77(12), 2	9903.7(2), 16
D_{calc} (Mg/m^3)	1.193	1.298
Absorption coefficient (mm^{-1})	0.543	0.686
F_{000}	1244	4080
Temperature (K)	183(2)	183(2)
Θ range for data collection (°)	1.25 to 20.00	1.19 to 23.27
Reflections collected	9883	30723
Unique Reflections	6054	7087
R	0.0905	0.0459
R_w	0.1016	0.0554
GoF	1.162	1.245

References begin on page 65

Table 1.3. Selected bond lengths and bond angles for $\{[N_3N]Mo\text{-}N{=}N\}_2Mg(THF)_2$ (**1**).

Bond Lengths (Å)					
Mo(1)-N(101)	1.876(11)	Mo(2)-N(201)	1.842(10)		
N(101)-N(102)	1.164(13)	N(201)-N(202)	1.193(13)		
Mg-N(102)	1.973(11)	Mg-N(202)	1.966(11)	Mo(1)-N(14)	2.215(10)
Mo(2)-N(24)	2.252(9)	Mo(1)-N(11)	1.998(12)	Mo(1)-N(12)	2.001(11)
Mo(1)-N(13)	2.010(11)	Mo(2)-N(21)	1.979(10)	Mo(2)-N(22)	2.017(9)
Mo(2)-N(23)	2.027(10)	Mg-O(1)	2.041(10)	Mg-O(2)	2.019(10)

Bond Angles (deg)			
Mo(1)-N(101)-N(102)	175.6(9)	Mo(2)-N(201)-N(202)	177.0(9)
Mg-N(102)-N(101)	178.2(9)	Mg-N(202)-N(201)	166.6(9)
Mo(1)-N(11)-Si(1)	127.7(6)	Mo(2)-N(23)-Si(6)	126.0(6)
N(102)-Mg-N(202)	134.7(5)	O(1)-Mg-O(2)	94.7(5)
N(102)-Mg-O(1)	107.9(4)	N(102)-Mg-O(2)	104.5(4)
N(202)-Mg-O(1)	105.1(4)	N(202)-Mg-O(2)	102.8(4)

Dihedral Angles (deg)[a]			
N(14)-Mo(1)-N(11)-Si(1)	179.45	N(14)-Mo(1)-N(13)-Si(3)	-180.00
N(24)-Mo(2)-N(21)-Si(5)	167.36	N(24)-Mo(2)-N(22)-Si(4)	-171.08

[a]Obtained from a Chem-3D Drawing

References begin on page 65

Table 1.4. Selected metrical parameters for crystallographically characterized complexes.

Complex	N-N (Å)	Mo-N (Å)	N-N-R (deg)
1	1.164(13)	1.876(11)	178.2(9)
	1.193(13)	1.842(10)	166.6(9)
4	1.085(5)	1.990(4)	
	1.083(6)	1.995(4)	
7	1.334(13)	1.747(10)	119.1(10)
			115.9(1)
8	1.206(9)	1.803(7)	170.5(8)
9	1.229(3)	1.789(2)	137.0(2)

Synthesis of a Mo(III) Terminal Dinitrogen Complex

Since **1** and **2** arise from the two electron reduction of $[N_3N]MoCl$ and the activation of dinitrogen, we wondered if the neutral terminal dinitrogen complex $[N_3N]Mo(N_2)$ (**4**) would be isolable. Although paramagnetic **4** can be isolated from the reduction of $[N_3N]MoCl$ in THF by sodium naphthalenide, the reaction is neither clean nor reproducible. The reaction is sensitive to a number of factors that include temperature, efficiency of stirring, and rate of addition of the reductant. For example, if one equivalent of sodium naphthalenide is added *dropwise* to a THF solution of $[N_3N]MoCl$ followed by addition of TMSCl, the ^1H NMR spectrum of the crude reaction mixture shows 0.5 equivalents of unreacted $[N_3N]MoCl$ and 0.5 equivalents of $[N_3N]MoN_2TMS$ (see below) to be present, indicating that two electron reduction of $[N_3N]MoCl$ has occurred exclusively. If one equivalent of sodium naphthalenide is added to $[N_3N]MoCl$ in THF *all at once*, the main product of the reaction is **4**, but it is contaminated with $[N_3N]MoCl$. In contrast, the one electron reduction of $[N_3N_F]MoOTf$ by sodium amalgam leads to the homobimetallic dinitrogen complex, $[N_3N_F]Mo\text{-}N{=}N\text{-}Mo[N_3N_F]$ and not the terminal dinitrogen complex.[22]

References begin on page 65

As **4** is formally the one electron oxidation product of $\{[N_3N]Mo(N_2)\}^-$, we reasoned that it might be accessible via oxidation of **1**. **1** reacts with $MCl_2(PPh_3)_2$ (M= Pd, Ni) according to equation 6 and **4** can be isolated as burgundy colored crystals from this reaction in >80% yield although occasionally samples are contaminated with 5-7% $[N_3N]MoCl$. To circumvent this problem other oxidants were sought and a cleaner, high-yield route to **4** results from the reaction of

$$\underset{\mathbf{1}}{\{[N_3N]Mo\text{-}N{=}N\}_2Mg(THF)_2} + ML_2Cl_2 \xrightarrow[-20\ ^\circ C]{THF} MgCl_2 + \underset{\mathbf{4}}{[N_3N]Mo(N_2)} + ML_x \qquad (6)$$

M = Pd, Ni; x is unknown

1 with $ZnCl_2$ (equation 7). Use of $ZnCl_2$ as the oxidant simplifies workup as metallic zinc precipitates out of solution during the course of the reaction and **4** is easily separated from $MgCl_2$ by extraction into pentane. Also, **4** is isolated free of any contamination by $[N_3N]MoCl$. It should be noted that oxidation of $[N_3N_F]Mo(N_2)\{Na(ether)_x\}$ by ferrocenium triflate yields the homobimetallic dinitrogen complex, $[N_3N_F]Mo\text{-}N{=}N\text{-}Mo[N_3N_F]$ and not the terminal dinitrogen complex $[N_3N_F]Mo(N_2)$.[22] This result suggests that the extent of backbonding into the π^* orbitals of dinitrogen is greater in $[N_3N]Mo$ complexes compared to $[N_3N_F]Mo$ complexes, allowing isolation of **4**. Such a suggestion is sensible in view of the fact that the $[N_3N]^{3-}$ ligand is more electron-donating then the $[N_3N_F]^{3-}$ ligand, giving rise to more electron-rich metal centers in $[N_3N]Mo$ complexes compared to $[N_3N_F]Mo$ complexes.

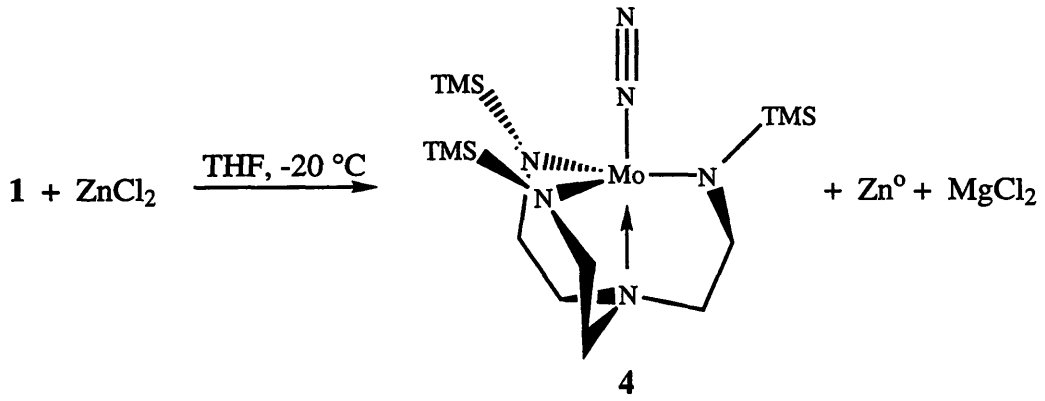

(7)

The ^{1}H NMR spectrum of **4** consists of two broad resonances at 14.02 and -40.57 ppm for the methylene protons of the ligand and a sharper resonance at -4.53 ppm assigned to the TMS groups of the ligand. Such a spectrum, that is one exhibiting a high field and a low field resonance for the ligand methylene protons is also characteristic of $[N_3N]W^{III}(L)$[29]and $[N_3N_F]W^{III}(L)$[30] complexes. The IR spectrum of **4** in pentane has a strong absorption at 1934 cm^{-1} that shifts to 1870 cm^{-1} in **4-$^{15}N_2$** (Table 1.1). The IR spectrum of **4** in Nujol consists of two strong absorptions at 1910 and 1901 cm^{-1}. We attribute the two absorptions in the solid state spectrum to the presence of two molecules in the unit cell (see below) and IR spectra of $[N_3N]MoCO$ exhibit similar features (see Chapter 3).

SQUID[31] magnetic susceptibility data for solid **4** is plotted versus temperature in Figure 1.2. Fitting these data to the Curie law over the temperature range 5-300 K yields $\mu = 1.75(1)\ \mu_B$. A trigonal bipyramidal complex possessing C_{3v} symmetry has a ligand field splitting pattern in which the lowest lying orbitals are the degenerate d_{xz}/d_{yz} pair. In the case of **4**, a Mo(III) complex, three electrons occupy these two orbitals giving rise to a single unpaired spin, as evidenced by the magnetic susceptibility data. Although **4** is stable under dinitrogen, dinitrogen exchange does take place slowly. If a toluene solution of **4** is stirred under an atmosphere of $^{15}N_2$ for one week, the IR spectrum of the resulting solid in Nujol reveals four strong absorptions at 1910, 1901, 1846 and 1839 cm^{-1} consistent with exchange of $^{14}N_2$ with $^{15}N_2$ to yield a roughly 2:1 mixture of **4-$^{14}N_2$** and **4-$^{15}N_2$**. In contrast, the dinitrogen ligand in $[N_3N_F]Re(N_2)$,[23] the only other example of a terminal dinitrogen complex in TREN-based systems, is not labile and consequently exchange with $^{15}N_2$ is not observed. We have found that the lability of N_2 in **4** can be exploited to isolate other $[N_3N]Mo^{III}(L)$ complexes and details of this chemistry are the subject of Chapter 3. **4** reacts with TMSOTf to give a mixture of $[N_3N]MoOTf$[21] and $[N_3N]MoN_2TMS$ (**6**) according to ^{1}H NMR spectroscopy. **4** is cleanly reduced by magnesium powder in THF to give **1** in high yield with no trace of the closely related species proposed to be **1a** that is formed upon reduction of $[N_3N]MoCl$ by Mg in THF (see above). The electrochemical behavior of **4** mirrors its chemical behavior. The cyclic voltammogram of **4** (obtained by Dr. Luis Baraldo of the

References begin on page 65

Cummins group) indicates that **4** is reduced at -1.9 eV (versus ferrocene/ferrocenium) to $\{[N_3N]Mo(N_2)\}^-$ and that the reduction is reversible. Oxidation of **4** is irreversible presumably due to loss of dinitrogen from the cationic d^2 metal center as a consequence of decreased backbonding into the π^* orbitals of dinitrogen.

Figure 1.2. Plot of χ_m (corrected for diamagnetism using Pascal's constants) versus T for $[N_3N]Mo(N_2)$, (**4**).

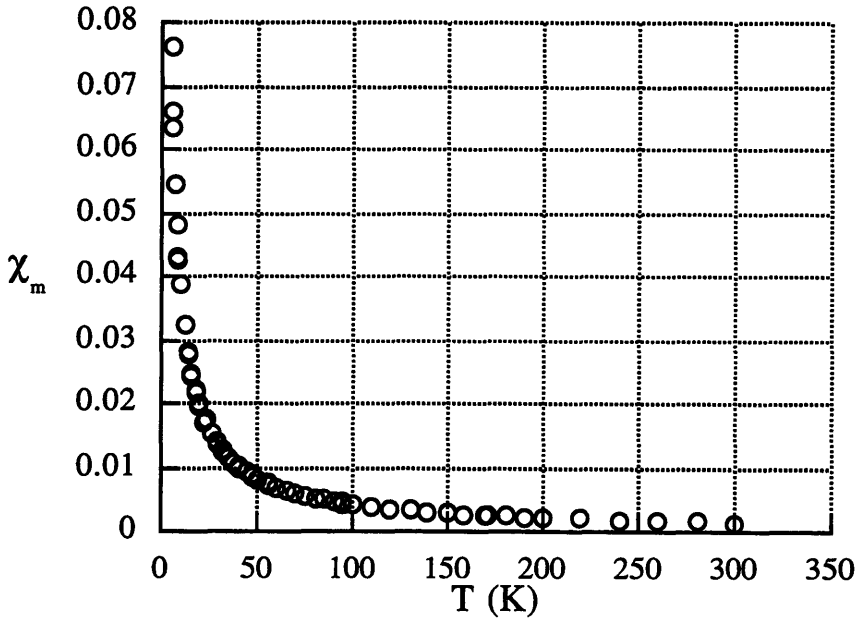

Single crystals of **4** were grown from saturated diethyl ether solutions at -20 °C and examined in an X-ray study. Crystallographic data and collection and refinement parameters are given in Table 1.2. The molecular structure of **4** along with the atom-labeling scheme is shown in Figure 1.3 while selected bond lengths and bond angles are listed in Table 1.5. Two statistically-identical molecules were found in the unit cell. The molybdenum atom is displaced from the plane defined by the amide nitrogens by 0.304 Å in the direction of N_α. **4** contains an "end-on" dinitrogen ligand with a linear Mo-N-N linkage. The N-N bond length at 1.085(5) Å is not

References begin on page 65

statistically different from that of free dinitrogen (1.098 Å[27]), which suggests that there is little reduction of the dinitrogen ligand in **4**. The short N-N bond length and long Mo-N bond length (1.990 Å) are consistent with the observed lability of dinitrogen. In **4** each MoN_2C_2 five-membered ring has an envelope conformation with $C_{\beta,\,ax}$ serving as the 'flap' of the envelope. Consequently, the TMS groups of **4** are all oriented upright, the N_{ax}-M-N_{eq}-Si dihedral angles averaging to 175.6°.

Figure 1.3. A view of the structure of $[N_3N]Mo(N_2)$ (**4**).

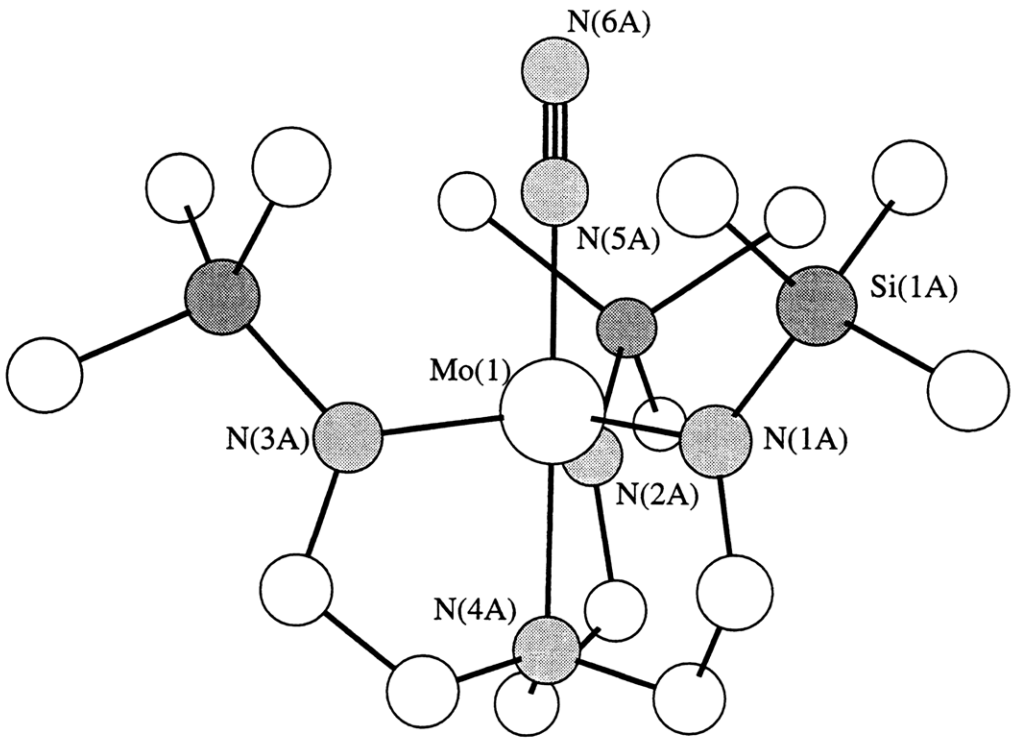

The isolation and structural characterization of **4** demonstrates, for the first time, the ability of a d^3 Mo center in a triamidoamine complex to bind dinitrogen, a question that work with $[N_3N_F]$Mo complexes had not answered. Although several examples of molybdenum terminal

Table 1.5. Selected bond lengths and bond angles for **4**.

Bond Lengths (Å)

N(5A)-N(6A) 1.085(5)	N(5B)-N(6B) 1.083(6)	Mo(1)-N(5A) 1.990(4)
Mo(2)-N(5B) 1.995(4)	Mo(1)-N(4A) 2.197(3)	Mo(2)-N(4B) 2.183(4)
Mo(1)-N(1A) 1.989(4)	Mo(1)-N(2A) 1.995(4)	Mo(1)-N(3A) 1.994(4)
Mo(2)-N(1B) 2.000(4)	Mo(2)-N(2B) 1.994(4)	Mo(2)-N(3B) 1.986(4)

Bond Angles (deg)

Mo(1)-N(5A)-N(6A) 179.1(4)	Mo(2)-N(5B)-N(6B) 179.4(4)
N(4A)-Mo(1)-N(5A) 179.36(14)	N(4B)-Mo(2)-N(5B) 179.1(2)
Mo(1)-N(1A)-Si(1A) 127.3(2)	Mo(2)-N(1B)-Si(1B) 128.1(2)
N(1A)-Mo(1)-N(2A) 118.4(2)	N(1B)-Mo(2)-N(2B) 120.6(2)

Dihedral Angles (deg)[a]

N(4A)-Mo(1)-N(1A)-Si(1A) -175.49	N(4A)-Mo(1)-N(2A)-Si(2A) 180.00
N(4A)-Mo(1)-N(3A)-Si(3A) 177.74	N(4B)-Mo(2)-N(1B)-Si(1B) 174.12
N(4B)-Mo(2)-N(2B)-Si(2B) 173.10	N(4B)-Mo(2)-N(3B)-Si(3B) 173.37

[a]Obtained from a Chem-3D Drawing

dinitrogen complexes of the type $Mo(N_2)_2(phosphine)_4$ have been structurally characterized,[7] **4** is the first example of a terminal dinitrogen complex containing molybdenum in a relatively high oxidation state. Recently, it has been shown that $Mo[N(R)Ar]_3$ (R = $C(CD_3)_2CH_3$, Ar = 3,5-$C_6H_3Me_2$) can homolytically cleave dinitrogen to give the nitrido complex $NMo[N(R)Ar]_3$.[13,14] Although the thermally-unstable, bridging dinitrogen complex $(\mu\text{-}N_2)\{Mo[N(R)Ar]_3\}_2$ can be observed spectroscopically, evidence for the formation of the terminal dinitrogen complex $(N_2)Mo[N(R)Ar]_3$ is lacking. We speculate that the presence of the nitrogen donor in $[N_3N]Mo$

References begin on page 65

destabilizes d_{z2} more than d_{xz} or d_{yz} resulting in a low spin configuration for $[N_3N]Mo$ and that such a spin state would appear optimal to bind dinitrogen.

Synthesis of a Homobimetallic Bridging Dinitrogen Complex

When a toluene solution of **4** is heated to 84 °C under dinitrogen, a dramatic color change from orange-red to royal purple is observed to occur over the course of 40 h as $[N_3N]Mo\text{-}N{=}N\text{-}Mo[N_3N]$ (**5**) is formed (equation 8). We propose that **5** forms by loss of dinitrogen from **4** to give the unobserved trigonal monopyramidal species "$[N_3N]Mo$" which is trapped by a second molecule of **4** to yield **5**. **5** can be isolated as black microcrystals in 78% yield. The ^1H NMR spectrum of paramagnetic **5** in C_6D_6 exhibits three broad, shifted resonances consistent with a species in which the $[N_3N]Mo$ portion is C_3-symmetric. The UV-visible spectrum of **5** in pentane has an intense absorption at 542 nm (ε = 17,872 M^{-1} cm^{-1}).

$$\underset{\mathbf{4}}{[N_3N]Mo(N_2)} \xrightarrow[-N_2]{\text{toluene, 84 °C}} \underset{\mathbf{5}}{[N_3N]Mo\text{-}N{=}N\text{-}Mo[N_3N]} \qquad (8)$$

SQUID magnetic susceptibility data for solid **5** is plotted versus temperature in Figure 1.4 and can be fit to the Curie-Weiss law ($\chi = \mu^2/8(T-\theta)$) over the temperature range 50-300 K to yield μ = 3.24(2) μ_B, θ = -1.1(5) K. The value for μ is close to the spin-only value for a system containing two unpaired electrons (2.83 μ_B), as predicted on the basis of **5** being a Mo(IV) diazenido complex analogous to $\{[(^tBuMe_2SiNCH_2CH_2)_3N]Mo\}_2(\mu\text{-}N_2)$.[24] For complexes such as **5**, one can construct two sets of degenerate π orbitals from the d_{xz} and d_{yz} orbitals on molybdenum and the p_x and p_y orbitals on the nitrogen atoms, into which are placed 10 electrons (3e from each Mo center and 4e from the π system of dinitrogen) resulting in two unpaired spins.[22] Such a picture is consistent with the magnetic susceptibility data.

References begin on page 65

Figure 1.4. Plot of χ_m (corrected for diamagnetism using Pascal's constants) versus T for $[N_3N]Mo\text{-}N{=}N\text{-}Mo[N_3N]$ (**5**).

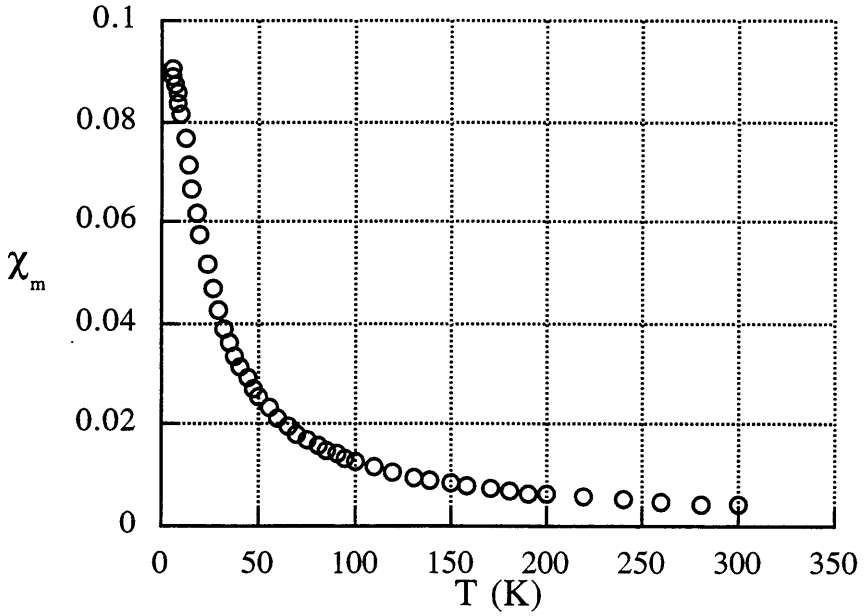

A toluene-d_8 solution of **5** shows no signs of decomposition upon being heated to 105 °C under dinitrogen for 72 h. In particular **5** is stable toward decomposition to $[N_3N]MoN$ (see below) via N-N bond homolysis. Unlike $[N_3N_F]Mo\text{-}N{=}N\text{-}Mo[N_3N_F]$[22] which can be reduced by sodium amalgam to yield $[N_3N_F]Mo(N_2)\{Na(ether)_x\}$, **5** is not reduced by magnesium to give **1.**

Functionalization of Dinitrogen

1 reacts cleanly with two equivalents of TMSCl to give $[N_3N]MoN_2TMS$ (**6**) as a yellow, pentane-soluble solid in 88% yield (equation 9). However, we have found that **1** need not be isolated and diamagnetic **6** can be obtained in high yield from the reduction of $[N_3N]MoCl$ by magnesium powder in the presence of TMSCl. The IR spectrum of **6** has a strong broad stretch at 1712 cm^{-1} that shifts to 1654 cm^{-1} in **6-$^{15}N_2$** (Table 1.1). The ^{15}N NMR spectrum of **6-$^{15}N_2$** in C_6D_6 consists of a pair of doublets at 356.9 and 238.1 ppm (J_{NN} = 12 Hz). For comparison, in

$[N_3N_F]$Mo-N=N-Si($^iPr_3$)[22] ν_{NN} is found at 1687 cm^{-1} and the ^{15}N NMR spectrum exhibits doublets at 366 and 228 ppm (J_{NN} = 15 Hz).

$$\underset{\mathbf{1}}{\{[N_3N]Mo\text{-}N{=}N\}_2Mg(THF)_2} + 2\ TMSCl \xrightarrow{THF} 2\ \underset{\mathbf{6}}{[N_3N]MoN_2TMS} + MgCl_2 \qquad (9)$$

1 also reacts cleanly with TMSOTf to give **6**. However, when other electrophiles are used the reactions are more complicated and product mixtures result. For example, reaction of MeOTf with **1** yields two diamagnetic products along with **4**. The IR spectrum of the product mixture has a strong stretch at 1713 cm^{-1} and so one of the diamagnetic products is tentatively formulated as the methyl analog of **6**. However, the nature of the supporting ligand in such circumstances cannot be stated with certainty in view of the tendency for a relatively small electrophile such as methyl to add to amido nitrogens in the triamidoamine ligand (see **7** and **8** below). **1** reacts with 2 equivalents of MeI to give a mixture of unidentified diamagnetic and paramagnetic species (according to ^1H NMR spectroscopy). If an excess of MeI is used the main product that can be identified by ^1H NMR spectroscopy is $[N_3N]MoI$.

In $[N_3N_F]$Mo complexes, efforts to reduce the dinitrogen ligand to the hydrazido level were unsuccessful and it was found that $[N_3N_F]$Mo-N=N-Si($^iPr_3$) does not react with dihydrogen, hydrazine or lithium aluminum hydride.[22] Drawing on these results, efforts to functionalize the dinitrogen ligand in **6** have consisted of attempts to alkylate **6**. Complex **6** does not react with TMSOTf, TMSI or MeI. However, it does react with excess MeOTf (4 equivalents) in toluene over 12 h to give a mixture of two diamagnetic products, **7** and **8**, typically in a ratio of 1:3 according to ^1H NMR spectroscopy (equation 10). These two products can be separated by fractional crystallization. Cooling THF/ether solutions of the product mixture yields the Mo(VI) dimethylhydrazido complex, $\{[N(CH_2CH_2NSiMe_3)_2(CH_2CH_2NCH_3)]MoN_2(CH_3)_2\}^+OTf^-$ (**7**) as an orange, crystalline solid in 20% yield. **7** is insoluble in pentane and slowly oils out of benzene and toluene. The ^{19}F NMR spectrum of **7** in C_6D_6 reveals a singlet at -77.3 ppm for the

References begin on page 65

triflate ion. The ^{1}H NMR spectrum of **7** in THF-d_8 has multiple resonances for the methylene protons of the ligand backbone, consistent with the fact that it is not a C_3-symmetric species. A singlet at 3.73 ppm integrates for 3H and is assigned to the amido methyl group. A singlet at 3.72 ppm integrates for 6H and is assigned to the methyl groups of the hydrazido ligand. The presence

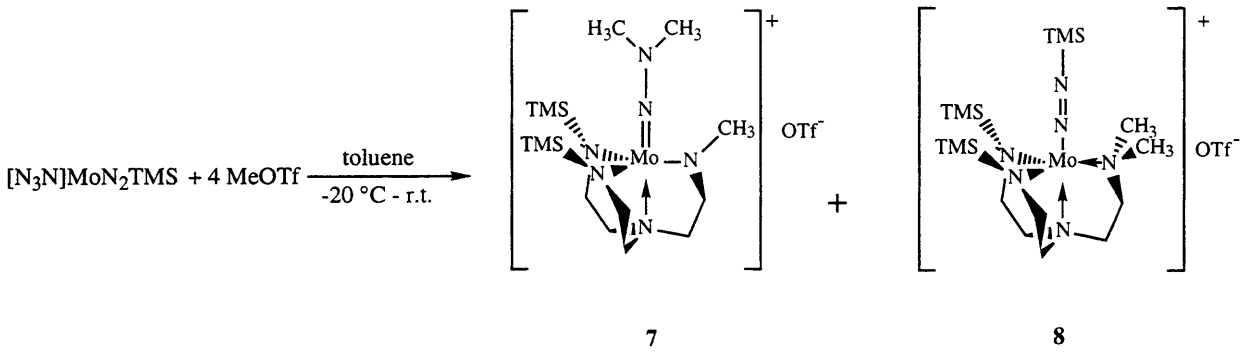

7 **8**

(10)

of a plane of symmetry in **7** is confirmed by the ^{13}C NMR spectrum which exhibits four resonances for the methylene backbone carbons of the ligand. The ^{15}N NMR spectrum of **7-$^{15}N_2$** in THF-d_8 consists of a pair of doublets at 374.8 and 157.2 ppm attributed to N_α and N_β of the hydrazido ligand, respectively.[25] The upfield shift of the resonance attributed to N_β compared to the chemical shift of N_β in **6** is consistent with the formulation of **7** as a hydrazido complex. Efforts to obtain a solid state IR spectrum of **7** were thwarted by its apparent aversion to Nujol and a ν_{NN} peak could not be assigned in an IR spectrum obtained in THF. **7** is thermally stable and a THF-d_8 solution of **7** shows no signs of decomposition on heating to 74 °C for 12 h.

Single crystals of **7** suitable for an X-ray study were grown from THF/pentane solutions at -20 °C. Crystallographic data and collection and refinement parameters are given in Table 1.6. The molecular structure of **7** (two views) along with the atom-labeling scheme is shown in Figure 1.5 while selected bond lengths and bond angles are listed in Table 1.7. Identification of **7** as a cationic, dimethyl hydrazido complex is consistent with the observed structure.

References begin on page 65

Figure 1.5. Two views of the structure of {[Me-N_3N]Mo=N-NMe_2}OTf (**7**) with the triflate ion omitted for clarity.

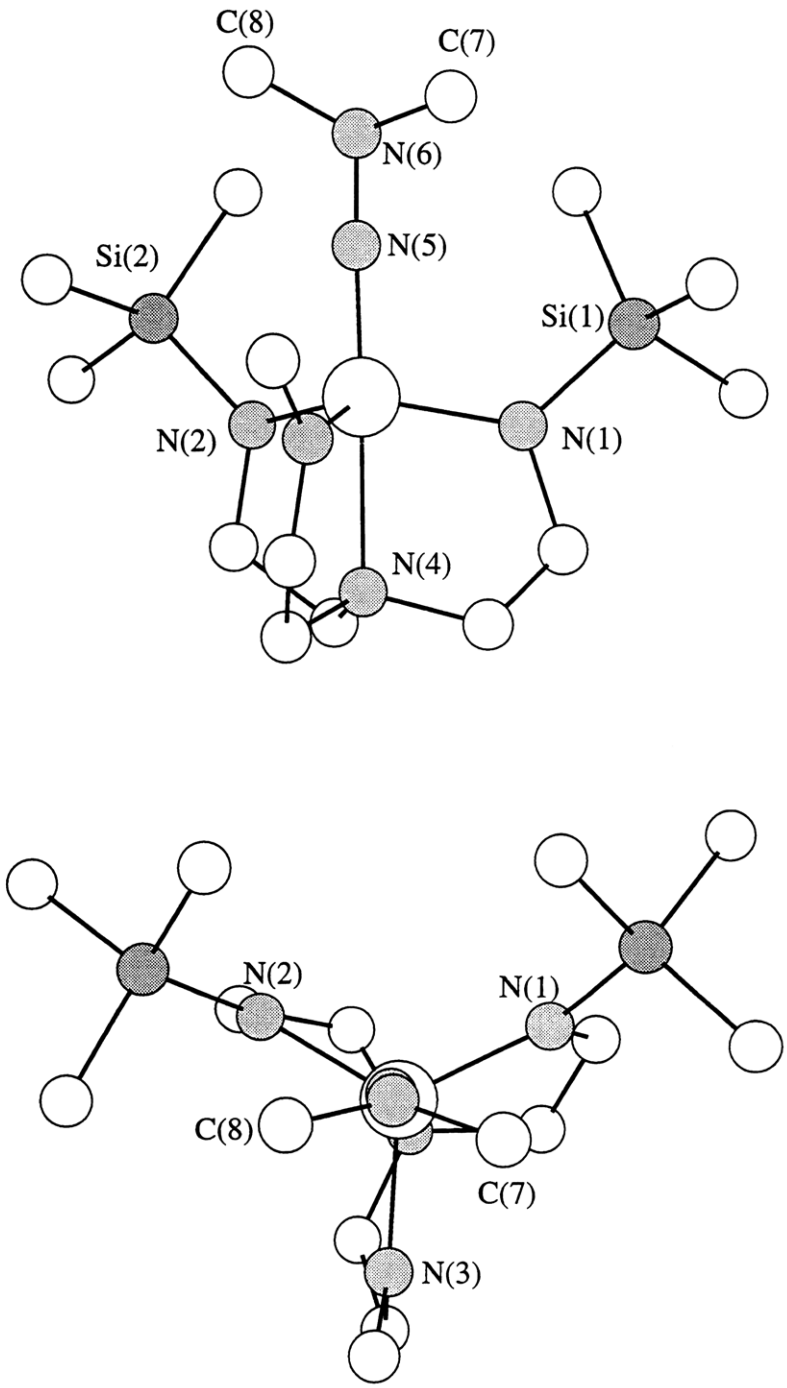

Table 1.6. Crystallographic data, collection parameters and refinement parameters for **7** and **8**.

	7	**8**
Empirical Formula	$C_{16}H_{39}F_3MoN_6O_3SSi_2$	$C_{18}H_{45}F_3MoN_6OSSi_3$
Formula Weight	604.71	662.87
Diffractometer	Siemens SMART/CCD	Siemens SMART/CCD
Crystal Dimensions (mm)	0.39 x 0.18 x 0.18	na
Crystal System	Orthorhombic	Orthorhombic
Space Group	Pbca	Pbca
a (Å)	14.723(3)	15.610(3)
b (Å)	14.417(3)	12.478(3)
c (Å)	26.243(4)	34.085(5)
α (°)	90	90
β (°)	90	90
γ (°)	90	90
V (Å^3), Z	5571(2), 8	6639(2), 2
D_{calc} (Mg/m^3)	1.442	1.326
Absorption coefficient (mm^{-1})	0.679	0.611
F_{000}	2512	2768
Temperature (K)	183(2)	183(2)
Θ range for data collection (°)	1.55 to 20.00	1.19 to 20.00
Reflections collected	15181	18299
Unique Reflections	2592	3088
R	0.0851	0.0452
R_w	0.1005	0.0531
GoF	1.293	0.855

References begin on page 65

Table 1.7. Selected bond lengths and bond angles for **7**.

Bond Lengths (Å)					
Mo(1)-N(5)	1.747(10)	Mo(1)-N(1)	1.960(9)	Mo(1)-N(2)	1.950(9)
Mo(1)-N(3)	1.962(9)	Mo(1)-N(4)	2.235(9)	N(5)-N(6)	1.334(13)

Bond Angles (deg)			
Mo(1)-N(5)-N(6)	173.6(8)	Mo(1)-N(1)-Si(1)	129.5(5)
Mo(1)-N(3)-C(31)	128.5(8)	Mo(1)-N(2)-Si(2)	125.1(5)
N(5)-N(6)-C(7)	119.1(10)	N(5)-N(6)-C(8)	115.9(10)
N(1)-Mo(1)-N(5)	103.5(4)	N(3)-Mo(1)-N(5)	94.5(4)

Dihedral Angles (deg)[a]			
N(4)-Mo-N(1)-Si(1)	175.3	N(4)-Mo-N(2)-Si(2)	165.0

[a]Obtained from a Chem-3D Drawing

An important feature of **7** is that one of the TMS groups of the ligand has been replaced by a methyl group giving rise to a molecule with C_s symmetry, consistent with the NMR data. This result also illustrates the susceptibility of Si-N bonds to undergo cleavage reactions leading to ligand degradation. Such decomposition pathways are believed to contribute to the low yield of $[N_3N]MoCl$ from the reaction of Li_3N_3N with $MoCl_4(THF)_2$.[21] The Mo-N(5)-N(6) linkage in **7** is essentially linear (173.6(8)°) and the N-N bond length (1.334(13) Å) is indicative of a bond order of ~1.5. Hence, the dinitrogen ligand in **7** is considerably reduced compared to structurally-characterized diazenido complexes such as **1**, $[Mo(t\text{-}BuMe_2SiNCH_2CH_2)_3N]_2(\mu\text{-}N_2)$[24] (N-N = 1.20(2) Å) and $[N_3N_F]MoN_2Si^iPr_3$[22] (N-N = 1.20(1) Å). The N-N bond length in **7** falls within

the range reported for other molybdenum and tungsten hydrazido complexes (1.28 - 1.39 Å).[32-36] Also, the short Mo-N(5) bond length (1.747(10) Å) is consistent with an increase in the multiple bonding between the metal center and N_α. N(6) is a planar nitrogen, the sum of the angles being 353°. This planarity allows for delocalization of the nitrogen lone pair throughout the Mo-N-N π system. The molybdenum atom is displaced from the plane defined by the amide nitrogens by 0.369 Å in the direction of N_α. The methyl groups of the hydrazido ligand point between the methylated ligand arm and a TMS-substituted ligand arm as opposed to pointing between two TMS-substituted ligand arms presumably for steric reasons. The $NNMe_2$ moiety is tilted ~10° toward the methylated ligand arm (N(5)-Mo-N(3) = 94.5(4)°, N(5)-Mo-N(1) = 103.5(4)°, N(5)-Mo-N(2) = 104.6(4)°). Both features can be attributed to greater steric demands of Si(1) and Si(2) compared to a methyl group. We can be certain that there is no proton present on N(3) in view of the virtual identity of the Mo-N(1), Mo-N(2), and Mo-N(3) bond lengths and the fact that they are all similar to $Mo\text{-}N_{amido}$ bond lengths in many other triamidoamine complexes.[17]

The second product of the reaction between **6** and MeOTf, $\{[(Me_3SiNCH_2CH_2)_2NCH_2CH_2NMe_2]Mo\text{-}N{=}NSiMe_3\}OTf$ (**8**), can be isolated in 35% yield as red crystals from THF/pentane solutions at -20 °C. The solubility properties of **8** are consistent with it being a cationic species. A singlet at 0.34 ppm in the ^1H NMR spectrum of **8** in THF-d_8 integrates as 27 protons and is assigned to the three TMS groups, the resonances for which are apparently accidentally equivalent. (In C_6D_6 two resonances are observed at 0.29 ppm (18H) and 0.16 ppm (9H)). A second singlet at 2.76 ppm integrates as 6 protons but is 1 ppm upfield of the methyl amido protons of **7**. There are six sets of multiplets for the twelve methylene protons of the ligand backbone and so **8** is not a C_3-symmetric complex. The ^{13}C NMR spectrum of **8** reveals TMS groups in two different environments and four methylene carbon resonances suggesting the presence of a plane of symmetry in **8**. The IR spectrum of **8** has a strong broad stretch at 1724 cm^{-1} that shifts to 1668 cm^{-1} in **8-$^{15}N_2$** and the ^{15}N NMR spectrum reveals resonances at 361.5 and 244.3 ppm (J_{NN} = 13 Hz) (Table 1.1). The position of ν_{NN} and the downfield shift of N_β in the ^{15}N NMR spectrum are suggestive of a diazenido complex (compare with **1** and **6** above) but

the complexity of the ^{1}H and ^{13}C NMR spectra precluded a determination of the molecular structure of **8** so an X-ray study was carried out to resolve the issue.

X-ray quality crystals of **8** were obtained by crystallization from THF/pentane at -20 °C. Crystallographic data and collection and refinement parameters are given in Table 1.6. The molecular structure of **8** along with the atom-labeling scheme is shown in Figure 1.6 while selected bond lengths and bond angles are listed in Table 1.8.

Figure 1.6. View of the structure of $\{[(Me_3SiNCH_2CH_2)_2NCH_2CH_2NMe_2]MoN_2TMS\}OTf$ (**8**) with the triflate ion omitted for clarity.

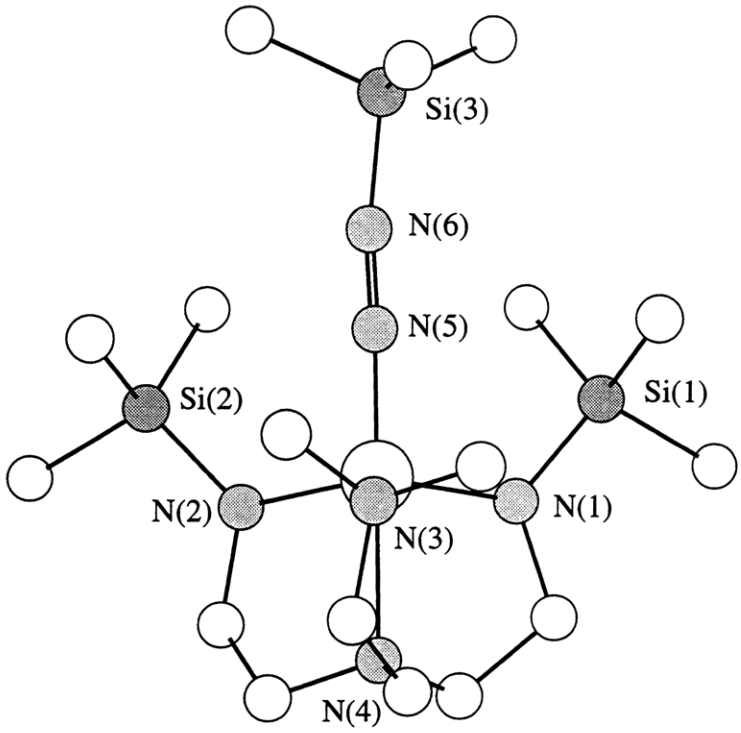

Two features of **8** are immediately apparent from Figure 1.6 and both serve to illustrate the lack of selectivity of the methylation reaction. Firstly, the diazenido ligand has emerged unscathed from the reaction and so further functionalization of dinitrogen has not been achieved. Secondly, one of the ligand arms has been doubly methylated thereby converting the triamidoamine ligand into a diamidodiamine ligand. This conversion explains the upfield shift of the methyl protons of **8**

References begin on page 65

relative to those of **7**. The Mo-N(3) bond length at 2.181(5) Å is typical of a dative amine bond and should be compared with the Mo-N(4) bond length of 2.229(6) Å. The dinitrogen bond length of 1.206(9) Å is within the range of N-N bond lengths of other crystallographically characterized diazenido complexes of the TMS-TREN system.[22,24] The Mo-N(5)-N(6) and N(5)-N(6)-Si(3) linkages are essentially linear with angles of 172.8° and 170.5° respectively.

Table 1.8. Selected bond lengths and bond angles for **8**.

Bond Lengths (Å)

Mo(1)-N(5)	1.803(7)	Mo(1)-N(1)	1.958(5)	Mo(1)-N(2)	1.950(5)
Mo(1)-N(3)	2.181(5)	Mo(1)-N(4)	2.229(6)	N(5)-N(6)	1.206(9)
N(1)-Si(1)	1.744(6)	N(2)-Si(2)	1.745(6)	N(6)-Si(3)	1.670(9)

Bond Angles (deg)

N(5)-Mo(1)-N(3)	95.2(2)	N(5)-Mo(1)-N(1)	100.3(3)
N(5)-Mo(1)-N(2)	100.8(3)	N(2)-Mo(1)-N(3)	116.5(2)
N(3)-Mo(1)-N(4)	80.2(2)	N(6)-N(5)-Mo(1)	172.8(7)
N(5)-N(6)-Si(3)	170.5(8)	N(4)-Mo(1)-N(5)	175.4(2)
Mo(1)-N(1)-Si(1)	126.2(2)	Mo(1)-N(2)-Si(2)	125.8(3)

Dihedral Angles (deg)[a]

N(4)-Mo(1)-N(1)-Si(1)	179.4	N(4)-Mo(1)-N(2)-Si(2)	173.0

[a]Obtained from a Chem-3D Drawing

References begin on page 65

Attempts have been made to improve the selectivity of the reaction shown in equation 10. If the reaction mixture is maintained at -20 °C, no reaction is observed over the course of 18 h and **6** is recovered. If less than 4 equivalents of MeOTf are used, the reaction does not go to completion (according to ^{1}H NMR spectroscopy). The reactivity of **1** with electrophiles such as MeI and MeOTf has been explored briefly in hopes of synthesizing hydrazido complexes in one step without isolation of the intermediate diazenido complexes. However, such reactions give rise to complex mixtures of diamagnetic and paramagnetic products and so this approach was abandoned.

The proposed mechanism for the formation of **7** and **8** is shown in Scheme 1.2. In the first step a methyl electrophile reacts with **6** by attacking an amido group of the ligand to give **A**. Loss of TMSOTf from **A** yields **B**. Sterically, the methylated amido nitrogen of **B** is probably more accessible than N_β of the diazenido ligand and further alkylation at the equatorial nitrogen would then produce **8**. Reaction of **8** with methyl triflate is unlikely due to its cationic nature which perhaps accounts for its isolation. In a competing reaction, alkylation at N_β of **B** yields **C** which loses TMSOTf to give **D**. Further alkylation of **D** could occur at the methylated amido nitrogen to produce **E** or at N_β, to yield **7**. In triamidoamine complexes one of the three linear combinations of p orbitals on the equatorial amido nitrogens is of A_2 symmetry and in the C_{3v} point group there is no metal-based orbital of matching symmetry. Presumably, it is the availability of this ligand-centered, nonbonding orbital that leads to alkylation of the equatorial amido nitrogen in **6**, **B** and **D**. The low yields of **7** and **8** suggest that competing pathways such as those that lead to **E** are accessible although products arising from such reactions have not been isolated. It should be noted that diazenido complexes of the type M-N=N-Me have not been isolated in any TREN-based systems. The reasons for this are not clear although the smaller size of a methyl group compared to a trimethylsilyl group may result in such species being prone to intermolecular decomposition. Whether the proposal outlined above is correct or not, it is clear that alkylation at the equatorial nitrogen competes with alkylation of N_β of the diazenido ligand at least when strong electrophiles such as methyl triflate are employed.

References begin on page 65

Scheme 1.2. Proposed mechanism for the formation of **7** and **8**.

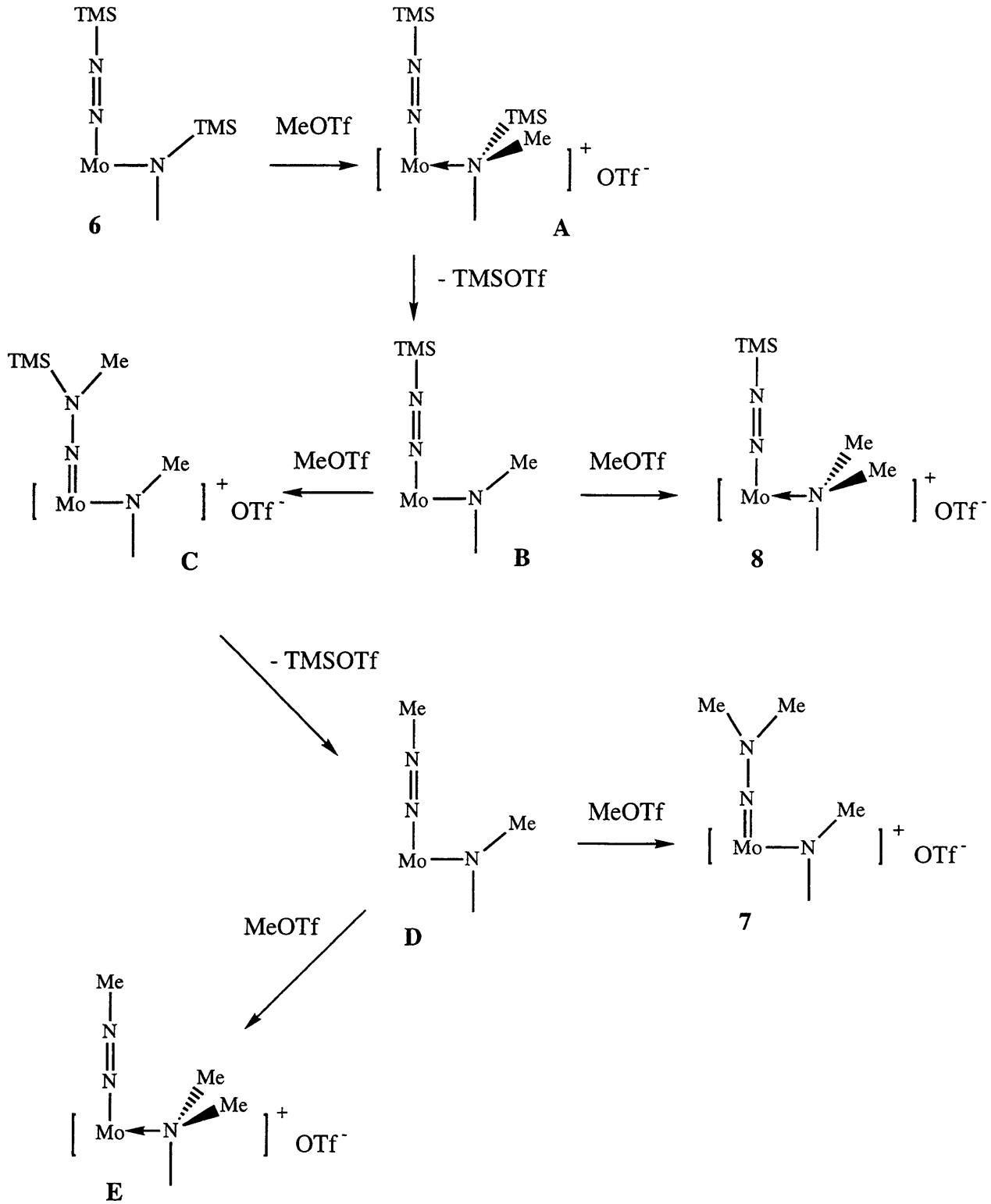

Having isolated and characterized **7** and **8** we began to explore their reactivity with a view to further functionalizing the dinitrogen ligand. In particular we examined the reactivity of **7** and **8** with MeMgCl in order to determine whether an alkyl nucleophile would add to N_α, to N_β, or to the metal center. **8** reacts instantaneously with MeMgCl in THF to give diamagnetic $[N(CH_2CH_2NSiMe_3)_2(CH_2CH_2NMe_2)]Mo(N_2TMS)(Me)$ (**9**) (equation 11). Resonances at

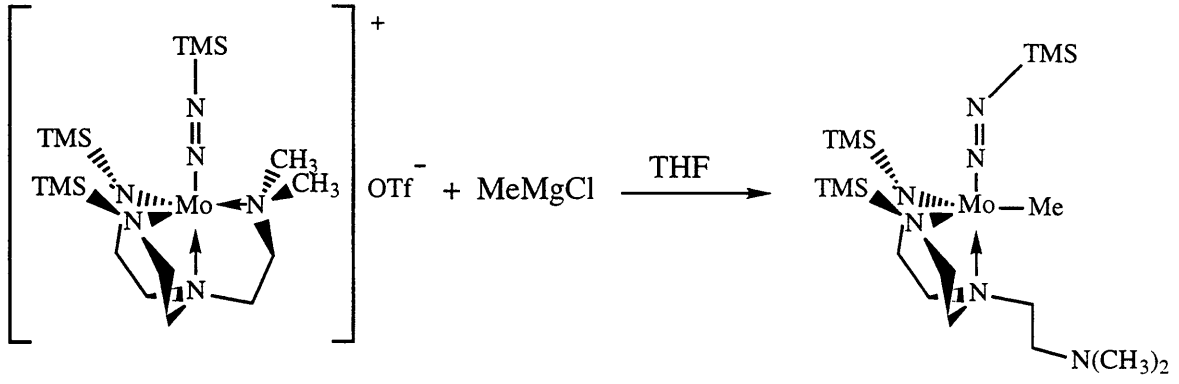

8 **9**

(11)

0.47 ppm in the ^1H NMR spectrum and at 23.9 ppm in the ^{13}C NMR spectrum of **9**, taken in C_6D_6, suggest that alkylation has occurred at molybdenum. In the ^1H NMR spectrum the resonance due to the methyl groups of the amine ligand arm appears at 1.90 ppm which is somewhat upfield of the corresponding resonance in **8** (2.76 ppm). The IR spectrum of **9** in Nujol shows a strong, broad absorption at 1640 cm^{-1} (1577 cm^{-1} in **9-$^{15}N_2$**) while the ^{15}N NMR spectrum taken in C_6D_6 consists of two doublets at 374.6 and 239.5 ppm (J_{NN} = 15 Hz) (Table 1.1). **9** decomposes to a black, oily solid upon prolonged exposure to vacuum (1 h). Satisfactory elemental analysis was obtained for a sample of **9** that was subjected to vacuum drying for ~ 10 min. Although these data do not reveal whether the amine donor is still bound to the metal or not, an X-ray structure revealed that it is not.

Single crystals of **9** were grown from saturated hexamethyldisiloxane solutions at -20 °C. The molecular structure of **9** along with the atom-labeling scheme is shown in Figure 1.7 while

selected bond lengths and bond angles are listed in Table 1.9. Crystallographic data and collection and refinement parameters are given in Table 1.10. The structure of **9** confirms that alkylation has occurred at molybdenum and that the amine ligand arm has dissociated to yield a trigonal bipyramidal environment around the metal center. The Mo-N(5)-N(6) linkage is linear and the N(5)-N(6) bond length at 1.229(3) Å is consistent with **9** being described as a diazenido complex. The diazenido ligand in **9** in quite bent at the β nitrogen, with N(5)-N(6)-Si(2) = 137.0(2)° (compare with the corresponding angle in **8** which is essentially linear at 170.5(8)°). We attribute the bending of the diazenido ligand to an absence of three approximately equal steric interactions that would oppose bending, rather than to electronic effects. The environment above C(7) is relatively open, so the trimethylsilyl group of the diazenido ligand bends away from the bulky TMS groups on the equatorial nitrogens toward C(7). A comparison of the ^{15}N NMR chemical shifts and the IR stretches for the diazenido ligands in **1**, **6**, **8** and **9** suggests that in triamidoamine complexes of the type being investigated here, ^{15}N NMR and IR data are not reliable parameters on which to base any conclusion as to whether the diazenido ligand is significantly bent at N_β or not in the solid state (Table 1.1).[37]

Table 1.9. Selected bond lengths and bond angles for **9**.

Bond Lengths (Å)

Mo(1)-N(5)	1.789(2)	Mo(1)-N(1)	1.983(2)	Mo(1)-C(7)	2.153(3)
Mo(1)-N(3)	1.981(2)	Mo(1)-N(4)	2.312(2)	N(5)-N(6)	1.229(3)
N(6)-Si(2)	1.726(2)				

Bond Angles (deg)

N(5)-Mo(1)-N(1)	98.65(8)	N(3)-Mo-(1)-N(1)	123.99(9)
N(5)-Mo(1)-C(7)	91.69(10)	N(3)-Mo(1)-C(7)	114.47(11)
C(4)-N(4)-Mo(1)	117.34(14)	N(6)-N(5)-Mo(1)	179.5(2)
N(5)-N(6)-Si(2)	137.0(2)		

References begin on page 65

Table 1.10. Crystallographic data, collection parameters and refinement parameters for **9**.

Empirical Formula	$C_{18}H_{49}MoN_6Si_3$
Formula Weight	529.84
Diffractometer	Siemens SMART/CCD
Crystal Dimensions (mm)	0.50 x 0.40 x 0.40
Crystal System	Monoclinic
Space Group	$P2_1/c$
a (Å)	10.235(3)
b (Å)	14.315(7)
c (Å)	20.277(7)
α (°)	90
β (°)	103.80
γ (°)	90
V (Å^3), Z	2885(2), 4
D_{calc} (Mg/m^3)	1.220
Absorption coefficient (mm^{-1})	0.594
F_{000}	1132
Temperature (K)	183(2)
Θ range for data collection (°)	1.76 to 23.28
Reflections collected	11505
Unique Reflections	4130
R	0.0251
R_w	0.0272
GoF	1.026

References begin on page 65

Figure 1.7. A view of the structure of **9** with the triflate ion omitted for clarity.

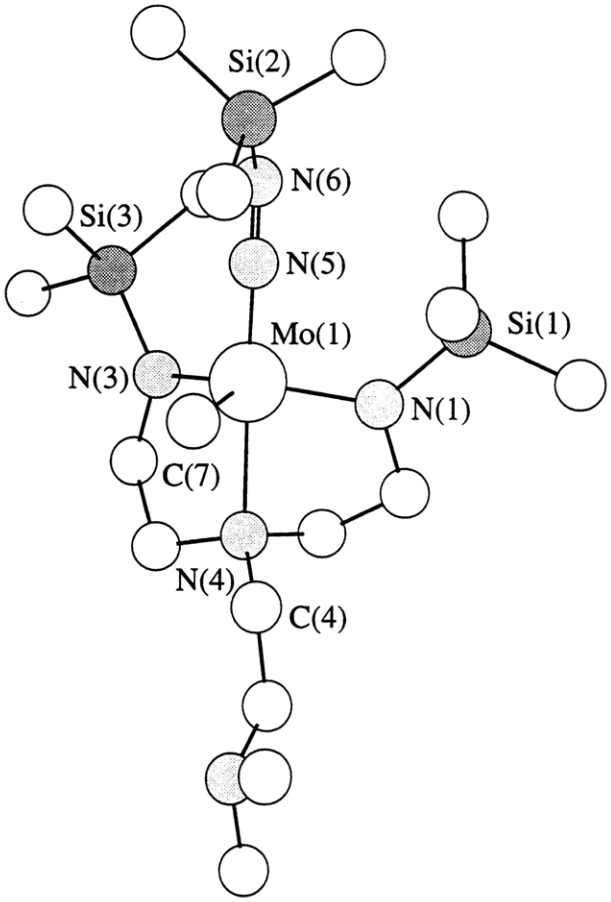

Addition of MeMgCl to a THF solution of **7** at -20 °C results in an immediate color change to blood red. The ^{1}H NMR spectrum of the product (**10**) in C_6D_6 is shown on the lower half of Figure 1.8. This spectrum is consistent with **10** being a complex of low symmetry. There are 10 sets of resonances for the 12 methylene protons of the ligand backbone and the singlet at 0.18 ppm indicates that methylation has occurred at molybdenum (cf. 0.74 ppm in **9**). Both the ^{1}H and ^{13}C NMR spectra of **10** have two resonances for the two TMS groups on the ligand which is also consistent with a complex of low symmetry. Two sets of doublets comprise the ^{15}N NMR spectrum of **10-$^{15}N_2$** with the resonance attributed to N_β appearing at 142.0 ppm. With these data in hand we formulate **10** as a pseudo-octahedral methylhydrazido complex shown in equation

12, alkylation between TMS- and Me-substituted amido nitrogens being the sterically more accessible position.

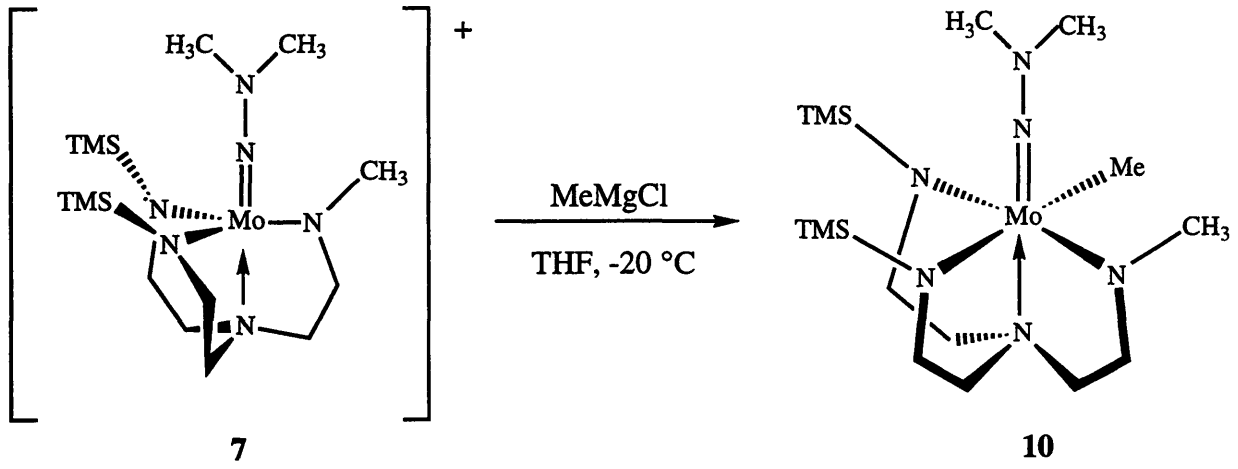

7 **10**

(12)

Efforts to crystallize **10** have been hampered by its high solubility in pentane and its thermal instability even at room temperature. Over 24 h, a C_6D_6 solution of **10** changes color from blood red to orange-brown. This transformation is accelerated by heating a sample to 65 °C. If the solvent is removed and the residue is extracted with pentane, a pale yellow, crystalline solid (**11**) can be isolated. The ^1H NMR spectrum of **11** is shown on the upper half of Figure 1.8. It is apparent from this spectrum that **11** is a complex of higher symmetry than **10**. There is a single resonance for the TMS groups on the ligand at 0.59 ppm and three sets of multiplets for the methylene protons (3.25, 2.78 and 2.21 ppm), consistent with a complex possessing mirror symmetry. The singlet at 4.08 ppm is assigned to the methyl group on the triamidoamine ligand arm. The ^{13}C NMR spectrum of **11** exhibits four resonances for the methylene carbons of the ligand backbone and a single resonance for the TMS groups of the ligand, suggesting that **11** contains a plane of symmetry. Spectroscopic and elemental analysis data support the formulation of **11** as the nitride complex [Me-N_3N]Mo≡N (equation 13). The ^1H NMR spectrum of **11** is a hybrid of that of [N_3N]Mo≡N (see below) and that of [$(MeNCH_2CH_2)_3N$]Mo≡N.[38] The IR spectra of **11** and **11-$^{15}N_2$** are superimposable except for a single absorption that occurs at 1002 cm^{-1} in the spectrum of **11** and shifts to 977 cm^{-1} in the spectrum of **11-$^{15}N_2$**, characteristic of a

References begin on page 65

References begin on page 65

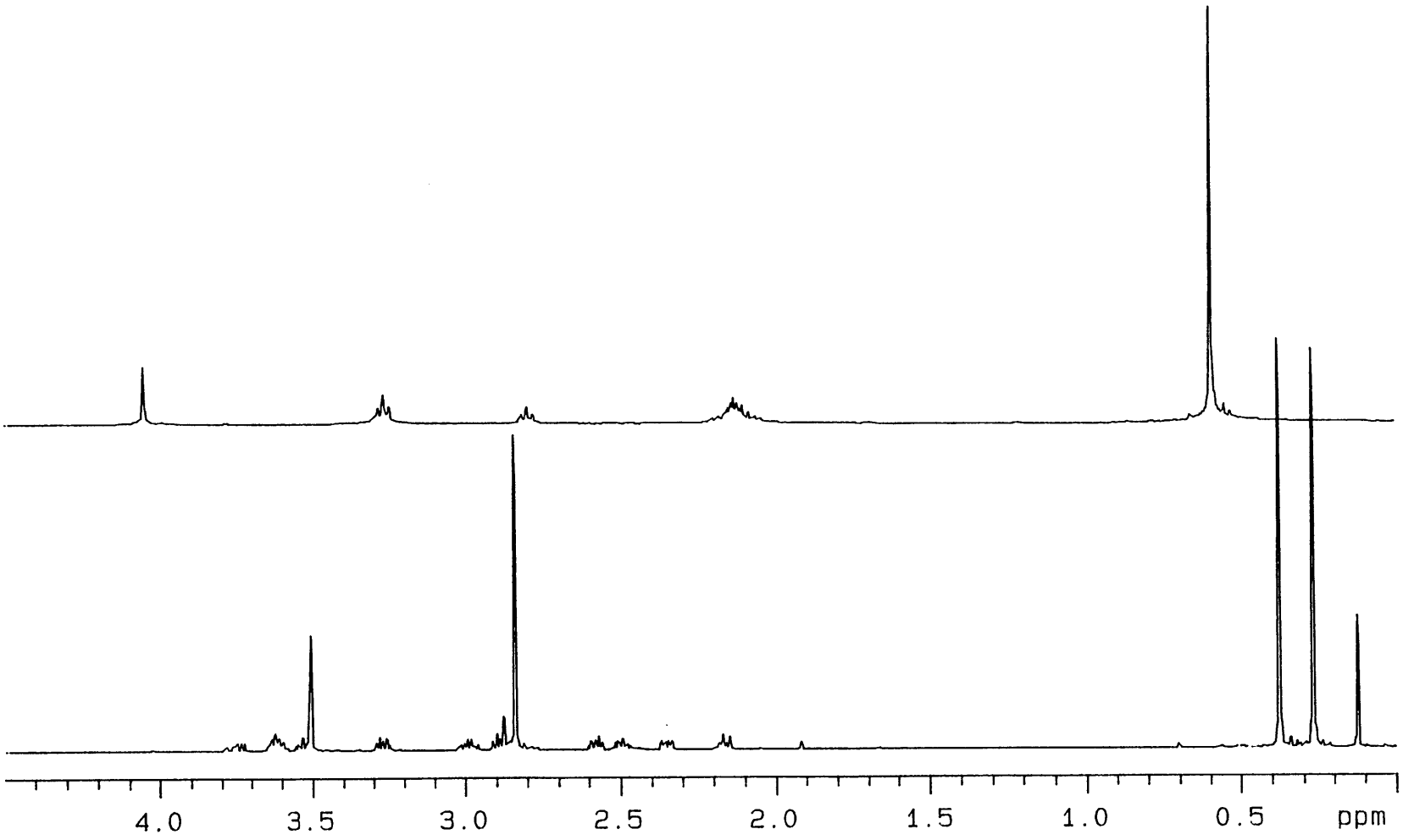

Figure 1.8. ^{1}H NMR spectra of **10** (lower spectrum) and **11** (upper spectrum) in C_6D_6.

M-N triple bond stretch.[39] Furthermore, the ^{15}N NMR spectrum of **11-$^{15}N_2$** consists of a singlet at 866.1 ppm which is also indicative of a metal nitride complex.[39]

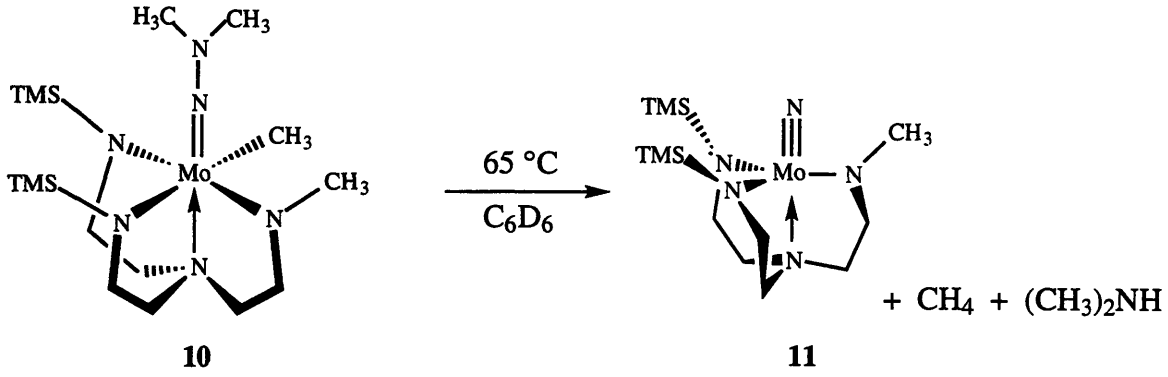

10 **11**

(13)

The thermolysis of **10** has also been carried out in THF-d_8 with essentially the same result. The yield of **11** (versus an internal standard) is 67% although the isolated yield (30%) is lowered due to its solubility in pentane. Among the organic products are methane (16% in solution) and dimethylamine (38% in solution), identified by comparison with ^1H and ^{13}C NMR spectra of authentic samples and measured via an internal standard. Resonances at 0.19 ppm in the ^1H NMR spectrum and at -1.22 ppm in the ^{13}C NMR spectrum are assigned to CH_4. The ^1H NMR spectrum also exhibits a doublet at 2.32 ppm ($^3J_{HH}$ = 6 Hz) attributed to $(CH_3)_2NH$. If the thermolysis is carried out employing **10-$^{15}N_2$** in THF-d_8, a doublet is observed at 10.74 ppm ($^1J_{NH}$ = 69 Hz) in the ^{15}N NMR spectrum consistent with the formation of $(CH_3)_2{}^{15}NH$. However, it is clear from the complexity of the NMR spectra of decomposed **10** that a fraction of the triamidoamine ligand has been attacked in some significant manner as evidenced in the ^1H NMR spectrum by numerous resonances between 0.4 and 0.0 ppm. We speculate that the decomposition of **10** to **11** proceeds initially via Mo-C bond homolysis to produce a methyl radical and the unstable Mo(V) species [Me-N_3N]Mo=N-N$(CH_3)_2$ which decomposes via homolytic N-N bond cleavage to give **11** and a dimethylamine radical. However, it is equally likely that the initial step may involve N-N bond homolysis followed by scission of the Mo-C bond. There is no

References begin on page 65

evidence for the incorporation of deuterium in the organic products that have been identified. This suggests that hydrogen atom abstraction from the $[N_3N]^{3-}$ ligand may be occurring and could explain the observed ligand degradation. Unfortunately, the long and low yield route to **10** has rendered a detailed study of its decomposition impractical. However, the progress we have made with regard to the functionalization of dinitrogen in [N$_3$N]Mo complexes and the difficulties that we have encountered with the lability of TMS groups in the $[N_3N]^{3-}$ ligand have prompted us to revisit the $[N_3N_F]^{3-}$ system and preliminary results suggest that this approach will be fruitful. For example, in a reaction analogous to that which yields **7** (see above), [N$_3$N$_F$]Mo-N=N-SiMe$_3$ has been found to react cleanly with MeOTf to give {[N$_3$N$_F$]Mo=NNMe$_2$}OTf.[40] {[N$_3$N$_F$]Mo=NNMe$_2$}OTf can be alkylated by MeMgCl and the resulting complex does decompose upon heating to give [N$_3$N$_F$]MoN as one of the products.[40] These results suggest that we will be able to establish the mechanism or mechanisms by which species analogous to **10** decompose by N-N bond cleavage.

Having functionalized dinitrogen to the nitrido stage we were compelled to explore the chemistry of such nitride complexes since in a catalytic cycle the second nitrogen must be removed from the metal center in order to regenerate a [N$_3$N]MoX complex which could then be reduced under dinitrogen to begin the cycle again. Since **11** is only available to us in low yield, we set out to synthesis [N$_3$N]MoN (**12**) by more direct routes. Although [N$_3$N]WN[19] can be synthesized from [N$_3$N]WCl and NaN$_3$, the analogous reaction with [N$_3$N]MoCl does not yield [N$_3$N]MoN in any appreciable amount. [N$_3$N]MoCl does react with TMSN$_3$ at elevated temperatures and **12** can be isolated from the reaction as a yellow, crystalline solid in 88% yield (equation 14). Presumably an azide complex is formed as an intermediate in this reaction and although decomposition of azide

$$[N_3N]MoCl + 4\ TMSN_3 \xrightarrow[90\ ^\circ C,\ 24\ h]{\text{toluene}} \underset{\mathbf{11}}{[N_3N]MoN} \qquad (14)$$

References begin on page 65

complexes is a common method for preparing nitride complexes, isolation of intermediate organoazide complexes has been documented in only a few cases.[41,42] The ^{1}H NMR spectrum of **12** taken in C_6D_6 is typical of C_3-symmetric complexes of this type and consists of a singlet for the TMS groups of the ligand at 0.56 ppm and a pair of triplets at 3.23 and 2.14 ppm assigned to the methylene protons of the ligand backbone. The IR spectrum of **12** has a strong absorption at 1001 cm^{-1} that is assigned to a M-N triple bond stretch and should be compared with that of **11**. **12** reacts readily with MeOTf or TMSOTf in toluene to give the corresponding cationic imido complexes, {[N_3N]MoNMe}OTf (**13**) and {[N_3N]MoNTMS}OTf (**14**) respectively (equation 15). Both **13** and **14** are isolated in high yield and have solubility properties that are consistent with their cationic nature e.g. both slowly oil out of toluene or benzene but are highly soluble in THF.

$$\underset{\textbf{12}}{[N_3N]MoN} + ROTf \xrightarrow{\text{toluene}} \underset{\begin{array}{l}\textbf{13 (R = Me)}\\ \textbf{14 (R = TMS)}\end{array}}{\{[N_3N]MoNR\}OTf} \qquad (15)$$

The chemistry of **13** and **14** has been explored by Dr. Klaus Wanninger. Both react readily with MeMgCl yielding complexes arising from alkylation at molybdenum. Complex **14** can be reduced by $Li_2C_8H_8$ or sodium naphthalenide to give the structurally-characterized Mo(V) imido complex [N_3N]MoNTMS. Further details of this chemistry can be found in the literature.[19] However, it is noted that efforts to remove the imido group from the metal center to generate a [N_3N]MoX complex have been unsuccessful to date. An alternative approach to this problem may involve reduction of **12** as the initial step although the cyclic voltammogram of **12** (obtained by Dr. Luis Baraldo) exhibits a reduction wave at -2.9 eV (versus ferrocene/ferrocenium) indicating that **12** is exceedingly difficult to reduce.

References begin on page 65

DISCUSSION

Our exploration of the dinitrogen chemistry of $[N_3N]Mo$ complexes has proved to be a fruitful one as evidenced by the plethora of complexes described above. The stepwise reduction and functionalization of dinitrogen has been achieved and examples of terminal dinitrogen, diazenido, hydrazido and nitrido complexes have been isolated. This work complements the extensive work carried out on the functionalization of dinitrogen in $[M(N_2)_2(P)_4]$ (P = phosphine; M = Mo, W) and $[M(N_2)_2(P\text{-}P)]$ (P-P = chelating diphosphine; M= Mo, W) complexes.[6-9] A facile entry to the chemistry is achieved by the reduction of $[N_3N]MoCl$ with magnesium powder to give **1** in high yield. **1** is noteworthy for a number of reasons. Firstly, as noted above, it provides us with an entry into dinitrogen chemistry in the TMS-TREN system. Secondly, in previous work in our group, efforts to crystallize $[N_3N_F]Mo(N_2)[Na(ether)_x]$[22] were unsuccessful and so **1** represents the first example of a structurally-characterized salt of a diazenido complex in the TREN-based systems. Thirdly, oxidation of **1** affords the neutral terminal dinitrogen complex **4** in high yield. Finally, heterometallic dinitrogen complexes containing Zr, V and Fe can be prepared by employing $\{[N_3N]Mo(N_2)\}^-$ as a nucleophile in the form of **1** and the synthesis of such complexes is the subject of Chapter 2.

Although the dinitrogen ligand in **4** is labile as suggested by exchange of $^{14}N_2$ with $^{15}N_2$ and by the decomposition of **4** to yield **5**, the "$[N_3N]Mo$" species formed by dissociation of dinitrogen from **4** has not be observed. Such a low spin species is expected to be of high energy and reactivity, the energy of the $d_{z}2$ orbital being much higher than that of the d_{xz} or d_{yz} orbital as a consequence of the presence of the apical amine donor. The high reactivity of such a species is demonstrated by the isolation of $[bitN_3N]Mo$, the product of C-H activation of one of the trimethylsilyl groups of the ligand, isolated from the reduction of $[N_3N]MoCl$ by magnesium in the absence of a donor ligand (see Chapter 3). In contrast to "$[N_3N]Mo$", $Mo[N(R)Ar]_3$ (R = $C(CD_3)_2CH_3$, Ar = 3,5-$C_6H_3Me_2$) is isolable and has a high spin configuration.[14] We suspect that this difference between the triamidoamine and trisanilide complexes is the crucial one that differentiates their chemistry with dinitrogen.

References begin on page 65

Although **7** is only available in low yield, it does represent a significant breakthrough in the context of the dinitrogen chemistry of TREN complexes being the first hydrazido complex to be isolated in such systems. Aside from the low yield, a further drawback of the chemistry is that the methylation reaction is non-selective and the TMS-TREN ligand has become involved in the chemistry. It appears that the nucleophilicity of the β nitrogen in **6** is not sufficiently different from that of the amido nitrogens to allow MeOTf to react preferentially with the diazenido ligand as further demonstrated by the isolation of **8**. However, **8** is an example of a new type of diamido/bisdonor complex that may be of use in future research provided more direct ways can be found to such ligands and complexes. The ability of the equatorial donor to associate and dissociate from the metal center as required may be a key feature of such chemistry.

Reaction of **7** with MeMgCl results in nucleophilic attack at the metal center to generate a methyl hydrazido complex, **10**. This result is perhaps not surprising in light of the crystal structure of **7**. The long N-N bond and shortened Mo-N bond are consistent with {[Me-N_3N]Mo^+=N-N$(CH_3)_2$}OTf as the major resonance structure for **7**. The decomposition of **10** to **11** is also not surprising in view of the documented propensity for triamidoamine complexes to form strong M-E bonds (E = CR, N, P, As).[19-21,43] The intimate details of this decomposition are not known at this stage and a complete investigation is hampered by the low yield of **7** in the preceding step.

Despite the limitations of TMS-TREN as a robust ligand, the present study demonstrates the feasibility of the stepwise reduction and functionalization of dinitrogen in molybdenum triamidoamine complexes. We have been able to isolate and crystallographically characterize several intermediates and the reduction of dinitrogen can be correlated with the N-N bond lengths in these complexes. These results have prompted us to revisit the C_6F_5-TREN[22] system and it appears likely that the salient features of the chemistry described herein will be transferable to such a system without the possibility of the side-reactions that plague the TMS-TREN system.

References begin on page 65

EXPERIMENTAL PROCEDURES

General Details. All experiments were performed under a nitrogen atmosphere in a Vacuum Atmospheres drybox or by standard Schlenk techniques unless otherwise specified. Pentane was washed with sulfuric acid/nitric acid (95/5 v/v), sodium bicarbonate, and water, stored over calcium chloride, and distilled from sodium benzophenone ketyl under nitrogen. Toluene was distilled from sodium, and CH_2Cl_2 was distilled from CaH_2. Anhydrous diethyl ether and THF were sparged with nitrogen and passed through alumina columns.[44] Hexamethyldisiloxane was purchased from Aldrich, dried over sodium and then vacuum transferred into a small storage flask. All solvents were stored in the dry box over activated 4 Å molecular sieves.

NMR data were obtained at 300 or 500 MHz (^1H), 75.4 MHz (^{13}C) and 50.7 MHz (^{15}N). Chemical shifts are listed in parts per million downfield from tetramethylsilane for proton and carbon. ^{15}N chemical shifts are referenced to external CH_3NO_2 whose shift is +380.2 ppm with respect to liquid ammonia (taken as 0 ppm). Coupling constants are listed in Hertz. Spectra were obtained at 25 °C unless otherwise noted. Benzene-d_6 and toluene-d_8 were pre-dried on CaH_2, vacuum transferred onto sodium and benzophenone, stirred under vacuum for two days and then vacuum transferred into small storage flasks and stored over molecular sieves. $[N_3N]MoCl$ was prepared as described in the literature.[21] TMSOTf, MeOTf, MeI, $PdCl_2(PPh_3)_2$, $NiCl_2(PPh_3)_2$, magnesium powder and MeMgCl were purchased from commercial vendors and used as received. $ZnCl_2$ was dried by heating to 80 °C for 24 h under active vacuum.

UV/visible spectra were recorded on a HP 8452 Diode Array spectrophotometer using a Hellma 221-QS quartz cell (path length = 10 mm) sealed to a gas adapter fitted with a Teflon stopcock. IR spectra were recorded on a Perkin-Elmer 1600 FT-IR spectrometer. Elemental analyses (C, H, N) were performed in our laboratory using a Perkin-Elmer 2400 CHN analyzer or by Microlytics Analytical Laboratories of Deerfield MA. X-ray data were collected on Siemens SMART/CCD diffractometer and general experimental details are described in the literature.[45]

References begin on page 65

SQUID Magnetic Susceptibility Measurements. Measurements were carried out on a Quantum Design SQUID magnetometer. Data were obtained at a field strength of 5000 Gauss. Straws and gel caps (Gelatin Capsule No. 4 Clear) were purchased from Quantum Design. The sample was prepared in the drybox by the following method. A gel cap and a square of parafilm were weighed. The sample was placed in the gel cap and the parafilm inserted above it. The gel cap was closed and the mass of the sample was ascertained by weighing the loaded gel cap. The gel cap was placed in a straw which was then mounted on the sample rod and placed in the magnetometer. Two runs were performed on the sample - one from 5 to 300 K and a second from 300 to 5 K. Measurements were made at the following increments: 5-10 K (every 1 K), 10-20 K (every 2 K), 20-50 K (every 3 K), 50-100 K (every 5 K), 100-200 K (every 10 K), 200-300 K (every 20 K).

{[(Me$_3$SiNCH$_2$CH$_2$)$_3$N]MoN$_2$}$_2$Mg(THF)$_2$ (1). [(Me$_3$SiNCH$_2$CH$_2$)$_3$N]MoCl (785 mg, 1.60 mmol) was dissolved in 30 mL of THF. Magnesium powder (100 mg, 4.16 mmol) was added to the solution which was then stirred for 17 h. THF was removed in vacuo and the residue was extracted with 30 mL toluene. 1,4-dioxane (560 mg, 6.37 mmol) was added and the solution stirred for 30 min. $MgCl_2$.(dioxane) was removed by filtration through a pad of Celite. Toluene was removed in vacuo and the orange solid was crystallized from diethyl ether; yield 820 mg (90%). ^{1}H NMR(C_6D_6) δ 3.98 (m, 8H, THF), 3.60 (t, 12H, NCH$_2$CH$_2$N), 2.21 (t, 12H, NCH$_2$CH$_2$N), 1.46 (m, 8H, THF), 0.61 (s, 54H, NSiMe$_3$). ^{13}C{^{1}H} NMR(C_6D_6) δ 71.0 (THF), 54.7 (NCH$_2$CH$_2$N), 52.0 (NCH$_2$CH$_2$N), 25.6 (THF), 4.8 (NSiMe$_3$). IR(THF, cm^{-1}) 1719 (N=N). Anal. Calcd. for $C_{38}H_{94}N_{12}Si_6O_2Mo_2Mg$: C, 40.18; H, 8.34; N, 14.80. Found: C, 40.35; H, 8.13; N, 14.76.

1-$^{15}N_2$. [(Me$_3$SiNCH$_2$CH$_2$)$_3$N]MoCl (520 mg, 1.06 mmol) was dissolved in 10 mL of THF and placed in a glass bomb with a stirring bar and an excess of magnesium powder. The vessel was subjected to three freeze-pump-thaw cycles to remove any $^{14}N_2$ present. $^{15}N_2$ (1 atm) was introduced and the solution stirred for 20 h. The product was isolated in a manner analogous

to that for $\{[(Me_3SiNCH_2CH_2)_3N]MoN_2\}_2Mg(THF)_2$. ^{15}N NMR(C_6D_6) δ 377.0 (J_{NN} = 12), 304.4 (J_{NN} = 12). IR(THF, cm^{-1}) 1662 (N=N).

$\{[(Me_3SiNCH_2CH_2)_3N]MoN_2\}[Na(15\text{-crown-}5)]$ (2). $[N_3N]MoCl$ (204 mg, 0.42 mmol) was dissolved in 5 mL of THF and cooled to -20 °C. Sodium naphthalenide (1654 μL, 0.85 mmol) was added dropwise to the stirred solution. After 40 min the solvent was removed under reduced pressure and the residue extracted with 7 mL diethyl ether. Removal of NaCl was effected by filtration through a pad of Celite. 15-crown-5 (83 μL, 0.42 mmol) was added to the ether solution which was chilled at -20 °C to afford the product as orange plates; yield 195 mg (64%). ^1H NMR(tol-d_8) δ 3.76 (t, 6H, NCH_2CH_2N), 3.10 (s, br, 15-crown-5), 2.27 (t, 6H, NCH_2CH_2N), 0.70 (s, 27H, $NSiMe_3$). $^{13}C\{^1H\}$ NMR(tol-d_8) δ 69.0 (15-crown-5), 55.0 (NCH_2CH_2N), 52.2 (NCH_2CH_2N), 4.6 ($NSiMe_3$). IR(Nujol, cm^{-1}) 1791(N=N).

$[(Me_3SiNCH_2CH_2)_3N]Mo(N_2)$ (4). Method 1. $\{[N_3N]MoN_2\}_2Mg(THF)_2$ (302 mg, 0.27 mmol) was dissolved in 10 mL THF and the solution was cooled to -20 °C. $Pd(PPh_3)_2Cl_2$ (187 mg, 0.27 mmol) was added all at once as a solid to the stirred solution of $\{[N_3N]MoN_2\}_2Mg(THF)_2$. Within one minute the solution had become deep green in color. After 45 min the solvent was removed and the residue extracted with 40 mL of pentane. The mixture was filtered through Celite and part of the pentane was removed in vacuo to yield red crystals; yield 205 mg (80%).

Method 2. $\{[N_3N]MoN_2\}_2Mg(THF)_2$ (302 mg, 0.27 mmol) was dissolved in 10 mL THF and $ZnCl_2$ (36 mg, 0.27 mmol) was dissolved in 2 ml THF. Both solutions were cooled to -20 °C and the $ZnCl_2$ solution was added to the stirred solution of $\{[N_3N]MoN_2\}_2Mg(THF)_2$. After 4 h the solution was filtered through Celite and the solvent removed in vacuo. The residue was extracted with 20 mL of pentane, filtered through Celite and dried in vacuo. Recrystallization from diethyl ether afforded the product as red crystals; yield 181 mg (70%, 2 crops). ^1H NMR (C_6D_6) δ 14.02 (CH_2), -4.53 (TMS), -40.57 (CH_2). IR(Pentane) cm^{-1} 1934 (N=N); IR(Nujol) cm^{-1} 1910, 1900 (N=N).

References begin on page 65

4-$^{15}N_2$. This compound was prepared in an analogous manner to **4** using **1-$^{15}N_2$**: IR (Pentane) cm^{-1} 1870 (N=N); IR(Nujol) cm^{-1} 1846, 1839 (N=N). Anal. Calcd. for $C_{15}H_{39}N_4{}^{15}N_2Si_3Mo$: C, 37.09; H, 8.09; N, 17.71. Found: C, 37.08; H, 8.49; N, 17.50.

[N_3N]Mo-N=N-Mo[N_3N] (5). [N_3N]Mo(N_2) (200 mg, 0.41 mmol) was dissolved in 5 mL of toluene and placed in a glass bomb along with a stirring bar. The bomb was sealed and heated to 84 °C for 40 h. During this time the reaction mixture turned deep purple in color. The toluene was removed in vacuo and the residue extracted with ether. Following filtration and reduction the ether solution was cooled to -20 °C and the product was obtained as a black microcrystalline solid; yield 152 mg (78%). ^1H NMR (C_6D_6) δ 3.74 (TMS), -17.05 (NCH_2CH_2N), -30.77 (NCH_2CH_2N). UV-visible(Toluene) λ = 542 nm, ε = 17,872 M^{-1} cm^{-1}. Anal. Calcd. for $C_{30}H_{78}N_{10}Si_6Mo_2$: C, 38.36; H, 8.37; N, 14.91. Found: C, 38.09; H, 8.45; N, 14.48.

[($Me_3SiNCH_2CH_2$)$_3$N]MoN_2SiMe_3 (6). Method 1. {[N_3N]MoN_2}$_2$Mg(THF)$_2$ (75 mg, 0.07 mmol) was dissolved in 5 mL THF. TMSCl (20 μL, 0.16 mmol) was added by syringe. The color of reaction mixture immediately lightened to yellow. The solution was stirred for 2 h. THF was removed and the residue extracted into pentane and filtered through Celite. The pentane solution was reduced and cooled to -30 °C to give a yellow solid; yield 60 mg (77%).

Method 2. [N_3N]MoCl (100 mg, 0.20 mmol) was dissolved in 5 mL THF. Magnesium powder and Me_3SiCl (80 mg, 0.74 mmol) were added. The solution was stirred and after 5 h the solution was yellow. After 20 h the THF was removed and the residue extracted into pentane and filtered through Celite. The pentane solution was reduced and cooled to -30 °C give a yellow solid; yield 100 mg (88 %). ^1H NMR(C_6D_6) δ 3.38 (t, 6H, NCH_2CH_2N), 2.10 (t, 6H, NCH_2CH_2N), 0.49 (s, 27H, $NSiMe_3$), 0.49 (s, 9H N_2SiMe_3). $^{13}C\{^1H\}$ NMR(C_6D_6) δ 54.1 (NCH_2CH_2N), 52.1 (NCH_2CH_2N), 4.1 ($NSiMe_3$), 4.0 (N_2SiMe_3). IR(THF, cm^{-1}) 1714 (N=N). IR(Nujol, cm^{-1}) 1712 (N=N). Anal. Calcd. for $C_{18}H_{48}N_6Si_4Mo$: C, 38.82; H, 8.69; N, 15.09. Found: C, 38.86; H, 8.73; N, 15.02.

References begin on page 65

6-$^{15}N_2$. This compound was prepared in a manner analogous to method 1 used to prepare **6**, except **1-$^{15}N_2$** was used. ^{15}N NMR(C_6D_6) δ 356.9 (J_{NN} = 12), 238.1 (J_{NN} = 12). IR(THF, cm^{-1}) 1654 (N=N).

{[N($CH_2CH_2NSiMe_3$)$_2$($CH_2CH_2NCH_3$)]MoN_2(CH_3)$_2$}$^+$OTf$^-$(THF)$_{0.5}$ (7). [N_3N]MoN_2SiMe_3 (500 mg, 0.90 mmol) was dissolved in 30 mL of toluene and cooled to -20 °C. Methyl triflate (408 μL, 3.60 mmol) was dissolved in 15 mL of toluene and cooled to -20 °C. The methyl triflate solution was added dropwise to the stirred solution of [N_3N]MoN_2SiMe_3. After 18 h the toluene was removed and the residue was washed with 7 mL of pentane to remove any unreacted [N_3N]MoN_2SiMe_3 (50 mg, 0.09 mmol). The brown-red solid was dissolved in minimum THF and filtered. Ether was added and the solution stored at -20 °C to give 102 mg of orange crystals (20%). A second recrystallization from THF/pentane was performed. ^1H NMR(THF-d_8) δ 3.96-3.79 (m, NCH_2CH_2, 6H), 3.73 (s, NCH_3, 3H), 3.72 (s, N(CH_3)$_2$, 6H), 3.43-3.26 (m, NCH_2CH_2, THF, 8H), 1.58 (m, THF), 0.27 (s, NTMS, 18H). ^{13}C NMR(THF-d_8) δ 71.50 (t, THF, $^1J_{CH}$ = 138), 64.10 (t, NCH_2CH_2N, $^1J_{CH}$ = 138), 56.79 (t, NCH_2CH_2N, $^1J_{CH}$ = 140), 55.50 (q, NCH_3, $^1J_{CH}$ = 136), 54.26 (t, NCH_2CH_2N, $^1J_{CH}$ = 140), 53.09 (t, NCH_2CH_2N, $^1J_{CH}$ = 140), 46.15 (q, N(CH_3)$_2$, $^1J_{CH}$ = 141), 27.82 (t, THF, $^1J_{CH}$ = 127), 2.73 (q, NTMS, $^1J_{CH}$ = 119). ^{19}F NMR(C_6D_6) δ -77.3 (s, CF_3SO_3). Anal. Calcd. for $C_{18}H_{43}F_3Si_2N_6MoO_{3.5}S$: C, 33.74; H, 6.76; N, 13.12. Found: C, 33.61; H, 6.83; N, 12.93

7-$^{15}N_2$. This complex was synthesized in an analogous manner to **7** except **6-$^{15}N_2$** was used. ^{15}N NMR(THF-d_8) δ 374.81 (d, $^1J_{NN}$ = 12), 157.15 (d, $^1J_{NN}$ = 12).

{[N($CH_2CH_2NSiMe_3$)$_2$($CH_2CH_2NMe_2$)]MoN_2TMS}$^+$OTf (8). Having isolated **7** from the reaction mixture, pentane was added to the mother liquor which was then cooled to -20 °C. The red solid obtained was subjected to a second crystallization from THF/pentane to give the product as a pink/red solid. ^1H NMR(THF-d_8) δ 4.17 (m, 2H, NCH_2CH_2N), 3.93 (m, 2H, NCH_2CH_2N), 3.35 (m, 2H, NCH_2CH_2N), 3.24 (m, 4H, NCH_2CH_2N), 2.96 (m, 2H, NCH_2CH_2N), 2.76 (s, 6H, N(CH_3)$_2$), 0.34 (s, 27H, NTMS). $^{13}C\{^1H\}$ NMR(THF-d_8) δ 61.42 (NCH_2CH_2N), 54.79 (NCH_2CH_2N), 54.40 (NCH_2CH_2N),

51.38 (NCH_2CH_2N), 48.26 ($N(CH_3)_2$), 2.99 (NTMS), 2.57 (NTMS). IR(Nujol) cm^{-1} 1724 (N=N). Anal. Calcd. for $C_{18}H_{45}F_3Si_3N_6MoO_3S$: C, 32.62; H, 6.84; N, 12.68. Found: C, 32.59; H, 6.93; N, 12.56.

8-$^{15}N_2$. This complex was synthesized in an analogous manner to **8** except **6-$^{15}N_2$** was used. IR(Nujol) cm^{-1} 1668 (N=N). ^{15}N NMR(THF-d_8) δ 361.50 (d, $^1J_{NN}$ = 13), 244.34 (d, $^1J_{NN}$ = 13).

{[N($CH_2CH_2NSiMe_3$)$_2$($CH_2CH_2NMe_2$)]$MoN_2TMS(CH_3)$ (9). {[$N(CH_2CH_2NSiMe_3)_2(CH_2CH_2NMe_2)$]$MoN_2TMS$}$^+$OTf (200 mg, 0.302 mmol) was dissolved in 5 mL of diethyl ether and cooled to -20 °C. 3.14 M MeMgCl (96 μL) was added dropwise to the stirred solution. After 20 min, the solvent was removed in vacuo and the residue extracted with pentane. Following filtration through Celite, the pentane was removed in vacuo to give the product as an orange/red solid; yield 153 mg (96%). ^1H NMR(C_6D_6) δ 3.54 (t, 1H, CH_2), 3.49 (t, 1H, CH_2), 3.35 (t, 1H, CH_2), 3.31 (t, 1H, CH_2), 2.97 (t, 2H, CH_2), 2.43 (t, 4H, CH_2), 2.03 (t, 2H, CH_2), 1.90 (s, 6H, NCH_3), 0.74 (s, 3H, $MoCH_3$), 0.53 (s, 18H, NTMS), 0.50 (s, 9H, NTMS). ^{13}C NMR(C_6D_6) δ 53.84 (t, NCH_2CH_2N), 52.86 (t, J_{CH} = 138, NCH_2CH_2N), 52.08 (t, J_{CH} = 134, NCH_2CH_2N), 51.65 (t, J_{CH} = 138, NCH_2CH_2N), 45.93 (q, J_{CH} = 135, CH_3NNCH_3), 23.92 (q, J_{CH} = 121, $MoCH_3$), 3.90 (q, J_{CH} = 118, NTMS), 3.56 (q, J_{CH} = 118, NTMS). IR(Nujol) cm^{-1} 1640 (N=N). Anal. Calcd. for $C_{18}H_{48}Si_3N_6Mo$: C, 40.88; H, 9.15; N, 15.89. Found: C, 40.72; H, 8.97; N, 15.55.

9-$^{15}N_2$. This complex was synthesized in an analogous manner to **9** except **8-$^{15}N_2$** was used. ^{15}N NMR(C_6D_6) δ 374.62 (d, $^1J_{NN}$ = 15), 239.46 (d, $^1J_{NN}$ = 15). IR(Nujol) cm^{-1} 1577 (N=N).

{[N($CH_2CH_2NSiMe_3$)$_2$($CH_2CH_2NCH_3$)]$Mo(CH_3)N_2(CH_3)_2$} (10). {[$N(CH_2CH_2NSiMe_3)_2(CH_2CH_2NCH_3)$]$MoN_2(CH_3)_2$}$^+$$OTf^-(THF)_{0.5}$ (178 mg, 0.294 mmol) was dissolved in 7 mL THF and cooled to -20 °C. 98 μL (1.05 eqs) of 3.14 M MeMgCl in THF was diluted to 3 mL with THF and cooled to -20 °C. Upon addition of MeMgCl to the stirred solution of {[$N(CH_2CH_2NSiMe_3)_2(CH_2CH_2NCH_3)$]$MoN_2(CH_3)_2$}$^+$$OTf^-(THF)_{0.5}$, the color

immediately changed from orange to blood-red. After 20 min the solvent was removed in vacuo and the residue extracted with pentane. Following filtration through Celite, the pentane was removed in vacuo to give the product as a red film; yield 125 mg (90%). ^{1}H NMR(C_6D_6) δ 3.79 - 3.72 (m, 1H, C*H*$_2$), 3.66 - 3.58 (m, 2H, CH_2), 3.56-3.52 (m, 1H, CH_2), 3.51 (s, 3H, NCH_3), 3.30 - 3.24 (m., 1H, CH_2), 3.02 - 2.95 (m, 1H, CH_2), 2.91 - 2.89 (m, 2H, CH_2), 2.84 (s, 6H, $N(CH_3)_2$), 2.61 - 2.55 (m, 1H, CH_2), 2.52 - 2.46 (m, 1H, CH_2), 2.38 - 2.33 (m, 1H, CH_2), 2.20 - 2.14 (m, 1H, CH_2), 0.38 (s, 9H, NTMS), 0.27 (s, 9H, NTMS), 0.18 (s, 3H, $MoCH_3$). ^{13}C NMR(C_6D_6) δ 67.19 (t, CH_2, J_{CH} = 129), 66.21 (t, CH_2, J_{CH} = 133), 64.76 (t, CH_2, J_{CH} = 136), 60.91 (t, CH_2, J_{CH} = 136), 56.29 (t, CH_2, J_{CH} = 131), 54.00 (q, NCH_3, J_{CH} = 136), 52.94 (t, CH_2, J_{CH} = 131), 44.30 (q, $N(CH_3)_2$, J_{CH} = 136), 17.79 (q, $MoCH_3$, J_{CH} = 124), 3.01 (q, NTMS, J_{CH} = 118), 2.54 (q, NTMS, J_{CH} = 118). Due to the thermal instability of this compound a sample for elemental analysis was not obtained.

10-$^{15}N_2$. This complex was synthesized in an analogous manner to **10**. ^{15}N NMR(THF-*d*$_8$) δ 354.85 (d, $^1J_{NN}$ = 12), 141.97 (d, $^1J_{NN}$ = 12).

[N(CH$_2$CH$_2$NSiMe$_3$)$_2$(CH$_2$CH$_2$NCH$_3$)]MoN (11). {[$N(CH_2CH_2NSiMe_3)_2(CH_2CH_2NCH_3)$]$Mo(CH_3)N_2(CH_3)_2$} (115 mg, 0.24 mmol) was dissolved in 1.5 mL of C_6D_6 and placed in a glass bomb along with a stirring bar. The bomb was sealed, removed from the dry box and the contents heated to 84 °C for 15 h. The volatiles were vacuum-transferred into an NMR tube which was then sealed. The bomb was returned to the dry box and the residue extracted with pentane and filtered. Following filtration the volume was reduced in vacuo and the solution chilled to -20 °C to give the product as yellow needles; yield 30 mg (30%). ^{1}H NMR(C_6D_6) δ 4.08 (s, 3H, NCH_3), 3.25 (t, 4H, NCH_2CH_2N), 2.78 (t, 2H, NCH_2CH_2N), 2.20-2.00 (m, 6H, NCH_2CH_2N), 0.59 (s, 18H, NTMS). ^{13}C NMR(C_6D_6) δ 60.38 (q, NCH_3), 59.73 (t, NCH_2CH_2N), 52.77 (t, NCH_2CH_2N), 51.17 (t, NCH_2CH_2N), 49.81 (t, NCH_2CH_2N), 3.18 (q, NTMS). IR(Nujol) cm^{-1} 1002 (Mo-N). Anal. Calcd. for $C_{13}H_{33}Si_2N_5Mo$: C, 37.94; H, 8.08; N, 17.02. Found: C, 37.96; H, 7.51; N, 16.69

References begin on page 65

11-$^{15}N_2$. This complex was synthesized in an analogous manner to **11**. ^{15}N NMR(C_6D_6) δ 866.08 (s). IR(Nujol) cm^{-1} 977 (Mo-N).

Thermolysis of 10 in THF-d_8; identification of methane and dimethylamine. {[$N(CH_2CH_2NSiMe_3)_2(CH_2CH_2NCH_3)$]$Mo(CH_3)N_2(CH_3)_2$} (38 mg, 0.08 mmol) was dissolved in 0.5 mL of THF-d_8 and placed in a teflon stoppered NMR tube. Cyclohexane (4.4 μL, 0.04 mmol) was added as an internal standard and the tube was sealed. The solution was heated at 76 °C for 12 h. ^1H NMR(THF-d_8) δ 3.97 (s, 3H, NMe), 3.56 (m, 4H, NCH_2CH_2N), 3.29 (t, 2H, NCH_2CH_2N), 3.26 (d, unassigned), 2.81 (t, 2H, NCH_2CH_2N), 2.65 (m, 4H, NCH_2CH_2N), 2.42 (s, unassigned), 2.31 (d, $(CH_3)_2NH$), 1.44 (s, cyclohexane), 0.32 (s, unassigned), 0.29 (s, 18H, NTMS), 0.20 (s, unassigned), 0.19 (s, CH_4), 0.13 (s, unassigned), 0.09 (s, unassigned), 0.07 (s, unassigned), 0.06 (s, unassigned), 0.01 (s, unassigned). ^{13}C NMR(THF-d_8) δ 60.3 (NCH_3), 60.1 (NCH_2CH_2N), 58.6 (unassigned), 56.2 (unassigned), 55.6 (unassigned), 55.5 (unassigned), 55.3 (unassigned), 53.7 (unassigned), 53.3 (NCH_2CH_2N), 52.3 (unassigned), 51.5 (NCH_2CH_2N), 50.4 (NCH_2CH_2N), 49.5 (unassigned), 44.7 (unassigned), 44.2 (unassigned), 39.3 ($(CH_3)_2NH$), 38.2 (unassigned), 27.8 (cyclohexane), 3.1 (unassigned), 2.73 (TMS), 2.5 (unassigned), 2.0 (unassigned), 1.3 (unassigned), -1.2 (CH_4).

[N_3N]Mo≡N (12). [N_3N]MoCl (106 mg, 0.22 mmol) was dissolved in 10 mL toluene and placed in a bomb. $TMSN_3$ (120 μL, 0.90 mmol) was added by syringe and the bomb was sealed. The solution was heated at 90 °C for 24 h during which time the color of the reaction mixture changed to brown/yellow. The solvent was removed and the residue was extracted into pentane and filtered. The filtrate was reduced in volume and cooled to -30 °C to give the product as a yellow crystalline compound; yield 89 mg (88%). ^1H NMR(C_6D_6) δ 3.23 (t, CH_2), 2.14 (t, CH_2), 0.56 (s, $SiMe_3$). $^{13}C\{^1H\}$ NMR(C_6D_6) δ 52.2 (CH_2), 51.6 (CH_2), 3.1 ($SiMe_3$); IR (Nujol) cm^{-1} 1001 (Mo-N). Anal. Calcd for $C_{15}H_{39}N_5Si_3Mo$: C, 38.36; H, 8.37; N, 14.91. Found: C, 37.99; H, 8.17; N, 14.65.

{[N_3N]Mo=NMe}OTf (13). [N_3N]Mo≡N (104 mg, 0.22 mmol) was dissolved in 3 mL toluene and MeOTf (30 μL, 0.27 mmol) was added by syringe. The reaction mixture

immediately deepened in color and a yellow solid precipitated. After 1 h the solvent was removed in vacuo and the resulting solid was dissolved in the minimum volume of THF. The solution was cooled to -30 °C to give the product as yellow needles; yield 129 mg (93%). ^{1}H NMR (CD_2Cl_2) δ 4.45 (s, 3, NCH_3), 4.00 (t, 6, CH_2), 3.24 (t, 6, CH_2), 0.30 (s, 27, $SiMe_3$). $^{13}C\{^1H\}$ NMR (CD_2Cl_2) δ 57.0 (NCH_3), 56.2 (CH_2), 54.5 (CH_2), 3.2 (TMS). Anal. Calcd for $C_{17}H_{42}N_5Si_3F_3SO_3Mo$: C, 32.22; H, 6.68; N, 11.05. Found: C, 32.07; H, 6.61; N, 11.17.

{[N_3N]Mo=NSiMe_3}OTf (14). [N_3N]Mo≡N (75 mg, 0.16 mmol) was dissolved in 3 mL toluene and TMSOTf (40 μL, 0.21 mmol) was added by syringe. The reaction mixture immediately deepened in color and a yellow solid precipitated. After 2 h the solvent was removed in vacuo and the resulting solid was dissolved in the minimum volume of THF. The solution was cooled to -30 °C to give the product as yellow needles; yield 92 mg (83%). ^{1}H NMR(CD_2Cl_2) δ 3.85 (t, CH_2), 3.11 (t, CH_2), 0.58 (s, 9, $SiMe_3$), 0.33 (s, 27, $SiMe_3$). $^{13}C\{^1H\}$ NMR (CD_2Cl_2) δ 58.2 (CH_2), 57.1 (CH_2), 3.9 ($SiMe_3$), 2.4 ($SiMe_3$). Anal. Calcd for $C_{19}H_{48}N_5Si_4F_3SO_3Mo$: C, 32.98; H, 6.99; N, 10.12. Found: C, 32.84; H, 6.47; N, 9.58.

REFERENCES

(1) Bazhenova, T. A.; Shilov, A. E. *Coord. Chem. Rev.* **1995**, *144*, 69.

(2) Eady, R. R.; Leigh, G. J. *J. Chem. Soc., Dalton Trans.* **1994**, 2739.

(3) Eady, R. R. *Chem. Rev.* **1996**, *96*, 3013.

(4) Chan, M. K.; Kim, J. S.; Rees, D. C. *Science* **1993**, *260*, 792.

(5) Allen, A. D.; Senoff, C. V. *J. Chem. Soc., Chem. Commun.* **1965**, 621.

(6) Hidai, M.; Mizobe, Y. *Chem. Rev.* **1995**, *95*, 1115.

(7) Chatt, J.; Dilworth, J. R.; Richards, R. L. *Chem. Rev.* **1978**, *78*, 589.

(8) Leigh, G. J. *Acc. Chem. Res.* **1992**, *25*, 177.

(9) Hidai, M.; Ishii, Y. *Bull. Chem. Soc. Jpn.* **1996**, *69*, 819.

(10) Schrock, R. R.; Glassman, T. E.; Vale, M. G. *J. Am. Chem. Soc.* **1991**, *113*, 725.

(11) Schrock, R. R.; Glassman, T. E.; Vale, M. G.; Kol, M. *J. Am. Chem. Soc.* **1993**, *115*, 1760.

(12) Vale, M. G.; Schrock, R. R. *Inorg. Chem.* **1993**, *32*, 2767.

(13) Laplaza, C. E.; Cummins, C. C. *Science* **1995**, *268*, 861.

(14) Laplaza, C. E.; Johnson, M. J. A.; Peters, J. C.; Odom, A. L.; Kim, E.; Cummins, C. C.; George, G. N.; Pickering, I. J. *J. Am. Chem. Soc.* **1996**, *118*, 8623.

(15) Fryzuk, M. D.; Love, J. B.; Rettig, S. J.; Young, V. G. *Science* **1997**, *275*, 1445.

(16) Verkade, J. G. *Acc. Chem. Res.* **1993**, *26*, 483.

(17) Schrock, R. R. *Acc. Chem. Res.* **1997**, *30*, 9.

(18) Cummins, C. C.; Schrock, R. R.; Davis, W. M. *Angew. Chem.* **1993**, *115*, 758.

(19) Mösch-Zanetti, N. C.; Schrock, R. R.; Davis, W. M.; Wanninger, K.; Seidel, S. W.; O'Donoghue, M. B. *J. Am. Chem. Soc.* **1997**, *119*, 11037.

(20) Schrock, R. R.; Seidel, S. W.; Mösch-Zanetti, N. C.; Dobbs, D. A.; Shih, K. -Y.; Davis, W. M. *Organometallics* **1997**, *16*, 5195.

(21) Schrock, R. R.; Seidel, S. W.; Mösch-Zanetti, N. C.; Shih, K. -Y.; O'Donoghue, M. B.; Davis, W. M.; Reiff, W. M. *J. Am. Chem. Soc.* **1997**, *119*, 11876.

(22) Kol, M.; Schrock, R. R.; Kempe, R.; Davis, W. M. *J. Am. Chem. Soc.* **1994**, *116*, 4382.

(23) Neuner, B.; Schrock, R. R. *Organometallics* **1996**, *15*, 5.

(24) Shih, K. -Y.; Schrock, R. R.; Kempe, R. *J. Am. Chem. Soc.* **1994**, *116*, 8804.

(25) Mason, J. *Chem. Rev.* **1981**, *81*, 205.

(26) K. -Y. Shih, unpublished observations.

(27) Wilkinson, P. G.; Houk, N. B. *J. Chem. Phys.* **1956**, *24*, 528.

(28) Hammer, R.; Klein, H. -F.; Schubert, U.; Frank, A.; Huttner, G. *Angew. Chem. Int. Ed. Engl.* **1976**, *15*, 612.

(29) D. A. Dobbs, unpublished observations.

(30) Seidel, S. W., Ph.D. Thesis, MIT, 1998.

(31) O'Connor, C. J. *Prog. Inorg. Chem.* **1982**, *29*, 203.

(32) Chatt, J.; Dilworth, J. R.; Dahlstrom, P. L.; Zubieta, J. *J. Chem. Soc., Chem. Comm.* **1980**, 786.

(33) Hidai, M.; Kodama, T.; Sato, M.; Harakawa, M.; Uchida, Y. *Inorg. Chem.* **1976**, *15*, 2694.

(34) Hidai, M.; Mizobe, Y.; Sato, M.; Kodama, T.; Uchida, Y. *J. Am. Chem. Soc.* **1978**, *100*, 5740.

(35) Oshita, H.; Mizobe, Y.; Hidai, M. *Organometallics* **1992**, *11*, 4116.

(36) Seino, H.; Ishii, Y.; Sasagawa, T.; Hidai, M. *J. Am. Chem. Soc.* **1995**, *117*, 12181.

(37) Haymore , B. L.; Hughes, M.; Mason, J.; Richards, R. L. *J. Chem. Soc., Dalton. Trans.* **1988**, 2935.

(38) Plass, W.; Verkade, J. G. *J. Am. Chem. Soc.* **1992**, *114*, 2275.

(39) Nugent, W. A.; Mayer, J. M. *Metal-Ligand Multiple Bonds*; Wiley: New York, 1988.

(40) G. E. Greco, unpublished observations.

(41) Fickes, M. G.; Davis, W. M.; Cummins, C. C. *J. Am. Chem. Soc.* **1995**, *117*, 6384.

(42) Proulx, G.; Bergman, R. G. *J. Am. Chem. Soc.* **1995**, *117*, 6382.

(43) Shih, K. -Y.; Totland, K.; Seidel, S. W.; Schrock, R. R. *J. Am. Chem. Soc.* **1994**, *116*, 12103.

(44) Pangborn, A. B.; Giardello, M. A.; Grubbs, R. H.; Rosen, R. K.; Timmers, F. J. *Organometallics* **1996**, *15*, 1518.

(45) Rosenberger, C.; Schrock, R. R.; Davis, W. M. *Inorg. Chem.* **1997**, *36*, 123.

CHAPTER 2

Heterometallic Dinitrogen Complexes Containing the $\{[N_3N]Mo(N_2)\}^-$ Ligand

A portion of the material covered in this chapter has appeared in print:

O'Donoghue, M. B., Zanetti, N. C., Davis, W. M., Schrock, R. R. *J. Am. Chem. Soc.* **1997**, *119*, 2753.

INTRODUCTION

Historically, transition metal dinitrogen complexes can be divided into two broad categories namely monometallic and bimetallic complexes, and conceptually it is possible to reduce dinitrogen to ammonia in either type of system. Numerous examples of monometallic[1,2] and homobimetallic[3] dinitrogen complexes have been described in the literature, yet examples of heterometallic dinitrogen complexes are comparatively rare. In fact, only four such complexes have been structurally characterized, namely dinuclear $[(PMe_2Ph)_4ClRe(N_2)MoCl_4(OMe)]$,[4] $[WI(PMe_2Ph)_3(py)(N_2)ZrCp_2Cl]$[5] and $[Cp^*Me_3Mo(N_2)WCp'Me_3]$,[6] and trinuclear $[MoCl_4\{(N_2)ReCl(PMe_2Ph)_4\}_2]$.[7]

The paucity of heterometallic dinitrogen complexes prompted us to explore the synthesis of such complexes and the results of our efforts are detailed in this chapter and are summarized in Scheme 2.1. Recall that $\{[N_3N]Mo\text{-}(N{=}N)\}_2Mg(THF)_2$ is isolated in high yield from the reduction of $[N_3N]MoCl$ under dinitrogen (Chapter 1). While initial efforts focused on the derivatization of dinitrogen at a single metal center, we realized that the $\{[N_3N]Mo\text{-}(N{=}N)\}^-$ fragment might be employed as a ligand in the synthesis of heterometallic dinitrogen complexes. In view of the crystal structure of nitrogenase[8] which confirms the presence of both iron and molybdenum in the active site, the synthesis of an iron/molybdenum dinitrogen complex was set as the initial goal in order to demonstrate how dinitrogen could be bound between these biologically relevant metals. The syntheses and structural characterization of iron/molybdenum, vanadium/molybdenum and zirconium/molybdenum dinitrogen complexes containing the $\{[N_3N]Mo(N_2)\}^-$ ligand are presented. As several of the resulting complexes are paramagnetic ^1H NMR spectroscopy has been of limited use as a method of characterization. X-ray crystallography has been used extensively and three structural studies are reported including that of $\{[N_3N]Mo\text{-}N{=}N\}_3Fe$, the first example of a structurally characterized iron/molybdenum dinitrogen complex. The oxidation state of iron in this complex and in $\{[N_3N]Mo\text{-}N{=}N\}_2Fe(DMPE)$ has been established by Mössbauer spectroscopy.

References begin on page 102

Scheme 2.1. Synthesis of heterometallic dinitrogen complexes.

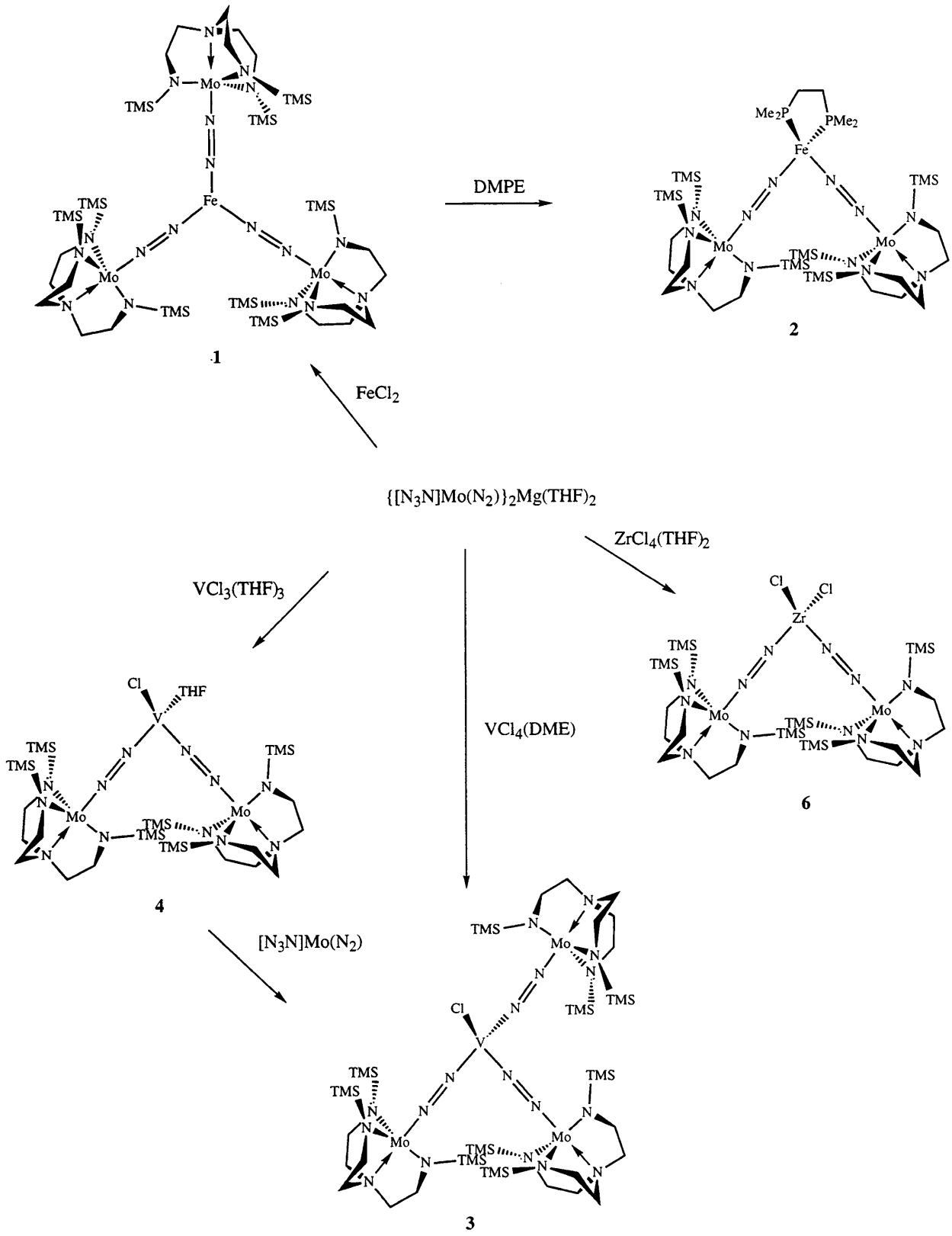

RESULTS AND DISCUSSION

Iron/Molybdenum Dinitrogen Complexes

Addition of $FeCl_2$ to a 10:2:1 Et_2O/THF/toluene solution of $\{[N_3N]Mo(N_2)\}_2Mg(THF)_2$ results in a darkening of the solution over the course of 15 min. $\{[N_3N]Mo(N_2)\}_3Fe$ (**1**) can be isolated in 38% yield from the pentane extract of the crude reaction product as plum-colored, paramagnetic crystals. Since a black magnetic solid, presumed to be iron, is formed during the course of the reaction and is observed clinging to the stir bar, the ideal stoichiometry for the reaction would be that shown in equation 1. The ^1H NMR spectrum of **1** in C_6D_6 exhibits three broad, shifted resonances at 9.25, -9.71 and -64.0 ppm consistent with a species in which the $[N_3N]Mo$ portion of the molecule is C_3-symmetric but the spectrum provides no information as to the molecular structure of **1**. An IR spectrum of **1** in Nujol shows primarily an absorption at 1703 cm^{-1}, although weaker absorptions are present between 1703 and 1600 cm^{-1} suggesting that dinitrogen is present and acting as a diazenido (2-) ligand. The UV-visible spectrum of **1** in pentane has an intense absorption at 516 nm (ε = 22,800 M^{-1} cm^{-1}) that shifts to 476 nm upon addition of THF (see below). Satisfactory elemental analyses of **1** have not been obtained due to the presence of trace amounts of $[N_3N]Mo(N_2)$ in the samples.

$$\{[N_3N]Mo\text{-}N{=}N\}_2Mg(THF)_2 + FeCl_2 \xrightarrow[-20\ ^\circ C\ -\ r.t.]{Et_2O/THF/toluene} \underset{\mathbf{1}}{2/3\ \{[N_3N]Mo\text{-}N{=}N\}_3Fe} + MgCl_2 + 1/3\ Fe^\circ \quad (1)$$

The molecular structure of **1** was elucidated by an X-ray crystallographic study. Crystals of **1** suitable for X-ray analysis were grown from saturated pentane solutions at -20 °C; a quarter of a molecule of pentane was found in the unit cell. Crystallographic data and collection and refinement parameters are given in Table 2.1. A view of the molecular structure of **1** along with the atom-labeling scheme is shown in Figure 2.1, while pertinent bond lengths and bond angles are listed in Table 2.2. Table 2.3 summarizes selected metrical parameters for all of the

References begin on page 102

crystallographically-characterized complexes reported in this chapter. Although the structure is not of high quality it does shed light on the remarkable connectivity of **1** which is a rare example of a complex with iron in a trigonal planar environment. The $[N_3N]Mo(N_2)$ unit can be viewed as a ligand with the bulky TMS groups of the triamidoamine precluding the attainment of higher coordination numbers. The three Mo-N-N linkages are essentially linear as are two of the Fe-N-N linkages. However, one of the Mo-N-N-Fe linkages is significantly bent at the nitrogen bound to iron (Fe-N(2)-N(1) = 156(2)°). The deviation from linearity of Fe-N(2)-N(1) is perhaps a consequence of steric crowding created by the $[N_3N]^{3-}$ ligand. In previous work,[9] it has been found that the twisting of a given TMS group out of the N_{ax}-M-N_{eq} plane and the resulting decrease in the N_{ax}-M-N_{eq}-Si dihedral angle are useful measures of the degree of steric strain in the pocket of $[N_3N]$ complexes. In **1** the dihedral angle defined by N(14)-Mo(1)-N(13)-Si(13) is found to be 142.5°, indicative of considerable steric pressure arising from three $[N_3N]Mo(N_2)$ units lying in the trigonal plane. However, all other N_{ax}-M-N_{eq}-Si dihedral angles are close to 180°. In view of the relatively large errors we cannot say that distances within the $[N_3N]Mo(N_2)$ units are statistically different. Nevertheless, the N-N bond distances suggest reduction of the dinitrogen ligands in **1** compared with free dinitrogen (1.098 Å).[10]

Three coordinate iron complexes have been known for some time and can be grouped into three broad classes, namely, dimeric Fe(II) complexes such as $\{Fe[O\text{-}(2,4,6\text{-}^tBu_3C_6H_2)_2]\}_2$[11] and $\{Fe(NPh_2)_2\}_2$[12] which contain terminal and bridging alkoxy or amide ligands, monomeric Fe(II) complexes such as $Fe[N(SiMe_3)_2]_2(THF)$[12] and $\{Fe[N(SiMe_3)_2]_3\}^-$[13] and monomeric Fe(III) complexes of which only two other examples are known namely, $Fe(NRAr)_3$[14] (R = $C(CD_3)_2CH_3$, Ar = 3,5-$C_6H_3Me_2$) and $Fe[N(SiMe_3)_2]_3$.[15] **1** is unique among these complexes for several reasons. Firstly, crystallographically-characterized, heterometallic complexes containing bridging dinitrogen are rare and to our knowledge **1** is the only reported example of a structurally characterized iron-molybdenum dinitrogen complex, a type of species that perhaps is especially relevant in view of the structure of Fe/Mo nitrogenase in one resting state.[8]

References begin on page 102

Table 2.1. Crystallographic data, collection parameters and refinement parameters for $\{[N_3N]Mo\text{-}N{=}N\}_3Fe$ (**1**) and $\{[N_3N]Mo\text{-}N{=}N\}_2VCl(THF)$ (**4**).

	1	**4**
Empirical Formula	$C_{46.25}H_{118.5}FeMo_3N_{18}Si_9$	$C_{39}H_{98.50}ClMo_2N_{12}O_{2.25}Si_6V$
Formula Weight	1521.05	1218.61
Diffractometer	SMART/CCD	SMART/CCD
Crystal Dimensions (mm)	0.14 x 0.14 x 0.12	na
Crystal System	Triclinic	Monoclinic
Space Group	$P\bar{1}$	$P2_1/n$
a (Å)	10.4926(2)	14.16110(10)
b (Å)	14.3300(10)	21.61220(10)
c (Å)	26.8875(6)	21.1463(3)
α (°)	97.2850(10)	90
β (°)	93.2670(10)	98.6770(10)
γ (°)	90.163(2)	90
V (Å^3), Z	4001.93(12), 2	6397.81(11), 4
D_{calc} (Mg/m^3)	1.262	1.265
Absorption coefficient (mm^{-1})	0.811	0.723
F_{000}	1595	2570
Temperature (K)	188(2)	183(2)
Θ range for data collection (°)	1.53 to 20.00	1.39 to 23.29
Reflections collected	11831	25386
Unique Reflections	7337	9183
R	0.1345	0.0660
R_w	0.1896	0.1080
GoF	1.280	1.085

References begin on page 102

Table 2.2. Selected bond lengths and bond angles for $\{[N_3N]Mo(N_2)\}_3Fe$ (**1**).

Bond Lengths (Å)

Fe-N(2)	1.86(2)	Fe-N(4)	1.84(2)	Fe-N(6)	1.82(2)
Mo(1)-N(1)	1.86(2)	Mo(2)-N(3)	1.81(2)	Mo(3)-N(5)	1.82(2)
N(1)-N(2)	1.20(3)	N(3)-N(4)	1.25(2)	N(5)-N(6)	1.27(2)
Mo(1)-N(11)	1.97(2)	Mo(2)-N(23)	2.03(2)	Mo(3)-N(32)	2.00(2)
Mo(1)-N(14)	2.24(2)	Mo(2)-N(24)	2.26(2)	Mo(3)-N(34)	2.24(2)

Bond Angles (deg)

Mo(1)-N(1)-N(2)	174(2)	Mo(2)-N(3)-N(4)	175(2)
Mo(3)-N(5)-N(6)	179(2)	Fe-N(2)-N(1)	156(2)
Fe-N(4)-N(3)	175(2)	Fe-N(6)-N(5)	176(2)
Mo(1)-N(11)-Si(11)	127.4(12)	Mo(2)-N(23)-Si(23)	123.7(10)
N(2)-Fe-N(4)	114.0(9)	N(2)-Fe-N(6)	119.2(10)
N(4)-Fe-N(6)	126.8(9)		

Dihedral Angles (deg)[a]

N(14)-Mo(1)-N(11)-Si(11)	170.4	N(14)-Mo(1)-N(13)-Si(13)	142.5
N(14)-Mo(1)-N(12)-Si(12)	-164.7	N(24)-Mo(2)-N(23)-Si(23)	176.3
N(34)-Mo(3)-N(32)-Si(32)	-177.9		

[a]Obtained from a Chem-3D Drawing

References begin on page 102

Figure 2.1. A view of the structure of $\{[N_3N]Mo\text{-}N{=}N\}_3Fe$ (**1**) with the trigonal plane lying in the plane of the paper.

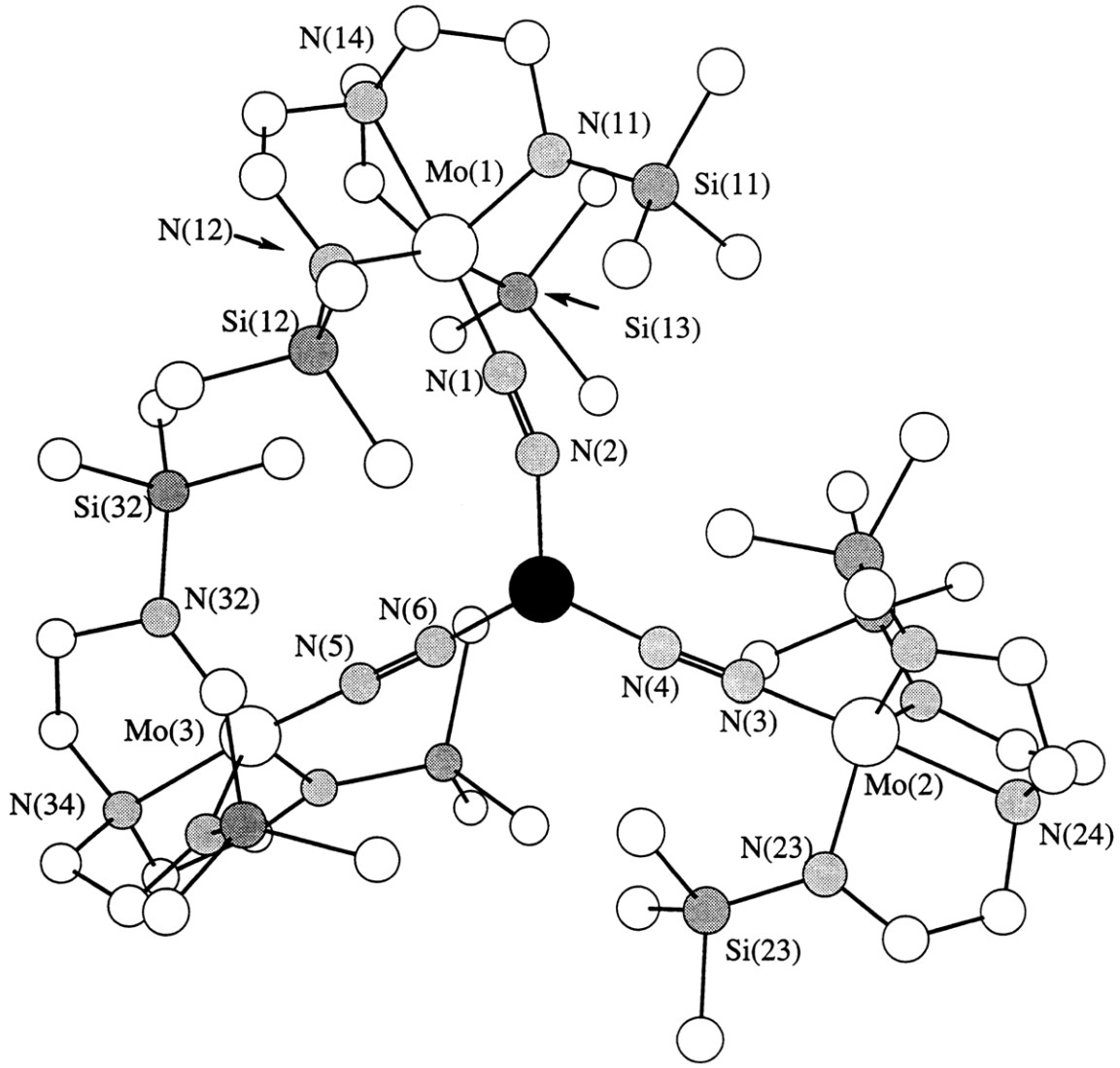

Secondly, the three ligands coordinated to iron are all derived from dinitrogen and finally, the dinitrogen-containing ligands can exist in both anionic and neutral forms (see Chapter 1).

In light of the extraordinary molecular geometry of **1**, magnetic susceptibility and Mössbauer studies were embarked upon with a view to establishing the spin state and oxidation state of iron in **1**, information that is not immediately apparent from the X-ray diffraction data.

Since the $[N_3N]Mo(N_2)$ ligand is stable as the terminal dinitrogen complex, $[N_3N]Mo(N_2)$ and the diazenido complex, $\{[N_3N]Mo(N_2)\}_2Mg(THF)_2$, **1** could be formulated, at the extremes, as an Fe(0) complex containing three neutral $[N_3N]Mo(N_2)$ ligands or as an Fe(III) complex containing three anionic $\{[N_3N]Mo\text{-}N{=}N\}^-$ ligands. Alternatively, **1** may exist as an Fe(II) complex with one neutral and two anionic ligands. The formulation of **1** as an Fe(0) complex can be ruled out on the basis of the N-N bond lengths. Although the errors are large, N-N bond lengths of 1.25(2) and 1.27(2) Å are more consistent with a diazenido complex. The significant bending of the Fe-N(2)-N(1) and the N(1)-N(2) bond length of 1.20(3) Å suggest that the three $[N_3N]Mo(N_2)$ ligands are inequivalent and so **1** might be viewed as an Fe(II) complex. However, magnetic susceptibility and Mössbauer studies unequivocally demonstrate that **1** is best formulated in the solid state as an Fe(III) complex (see below).

Table 2.3. Selected metrical parameters for heterometallic dinitrogen complexes.

Complex	N-N (Å)	Mo-N (Å)	M-N (Å)	N-M-N (deg)	L-M-L (deg)
Mo/Fe (**1**)	1.20(3)	1.86(2)	1.86(2)	119.2(10)	
	1.25(2)	1.81(2)	1.84(2)	114.0(9)	
	1.27(2)	1.82(2)	1.82(2)	126.8(9)	
Mo/V (**4**)	1.217(7)	1.827(6)	1.860(6)	119.8(3)	96.5(2)
	1.221(7)	1.836(6)	1.864(4)		
Mo/Zr (**6**)	1.249(8)	1.796(6)	1.974(6)	114.6(2)	107.14(9)
	1.245(8)	1.797(6)	1.978(6)		

SQUID[16] magnetic susceptibility data for solid **1** is plotted versus temperature in Figure 2.2 and can be fit to the Curie-Weiss law ($\chi = \mu^2/8(T-\theta)$) over the temperature range 5-300 K to yield $\mu = 6.02(3)\ \mu_B$, $\theta = 0.74(5)$ K. These data are unremarkable other than that the value for μ

References begin on page 102

is close to the spin-only value for a system containing five unpaired electrons (5.92 μ_B) and is consistent with the formulation of **1** as a high-spin Fe(III) complex.

Figure 2.2. Plot of χ_m (corrected for diamagnetism using Pascal's constants) versus T for $\{[N_3N]Mo\text{-}N{=}N\}_3Fe$, (**1**).

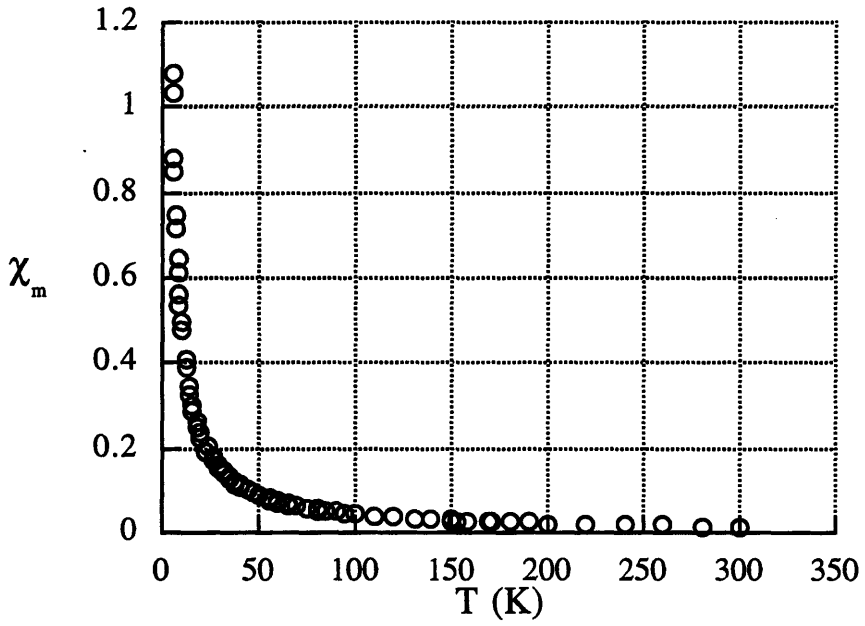

Further evidence confirming the identity of **1** as a high-spin Fe(III) complex was obtained from Mössbauer spectroscopic studies (carried out by Professor William Reiff). Figure 2.3 shows the Mössbauer spectrum of **1** obtained at 77 K. It consists of a quadrupole doublet with quadrupole splitting of 3.15 mm/sec and an isomer shift of 0.65 mm/sec relative to natural iron foil. The high energy peak is broadened, a common feature in high-spin Fe(III) complexes[17] which arises from paramagnetic relaxation phenomena.[18] The quadrupole splitting arises from the presence of an electric field gradient at the Mössbauer nucleus and the magnitude of the quadrupole splitting reflects the asymmetry of the electron density around the nucleus.[19] In **1**, the absence of axial ligands gives rise to an unusually large electric field gradient and hence the large quadrupole splitting. The magnitude of the isomer shift is reasonable for a ferric complex and is also

References begin on page 102

References begin on page 102

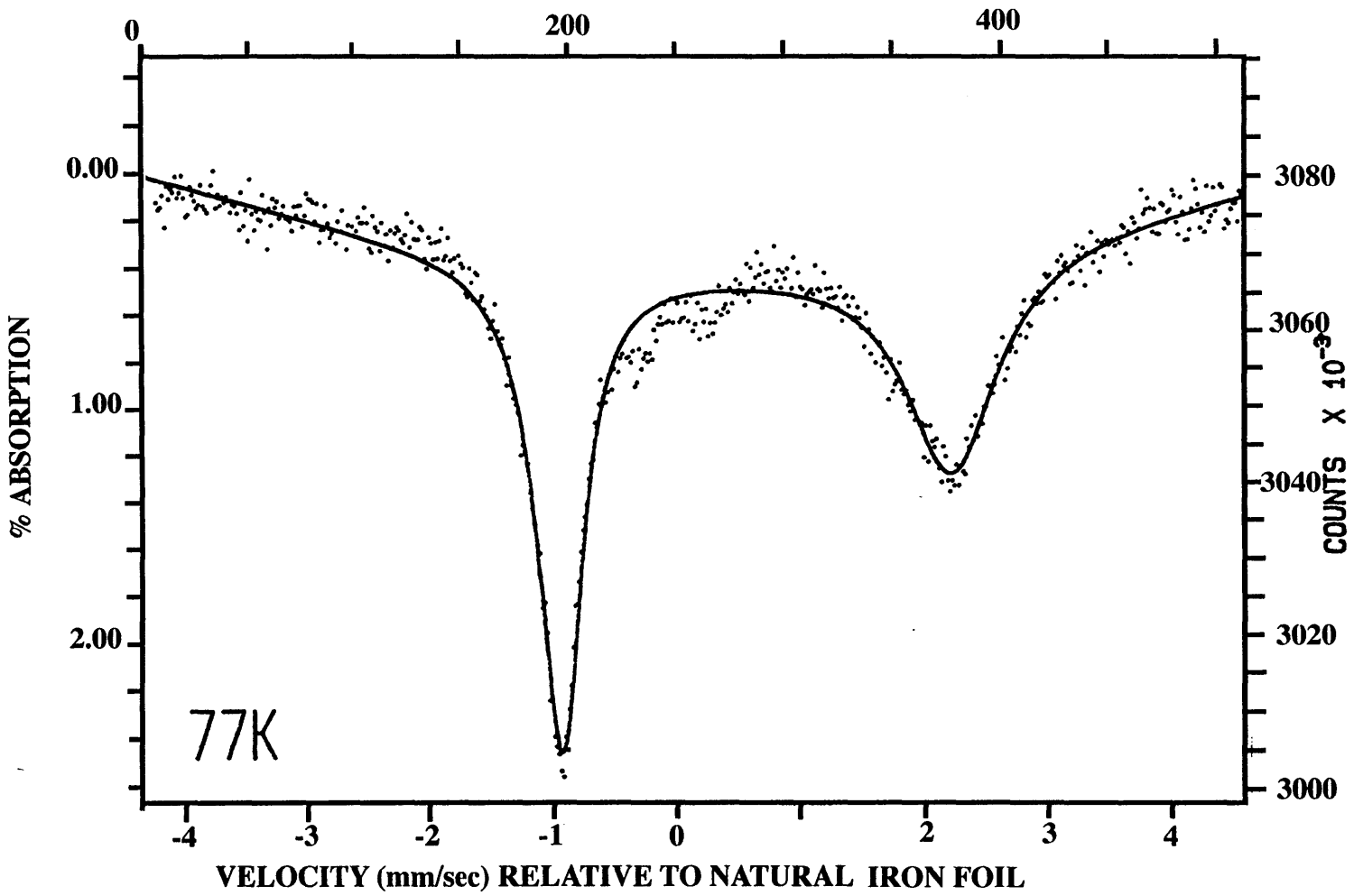

Figure 2.3. Mössbauer spectrum of $\{[N_3N]Mo\text{-}N{=}N\}_3Fe$ (**1**) at 77 K.

consistent with the low coordination number.[19] $Fe[N(SiMe_3)_2]_3$ is the only other example of an Fe(III) complex containing trigonal planar iron which has been studied in detail by X-ray crystallography,[15] magnetic susceptibility measurements[20] and Mössbauer spectroscopy.[17] Unlike **1**, resonances were not found in the ^1H NMR spectrum of $Fe[N(SiMe_3)_2]_3$, presumably due to the proximity of the TMS groups to the paramagnetic center.[21] The magnetic moment of $Fe[N(SiMe_3)_2]_3$ obtained between 98-298 K is 5.94 μ_B which like that of **1** is close to the spin-only moment for a system with five unpaired spins. Finally, the Mössbauer spectrum of $Fe[N(SiMe_3)_2]_3$ at 77 K is strikingly similar to that of **1**, consisting of an asymmetric quadrupole doublet with quadrupole splitting of 5.12 mm/sec. The Mössbauer spectral parameters of **1** and $Fe[N(SiMe_3)_2]_3$ allow a qualitative comparison of the bonding in these complexes to be made. σ donation by the ligands increases the total electron density at the nucleus and π acceptance by the ligands decreases shielding of the s electron density, both of which have the effect of decreasing the isomer shift. Since the $\{[N_3N]Mo\text{-}N{=}N\}^-$ ligand is expected to be a weak π acceptor, the smaller isomer shift of $Fe[N(SiMe_3)_2]_3$ (0.30 mm/sec) reflects the better σ donating ability of the $[N(SiMe_3)_2]^-$ ligand compared to the $\{[N_3N]Mo\text{-}N{=}N\}^-$ ligand. The larger quadrupole splitting in $Fe[N(SiMe_3)_2]_3$ suggests stronger Fe-N bonding in this complex compared with **1** but an examination of the available crystallographic data would appear to indicate the opposite bonding picture (Fe-N in $Fe[N(SiMe_3)_2]_3$ = 1.92 Å,[15] Fe-N in **1** ≈ 1.84 Å). However, the large errors associated with the bond lengths in **1** probably render such a comparison meaningless.

The reaction that produces **1** is relatively complex and is sensitive to a number of factors including temperature and solvent. For example, if the reaction is carried out at room temperature in THF the main product isolated is $[N_3N]Mo(N_2)$ suggesting that oxidation of $\{[N_3N]Mo(N_2)\}_2Mg(THF)_2$ occurs exclusively (equation 2). If THF is employed as the solvent and the reaction is conducted at low temperature, the major species produced is "$\{[N_3N]Mo\text{-}N{=}N\}_2Fe(THF)_2$" (see below) according to ^1H NMR spectroscopy.

References begin on page 102

$$\{[N_3N]Mo\text{-}N{=}N\}_2Mg(THF)_2 + FeCl_2 \xrightarrow[r.t.]{THF} 2\,[N_3N]Mo(N_2) + Fe^{\circ} + MgCl_2 \qquad (2)$$

Toluene and pentane solutions of **1** are an intense purple color whereas THF solutions are orange-brown in color. As noted previously, the UV-visible spectrum of **1** in pentane has an intense absorption at 516 nm (ε = 22,800 M^{-1} cm^{-1}) that shifts to 476 nm upon addition of THF. ^1H NMR spectroscopy was used to determine the nature of this color change. The lower half of Figure 2.4 shows a portion of the ^1H NMR spectrum of **1** in C_6D_6. The resonance at 9.25 ppm is assigned to the TMS groups of the TREN ligand and the resonance at -9.71 ppm is attributed to one set of the methylene protons of the ligand backbone. The relatively sharp resonance at -4.5 ppm is due to the presence of a small amount of $[N_3N]Mo(N_2)$ in the sample. Upon addition of 10 equivalents of THF-d_8 to the sample, a color change from purple to orange-brown is discernible and the upper spectrum in Figure 2.4 is obtained. It is seen that the resonance at 9.25 ppm has decreased significantly in intensity and a new resonance at 6.57 ppm has grown in. Furthermore, the resonance assigned to $[N_3N]Mo(N_2)$ has increased dramatically in intensity. This result suggests that coordination of THF to the iron center effects Fe-N bond homolysis thereby reducing Fe(III) to Fe(II) and induces the extrusion of an equivalent of $[N_3N]Mo(N_2)$ (as evidenced in the ^1H NMR spectrum by the increase in the intensity of the resonance at -4.5 ppm), yielding a tetrahedral Fe(II) complex tentatively formulated as $\{[N_3N]Mo(N_2)\}_2Fe(THF)_2$ (equation 3). This reaction is reversible and it has been shown by ^1H NMR spectroscopy that $\{[N_3N]Mo(N_2)\}_2Fe(THF)_2$ reacts with $[N_3N]Mo(N_2)$ to give free THF and **1**. Similar redox behavior has been found to occur in vanadium/molybdenum dinitrogen complexes (see below).

$$\{[N_3N]Mo\text{-}N{=}N\}_3Fe \underset{-\,THF}{\overset{+\,THF}{\rightleftharpoons}} \{[N_3N]Mo\text{-}N{=}N\}_2Fe(THF)_2 + [N_3N]Mo(N_2) \qquad (3)$$

References begin on page 102

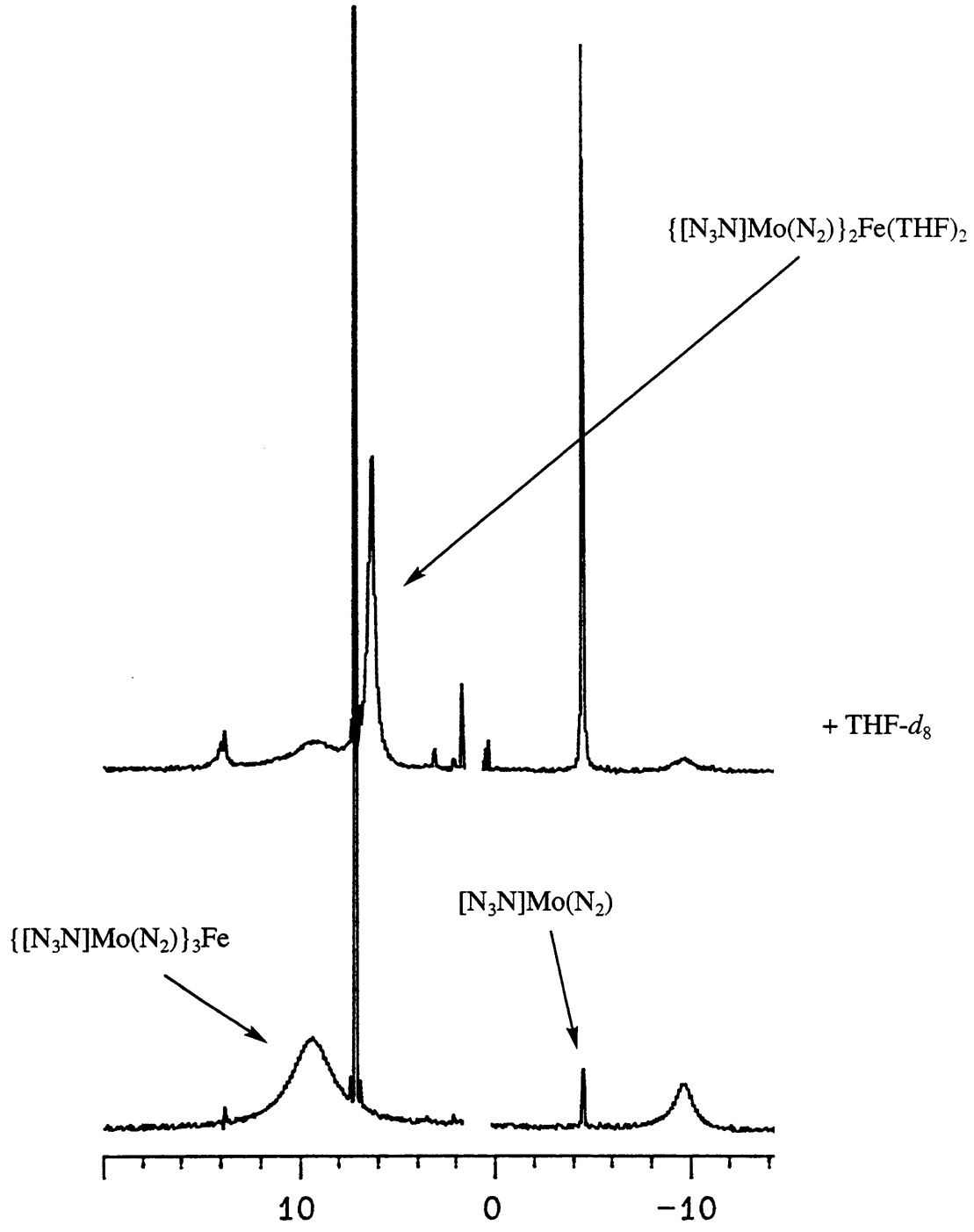

Figure 2.4. ^{1}H NMR spectrum of $\{[N_3N]Mo\text{-}N{=}N\}_3Fe$ (lower spectrum) and ^{1}H NMR spectrum of $\{[N_3N]Mo\text{-}N{=}N\}_3Fe$ after addition of 10 equivalents of THF-d_8 (upper spectrum).

References begin on page 102

Two plausible mechanisms for the formation of **1** are shown in Scheme 2.2. In the first, nucleophilic substitution and redox reactions occur at similar rates to generate $\{[N_3N]Mo(N_2)\}_2Fe(THF)_2$ and $[N_3N]Mo(N_2)$ in solution. $\{[N_3N]Mo(N_2)\}_2Fe(THF)_2$ then reacts with $[N_3N]Mo(N_2)$ to yield **1**. Alternatively, if the rate of nucleophilic substitution is faster than the rate by which $\{[N_3N]Mo(N_2)\}_2Mg(THF)_2$ is oxidized then "$\{([N_3N]Mo(N_2))_3Fe\}^-\{MgCl\}^+$" might be generated in situ and subsequently oxidized by $FeCl_2$ to give **1**. Interestingly, the related Fe(III) complex $Fe(NRAr)_3$ is synthesized by oxidation of the "ate" complex $(ArRN)Fe(\mu\text{-}NRAr)_2Li(OEt_2)$.[14] The observations that reaction of $\{[N_3N]Mo(N_2)\}_2Mg(THF)_2$ and $FeCl_2$ at room temperature yields $[N_3N]Mo(N_2)$ and that the species proposed to be $\{[N_3N]Mo(N_2)\}_2Fe(THF)_2$ reacts with $[N_3N]Mo(N_2)$ to give free THF and **1**, suggest that formation of **1** occurs by the first mechanism. Therefore, it appears that isolation of **1** is contingent on the facility of $\{[N_3N]Mo(N_2)\}^-$ to act as both a nucleophile and a reductant.

Attempts to find a more direct route to **1** have been unsuccessful. Addition of $FeCl_3$ to THF solutions of $\{[N_3N]Mo(N_2)\}_2Mg(THF)_2$ at -20 °C results in a vigorous reaction yielding complex product mixtures. Among the products identifiable by ^1H NMR spectroscopy are $[N_3N]MoCl$, $[N_3N]Mo(N_2)$ and $\{[N_3N]Mo(N_2)\}_2Fe(THF)_2$, along with **1** and unreacted $\{[N_3N]Mo(N_2)\}_2Mg(THF)_2$.

Efforts to isolate $\{[N_3N]Mo(N_2)\}_2Fe(THF)_2$ were unsuccessful presumably due to the lability of the THF ligands. Isolation of an Fe(II) complex was effected by replacement of the THF ligands with a chelating diphosphine, dimethylphosphinoethane (DMPE). Addition of DMPE to a toluene solution of **1** produces $\{[N_3N]Mo\text{-}N{=}N\}_2Fe(DMPE)$ (**2**) that can be isolated as black blocks from diethyl ether in moderate yield (43% based on the number of equivalents of $\{[N_3N]Mo(N_2)\}_2Mg(THF)_2$ used to generate **1**) (equation 4).

$$\{[N_3N]Mo\text{-}N{=}N\}_3Fe \xrightarrow[\text{toluene}]{\text{DMPE}} \underset{\mathbf{2}}{\{[N_3N]Mo\text{-}N{=}N\}_2Fe(DMPE)} + [N_3N]Mo(N_2) \qquad (4)$$

References begin on page 102

Scheme 2.2. Possible mechanisms for the formation of $\{[N_3N]Mo(N_2)\}_3Fe$ (**1**).

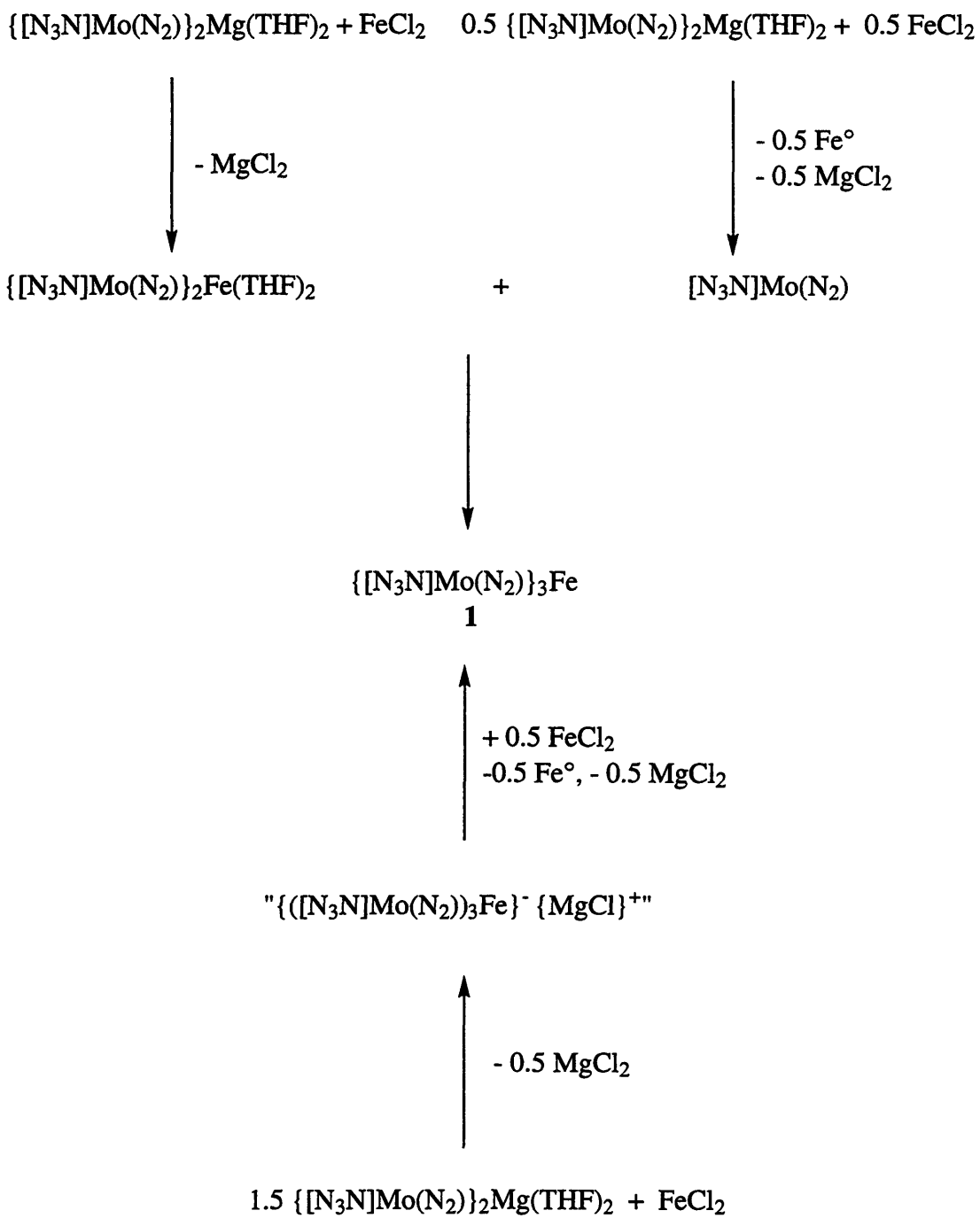

References begin on page 102

A preliminary X-ray study of **2** established the connectivity, showing it to be a tetrahedral iron complex but a disorder in the trimethylsilyl groups of the $[N_3N]^{3-}$ ligand prevented satisfactory refinement.[22] The ^1H NMR spectrum of **2** in C_6D_6 consists of five broad resonances between +40 ppm and -118 ppm. The $[N_3N]$Mo portion of **2** appears C_3-symmetric and two broad resonances at +37.00 ppm and -117.46 ppm are ascribed to the methyl and methylene protons of the DMPE ligand. Due to the proximity of the phosphorus nuclei to the paramagnetic iron center a resonance could not be located in the ^{31}P NMR spectrum of **2**. The IR spectrum of **2** has a strong, sharp band at 1706 cm^{-1} that is assigned to ν_{NN} and is consistent with the formulation of **2** as a diazenido species. The UV-visible spectrum of **2** has two intense absorptions at 360 nm (ε = 23,306 M^{-1} cm^{-1}) and 508 nm (ε = 13,997 M^{-1} cm^{-1}) that are unaffected by the addition of THF (in contrast to the behavior of **1**). **2** apparently decomposes rapidly in the solid state when exposed to high vacuum as evidenced by a color change from purple to dark brown. We speculate that loss of DMPE is the first step in this decomposition although no products of the reaction have been identified.

SQUID magnetic susceptibility studies have been carried out on solid **2** and the data can be fit to the Curie-Weiss law ($\chi = \mu^2/8(T-\theta)$) over the temperature range 50-300 K to yield μ = 5.08(3) μ_B, θ = 2.4(6) K, consistent with a system containing four unpaired electrons. A Mössbauer study of **2** was undertaken to unequivocally establish the oxidation state and spin state of iron. The Mössbauer spectrum of **2**, taken at 77 K, is shown in Figure 2.5. The appearance of a symmetric quadrupole doublet and the magnitude of the parameters associated with it (quadrupole splitting = 1.15 mm/sec and isomer shift = 0.67 mm/sec) are fully consistent with the formulation of **2** as a high-spin Fe(II) complex.[19]

In an attempt to improve the yield of **2**, $[DMPE]FeCl_2$ was reacted with $\{[N_3N]Mo(N_2)\}_2Mg(THF)_2$ in THF. Over the course of 12 h the color of the reaction mixture turned deep green and then purple as a mixture of **2** and $[N_3N]Mo(N_2)$ was formed. **2** could not be isolated in good yield by this method and this reaction illustrates the delicate balance required to favor metathesis over redox chemistry in these systems.

References begin on page 102

References begin on page 102

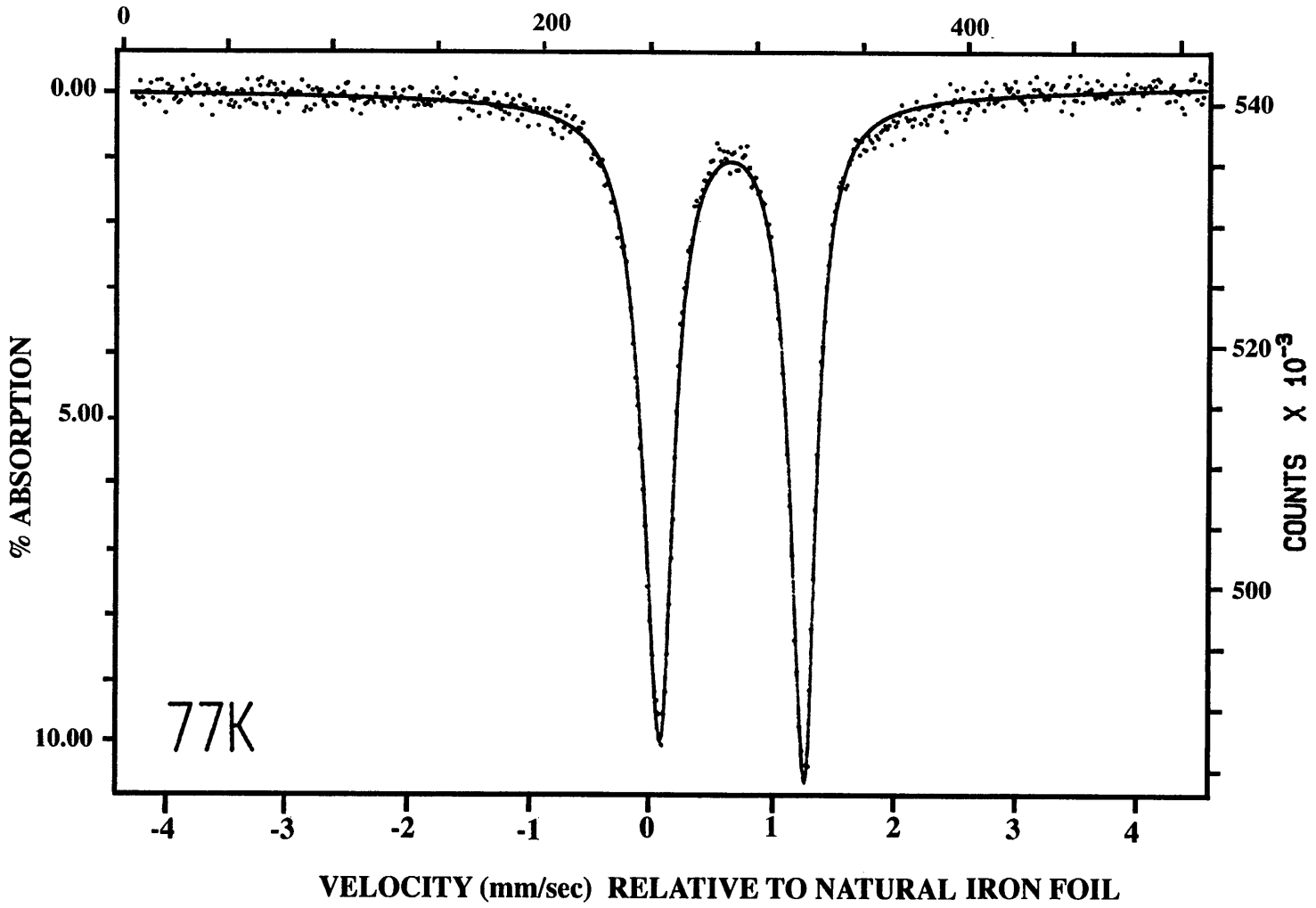

Figure 2.5. Mössbauer spectrum of $\{[N_3N]Mo\text{-}N{=}N\}_2Fe(DMPE)$ (**2**) at 77 K.

Vanadium/Molybdenum Dinitrogen Complexes

Spurred on by the successful isolation of iron/molybdenum dinitrogen complexes, a study of related vanadium complexes was initiated. Initial efforts focused on the reaction of $VCl_3(THF)_3$ with $\{[N_3N]Mo(N_2)\}_2Mg(THF)_2$ with a view to preparing a trigonally symmetric vanadium complex analogous to **1**. However, as discussed below, the chemistry is complicated by redox reactions but by drawing on the experience gained in the iron system it has been possible to isolate examples of V(III) and V(IV) heterometallic dinitrogen complexes.

VCl_4(DME) reacts with 1.5 equivalents of $\{[N_3N]Mo(N_2)\}_2Mg(THF)_2$ in THF to yield deep purple solutions. ^{1}H NMR spectra of the crude reaction mixture reveal the presence of two paramagnetic and one diamagnetic species as well as traces of $[N_3N]Mo(N_2)$, $[N_3N]MoH$ and $[bitN_3N]Mo$ (see Chapter 3). Paramagnetic $\{[N_3N]Mo(N_2)\}_3VCl$ (**3**) can be separated from the reaction mixture by crystallization from THF/pentane as black plates and is isolated in 42% yield. The actual yield of **3** is higher according to ^{1}H NMR spectra of the mother liquor but efforts to increase the isolated yield have been unsuccessful. The connectivity of **3** has been established by a single crystal diffraction study of low resolution (1.6 Å) which clearly shows three $[N_3N]Mo(N_2)$ ligands and one chloride ligand bound to vanadium.[22] The ^{1}H NMR spectrum of **3** consists of three relatively sharp resonances at 1.36 ($\Delta\nu_{1/2}$ = 14 Hz), 0.94 ($\Delta\nu_{1/2}$ = 6 Hz) and -0.55 ppm ($\Delta\nu_{1/2}$ = 14 Hz) with the resonance at 0.94 ppm being assigned to the TMS groups of the ligand. Complex **3** appears stable in solution and C_6D_6 solutions of **3** remain unchanged when stored under dinitrogen for a period of days (according to ^{1}H NMR spectroscopy). The IR spectrum of **3** in Nujol exhibits a broad N-N stretch at 1579 cm^{-1} and the UV-visible spectrum of **3** in pentane has an intense absorption at 540 nm (ε = 29,787 M^{-1} cm^{-1}). SQUID magnetic susceptibility measurements on solid **3** are in accord with its formulation as a d^1 V(IV) complex and the data is plotted in Figure 2.6. Fitting the data to the Curie law yields μ = 1.50(1) μ_B (R = 0.9998).

The second paramagnetic species that is present in the reaction mixture is characterized by broad, unassigned resonances at 6.00, 1.28 and -5.56 ppm. Although this complex has not been isolated, it is formulated as the V(III) complex $\{[N_3N]Mo(N_2)\}_2VCl(THF)$ (**4**) on the basis of

References begin on page 102

investigations of reactions between $VCl_3(THF)_3$ and $\{[N_3N]Mo(N_2)\}_2Mg(THF)_2$ (see below). The diamagnetic species appears to be the diazenido complex $[N_3N]Mo\text{-}N{=}N\text{-}TMS$ with a pair of triplets being observed at 3.38 and 2.10 ppm in addition to a singlet at 0.50 ppm.

Figure 2.6. Plot of χ_m (corrected for diamagnetism using Pascal's constants) versus T for $\{[N_3N]Mo\text{-}N{=}N\}_3VCl$, (**4**).

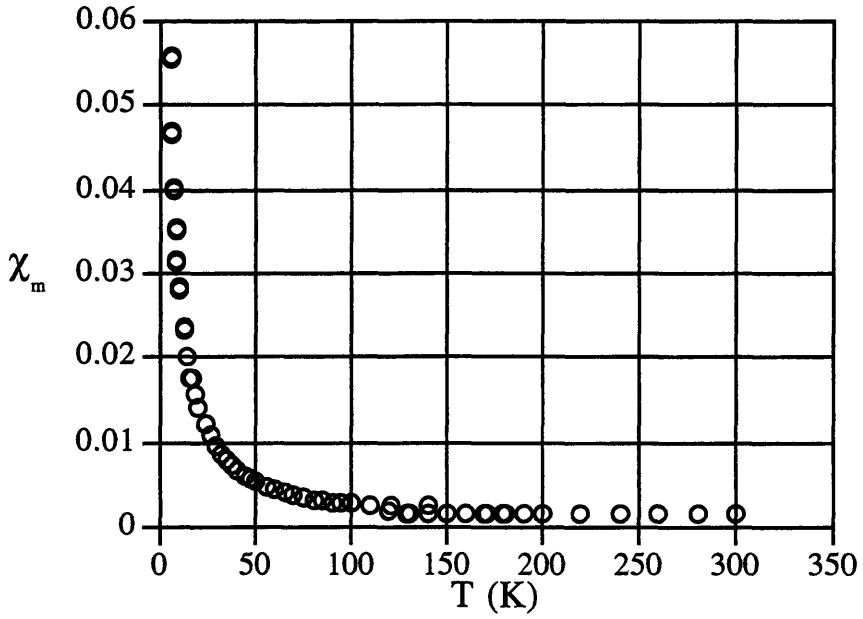

Reaction of $VCl_3(THF)_3$ with one equivalent of $\{[N_3N]Mo(N_2)\}_2Mg(THF)_2$ also yields deep purple solutions from which **3** can be isolated in 28% yield. The formation of **3** was unanticipated and suggests that a fraction of $VCl_3(THF)_3$ is being reduced during the course of the reaction although no reduced vanadium species has been isolated from the reaction mixture. Furthermore, ^1H NMR spectra of the crude reaction mixture are complex revealing the presence of **3** and **4** along with traces of $[N_3N]MoH$, $[bitN_3N]Mo$ and $[N_3N]Mo(N_2)$. Reaction of $VCl_3(THF)_3$ with 1.5 equivalents of $\{[N_3N]Mo(N_2)\}_2Mg(THF)_2$ does not yield the trigonal planar complex $\{[N_3N]Mo(N_2)\}_3V$. Red-purple solutions are obtained (as opposed to the deep

purple color observed in previous reactions) and ^{1}H NMR spectra again reveal the presence of **3** and **4** as well as trace amounts of [N_3N]MoH, [bitN_3N]Mo and [N_3N]Mo(N_2). Resonances at -0.55 ppm (**3**) and -5.56 ppm (**4**) integrate to a ratio of 1:2 suggesting that **4** is formed in higher yield than in the reaction of VCl_4(DME) and 1.5 equivalents of {[N_3N]Mo(N_2)}$_2$Mg(THF)$_2$ where the resonances integrate to a ratio of approximately 2:1. Upon standing under dinitrogen for a period of hours, C_6D_6 solutions of the mixture of **3** and **4** take on a deep purple color as **3** becomes the major species present in solution. ^{1}H NMR spectra of the purple solutions reveal that the resonances attributable to **4**, most noticeably those at 1.28 and -5.56 ppm, have diminished in intensity with a concomitant increase in intensity of the resonances for **3**. These results clearly indicate that **4** is unstable in solution, undergoing a disproportionation reaction that yields **3** as one of the products. Unfortunately, no other products of this reaction have been identified.

By analogy to the reaction of {[N_3N]Mo(N_2)}$_2$Fe(THF)$_2$ with [N_3N]Mo(N_2) that produces **1**, it was reasoned that **4** should react with [N_3N]Mo(N_2) to yield **3** (equation 5). The ^{1}H NMR spectrum of the mixture of **3** and **4** is shown in Figure 2.7 (lower spectrum) along with the ^{1}H NMR spectrum of a sample to which [N_3N]Mo(N_2) has been added. Upon addition of [N_3N]Mo(N_2) to the mixture of **3** and **4** an immediate color change to deep purple is observed and resonances attributable to **4** are no longer present in the ^{1}H NMR spectrum while those of **3** have increased significantly in intensity (upper spectrum, Figure 2.7). These results are consistent with coordination of [N_3N]Mo(N_2) and oxidation of the vanadium center. The reverse reaction does occur but the equilibrium lies far to the right. Upon addition of THF-d_8 (~ 400 eqs) to C_6D_6 solutions of **3** resonances attributable to trace amounts of [N_3N]Mo(N_2) and **4** are observed in the ^{1}H NMR spectrum but after 24 h the main species present in solution is **3**.

$$\underset{\mathbf{4}}{\{[N_3N]Mo(N_2)\}_2VCl(THF)} + [N_3N]Mo(N_2) \xrightarrow[-\,THF]{C_6D_6} \underset{\mathbf{3}}{\{[N_3N]Mo(N_2)\}_3VCl} \qquad (5)$$

In an attempt to synthesize {[N_3N]Mo(N_2)}$_4$V, VCl_4(DME) was reacted with two equivalents of {[N_3N]Mo(N_2)}$_2$Mg(THF)$_2$ in THF at -20 °C. ^{1}H NMR spectra of the crude

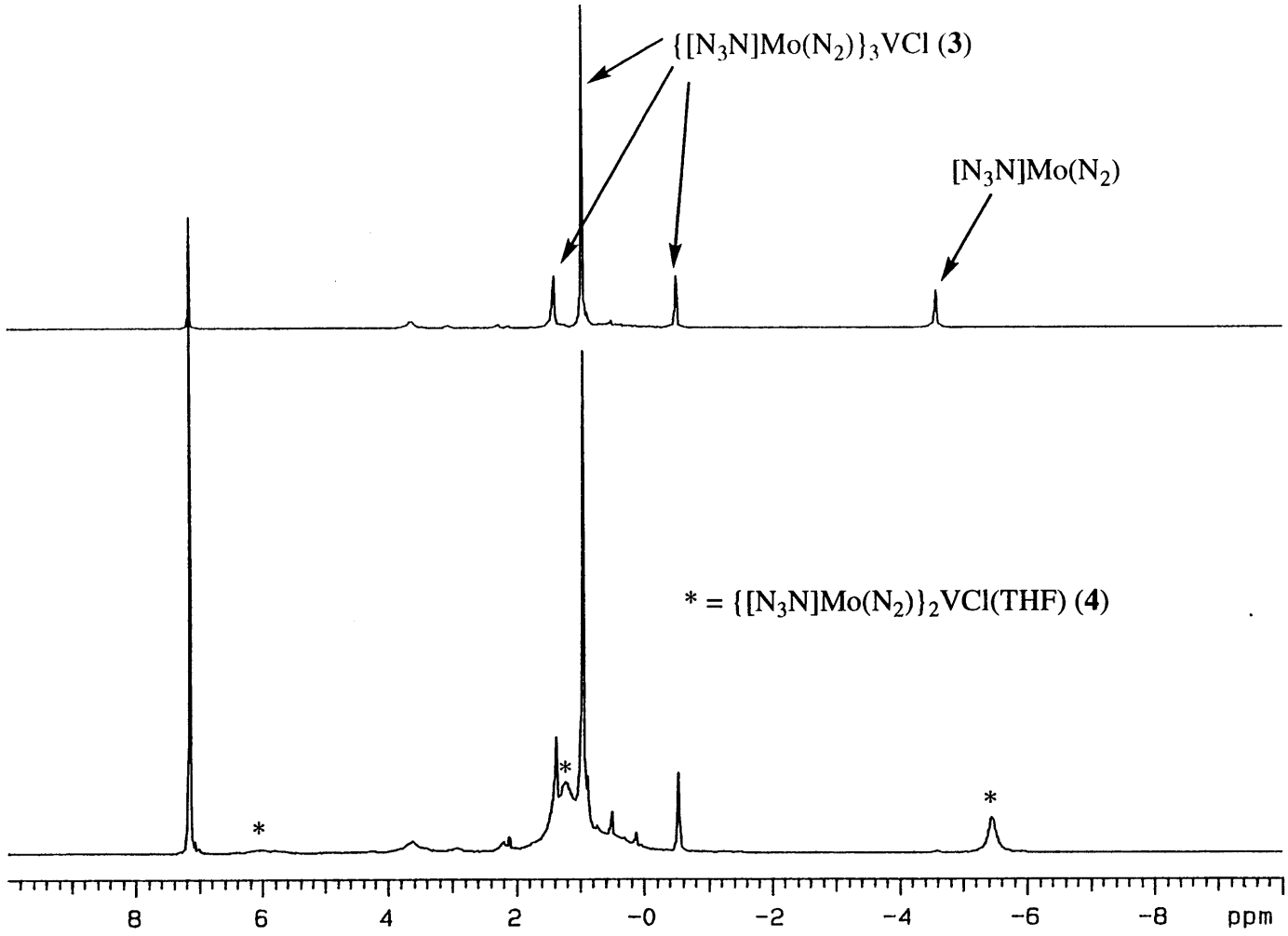

Figure 2.7. ^{1}H NMR spectrum of a mixture of **3** and **4** in C_6D_6 (lower spectrum) and ^{1}H NMR spectrum of a sample to which $[N_3N]Mo(N_2)$ was added (upper spectrum).

References begin on page 102

reaction mixture reveal that **3** and **4** are formed along with traces of $[N_3N]MoH$ and $[bitN_3N]Mo$. It is believed that $\{[N_3N]Mo(N_2)\}_4V$ is not accessible for steric reasons and the synthesis of this complex was not pursued further.

Although the instability of **4** in solution has precluded its isolation on a preparative scale, crystals of **4** suitable for an X-ray diffraction study were grown from THF/Et_2O solutions of the reaction mixture at -20 °C. 1.25 molecules of diethyl ether were found in the unit cell. Crystallographic data and collection and refinement parameters are given in Table 2.1. The molecular structure of **4** along with the atom-labeling scheme is shown in Figure 2.8 while selected bond lengths and bond angles are listed in Table 2.4. **4** is comprised of two $\{[N_3N]Mo(N_2)\}^-$ units bound to pseudo-tetrahedral vanadium, the coordination sphere being completed by one molecule of THF and one chloride ligand. The N-V-N bond angle opens to 119.8° in order to accommodate the sterically bulky $\{[N_3N]Mo(N_2)\}^-$ ligands. The Mo-N-N linkages are essentially linear and the N-N bond lengths at 1.217(7) and 1.221(7) Å are indicative of some reduction of the dinitrogen ligands in **4** compared with free dinitrogen (1.098 Å) and are consistent with formulation of **4** as a diazenido complex with Mo and V in formal oxidation states of 4+ and 3+, respectively. The N_{ax}-Mo-N_{eq}-Si dihedral angles are all close to 180°, suggesting that there is little steric pressure in the pocket defined by the $[N_3N]^{3-}$ ligand. The first structurally characterized vanadium dinitrogen complex[23] was reported in 1989 but examples of V(III) dinitrogen complexes remain comparatively rare. The homobimetallic complexes $[(Np)_3V]_2(\mu\text{-}N_2)$,[24] $[CH_3C\{(CH_2)N(^iPr)\}_3V]_2(\mu\text{-}N_2)$[25] and $[(^iPr_2N)_3V]_2(\mu\text{-}N_2)$[26] have been crystallographically characterized but **4** is the first example of a heterometallic vanadium dinitrogen complex. The N-N bonds in **4** are slightly shorter than the corresponding bonds in the homobimetallic complexes (~ 1.26 Å). Interestingly, the V-N bond lengths of the homobimetallic complexes (~ 1.72 Å) are significantly shorter than those in **4** (1.86 Å). These bonding parameters suggest that the homobimetallic complexes are perhaps better formulated as V(IV) or V(V) complexes with the dinitrogen ligand reduced to the diazenido or hydrazido stage.

References begin on page 102

Figure 2.8. A view of the structure of $\{[N_3N]Mo\text{-}N{=}N\}_2VCl(THF)$ (**4**).

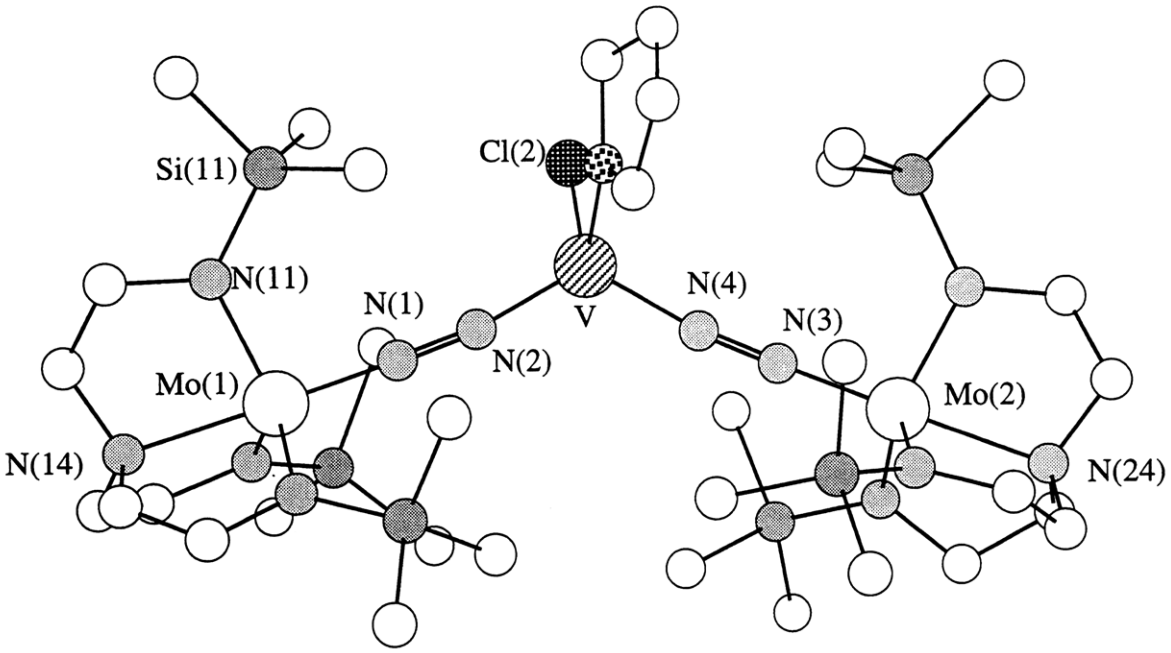

Table 2.4. Selected bond lengths and bond angles for $\{[N_3N]Mo\text{-}N{=}N\}_2VCl(THF)$ (**4**).

Bond Lengths (Å)

N(1)-N(2)	1.217(7)	N(3)-N(4)	1.221(7)	Mo(1)-N(1)	1.836(6)
Mo(2)-N(3)	1.827(6)	V-N(2)	1.864(4)	V-N(4)	1.860(6)
Mo(1)-N(14)	2.244(6)	V-Cl	2.288(2)	V-O	2.061(5)

Bond Angles (deg)

Mo(1)-N(1)-N(2)	178.2(5)	Mo(2)-N(3)-N(4)	178.3(5)		
V-N(2)-N(1)	169.2(5)	V-N(4)-N(3)	172.1(5)	N(2)-V-N(4)	119.8(3)
Cl-V-N(2)	114.9(2)	O-V-Cl	96.5(2)	O-V-N(4)	104.2(2)

References begin on page 102

Zirconium/Molybdenum Dinitrogen Complexes

From our excursions into iron and vanadium chemistry, coupled with the observation that reactions of $\{[N_3N]Mo(N_2)\}_2Mg(THF)_2$ with halides of transition metals such as palladium, nickel and zinc proceed via oxidative pathways yielding $[N_3N]Mo(N_2)$ (see Chapter 1), it is clear that the tendency for redox chemistry to prevail increases as we move to the right of the transition metal series. Drawing on these results it seemed reasonable that redox chemistry might be avoided by employing halides of earlier transition metals such as zirconium. This approach has been successful and several zirconium/molybdenum dinitrogen complexes have been isolated.

$ZrCl_4(THF)_2$ proved to be a versatile reagent for the synthesis of zirconium/molybdenum heterometallic dinitrogen complexes and $\{[N_3N]Mo(N_2)\}_2Mg(THF)_2$ reacts cleanly with two equivalents of $ZrCl_4(THF)_2$ in THF to give $\{[N_3N]Mo\text{-}N{=}N\}ZrCl_3(THF)_2$ (**5**) as salmon-colored needles in 77% yield (equation 6). The ^1H NMR spectrum of diamagnetic **5**, taken in THF-d_8, consists of a single TMS resonance and a pair of triplets for the methylene protons on the ligand backbone characteristic of compounds in which the $[N_3N]Mo$ portion of the molecule is C_3-symmetric. Resonances attributed to coordinated THF are also observed in the spectrum and elemental analyses are consistent with there being two molecules of THF present per zirconium center. The IR spectrum of **5** in Nujol has a broad N-N stretch at 1515 cm^{-1} which is within the range reported for related Group 4 heterobimetallic bridging dinitrogen complexes (1468 - 1545 cm^{-1}).[5]

$$\{[N_3N]Mo\text{-}N{=}N\}_2Mg(THF)_2 + 2\,ZrCl_4(THF)_2 \xrightarrow{THF} 2\,\{[N_3N]Mo\text{-}N{=}N\}ZrCl_3(THF)_2 \quad \textbf{5} \quad + MgCl_2 \qquad (6)$$

By varying the stoichiometry of the reaction depicted in equation 6, two other zirconium/molybdenum dinitrogen complexes can be isolated. Reaction of one equivalent of

References begin on page 102

$\{[N_3N]Mo(N_2)\}_2Mg(THF)_2$ with one equivalent of $ZrCl_4(THF)_2$ yields the diamagnetic complex $\{[N_3N]Mo(N_2)\}_2ZrCl_2$ (**6**) as red cubes in moderate yield (54%, equation 7). The ^1H NMR spectrum of **6** in C_6D_6 reveals the presence of one equivalent of THF per zirconium center, an observation that is corroborated by elemental analysis data. The IR spectrum of **6** in Nujol is characterized by a strong N-N stretch at 1556 cm^{-1}. **6** is unstable in solution undergoing a ligand redistribution reaction that produces **5** and $\{[N_3N]Mo(N_2)\}_3ZrCl$ (**7**, see below) and after 48 h ^1H NMR spectra of C_6D_6 solutions indicate that **5**, **6** and **7** are present in an approximate ratio of 1:3:1.

$$\{[N_3N]Mo\text{-}N{=}N\}_2Mg(THF)_2 + ZrCl_4(THF)_2 \xrightarrow{THF} \underset{\mathbf{6}}{\{[N_3N]Mo\text{-}N{=}N\}_2ZrCl_2} + MgCl_2 \qquad (7)$$

Single crystals of **6** were grown from saturated diethyl ether solutions at -20 °C and examined in an X-ray study; a half a molecule of diethyl ether was found in the unit cell. Crystallographic data and collection and refinement parameters are given in Table 2.5. The molecular structure of **6** along with the atom-labeling scheme is shown in Figure 2.9 while selected bond lengths and bond angles are listed in Table 2.6. The data confirm that two $[N_3N]Mo(N_2)$ ligands are coordinated to pseudo-tetrahedral zirconium with two chloride ligands completing the coordination sphere. The Mo-N-N and Zr-N-N linkages are essentially linear and the large size of Zr(IV) and its ability to accommodate the sterically bulky $[N_3N]Mo(N_2)$ ligands is reflected in the N(16)-Zr-N(26) bond angle of 114.6(2)°. The Mo-N_α bond lengths at 1.797(6) and 1.796(6) Å are the shortest of all the crystallographically-characterized heterometallic complexes reported in this chapter, suggesting extensive d_π-p_π multiple bonding between these atoms. We can assign oxidation states of 4+ to the molybdenum and zirconium centers and so **6** is formally a diazenido complex with dinitrogen functioning as a $(N_2)^{2-}$ ligand. The N-N bond lengths in **6** straddle the ranges reported for bimetallic diazenido (1.20-1.25 Å) and hydrazido (1.25-1.34 Å) complexes[2]

References begin on page 102

and are comparable to the N-N bond length of 1.24(2) Å in the related heterobimetallic dinitrogen complex $WI(PMe_2Ph)_3(py)(\mu\text{-}N_2)ZrCp_2Cl$.[5] In **6** the TMS groups are all oriented upright with the N_{ax}-Mo-N_{eq}-Si dihedral angles close to 180°, consistent with minimal steric pressure within the pocket. Finally, the Mo-N_{amido} bond lengths are not statistically different and are similar to Mo-N_{amido} bond lengths in many other triamidoamine complexes.[27]

Figure 2.9. A view of the structure of $\{[N_3N]Mo\text{-}N{=}N\}_2ZrCl_2$ (**6**).

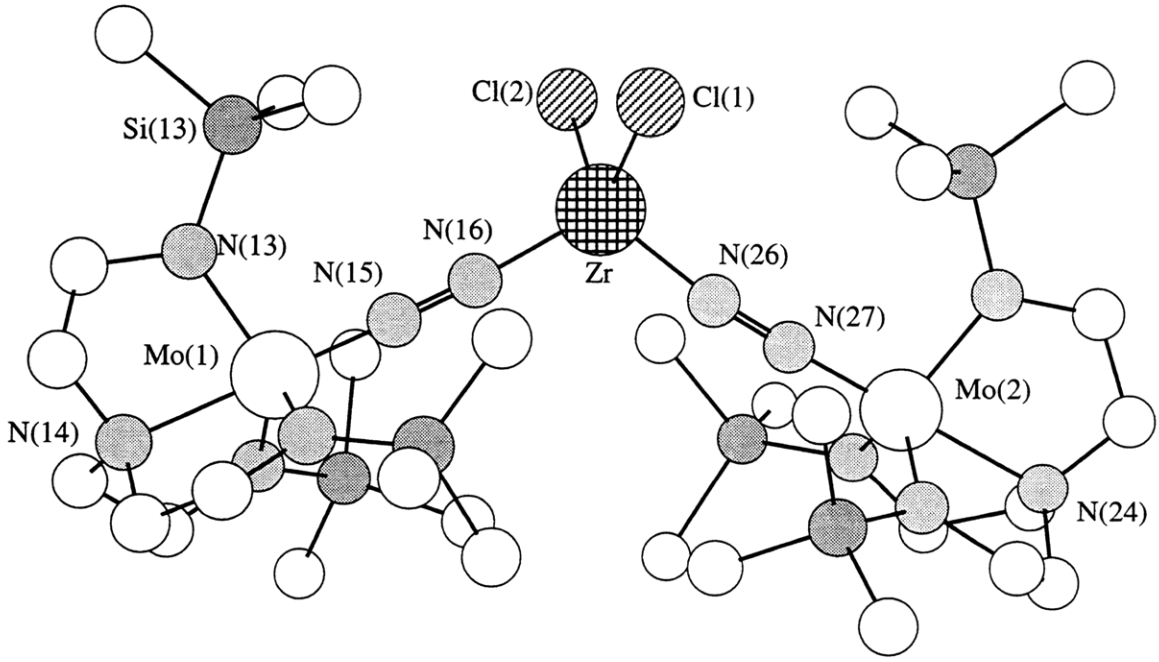

Table 2.5. Crystallographic data, collection parameters and refinement parameters for $\{[N_3N]Mo\text{-}N{=}N\}_2ZrCl_2$ (**6**).

	6
Empirical Formula	$C_{32}H_{88}Cl_2Mo_2N_{12}O_{0.50}Si_6Zr$
Formula Weight	1171.68
Diffractometer	SMART/CCD
Crystal Dimensions(mm)	na
Crystal System	Monoclinic
Space Group	$P2_1/c$
a (Å)	16.4150(3)
b (Å)	18.5686(4)
c (Å)	19.8964(4)
α (°)	90
β (°)	100.2590(10)
γ (°)	90
V (Å^3), Z	5967.5(2), 4
D_{calc} (Mg/m^3)	1.304
Absorption coefficient (mm^{-1})	0.829
F_{000}	2420
Temperature (K)	183(2)
Θ range for data collection (°)	1.26 to 23.29
Reflections collected	23769
Unique Reflections	8552
R	0.0559
R_w	0.0986
GoF	1.056

References begin on page 102

Table 2.6. Selected bond lengths and bond angles for $\{[N_3N]Mo(N_2)\}_2ZrCl_2$ (**6**).

Bond Lengths (Å)

Mo(1)-N(15)	1.797(6)	Mo(2)-N(25)	1.796(6)	N(15)-N(16)	1.249(8)
N(25)-N(26)	1.245(8)	Zr-N(16)	1.978(6)	Zr-N(26)	1.974(6)
Zr-Cl(1)	2.394(2)	Zr-Cl(2)	2.408(2)	Mo(1)-N(14)	2.236(6)
Mo(2)-N(24)	2.251(6)				

Bond Angles (degrees)

Mo(1)-N(15)-N(16)	176.9(5)	Mo(2)-N(25)-N(26)	177.9(5)
Zr-N(16)-N(15)	175.9(6)	Zr-N(26)-N(25)	170.6(5)
N(16)-Zr-N(26)	114.6(2)	Cl(1)-Zr-Cl(2)	107.14(9)

Dihedral Angles (degrees)[a]

N(14)-Mo(1)-N(13)-Si(13)	174.4	N(24)-Mo(2)-N(21)-Si(21)	-173.6

[a]Obtained from a Chem 3D drawing

To further probe the ability of Zr(IV) to accommodate the sterically bulky $[N_3N]Mo(N_2)$ ligand, $ZrCl_4(THF)_2$ was reacted with 1.5 equivalents of $\{[N_3N]Mo(N_2)\}_2Mg(THF)_2$ according to equation 8. $\{[N_3N]Mo(N_2)\}_3ZrCl$ (**7**) can be isolated as deep red needles from diethyl ether in 68% yield. Similar to **5** and **6** above, ^1H and ^{13}C NMR spectra of **7** are characteristic of a complex in which the $[N_3N]Mo$ portion of the molecule is C_3-symmetric. The IR spectrum of **7** taken in Nujol has a strong broad stretch at 1576 cm^{-1}. **7** appears to be thermally stable and C_6D_6 solutions of **7** show no signs of decomposition when stored at room temperature under dinitrogen for 72 h (according to ^1H NMR spectroscopy).

References begin on page 102

$$1.5\ \{[N_3N]Mo\text{-}N{=}N\}_2Mg(THF)_2 + ZrCl_4(THF)_2 \xrightarrow{Et_2O/tol} \underset{\mathbf{7}}{\{[N_3N]Mo\text{-}N{=}N\}_3ZrCl} + 1.5\ MgCl_2 \quad (8)$$

Efforts to prepare $\{[N_3N]Mo(N_2)\}_4Zr$ were unsuccessful; reaction of $ZrCl_4(THF)_2$ with two equivalents of $\{[N_3N]Mo(N_2)\}_2Mg(THF)_2$ yielded **7** as the sole identifiable product suggesting that $\{[N_3N]Mo\text{-}N{=}N\}_4Zr$ is not accessible on steric grounds.

CONCLUSIONS

The concept of $\{[N_3N]Mo(N_2)\}^-$ as a ligand has been explored and implemented in the synthesis of heterometallic dinitrogen complexes. The $\{[N_3N]Mo(N_2)\}^-$ ligand is unique not only in that it is derived from dinitrogen but also in its ability to exist in both anionic and neutral forms. The non-innocent nature of the ligand coupled with the presence of a redox active metal center facilitates the interconversion of Fe(II)/Fe(III) and V(III)/V(IV) dinitrogen complexes as evidenced by ^1H NMR spectroscopic studies. It is clear that upon coordination of $[N_3N]Mo(N_2)$ to the Fe(II) or V(III) center, an electron is transferred from the metal to the ligand, and as a result complexes containing the neutral ligand have not been isolated. Reduction of the metal center with the concomitant oxidation of $\{[N_3N]Mo(N_2)\}^-$ has thwarted efforts to synthesize heterometallic complexes containing later transition metals although such reactions do allow isolation of the neutral terminal dinitrogen complex $[N_3N]Mo(N_2)$ (see Chapter 1). Complexes containing four $\{[N_3N]Mo(N_2)\}^-$ ligands have not been isolated and it is proposed that the steric bulk of the ligand prevents the formation of such complexes.

References begin on page 102

EXPERIMENTAL PROCEDURES

General Details. All experiments were performed under a nitrogen atmosphere in a Vacuum Atmospheres drybox or by standard Schlenk techniques unless otherwise specified. Pentane was washed with sulfuric acid/nitric acid (95/5 v/v), sodium bicarbonate, and water, stored over calcium chloride, and distilled from sodium benzophenone ketyl under nitrogen. Toluene was distilled from sodium, and CH_2Cl_2 was distilled from CaH_2. Anhydrous diethyl ether and THF were sparged with nitrogen and passed through alumina columns.[28] All solvents were stored in the dry box over activated 4 Å molecular sieves.

NMR data were obtained at 300 or 500 MHz (^1H), 75.4 MHz (^{13}C) and 121.8 MHz (^{31}P) and are listed in parts per million downfield from tetramethylsilane for proton and carbon and in parts per million downfield from 85% H_3PO_4 for phosphorus. Coupling constants are listed in Hertz. Spectra were obtained at 25 °C unless otherwise noted. Benzene-d_6 and toluene-d_8 were pre-dried on CaH_2, vacuum transferred onto sodium and benzophenone, stirred under vacuum for two days and then vacuum transferred into small storage flasks and stored over molecular sieves. $[N_3N]MoCl$,[9] $[DMPE]FeCl_2$,[29] $VCl_3(THF)_3$,[30] $VCL_4(DME)$[31] and $ZrCl_4(THF)_2$[30] were prepared as described in the literature. $PdCl_2(PPh_3)_2$, $NiCl_2(PPh_3)_2$, $FeCl_2$ and $FeCl_3$ were purchased from commercial vendors and used as received.

UV/visible spectra were recorded on a HP 8452 Diode Array spectrophotometer using a Hellma 221-QS quartz cell (path length = 10 mm) sealed to a gas adapter fitted with a Teflon stopcock. IR spectra were recorded on a Perkin-Elmer 1600 FT-IR spectrometer. Elemental analyses (C, H, N) were performed in our laboratory using a Perkin-Elmer 2400 CHN analyzer or by Microlytics Analytical Laboratories of Deerfield MA. X-ray data were collected on Siemens SMART/CCD diffractometer and general experimental details are described in the literature.[32]

SQUID Magnetic Susceptibility Measurements. Measurements were carried out on a Quantum Design SQUID magnetometer. Data were obtained at a field strength of 5000 Gauss. Straws and gel caps (Gelatin Capsule No. 4 Clear) were purchased from Quantum Design. The sample was prepared in the drybox by the following method. A gel cap and a square of

References begin on page 102

parafilm were weighed. The sample was placed in the gel cap and the parafilm inserted above it. The gel cap was closed and the mass of the sample was ascertained by weighing the loaded gel cap. The gel cap was placed in a straw which was then mounted on the sample rod and placed in the magnetometer. Two runs were performed on the sample - one from 5 to 300 K and a second from 300 to 5 K. Measurements were made at the following increments: 5-10 K (every 1 K), 10-20 K (every 2 K), 20-50 K (every 3 K), 50-100 K (every 5 K), 100-200 K (every 10 K), 200-300 K (every 20 K).

$\{[N_3N]MoN_2\}_3Fe$ (1). $\{[N_3N]Mo(N_2)\}_2Mg(THF)_2$ (316 mg, 0.28 mmol) was dissolved in 10 mL Et_2O/ 2 mL THF/ 1 mL toluene and the solution was cooled to -20 °C. $FeCl_2$ (35 mg, 0.28 mmol) was slurried in 1 mL Et_2O, cooled to -20 °C and then was added all at once to the stirred solution of $\{[N_3N]Mo(N_2)\}_2Mg(THF)_2$. Over the course of 15 min $FeCl_2$ was taken into solution as the color of the solution darkened to a burnt orange color. After 90 min the solvent was removed to give a black purple residue. This residue was extracted with 30 mL of pentane and the purple solution was filtered through Celite. Upon reducing the pentane solution purple crystals began to form. The solution was cooled to -20 °C and the product obtained as a black-purple crystalline solid; yield 105 mg (38%) ^1H NMR (C_6D_6) δ 9.25 ($\Delta\nu_{1/2}$ = 705 Hz, TMS), -9.71 ($\Delta\nu_{1/2}$ = 288 Hz, NCH_2CH_2N), -64.0 ($\Delta\nu_{1/2}$ = 241 Hz, NCH_2CH_2N). IR(Nujol, cm^{-1}) 1703 (N=N). UV-visible(Pentane) λ = 516 nm, ε = 22,818 M^{-1} cm^{-1}. μ = 6.03 μ_B.

$\{[N_3N]MoN_2\}_2Fe(DMPE)$.ether (2). $\{[N_3N]Mo(N_2)\}_2Mg(THF)_2$ (454 mg, 0.40 mmol) was dissolved in 10 mL of THF and the solution was cooled to -20 °C. $FeCl_2$ (51 mg, 0.40 mmol) was added all at once to the stirred solution. After 1 min the solution began to darken in color and took on a dark burnt-orange color. After 45 min the solvent was removed in vacuo and the residue extracted with 40 mL of pentane. The purple pentane solution was filtered through Celite and the pentane removed to give a black/purple solid. This solid was dissolved in 10 mL of toluene and DMPE (60 mg, 0.40 mmol) in 3 mL of toluene was added dropwise to the stirred solution. After stirring for 20 min the solvent was removed in vacuo. The residue was extracted with 15 mL of diethyl ether, filtered and the volume of the filtrate was reduced to 7 mL. Upon

References begin on page 102

cooling this solution to -20 °C the product was obtained as black blocks; yield 200 mg (43%). ^{1}H NMR (C_6D_6) δ 37.0 (P(C*H*$_3$)$_2$ or PC*H*$_2$), 6.62 ($\Delta\nu_{1/2}$ = 690 Hz, TMS), -4.67 ($\Delta\nu_{1/2}$ = 337 Hz, NCH_2CH_2N), -47.43 ($\Delta\nu_{1/2}$ = 591 Hz, NCH_2CH_2N), -117.46 (P(C*H*$_3$)$_2$ or PC*H*$_2$). IR(Nujol, cm^{-1}) 1706 (N=N). UV-visible(Pentane) λ = 360 nm, ε = 23,306 M^{-1} cm^{-1}, λ = 508 nm, ε = 13,997 M^{-1} cm^{-1}. μ = 5.08 μ_B. Anal. Calcd. for $C_{40}H_{104}N_{12}Si_6Mo_2FeP_2O$: C, 38.51; H, 8.40; N, 13.47. Found: C, 38.55; H, 8.43; N, 13.53.

{[N_3N]MoN_2}$_3$VCl (3). Method 1. {[N_3N]Mo(N_2)}$_2$Mg(THF)$_2$ (300 mg, 0.264 mmol) was dissolved in 10 mL THF and cooled to -20 °C. VCl_4(DME) (50 mg, 0.177 mmol) was dissolved in 3 mL THF, cooled to -20 °C and then added to the stirred solution of {[N_3N]Mo(N_2)}$_2$Mg(THF)$_2$. The solution was stirred for 15 h to give a purple solution. The solvent was removed and the residue extracted with 15 mL of toluene. Following filtration through Celite, the toluene was removed in vacuo and the resulting residue was recrystallized from THF/pentane to give the product as black plates; yield 112 mg (42%).

Method 2. {[N_3N]Mo(N_2)}$_2$Mg(THF)$_2$ (290 mg, 0.255 mmol) was dissolved in 7 mL THF and cooled to -20 °C. VCl_3(THF)$_3$ (95 mg, 0.255 mmol) was dissolved in 2 mL THF, cooled to -20 °C and then added to the stirred solution of {[N_3N]Mo(N_2)}$_2$Mg(THF)$_2$. The solution was stirred for 25 h to give a purple solution. The solvent was removed and the residue extracted with 15 mL of toluene. Following filtration through Celite, the toluene was removed in vacuo and the resulting residue was recrystallized from THF/pentane to give the product as black plates; yield 108 mg (28%). ^{1}H NMR(C_6D_6) δ 1.36 ($\Delta\nu_{1/2}$ = 20 Hz, NCH_2CH_2N), 0.94 ($\Delta\nu_{1/2}$ = 6 Hz, TMS), -0.55 ($\Delta\nu_{1/2}$ = 14 Hz, NCH_2CH_2N). IR(Nujol, cm^{-1}) 1579 (N=N). μ = 1.50 μ_B.

{[N_3N]Mo(N_2)}ZrCl$_3$(THF)$_2$ (5). {[N_3N]Mo(N_2)}$_2$Mg(THF)$_2$ (150 mg, 0.136 mmol) was dissolved in 7 mL of THF and cooled to -20 °C. $ZrCl_4$(THF)$_2$ (100 mg, 0.265 mmol) was added as a solid to the stirred solution of {[N_3N]Mo(N_2)}$_2$Mg(THF)$_2$. After 3 h the solvent was removed in vacuo and the residue was extracted with 15 mL of toluene. Following filtration through a pad of Celite, the toluene was removed under reduced pressure. Crystallization from

THF/pentane afforded the product as salmon-colored needles; yield 153 mg (77%). ^{1}H NMR(THF-d_8) δ 3.75 (t, NCH_2CH_2N), 3.62 (m, THF), 2.90 (t, NCH_2CH_2N), 1.78 (m, THF), 0.35 (s, TMS). $^{13}C\{^1H\}$ NMR(THF-d_8) δ 68.4 (THF), 54.9 (NCH_2CH_2N), 53.4 (NCH_2CH_2N), 26.5 (THF), 4.2 (TMS). IR(Nujol, cm^{-1}) 1515 (N=N). Anal. Calcd. for $C_{23}H_{55}N_6Si_3MoZrCl_3O_2$: C, 33.46; H, 6.72; N, 10.18, Cl, 12.88. Found: C, 33.90; H, 6.54; N, 9.81, Cl, 12.81.

{[N_3N]Mo(N_2)}$_2$ZrCl$_2$.THF (6). {[N_3N]Mo(N_2)}$_2$Mg(THF)$_2$ (300 mg, 0.264 mmol) was dissolved in 10 mL of THF and cooled to -20 °C. $ZrCl_4(THF)_2$ (100 mg, 0.265 mmol) was added as a solid to the stirred solution of {[N_3N]Mo(N_2)}$_2$Mg(THF)$_2$. After 29 h the solvent was removed in vacuo and the residue was extracted with toluene. Following filtration through a pad of Celite, the toluene was removed in vacuo. Crystallization from THF/pentane afforded the product as red cubes; yield 160 mg (54%, 2 crops). ^{1}H NMR(C_6D_6) δ 3.60 (m, THF), 3.29 (t, NCH_2CH_2N), 2.04 (t, NCH_2CH_2N), 1.40 (m, THF), 0.65 (s, TMS). $^{13}C\{^1H\}$ NMR(C_6D_6) δ 54.2 (NCH_2CH_2N), 52.5 (NCH_2CH_2N), 26.1 (THF), 4.5 (NTMS). IR(Nujol, cm^{-1}) 1556 (N=N). Anal. Calcd. for $C_{34}H_{86}N_{12}Si_6Mo_2ZrCl_2O$: C, 33.98; H, 7.21; N, 13.99. Found: C, 33.51; H, 7.21; N, 14.00.

{[N_3N]Mo(N_2)}$_3$ZrCl (7). {[N_3N]Mo(N_2)}$_2$Mg(THF)$_2$ (155 mg, 0.136 mmol) was dissolved in 5 mL of a 2:1 ether/toluene solution and cooled to -20 °C. $ZrCl_4(THF)_2$ (34 mg, 0.09 mmol) was added as a solid to the stirred solution of {[N_3N]Mo(N_2)}$_2$Mg(THF)$_2$. The solution was stirred for 17 h and then filtered through a pad of Celite to give a clear, blood-red solution. The solvent was removed and the residue dissolved in the minimum diethyl ether. Cooling this solution to -20 °C afforded the product as deep red needles; yield 97 mg (68%). ^{1}H NMR(C_6D_6) δ 3.37 (t, NCH_2CH_2N), 2.10 (t, NCH_2CH_2N), 0.69 (s, TMS). $^{13}C\{^1H\}$ NMR(C_6D_6) δ 55.0 (NCH_2CH_2N), 52.0 (NCH_2CH_2N), 4.7 (NTMS). IR(Nujol, cm^{-1}) 1576 (N=N).

References begin on page 102

REFERENCES

(1) Chatt, J.; Dilworth, J. R.; Richards, R. L. *Chem. Rev.* **1978**, *78*, 589.

(2) Hidai, M.; Mizobe, Y. *Chem. Rev.* **1995**, *95*, 1115.

(3) Laplaza, C. E.; Johnson, M. J. A.; Peters, J. C.; Odom, A. L.; Kim, E.; Cummins, C. C.; George, G. N.; Pickering, I. J. *J. Am. Chem. Soc.* **1996**, *118*, 8623 and references therein.

(4) Mercer, M. J. *J. Chem. Soc., Dalton Trans.* **1974**, 1637.

(5) Mizobe, Y.; Yokobayashi, Y.; Oshita, H.; Takahashi, T.; Hidai, M. *Organometallics* **1994**, *13*, 3764.

(6) Schrock, R. R.; Kolodziej, R. M.; Liu, A. H.; Davis, W. M.; Vale, M. G. *J. Am. Chem. Soc.* **1990**, *112*, 4338.

(7) Cradwick, P. D.; Chatt, J.; Crabtree, R. H.; Richards, R. L. *J. Chem. Soc., Chem. Commun.* **1975**, 351.

(8) Chan, M. K.; Kim, J. S.; Rees, D. C. *Science* **1993**, *260*, 792.

(9) Schrock, R. R.; Seidel, S. W.; Mösch-Zanetti, N. C.; Shih, K. -Y.; O'Donoghue, M. B.; Davis, W. M.; Reiff, W. M. *J. Am. Chem. Soc.* **1997**, *119*, 11876.

(10) Wilkinson, P. G.; Houk, N. B. *J. Chem. Phys.* **1956**, *24*, 528.

(11) Bartlett, R. A.; Ellison, J. J.; Power, P. P.; Shoner, S. C. *Inorg. Chem.* **1991**, *30*, 2888.

(12) Olmstead, M. M.; Power, P. P.; Shoner, S. C. *Inorg. Chem.* **1991**, *30*, 2547.

(13) Putzer, M. A.; Neumüller, B.; Dehnicke, K.; Magull, J. *Chem. Ber.* **1996**, *129*, 715.

(14) Stokes, S. L.; Davis, W. M.; Odom, A. L.; Cummins, C. C. *Organometallics* **1996**, *15*, 4521.

(15) Bradley, D. C.; Hursthouse, M. B.; Rodesiler, P. F. *Chem. Comm.* **1969**, 14.

(16) O'Connor, C. J. *Prog. Inorg. Chem.* **1982**, *29*, 203.

(17) Fitzsimmons, B. W.; Johnson, C. E. *Chem. Phys. Letters* **1974**, *24*, 422.

(18) Blume, M. *Phys. Rev. Letters* **1965**, *14*, 96.

(19) Parish, R. V. *NMR, NQR, EPR and Mössbauer Spectroscopy in Inorganic Chemistry*; Ellis Horwood Limited: Chichester, 1990.

(20) Alyea, E. C.; Bradley, D. C.; Copperthwaite, R. G.; D., S. K. *J. Chem. Soc., Dalton Trans.* **1973**, 185.

(21) Eller, P. G.; Bradley, D. C.; Hursthouse, M. B.; Meek, D. W. *Coord. Chem. Rev.* **1977**, *24*, 1.

(22) W. M. Davis, personal communication.

(23) Edema, J. J. H.; Meetsma, A.; Gambarotta, S. *J. Am. Chem. Soc.* **1989**, *111*, 6878.

(24) Buijink, J. -K. F.; Meetsma, A.; Teuben, J. H. *Organometallics* **1993**, *12*, 2004.

(25) Desmangles, N.; Jenkins, H.; Ruppa, K. B.; Gambarotta, S. *Inorg. Chim. Acta.* **1996**, *250*, 1.

(26) Song, J. -I.; Berno, P.; Gambarotta, S. *J. Am. Chem. Soc.* **1994**, *116*, 6927.

(27) Schrock, R. R. *Acc. Chem. Res.* **1997**, *30*, 9.

(28) Pangborn, A. B.; Giardello, M. A.; Grubbs, R. H.; Rosen, R. K.; Timmers, F. J. *Organometallics* **1996**, *15*, 1518.

(29) Girolami, G. S.; Wilkinson, G.; Galas, A. M. R.; Thorton-Pett, M.; Hursthouse, M. B. *J. Chem. Soc., Dalton Trans.* **1985**, 1339.

(30) Manzer, L. E. *Inorg. Synth.* **1982**, *21*, 135.

(31) Bridgland, B. E.; Fowles, G. W. A.; Walton, R. A. *J. Inorg. Nucl. Chem.* **1965**, *27*, 383.

(32) Rosenberger, C.; Schrock, R. R.; Davis, W. M. *Inorg. Chem.* **1997**, *36*, 123.

CHAPTER 3

Organometallic Chemistry of Trimethylsilyl-Substituted Triamidoamine Complexes of Molybdenum

A portion of the material covered in this chapter has appeared in print:

Schrock, R. R., Seidel, S. W., Mösch-Zanetti, N. C., Shih, K. -Y., O'Donoghue, M. B., Davis, W. M., Reiff, W. M. *J. Am. Chem. Soc.* **1997**, *119*, 11876.

INTRODUCTION

In recent years a wide variety of transition metal complexes containing the triamidoamine ligands $[(RNCH_2CH_2)_3N]^{3-}$ (R = C_6F_5, Me_3Si) have been synthesized in our laboratories.[1] The salient features of such complexes are the sterically protected, three-fold-symmetric, apical coordination site and the spatial arrangement of three orbitals of the metal center within this pocket. The use of bulky R groups such as Me_3Si is believed to impart kinetic stability on what would otherwise be reactive species. This strategy has allowed us to isolate examples of rarely observed complexes such as trigonal monopyramidal complexes from titanium to iron,[2] a tantalum phosphinidene complex,[3] and tungsten and molybdenum phosphido and arsenido complexes.[4] In triamidoamine complexes the frontier orbitals of the metal that are available to bind other ligands consist of an orbital of σ symmetry (d_{z2}) and two degenerate orbitals of π symmetry (d_{xz} and d_{yz}). Such an orbital arrangement is ideal for the formation of M-E triple bonds as exemplified by the synthesis of $[N_3N]ME$ complexes (M = Mo, W; E = CR, N, P, As).[1] Alternatively, rehybridization allows the metal center to bind two ligands via a single and a double bond as is the case in the alkylidene hydride complex $[N_3N]W(C_5H_8)(H)$.[5] The third bonding picture in which the metal forms single bonds to three ligands is uncommon with $[N_3N]W(H)_3$[5,6] being a rare example of such a complex.

One of the original drives behind our foray into the chemistry of transition metal triamidoamine complexes was to understand how dinitrogen might be activated and reduced in a C_3-symmetric environment. In this context the exploration of the chemistry of $[N_3N_F]Mo$[7] and $[N_3N]Mo$ complexes has been especially rewarding and Chapter 1 details progress made toward the derivatization of dinitrogen in $[N_3N]Mo$ complexes. With the isolation of paramagnetic $[N_3N]Mo(N_2)$, we demonstrated that a dinitrogen adduct of trigonal monopyramidal $[N_3N]Mo$ is a viable species. Drawing on this result, we reasoned that other $[N_3N]Mo(L)$ complexes where L = CO, RNC, or olefin should be accessible. It should be noted that the organometallic chemistry of molybdenum in the 3+ oxidation state is relatively little explored and that studies of the organometallic chemistry of $[N_3N]Mo$ complexes have focused almost exclusively on Mo(IV)

References begin on page 137

alkyl complexes and their decomposition to Mo(VI) alkylidynes, culminating with the unequivocal demonstration that such decompositions occur via α elimination processes that are as much as six orders of magnitude faster than β elimination processes.[8]

Two synthetic approaches to $[N_3N]Mo(L)$ complexes have been devised. In the first approach, $[N_3N]MoCl$ is reduced by magnesium powder in the presence of the donor ligand, L. However, only $[N_3N]Mo(C_2H_4)$ has been successfully synthesized in this manner. In the cases of CO and ^{t}BuNC no reaction occurs and the starting material is recovered. Having observed that the dinitrogen ligand in $[N_3N]Mo(N_2)$ is labile (see Chapter 1), we reasoned that $[N_3N]Mo(N_2)$ could serve as a source of the as-yet-unobserved trigonal monopyramidal complex, $[N_3N]Mo$. Hence, we embarked on a series of ligand exchange reactions leading to the high yield syntheses of $[N_3N]Mo(C_2H_4)$, $[N_3N]Mo(CO)$ and $[N_3N]Mo(CN^tBu)$. These and other reactions described in this chapter are summarized in Scheme 3.1.

As noted previously, examples of trigonal monopyramidal triamidoamine complexes are known for a variety of first row metals yet such complexes are unknown for second and third row metals. Since the elusive species $[N_3N]Mo$ is implicated in the ligand exchange reactions (assuming a dissociative mechanism is operating), we felt it a worthy endeavor to attempt to isolate it. However, reduction of $[N_3N]MoCl$ in the absence of a donor ligand leads to C-H activation of one of the trimethylsilyl groups of the ligand and $[bitN_3N]Mo$ is isolated. An X-ray study of $[bitN_3N]Mo$ is reported, highlighting the vulnerability of the $[N_3N]^{3-}$ ligand to ligand degradation reactions other than those involving Si-N bond cleavage (see Chapter 1).

References begin on page 137

Scheme 3.1. Organometallic chemistry of $[N_3N]Mo$ complexes.

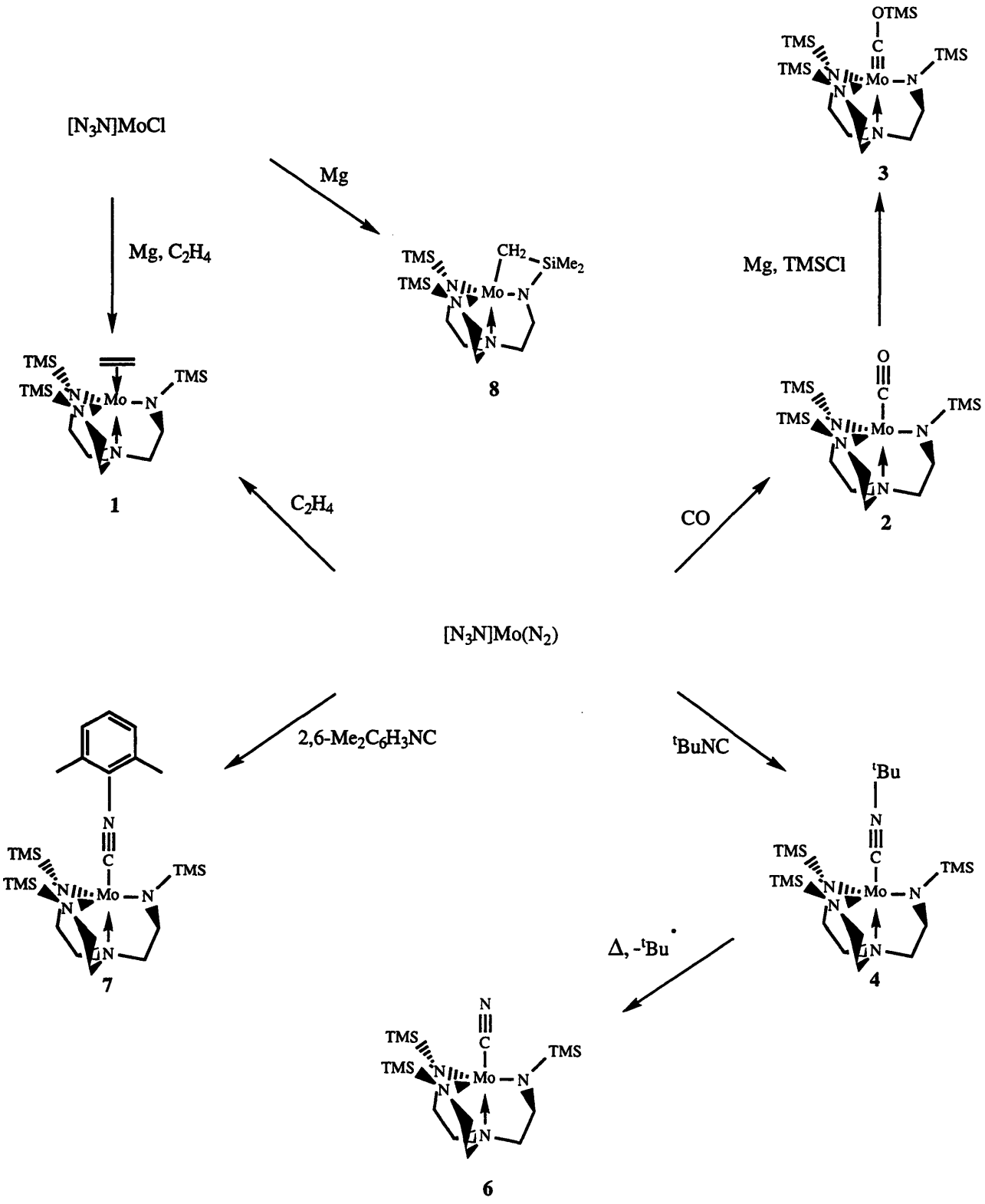

RESULTS

Synthesis of $[N_3N]Mo(C_2H_4)$

Reduction of $[N_3N]MoCl$ in THF with an excess of magnesium powder in the presence of 5 equivalents of ethylene proceeds smoothly over a period of 12 h to give a purple solution (equation 1). Paramagnetic $[N_3N]C_2H_4$ (**1**) can be isolated as analytically-pure, purple needles in 97% yield by recrystallization from hexamethyldisiloxane. Exposure of C_6D_6 solutions of $[N_3N]Mo(N_2)$ to an excess of ethylene (10 equivalents) results in an immediate color change from orange to purple as **1** is formed cleanly according to ^1H NMR spectroscopy. Unlike other Mo(III) adducts (see below) resonances for the methylene protons of the ligand backbone are not observed in the ^1H NMR spectrum of **1**. Instead a single broad resonance at 3.63 ppm ($\Delta\nu_{1/2}$ = 414 Hz) assigned to the TMS groups of the ligand is observed. A resonance attributable to the ethylene ligand is not observed, presumably due to its proximity to the paramagnetic center. Triamidoamine complexes of ethylene are known and Ta,[9,10] W[11] and Re[12] analogs of **1** have been synthesized

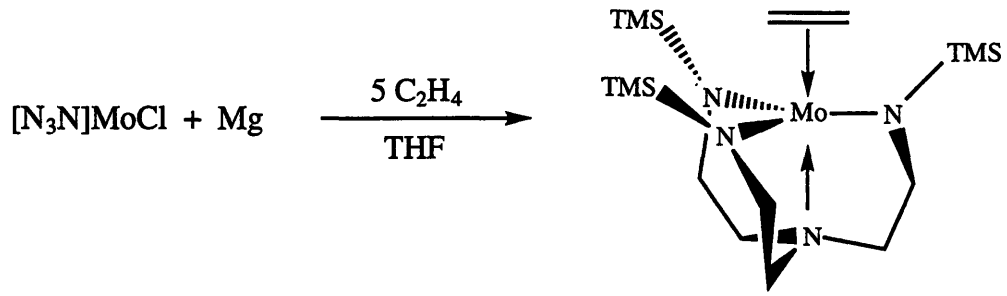

1

(1)

in our group. $[Et_3Si\text{-}N_3N]Ta(C_2H_4)$[10] has been shown to be thermally unstable and undergoes decomposition via a unique pathway involving intramolecular abstraction of a proton α to the equatorial nitrogen in the ligand methylene backbone. **1** is thermally quite stable; toluene-d_8 solutions of **1** remain unchanged after heating under vacuum at 60 °C for 14 h. However, when a sample of **1** is heated to 90 °C in toluene under 1 atmosphere of dinitrogen for a period of 1 week, the ^1H NMR spectrum reveals the presence of $[N_3N]Mo\text{-}N{=}N\text{-}Mo[N_3N]$ and $[N_3N]Mo(N_2)$ along

with unreacted **1** (equation 2). Presumably, the ethylene ligand is first replaced with dinitrogen to form $[N_3N]Mo(N_2)$ which upon further heating is converted to $[N_3N]Mo\text{-}N{=}N\text{-}Mo[N_3N]$ (see Chapter 1). The broadness of the TMS resonance of **1** and its coincidental overlap with the TMS resonance of $[N_3N]Mo\text{-}N{=}N\text{-}Mo[N_3N]$ precluded an estimate of the extent of decomposition. **1** decomposes rapidly in the solid state when exposed to high vacuum as evidenced by the formation of a black, oily solid. We speculate that loss of ethylene is the first step in this decomposition although no products of the reaction have been identified.

$$\mathbf{1} \xrightarrow[N_2]{90\ ^\circ C,\ tol} \mathbf{1} + [N_3N]Mo(N_2) + \{[N_3N]Mo\}_2(\mu\text{-}N_2) \qquad (2)$$

1 is oxidized by ferrocenium triflate to give known $[N_3N]MoOTf$[8] as the only identifiable product, according to ^1H NMR spectroscopy (equation 3). Upon oxidation, it appears that backbonding from the cationic d^2 metal center is weak and the ethylene ligand is lost with the resulting formation of $[N_3N]MoOTf$. In contrast, $\{[N_3N_F]W(C_2H_4)\}OTf$[11] is isolable (the analogous molybdenum complex has not been synthesized). Presumably, backbonding from the reducing tungsten center to the ethylene ligand is more efficient in this complex, despite the presence of the more electron-withdrawing $[N_3N_F]^{3-}$ ligand.

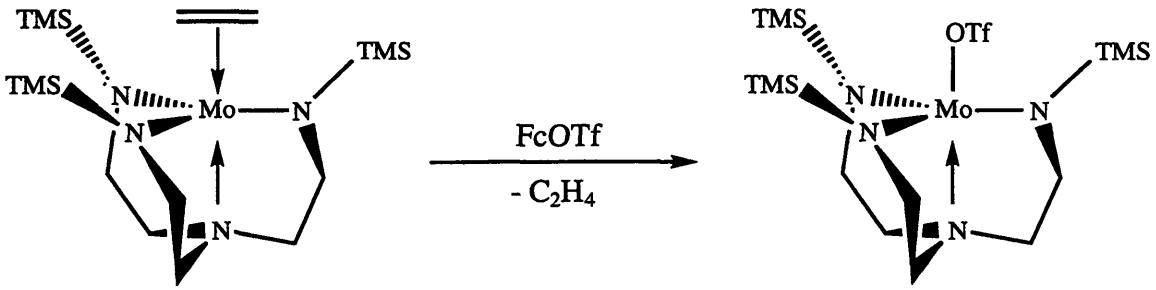

1 (3)

SQUID[13] magnetic susceptibility studies have been carried out on solid **1** and a plot of the molar magnetic susceptibility versus temperature is shown in Figure 3.1. The data can be fit to the

Curie law over the temperature range 5-300 K to give μ = 1.73(1) μ_B (R = 0.9999), consistent with **1** being a low-spin Mo(III) complex. It should be noted that in trigonal bipyramidal complexes of the type [N_3N]Mo(L) the lowest lying orbitals are the degenerate d_{xz}/d_{yz} pair. Three electrons occupy these two orbitals giving rise to a single unpaired spin.

Figure 3.1. Plot of χ_m (corrected for diamagnetism using Pascal's constants) versus T for [N_3N]Mo(C_2H_4) (**1**).

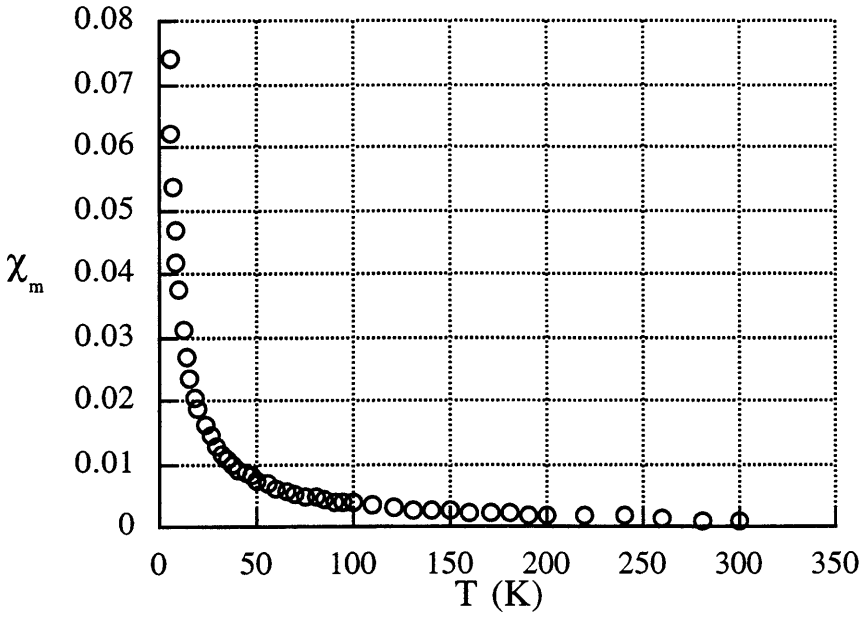

Synthesis and Reactivity of [N_3N]Mo(CO)

Attempts to synthesize [N_3N]Mo(CO) (**2**) directly from [N_3N]MoCl have been unsuccessful as no reaction is observed between [N_3N]MoCl and magnesium powder in the presence of one equivalent of CO and [N_3N]MoCl is recovered. A preassociation of CO with [N_3N]MoCl that might prevent reduction from occurring is ruled out on the basis that resonances in the ^{1}H NMR spectrum of [N_3N]MoCl under 1 atmosphere of CO are not shifted relative to those in the ^{1}H NMR spectrum of [N_3N]MoCl under 1 atmosphere of dinitrogen. In contrast, [N_3N]MoOTf is reduced by magnesium in the presence of CO but the product is not

References begin on page 137

$[N_3N]Mo(CO)$ but rather the dimeric complex $\{(TMSNCH_2CH_2)_2N(CH_2CH_2N)Mo\}_2$[14] formed by formal loss of TMSOTf. Similar results are obtained when $[N_3N]MoOTf$ is reduced by magnesium under dinitrogen (see Chapter 1). It should also be noted that $[N_3N_F]WOTf$ can be reduced by sodium amalgam in the presence of carbon monoxide to yield $[N_3N_F]W(CO)$ but $[N_3N_F]WCl$ does not react under the same conditions.[11] However, $[N_3N_F]W(CN^tBu)$ can be synthesized by reduction of $[N_3N_F]WOTf$ *or* $[N_3N_F]WCl$ in the presence of ^tBuNC.[11] The results described above are puzzling and no satisfactory explanation of them has been arrived at to date.

Complex **2** can be accessed through the ligand exchange reaction depicted in equation 4. Exposure of benzene solutions of $[N_3N]Mo(N_2)$ to one equivalent of CO results in a color change from orange to emerald green over the course of 15 min and **2** can be isolated from the reaction as green needles in 85% yield. If an excess of CO is used in this reaction a mixture of **2** and $[N_3N]MoCOTMS$ (**3**, see below) is formed. Complex **3** presumably arises from intermolecular migration of a TMS group and the formation of **3** serves to further illustrate the susceptibility of the $[N_3N]^{3-}$ ligand to degradation via Si-N bond cleavage (see Chapter 1).

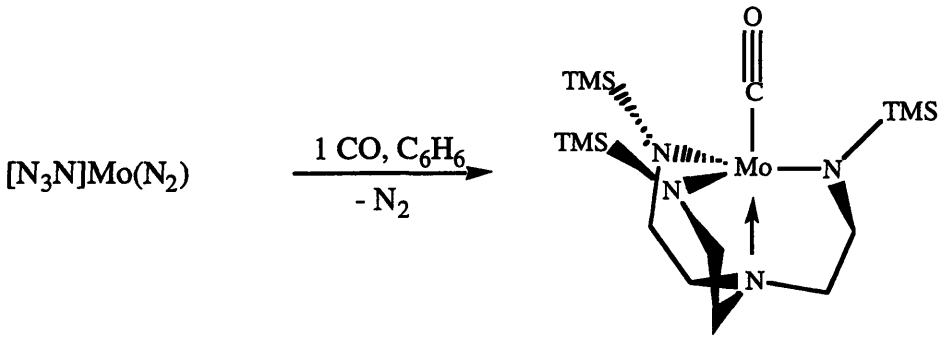

2

(4)

The ^1H NMR spectrum of **2** consists of two broad resonances at 13.17 and -38.04 ppm for the methylene protons of the ligand backbone and a sharper resonance at -2.03 ppm which is assigned to the TMS groups of the ligand. This spectrum is reminiscent of the ^1H NMR spectrum of $[N_3N]Mo(N_2)$ (see Chapter 1) and the observation of a high field and a low field resonance for

References begin on page 137

the methylene protons with the TMS resonance falling between them is characteristic of $[N_3N]Mo(L)$ complexes with the exception of **1** (see above). The IR spectrum of **2** in pentane has a strong, sharp C-O stretch at 1859 cm^{-1} which lies on the low end of the range of typical stretching frequencies for neutral, terminal CO complexes,[15] indicating that there is considerable backbonding from the metal into the π^* orbitals of the CO ligand. The IR spectrum of **2** in Nujol exhibits two strong absorptions at 1841 and 1832 cm^{-1}. A similar trend of one absorption being observed in solution and two absorptions observed in the solid state is seen in the IR spectra of $[N_3N]Mo(N_2)$ and in that case we attribute the two absorptions in the solid state spectrum to the presence of two molecules in the unit cell (see Chapter 1).

Efforts to reduce $[N_3N]WCl$ have been unsuccessful but $[N_3N]W(CO)$ has been prepared in low yield by exposure of $[N_3N]WCl$ or $[N_3N]WI$ to excess carbon monoxide.[16] A comparison of the position of the CO stretches in the IR spectra of **2**, $[N_3N]W(CO)$ and $[N_3N_F]W(CO)$[11] is instructive. The C-O stretch for $[N_3N]W(CO)$ in Nujol is found at 1789 cm^{-1}, 40-50 cm^{-1} lower than the corresponding stretch for **2**, consistent with the more reducing nature of tungsten compared to molybdenum. The IR spectrum of $[N_3N_F]W(CO)$ in Nujol reveals a C-O stretch at 1846 cm^{-1} which is almost identical to the position of that of **2** suggesting that the extent of backbonding is similar in these complexes and that substitution of W for Mo is offset by the more electron-withdrawing nature of the $[N_3N_F]^{3-}$ ligand.

Heating C_6D_6 solutions of **2** at 80 °C for one week results in a slight darkening of the color of the solution. ^1H NMR spectroscopy reveals the presence of ~10% $[N_3N]MoCOTMS$ (**3**), reinforcing Si-N bond cleavage as a common decomposition route for complexes containing the $[N_3N]^{3-}$ ligand.

SQUID magnetic susceptibility data for solid **2** are plotted versus temperature in Figure 3.2. The data reveal that **2** behaves as a Curie paramagnet over the temperature range 5-300 K and fitting the data to the Curie law yields $\mu = 1.74(1)\ \mu_B$ ($R = 0.9998$), a value that is close to the spin-only moment for a system containing one unpaired electron.

References begin on page 137

Figure 3.2. Plot of χ_m (corrected for diamagnetism using Pascal's constants) versus T for $[N_3N]Mo(CO)$ (**2**).

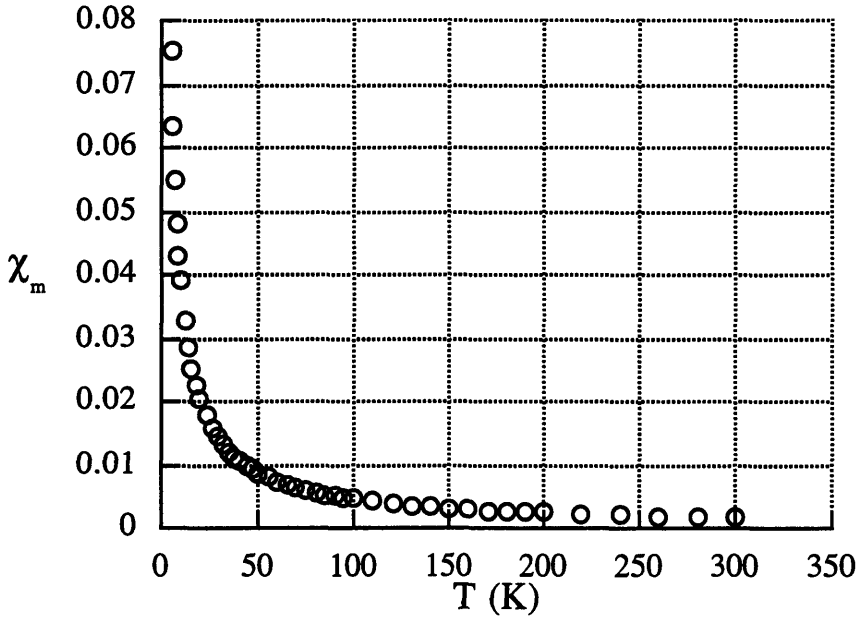

When THF solutions of **2** are stirred over magnesium powder in the presence of TMSCl a color change from deep green to yellow is observed over the course of fifteen minutes. The diamagnetic oxycarbyne complex $[N_3N]MoCOTMS$ (**3**) can be isolated from the reaction as pale yellow needles in 91% yield (equation 5). In the absence of TMSCl, two other diamagnetic complexes are observed by ^1H NMR spectroscopy and are tentatively formulated as $\{[N_3N]Mo(CO)\}_2Mg(THF)_2$ and $\{[N_3N]Mo(CO)\}MgCl(THF)_2$, the CO analogs of $\{[N_3N]Mo(N_2)\}_2Mg(THF)_2$ and $\{[N_3N]Mo(N_2)\}MgCl(THF)_2$, respectively (see Chapter 1). No attempt has been made to isolate these complexes. The ^1H NMR spectrum of **3** consists of two TMS resonances and a pair of triplets for the methylene protons on the ligand backbone. The ^{13}C NMR spectrum of **3** also reveals TMS groups in two environments and the resonance for the alkylidyne carbon is found at 208.3 ppm. The IR spectrum of **3** taken in Nujol does not have a readily assignable C-O stretch. The formation of **3** is perhaps not surprising in light of the documented propensity for tungsten and molybdenum triamidoamine complexes to form strong M-

References begin on page 137

E bonds (E = CR, N, P, As)[1] and analogs of **3**, namely [N_3N]WCOTMS[6] and [N_3N_F]WCOTMS,[11] have been synthesized in our laboratory. In general though, siloxycarbyne

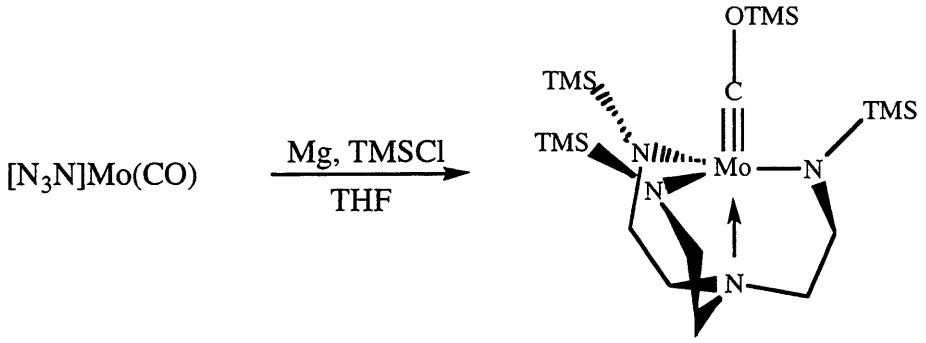

3

(5)

complexes are rare, although examples such as M(CO)($COSiR_3$)$(DMPE)_2$ (M= V,[17] Ta,[18,19] Nb[18]) have been isolated as intermediates in the reductive coupling of CO to form acetylene diethers at V, Ta and Nb metal centers.

Alkyl- and Arylisocyanide Complexes

As with carbon monoxide, no reaction is observed between [N_3N]MoCl and magnesium powder in the presence of one equivalent of ^{t}BuNC. However, paramagnetic [N_3N]Mo(CN^tBu) (**4**) can be isolated from the reduction of [N_3N]MoCl by Na/Hg amalgam in the presence of ^{t}BuNC but the reaction is not clean and **4** is contaminated with [N_3N]MoCl. A clean, high-yielding route to **4** was found in the reaction of [N_3N]Mo(N_2) with ^{t}BuNC (equation 6). Upon addition of ^{t}BuNC to toluene solutions of [N_3N]Mo(N_2) a color change to deep orange is discernible and **4** is isolated from the reaction as rust-colored needles in 96% yield. The ^{1}H NMR spectrum of **4** exhibits broad resonances at 13.37 and -39.00 ppm for the methylene protons of the TREN ligand, the resonances for the ^{t}Bu and TMS groups being observed at 3.76 and 0.12 ppm, respectively. The IR spectrum of **4** in Nujol has a broad absorption at 1838 cm^{-1} (free ^{t}BuNC = 2143 cm^{-1}). This value should be compared with that of [N_3N_F]W(CN^tBu) (1684 cm^{-1}), the crystal structure of which revealed that the isocyanide ligand is quite bent (C-N-C = 132.2(10)°).[11]

This result and the low C-N stretching frequency were attributed to extensive π backbonding from the metal center to the isocyanide ligand and it was suggested that $[N_3N_F]W(CN^tBu)$ is best formulated as a W(V) imido carbene complex. The higher C-N stretching frequency of **4** suggests that the degree of π backbonding is less in **4** and that it contains a linear isocyanide ligand and so is best viewed as a Mo(III) isocyanide complex.

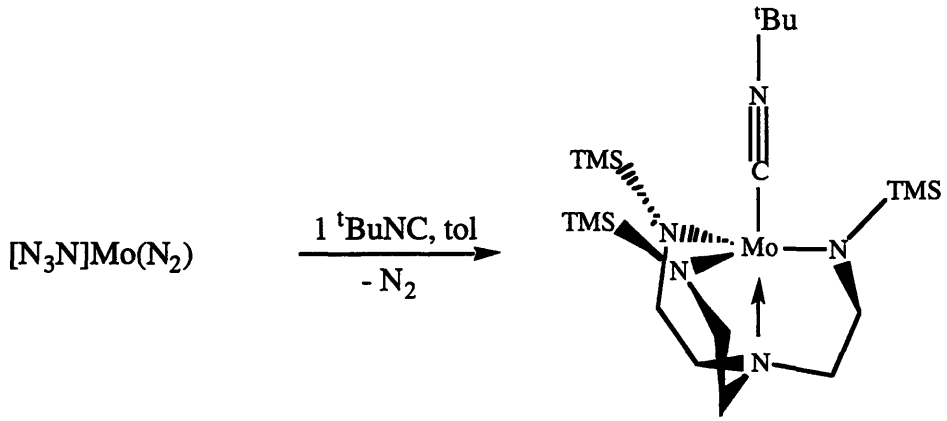

4 (6)

SQUID magnetic susceptibility measurements on solid **4** have been carried out and a plot of the molar magnetic susceptibility versus temperature is shown in Figure 3.3. Like **1** and **2**, **4** behaves as a Curie paramagnet over the temperature range 5-300 K and the data can be fit to the Curie law yielding $\mu = 1.74(1)\ \mu_B$, consistent with **4** being a low spin d^3 complex with one unpaired electron.

4 reacts smoothly with ferrocenium triflate in THF to give $\{[N_3N]Mo(CN^tBu)\}OTf$ (**5**) quantitatively as a burnt-orange powder. The ^1H NMR spectrum of **5** is typical of d^2 $[N_3N]Mo$ complexes, the resonances for the methylene protons of the ligand backbone (-29.38 and -98.14 ppm) occurring upfield of the resonance attributed to the TMS groups of the ligand (12.83 ppm). The C-N stretching frequency of **5** in THF appears at 2147 cm^{-1}, reflecting the weak π backbonding from the cationic d^2 metal center compared to that of the d^3 metal center of **4**. Efforts to crystallize **5** have been unsuccessful and so satisfactory elemental analyses have not been obtained.

SQUID magnetic susceptibility measurements on **5** over the temperature range 5-300 K reveal a behavior analogous to that observed for $[N_3N]MoMe$ and $[N_3N]MoCl$ (χ approaches a constant as T approaches 0 K),[8] and which we now assume to be characteristic of paramagnetic d^2 $[N_3N]Mo$ complexes of this general type (Figure 3.4). The data can be fit to the Curie-Weiss law ($\chi = \mu^2/8(T-\theta)$) over the temperature range 30-300 K (μ = 2.71(4) μ_B, θ = -5(1) K), consistent with two unpaired electrons being present. In C_3-symmetric triamidoamine complexes the frontier π orbitals (d_{xz} and d_{yz}) are strictly degenerate and in **5** we assume these orbitals are singly-occupied giving rise to two unpaired spins in the molecule. In contrast to **5**, $\{[N_3N_F]W(CN^tBu)\}OTf$[11] is diamagnetic suggesting that backbonding from tungsten into the π^* orbitals of the isocyanide ligand is sufficient to break the degeneracy of the d_{xz}/d_{yz} orbitals.

4 does not decompose in solution when stored at room temperature for a period of days according to ^1H NMR spectroscopy. However, **4** proved to be thermally unstable at elevated temperatures and upon heating toluene solutions of **4** to 86 °C for 36 h, a color change from orange to yellow is observed. If the thermolysis is carried out in C_6D_6 in a sealed NMR tube, ^1H NMR spectra of the crude reaction mixture reveal three broad, paramagnetically-shifted resonances at 7.73, -25.7 and -112.4 ppm suggesting formation of a new C_3-symmetric complex. Resonances at 4.80, 1.61 and 0.95 ppm are also observed and are assigned to isobutylene, isobutane and hexamethylethane, products arising from the disproportionation and coupling of ^{t}Bu radicals. $[N_3N]MoCN$ (**6**) can be isolated from the reaction as a yellow, crystalline solid in 88% yield. A C-N stretch could not be located in the IR spectrum of **6**. It should be noted that the IR spectrum of the analogous tungsten complex, $[N_3N]WCN$,[16] also lacks an absorption in the region 2200-2000 cm^{-1}.

The reaction depicted in equation 7, that is, formation of a cyanide complex via dealkylation of an isocyanide complex has some precedent in the literature. Upon refluxing in ethanol, $[(^tBuNC)_7Mo]^{2+}$ loses a carbonium ion to form $[(^tBuNC)_6Mo(CN)]^+$, although the organic products of the reaction were not isolated.[20] Reaction of $[(^tBuNC)_7Mo]^{2+}$ with zinc in THF yields $[(^tBuNC)_4Mo(^tBuHNCCNH^tBu)(CN)]^+$, a product in which both reductive coupling and

Figure 3.3. Plot of χ_m (corrected for diamagnetism using Pascal's constants) versus T for [N_3N]Mo(CN^{t}Bu) (**4**).

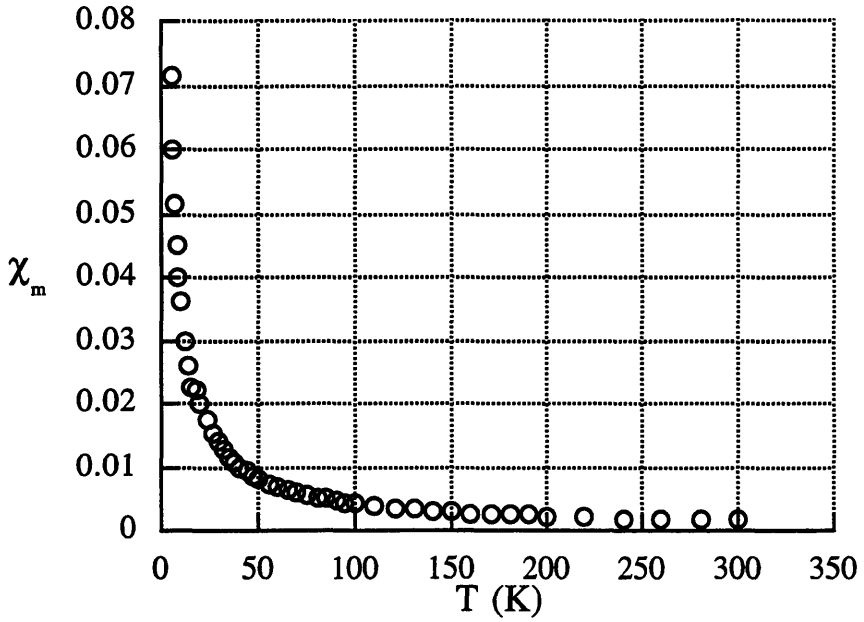

Figure 3.4. Plot of χ_m (corrected for diamagnetism using Pascal's constants) versus T for {[N_3N]Mo(CN^{t}Bu)}OTf (**5**).

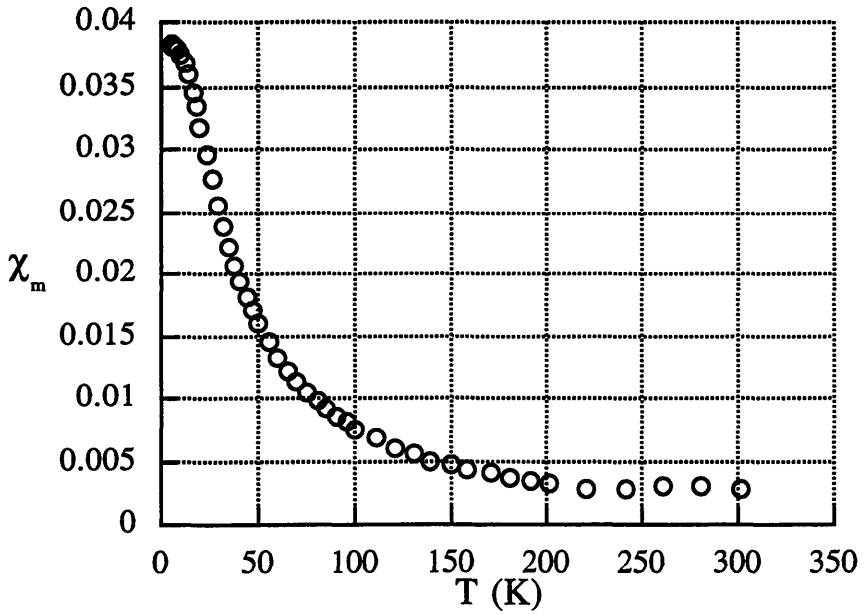

References begin on page 137

dealkylation of the isocyanide ligands has occurred.[21] Perhaps the most closely related example to **6** is that of *trans*-$Mo(CN)_2(Me_8[16]aneS_4)$ ($Me_8[16]aneS_4$ = 3,3,7,7,11,11,15,15,-octamethyl-1,5,9,13-tetrathiacyclohexadecane).[22] The precursor complex, $Mo(CN)(^tBuNC)(Me_8[16]aneS_4)$ is formed by a ligand exchange reaction from the bis-dinitrogen complex and it decomposes even at -30 °C to the dicyanide complex.

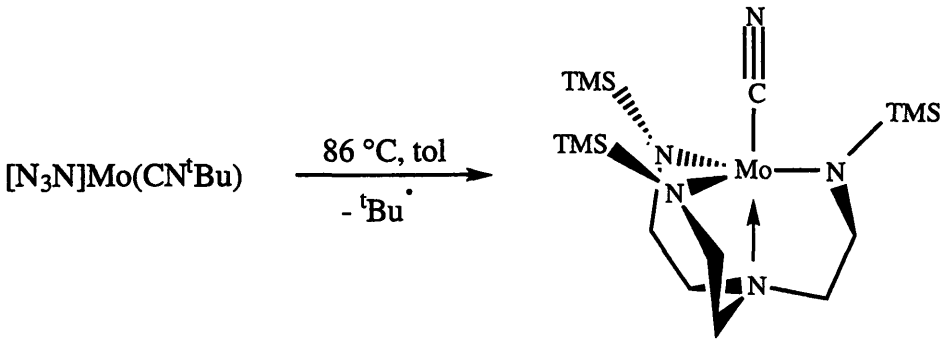

6

(7)

Single crystals of **6** were grown from saturated diethyl ether solutions at -30 °C and examined in an X-ray study; a half a molecule of diethyl ether was found in the unit cell. Crystallographic data and collection and refinement parameters are given in Table 3.1. The molecular structure of **6** along with the atom-labeling scheme is shown in Figure 3.5 while selected bond lengths, bond angles and dihedral angles are listed in Table 3.2. As expected, the structure of **6** bears a striking resemblance to that of $[N_3N]MoCl$.[23] The $Mo\text{-}N_{amide}$ bond distances are statistically identical in the two complexes, as are the $Mo\text{-}N_{ax}$ bond distances. In **6** and $[N_3N]MoCl$ the TMS groups are all oriented upright with the $N_{ax}\text{-}Mo\text{-}N_{eq}\text{-}Si$ dihedral angles close to 180°, indicative of little steric pressure within the pocket. For comparison, in $[N_3N]MoOTf$ the dihedral angles range from 136-143° as the TMS groups twist in response to the presence of the sterically-bulky triflate ligand within the pocket.[8] The Mo-C(7) and C(7)-N(5) bond lengths of 2.182 and 1.113 Å in **6** are close to the corresponding bond lengths in *trans*-$Mo(CN)_2(Me_8[16]aneS_4)$ (2.219(7) and 1.086(10) Å, respectively).[22]

Figure 3.5. A view of the structure of [N_3N]MoCN (**6**).

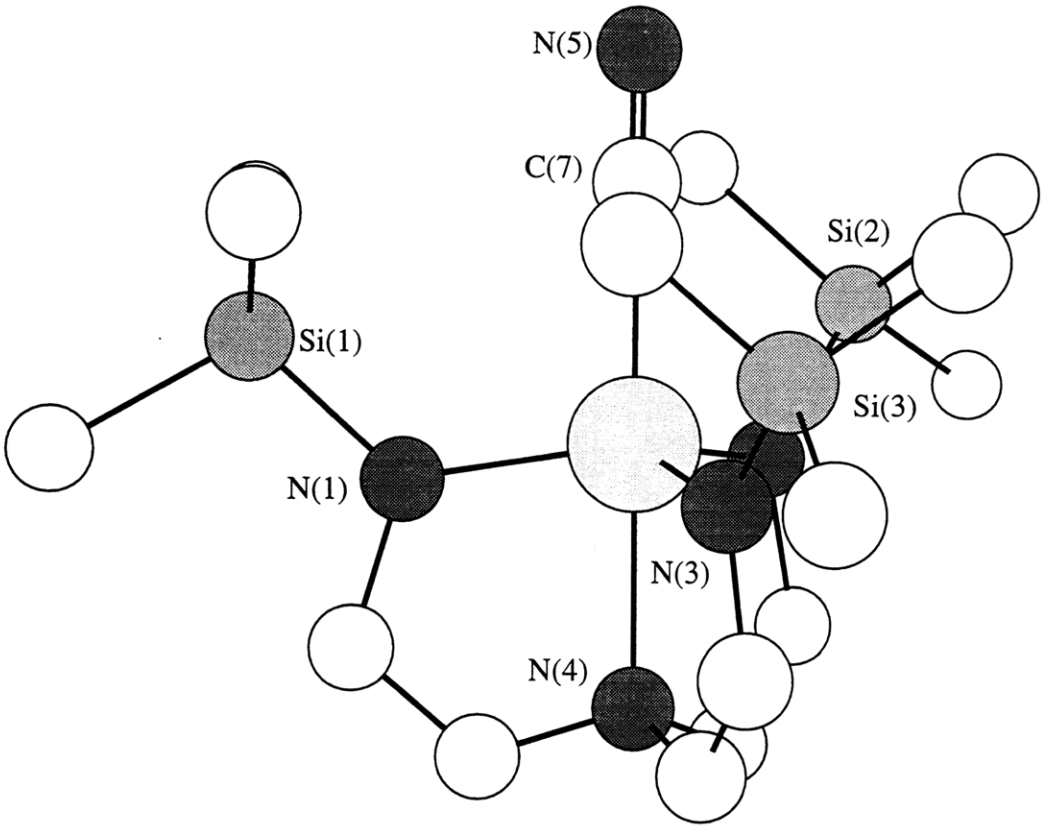

A plot of the molar magnetic susceptibility of **6** versus temperature is shown in Figure 3.6 and is characteristic of paramagnetic d^2 [N_3N]MoX complexes of this general type (see **5** above). The data can be fit to the Curie-Weiss law ($\chi = \mu^2/8(T-\theta)$) over the temperature range 30-300 K to give μ = 2.73(1) μ_B and $\theta = -7.1(3)$. A plot of μ_{eff} versus temperature for **6** is shown in Figure 3.7 and illustrates how μ_{eff} decreases rapidly below 50 K. Similar behavior has been observed for [N_3N]MoCl[8] and is attributed to a combination of spin-orbit coupling and low-symmetry ligand field components that result in zero field splitting of the d^2 ground-state spin triplet.[24]

References begin on page 137

Table 3.1. Crystallographic data, collection parameters and refinement parameters for **6** and **8**.

	6	**8**
Empirical Formula	$C_{18}H_{44}MoN_5O_{0.50}Si_3$	$C_{15}H_{38}MoN_4Si_3$
Formula Weight	518.79	454.70
Diffractometer	SMART/CCD	SMART/CCD
Crystal Dimensions (mm)	0.37 x 0.32 x 0.23	0.60 x 0.43 x 0.34
Crystal System	Tetragonal	Monoclinic
Space Group	$P\bar{4}2_1m$	$P2_1/n$
a (Å)	16.5384(4)	8.972(3)
b (Å)	16.5384(4)	17.308(4)
c (Å)	9.8908(3)	15.398(3)
α (°)	90	90
β (°)	90	100.61(3)
γ (°)	90	90
V (Å^3), Z	2705.32(12), 4	2350.2(11), 4
D_{calc} (Mg/m^3)	1.274	1.285
Absorption coefficient (mm^{-1})	0.633	0.716
F_{000}	1100	960
Temperature (K)	183(2)	188(2)
Θ range for data collection (°)	1.74 to 23.23	1.79 to 23.26
Reflections collected	11177	9331
Unique Reflections	2052	3337
R	0.0292	0.0231
R_w	0.0320	0.0242
GoF	0.936	1.125

References begin on page 137

Table 3.2. Selected bond lengths and bond angles for $[N_3N]MoCN$ (**6**).

Bond Lengths (Å)					
Mo-C(7)	2.182(6)	Mo-N(1)	1.980(5)	Mo-N(2)	1.970(3)
Mo-N(3)	1.970(3)	Mo-N(4)	2.210(5)	C(7)-N(5)	1.113(8)

Bond Angles (deg)			
Mo-C(7)-N(5)	179.8(6)	C(7)-Mo-N(4)	179.1(2)
N(1)-Mo-N(2)	118.54(11)	N(1)-Mo-N(3)	118.53(11)
Si(1)-N(1)-Mo	128.1(2)	Si(2)-N(2)-Mo	128.3(3)
N(1)-Mo-N(4)	80.9(2)	N(2)-Mo-N(4)	80.92(12)

Dihedral Angles (deg)[a]			
N(4)-Mo-N(3)-Si(3)	179.34	N(4)-Mo-N(2)-Si(2)	-179.55
N(4)-Mo-N(1)-Si(1)	-180.00	N(4)-Mo-C(7)-N(5)	0.00

[a]Obtained from a Chem-3D Drawing

References begin on page 137

Figure 3.6. Plot of χ_m (corrected for diamagnetism using Pascal's constants) versus T for [N_3N]MoCN (**6**).

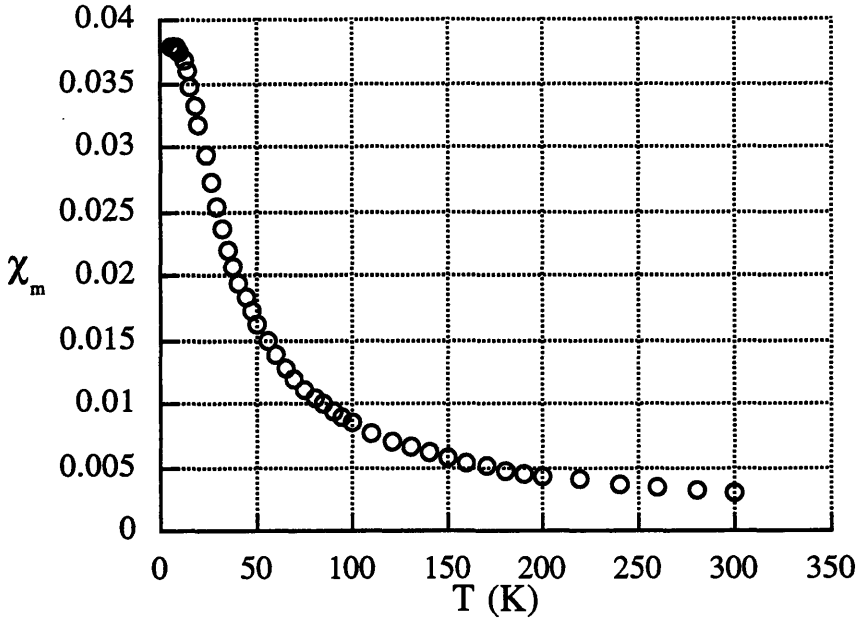

Figure 3.7. Plot of μ_{eff} versus T for [N_3N]MoCN (**6**).

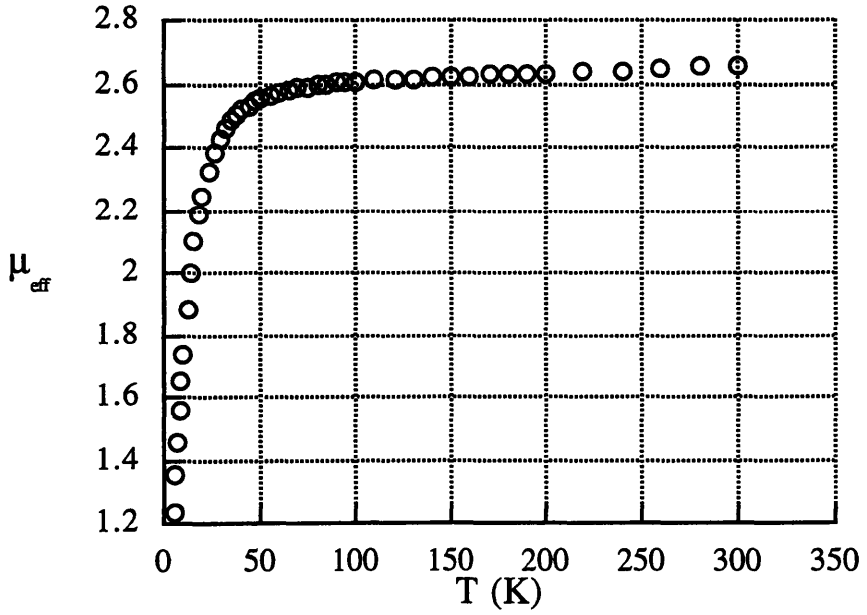

Reaction of $[N_3N]Mo(N_2)$ with ArNC (Ar = 2,6-$Me_2C_6H_3$) yields $[N_3N]MoCNAr$ (**7**) in good yield as deep red plates. Unlike **4**, **7** is thermally stable and C_6D_6 solutions of **7** show no evidence for decomposition when heated to 80 °C for 12 h. The C-N stretch for **7** is found at 1740 cm^{-1} and lies between that of the linear (1959 cm^{-1}) and bent (1658 cm^{-1}) PhNC ligands of *trans*-$Mo(PhNC)_2(Me_8[16]aneS_4)$.[22]

Attempted Synthesis of Other $[N_3N]Mo(III)$ Complexes

Attempts to synthesize $[N_3N]Mo(L)$ complexes where L is a σ donor such as a phosphine or nitrile have been unsuccessful. $[N_3N]MoCl$ is reduced by magnesium in the presence of two equivalents of PMe_3. If the reaction is carried out under dinitrogen, ^1H NMR spectroscopy reveals the presence of two diamagnetic complexes whose resonances are consistent with their formulation as $\{[N_3N]Mo(N_2)\}_2Mg(PMe_3)_2$ and $\{[N_3N]Mo(N_2)\}MgCl(PMe_3)_2$. Carrying out the reaction in the absence of dinitrogen yields $[bitN_3N]Mo$ (**8**, see below) and $[N_3N]MoH$ as the only identifiable species according the ^1H NMR spectroscopy. It is abundantly clear from these observations that PMe_3 does not inhibit reduction (unlike CO and ^tBuNC). Arguably, $[N_3N]Mo(PMe_3)$ may not be accessible on steric grounds and reactions with other phosphines have not been attempted. However, attempts to synthesize $[N_3N_F]W(PMe_3)$ have also been unsuccessful despite the larger bowl-like pocket of these complexes.[11] It appears that d_π-p_π backbonding is an important component of the bonding picture in $[N_3N]Mo(L)$ complexes and is inherent to their stability. If $[N_3N]Mo(PMe_3)$ is generated in situ, the weak π acceptor ability of PMe_3 would render this ligand extremely labile and easily replaced by dinitrogen. $[N_3N]Mo(NCCH_3)$ has also proved inaccessible. $[N_3N]MoCl$ is not reduced by magnesium in THF in the presence of two equivalents of acetonitrile. Similarly, no reaction is observed when acetonitrile is used as the solvent and in both cases $[N_3N]MoCl$ is recovered. Furthermore, the dinitrogen ligand in $[N_3N]Mo(N_2)$ does not undergo exchange with CH_3CN. Since $[N_3N]W(PhNNPh)(H)$ has been isolated,[6] synthesis of $[N_3N]Mo(PhNNPh)$ seemed a reasonable

proposition on steric grounds. Unfortunately, once again our efforts were thwarted by the inability of magnesium to reduce [N_3N]MoCl in the presence of azobenzene.

Synthesis and Reactivity of [bitN_3N]Mo

In an attempt to isolate the elusive trigonal monopyramidal complex [N_3N]Mo, we began to explore the reduction of [N_3N]MoCl in the absence of donor ligands. Reaction of [N_3N]MoCl with magnesium powder in an evacuated vessel over the course of seven days leads to a color change from orange to blood-red. ^1H NMR spectra of the crude reaction mixture taken under dinitrogen reveal the presence of two paramagnetic products, one of which is readily identified as the known hydride complex, [N_3N]MoH.[8] The second product, [bitN_3N]Mo (**8**) exhibits eight resonances between +19 ppm and -126 ppm and has apparent mirror symmetry (equation 8). **8** can be separated from [N_3N]MoH by recrystallization from hexamethyldisiloxane and is isolated as a blood-red, crystalline solid in good yield.

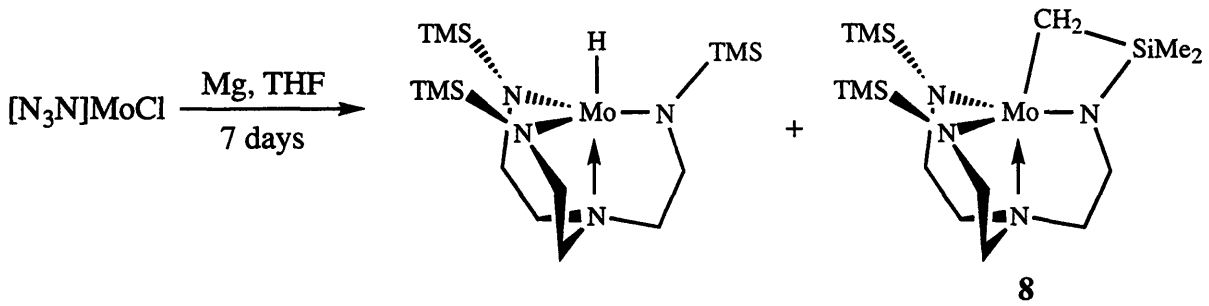

8

(8)

The molecular structure of **8** was confirmed by an X-ray study. Single crystals of **8** were grown from saturated hexamethyldisiloxane solutions at -20 °C. Crystallographic data, collection parameters, and refinement parameters for **8** are given in Table 3.1. The molecular structure of **8** (two views) along with the atom-labeling scheme are shown in Figure 3.8 while selected bond lengths, bond angles and dihedral angles are given in Table 3.3. The Mo-C(11) bond is somewhat longer than the Mo-C bonds in [N_3N]MoMe[8] (2.188 Å) and [N_3N]Mo(cyclohexyl)[8] (2.167 Å) but

References begin on page 137

Figure 3.8. Two views of the structure of [bitN_3N]Mo (**8**).

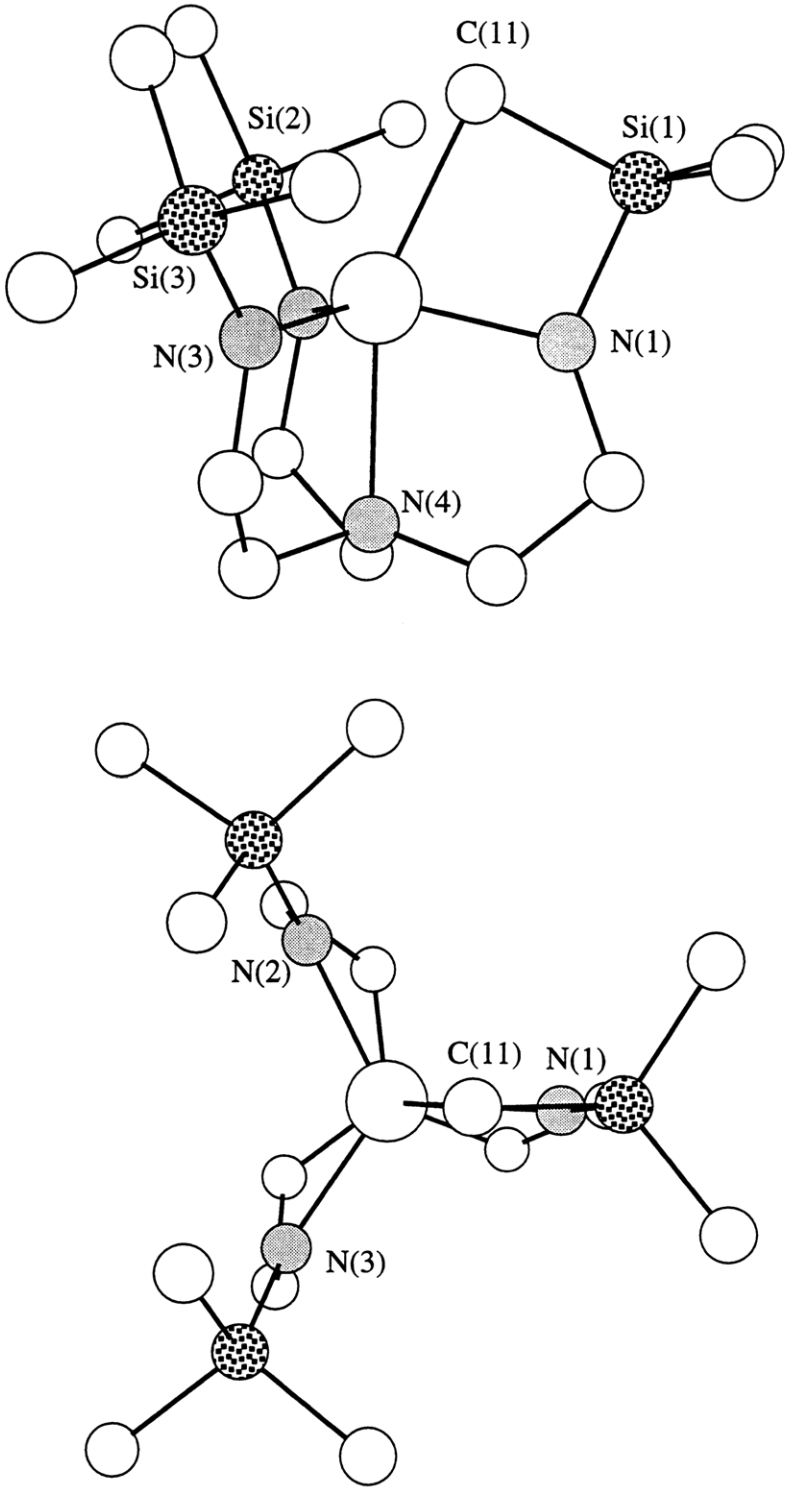

Table 3.3. Selected bond lengths and bond angles for **8**.

Bond Lengths (Å)

Mo-N(1)	1.948(2)	Mo-N(2)	1.983(2)	Mo-N(3)	1.994(2)
Mo-N(4)	2.237(2)	Mo-C(11)	2.249(3)	N(1)-Si(1)	1.734(2)
N(2)-Si(2)	1.743(2)	N(3)-Si(3)	1.743(2)	C(11)-Si(1)	1.849(3)
C(22)-Si(2)	1.873(3)	C(33)-Si(3)	1.869(3)		

Bond Angles (deg)

Mo-N(1)-Si(1)	102.30(10)	Mo-N(2)-Si(2)	127.08(10)
Mo-N(3)-Si(3)	125.87(11)	N(1)-Si(1)-C(11)	92.93(11)
N(2)-Si(2)-C(22)	108.99(11)	N(3)-Si(3)-C(33)	110.56(12)
Mo-C(11)-Si(1)	88.35(10)	N(1)-Mo-C(11)	76.13(9)
N(4)-Mo-C(11)	155.16(8)	N(1)-Mo-N(2)	116.95(8)
N(1)-Mo-N(3)	118.27(8)	N(2)-Mo-N(3)	116.83(8)
N(1)-Mo-N(4)	79.03(8)	N(2)-Mo-N(4)	81.40(8)
N(3)-Mo-N(4)	81.20(7)		

Dihedral Angles (deg)[a]

N(4)-Mo-N(1)-Si(1)	176.08	N(4)-Mo-N(2)-Si(2)	178.86
N(4)-Mo-N(3)-Si(3)	170.94	Mo-N(1)-Si(1)-C(11)	-3.99

[a]Obtained from a Chem-3D Drawing

References begin on page 137

the Mo-N_{amide} bond distances are comparable to those found in **6** and the N_{ax}-Mo-N_{eq}-Si dihedral angles are all close to 180° consistent with little steric strain in the molecule. The Mo atom lies 0.325 Å out of the plane defined by the amide nitrogens in the direction of C(11) and the four-membered ring is almost planar (Mo-N(1)-Si(1)-C(11) = -4°). The absence of distortion in the MoN_4 core is somewhat surprising in view of the presence of the Mo-C-Si-N ring and relatively small N(4)-Mo-C(11) angle (155.16(8)°). **8** has approximate mirror symmetry in the solid state as highlighted by the view down the Mo-N(4) axis and is in complete accord with the NMR data. Since resonances for protons on carbons bound directly to Mo are not observed for paramagnetic [N_3N]Mo(alkyl) complexes, presumably due to their proximity to the paramagnetic center, eight resonances would be expected and are observed in the ^{1}H NMR spectrum of **8**. Although C-H activation in TMS amido complexes is relatively well-known,[25-28] X-ray structures of complexes that contain a MNSiC ring are rare.[29-31] One such species is $Zr[CH_2SiMe_2N(SiMe_3)]_2(dmpe)$[29] which contains two planar, four-membered metallacyclic rings analogous to that found in **8** (C-Zr-N = 76°; Zr-N-Si = 97°; N-Si-C = 99°; Si-C-Zr = 87°).

A plot of the molar magnetic susceptibility of **8** versus temperature is shown in Figure 3.9 and is similar to other d^2 complexes (see **5** and **6** above). Fitting the data to the Curie-Weiss law ($\chi = \mu^2/8(T-\theta)$) over the temperature range 30-300 K yields μ = 2.84(1) and 2.53(1) μ_B and θ = -4.1(4) and -3.4(3) K (2 runs).

8 is thermally stable and ^{1}H NMR spectra of toluene-d_8 solutions of **8** show no evidence for decomposition when heated to 90 °C under dinitrogen or under vacuum for one week. Andersen has demonstrated that related thorium and uranium metallacycles undergo insertion reactions with CO and ^{t}BuNC to yield five-membered metallacyclic complexes resulting from formal insertion of ^{t}BuNC and CO into a silicon-carbon bond.[32] The dimeric metallacyclic complex, $\{[(Me_3Si)_2N]V[\mu\text{-}CH_2SiMe_2N(SiMe_3)]\}_2$ also reacts with CO in a similar manner[30] and so an investigation of addition/insertion reactions of **8** was undertaken. However, **8** does not react with ethylene or CO but exposure of THF solutions of **8** to D_2 (1 atm) results in a color change from blood-red to yellow over a period of 2 days. [d_1-N_3N]MoD (**9**) is formed quantitatively

References begin on page 137

Table 3.4. Selected characterization data for paramagnetic $[N_3N]Mo$ complexes.

Complex	% Yield	Morphology	μ_{so}	μ_{eff}
$[N_3N]MoC_2H_4$ (**1**)	97	purple needles	1.73	1.73
$[N_3N]MoCO$ (**2**)	85	green needles	1.73	1.77
$[N_3N]MoCN^tBu$ (**4**)	96	rust needles	1.73	1.74
$\{[N_3N]MoCN^tBu\}OTf$ (**5**)	92	orange powder	2.83	2.71
$[N_3N]MoCN$ (**6**)	88	yellow cubes	2.83	2.73
$[N_3N]MoCNAr$ (**7**)	62	red plates	1.73	na
$[bitN_3N]Mo$ (**8**)	72	red cubes	2.83	2.87
$[d_1\text{-}N_3N]MoD$ (**9**)	100	yellow needles	2.83	2.83

Figure 3.9. Plot of χ_m (corrected for diamagnetism using Pascal's constants) versus T for $[bitN_3N]Mo$ (**8**).

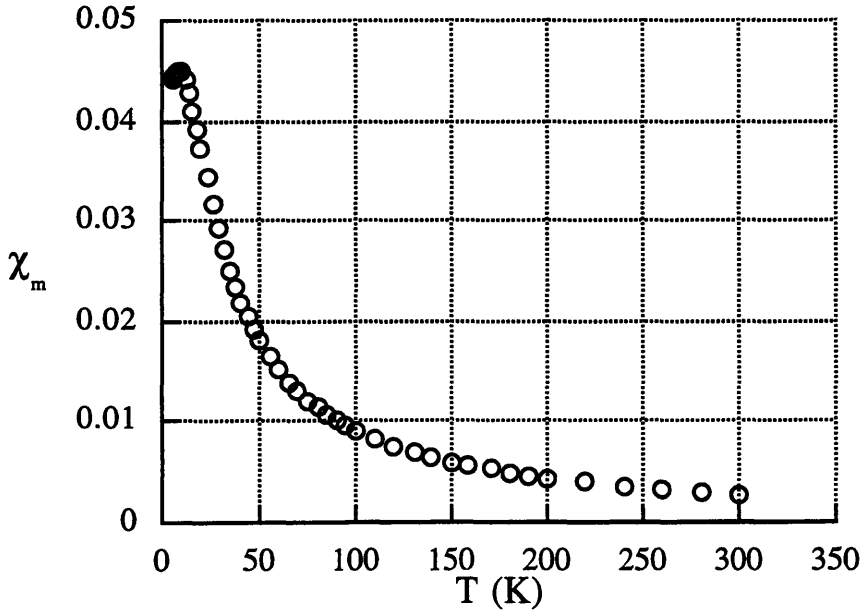

References begin on page 137

according to ^{1}H NMR spectroscopy and the ^{2}H NMR spectrum of **9** in benzene reveals a singlet at 16.48 ppm indicating that the second deuterium is located in a TMS group of the ligand (equation 9). The reversibility of the cyclometallation reaction has been confirmed by Dr. Scott Seidel and upon heating toluene solutions of [N_3N]MoH to 105 °C formation of **8** and dihydrogen is observed.[8] SQUID magnetic susceptibility data for **9** can be fit to the Curie-Weiss law over the temperature range 30-300 K yielding $\mu = 2.87(3)\ \mu_B$ and $\theta = -0.2(6)$.

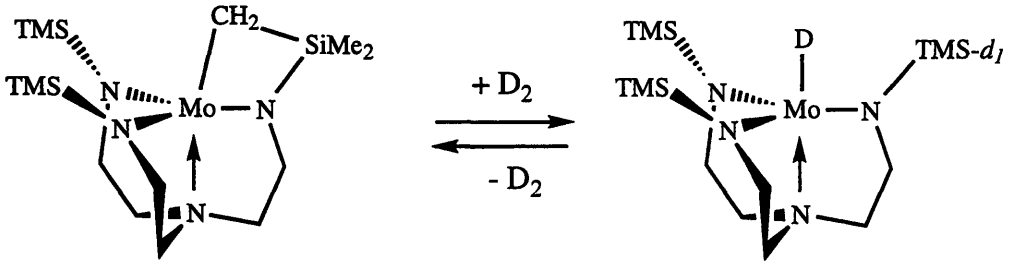

9 (9)

8 reacts rapidly with ^{t}BuNC and upon addition of ^{t}BuNC to a toluene solution of **8** an immediate and dramatic color change to deep green is evident. This green color fades within minutes to give a clear, orange solution. The product (**10**) can be isolated by crystallization from hexamethyldisiloxane as orange, diamagnetic crystals (equation 10, TMS groups of **10** omitted for clarity). The ^{1}H NMR spectrum of **10** in C_6D_6 has multiple resonances for the methylene protons

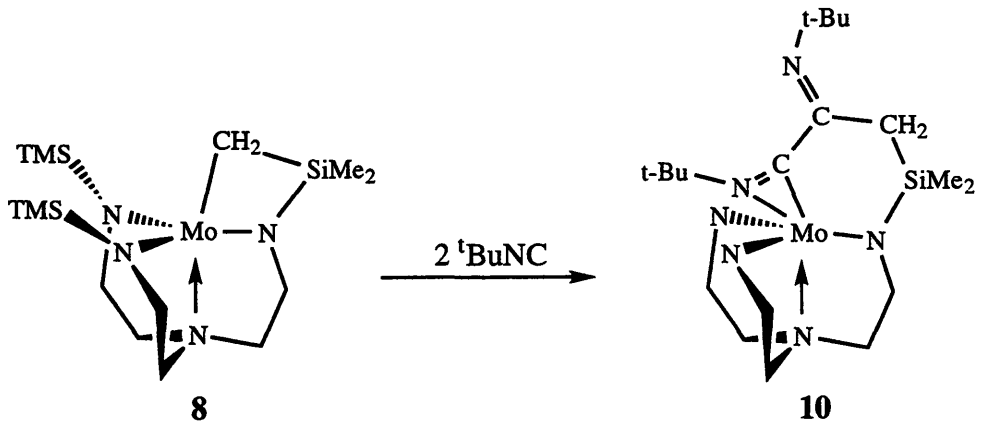

8 **10** (10)

of the ligand backbone and a pair of singlets at 1.50 and 1.45 ppm integrate for 18H, consistent with incorporation of two equivalents of ^{t}BuNC. A single resonance is observed for the TMS

groups of the ligand and the presence of a plane of symmetry in **10** is confirmed by the ^{13}C NMR spectrum which exhibits four resonances for the methylene carbons of the ligand backbone. The ^{13}C NMR spectrum also reveals quaternary carbon resonances at 247.4 and 167.2 ppm. The IR spectrum of **10** has a strong absorption at 1586 cm^{-1}, characteristic of a C-N double bond stretch. On the basis of the available data, **10** is tentatively formulated as an η^2-iminoacyl imine complex as shown in equation 10, the downfield shifts in the ^{13}C NMR spectrum of the quaternary carbons being characteristic of the iminoacyl and imine functionalities (247.4 and 167.2 ppm respectively). Insertion of isocyanides into metal-carbon bonds[33-35] and coupling of isocyanides at metal centers[36-38] are well-documented reactions. Futhermore, Zr[39] and Hf[40] metallacyclobutane complexes have been shown to undergo double insertion/coupling reactions with ^{t}BuNC, analogous to that proposed for **8**, yielding related η^2-iminoacyl imine complexes.

DISCUSSION

The central theme of the chemistry discussed in this chapter is the use of $[N_3N]Mo(N_2)$ to synthesize organometallic complexes of molybdenum in the relatively rare oxidation state of 3+ via ligand exchange reactions. However, we have not determined whether these reactions are proceeding via an associative or dissociative mechanism. In general, $[N_3N]Mo(L)$ complexes cannot be synthesized directly by reduction of $[N_3N]MoCl$ in the presence of the appropriate ligand for reasons that are not entirely clear. $[N_3N]Mo(L)$ complexes show a tendency to be oxidized to Mo(IV) complexes either by treatment with an oxidant or, as in the case of $[N_3N]Mo(CN^tBu)$ (**4**), by expulsion of an organic radical. In the case of $[N_3N]Mo(C_2H_4)$ (**1**), the ethylene ligand is lost upon oxidation consistent with the bonding picture in $[N_3N]Mo(C_2H_4)$ being closer to the Dewar-Chatt model rather than the metallacyclopropane model.

In general, comparison of the reactivity of $[N_3N]Mo(L)$ complexes with that of the analogous $[N_3N_F]Mo(L)$ complexes has not been possible, as the organometallic chemistry of such complexes is relatively unexplored. However, comparisons with $[N_3N_F]W(L)$ complexes have been made where possible and reveal striking differences between the two systems. For

References begin on page 137

example, both {[N_3N_F]W(C_2H_4)}OTf[11] and {[N_3N_F]W(CN^{t}Bu)}OTf[11] are diamagnetic whereas {[N_3N]Mo(CN^{t}Bu)}OTf (**5**) is paramagnetic. The diamagnetism of the [N_3N_F]W complexes might be explained by an increase in d_π-p_π backbonding as would be expected for tungsten relative to molybdenum i.e."oxidation" to W(VI). Alternatively, it may indicate coordination of triflate in these complexes. Such coordination of triflate would break the degeneracy of the d_{xz}/d_{yz} orbitals, accounting for the observed diamagnetism. In contrast, coordination of triflate in **5** is unlikely due to steric congestion in the apical pocket as a result of the bulky TMS groups on the ligand.

An interesting difference between [N_3N]Mo and [N_3N]W complexes has also been uncovered. As evidenced by the mode of synthesis, [N_3N]MoCN (**6**) is thermally stable, in stark contrast to the behavior of [N_3N]WCN which decomposes at room temperature yielding two diamagnetic products.[16] Neither of these products was fully characterized but it was proposed that one arose from the intermolecular coupling of cyanide ligands by analogy to the coupling of acetylides in [N_3N]Mo complexes.[41] In light of the X-ray structure and paramagnetism of [N_3N]MoCN we are confident in our formulation of [N_3N]MoCN as a monomeric cyanide complex.

The mechanism by which [bitN_3N]Mo (**8**) might be formed deserves some comment. We propose that [N_3N]MoCl is reduced by magnesium to {[N_3N]MoCl}$^-$ which loses Cl^- to form the trigonal monopyramidal species **A** (equation 11). Oxidative addition of a C-H bond of a TMS group of the ligand to the metal center, possibly in a reversible manner, yields the Mo(V) species **B**. Loss of a hydrogen radical then produces **8**. The fate of the hydrogen radical is uncertain (equation 12). It may react with **A** to give [N_3N]MoH. Alternatively, coupling of two hydrogen

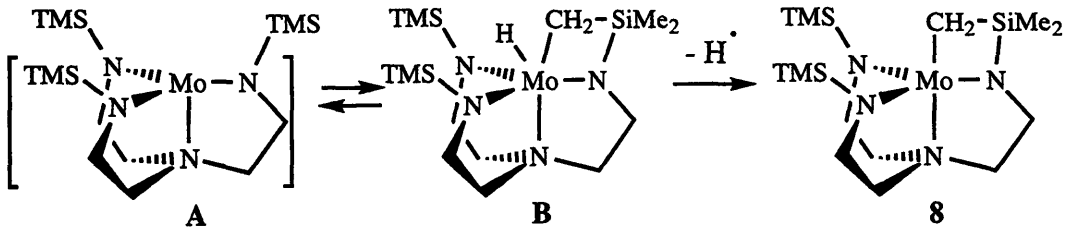

(11)

References begin on page 137

radicals would produce dihydrogen which could then react with **8** to give $[N_3N]MoH$ (see equation 9 above). Either of these scenarios would lower the yield of **8** and ^1H NMR spectra of the crude reaction mixture indicate that $[N_3N]MoH$ and **8** are formed in an approximate ratio of 1:4. The related complex $[bitN_3N]Ti$ has been synthesized by thermal decomposition of

$$[N_3N]MoH \xleftarrow{A} H^{\cdot} \xrightarrow{+H^{\cdot}} H_2 \xrightarrow{8} [N_3N]MoH \qquad (12)$$

$[N_3N]Ti(s\text{-}Bu)$ and upon heating $[N_3N]Ti(s\text{-}Bu)$ in the presence of dihydrogen a resonance attributed to the Ti(IV) hydride complex is observed by ^1H NMR spectroscopy.[28] Also, $[N_3N]WH$ decomposes slowly upon heating to 85 °C to give the known trihydride complex, $[N_3N]W(H)_3$ and a complex possessing mirror symmetry which was purported to be $[bitN_3N]W$ but which was not isolated.[16] These observations confirm that $[N_3N]MH$ complexes where M = Ti, Mo, W are, to varying degrees, susceptible to cyclometallation reactions via C-H activation of a TMS group of the ligand and that, in some cases, this reaction is reversible.

A major impetus for this work was to determine whether the trigonal monopyramidal complex $[N_3N]Mo$ could be isolated. First row analogs of this complex from titanium to iron have been synthesized and were found to be high-spin.[2] The related trigonal complex $Mo[N(C(CD_3)_2CH_3)(3,5\text{-}Me_2C_6H_3)]_3$ is also isolable and has a high-spin configuration.[42] A detailed investigation of the dinitrogen chemistry of $[N_3N]Mo$ complexes (see Chapter 1) suggests that a low-spin configuration of $[N_3N]Mo$ is optimal to bind dinitrogen. In such a configuration the presence of an empty orbital on the metal center would also render $[N_3N]Mo$ susceptible to oxidative addition reactions which are proposed to account for the formation of $[bitN_3N]Mo$ (see above). These results suggest that $[N_3N]Mo$ is an unstable species and that its high energy and reactivity could be a consequence of its low-spin configuration. Clearly, isolation of a molybdenum trigonal monopyramidal complex in TREN-based systems will require employment of a more robust ligand.

References begin on page 137

EXPERIMENTAL PROCEDURES

General Details. All experiments were performed under a nitrogen atmosphere in a Vacuum Atmospheres drybox or by standard Schlenk techniques unless otherwise specified. Pentane was washed with sulfuric acid / nitric acid (95/5 v/v), sodium bicarbonate, and water, stored over calcium chloride, and distilled from sodium benzophenone ketyl under nitrogen. Toluene was distilled from sodium, and CH_2Cl_2 was distilled from CaH_2. Anhydrous diethyl ether and THF were sparged with nitrogen and passed through alumina columns.[43] Hexamethyldisiloxane was purchased from Aldrich, dried over sodium and then vacuum transferred into a small storage flask. All solvents were stored in the dry box over activated 4 Å molecular sieves.

NMR data were obtained at 300 or 500 MHz (^1H), 75.4 MHz (^{13}C), 46.0 MHz (^2H) and 282 MHz (^{19}F). Chemical shifts are listed in parts per million downfield from tetramethylsilane for proton and carbon. ^{19}F chemical shifts are listed in parts per million downfield from $CFCl_3$ as an external standard and ^2H NMR spectra were referenced to external C_6D_6. Coupling constants are listed in Hertz. Spectra were obtained at 25 °C unless otherwise noted. Benzene-d_6 and toluene-d_8 were pre-dried on CaH_2, vacuum transferred onto sodium and benzophenone, stirred under vacuum for two days and then vacuum transferred into small storage flasks and stored over molecular sieves. THF-d_8 was dried over sodium and vacuum transferred into a small storage flask and stored over molecular sieves. $[N_3N]MoCl$[8] and ferrocenium triflate[44] were prepared as described in the literature. Magnesium powder, ^{t}BuNC, ethylene, carbon monoxide and TMSCl were purchased from commercial vendors and used as received.

Elemental analyses (C, H, N) were performed in our laboratory using a Perkin-Elmer 2400 CHN analyzer or by Microlytics Analytical Laboratories of Deerfield MA. X-ray data were collected on Siemens SMART/CCD diffractometer and general experimental details are described in the literature.[45]

SQUID Magnetic Susceptibility Measurements. Measurements were carried out on a Quantum Design SQUID magnetometer. Data were obtained at a field strength of 5000

References begin on page 137

Gauss. Straws and gel caps (Gelatin Capsule No. 4 Clear) were purchased from Quantum Design. The sample was prepared in the drybox by the following method. A gel cap and a square of parafilm were weighed. The sample was placed in the gel cap and the parafilm inserted above it. The gel cap was closed and the mass of the sample was ascertained by weighing the loaded gel cap. The gel cap was placed in a straw which was then mounted on the sample rod and placed in the magnetometer. Two runs were performed on the sample - one from 5 to 300 K and a second from 300 to 5 K. Measurements were made at the following increments: 5-10 K (every 1 K), 10-20 K (every 2 K), 20-50 K (every 3 K), 50-100 K (every 5 K), 100-200 K (every 10 K), 200-300 K (every 20 K).

$[N_3N]MoC_2H_4$ (1). $[N_3N]MoCl$ (650 mg, 1.32 mmol) was dissolved in 15 mL THF and placed in a glass bomb with a stirring bar and magnesium powder (64 mg, 2.67 mmol). The vessel was sealed and subjected to three freeze-pump-thaw cycles to remove any dinitrogen present. Ethylene (~5eqs) was condensed onto the frozen solution. Upon thawing the solution was stirred for 12 h during which time the color of the solution changed from orange/red to purple. The solvent was removed in vacuo and the residue extracted with 20 mL pentane. After filtration through Celite, the pentane was removed in vacuo to give a purple solid. Recrystallization from hexamethyldisiloxane at -20 °C afforded the product as purple needles; yield 623 mg (97%). ^1H NMR(C_6D_6) δ 3.63 (TMS). $\mu = 1.73\ \mu_B$. Anal. Calcd. for $C_{17}H_{43}N_4Si_3Mo$: C, 42.21; H, 8.96; N, 11.58. Found: C, 42.39; H, 9.31; N, 11.55.

$[N_3N]Mo(CO)$ (2). $[N_3N]Mo(N_2)$ (100 mg, 0.21 mmol) was dissolved in 5 mL of benzene and sealed in a 25 mL bomb. The solution was subjected to two freeze-pump-thaw cycles and 1 equivalent of carbon monoxide was introduced. Over 15 min the solution changed color from orange-red to emerald green. After 3 h the solvent was removed in vacuo and the residue extracted with 5 mL of pentane. The pentane solution was cooled to -20 °C to give the product as green needles; yield 85 mg (85%). ^1H NMR(C_6D_6) δ 13.17 (CH_2), -2.03 (TMS), -38.04 (CH_2). IR(Nujol, cm^{-1}) 1841, 1832 (C-O). IR(Pentane, cm^{-1}) 1859 (C-O). $\mu = 1.77\ \mu_B$. Anal. Calcd.

References begin on page 137

for $C_{16}H_{39}N_4Si_3MoO$: C, 39.73; H, 8.13; N, 11.58. Found: C, 39.54; H, 8.18; N, 11.55.

[N_3N]MoCOTMS (3). [N_3N]MoCO (100 mg, 0.21 mmol) was dissolved in 5 mL of THF. Magnesium powder (20 mg, 0.87 mmol) and TMSCl (45 μL, 0.36 mmol) were added and the mixture was stirred for 3.5 h. The solvent was removed in vacuo and the residue extracted with 7 mL of pentane. The pentane solution was filtered through a pad of Celite and the volume was reduced to 3 mL. The pentane solution was cooled to -20 °C to give the product as pale yellow needles; yield 105 mg (91%). ^{1}H NMR(C_6D_6) δ 3.48 (t, NCH_2CH_2N), 3.24 (t, NCH_2CH_2N), 0.49 (s, TMS), 0.40 (s, TMS). ^{13}C NMR(C_6D_6) δ 208.34 (Mo*C*OTMS), 53.53 (NCH_2CH_2N), 52.56 (NCH_2CH_2N), 5.07 (TMS), 2.55 (TMS). Anal. Calcd. for $C_{19}H_{48}N_4Si_4MoO$: C, 40.98; H, 8.69; N, 10.06. Found: C, 40.69; H, 8.70; N, 10.07.

[N_3N]Mo(CN^{t}Bu) (4). [N_3N]Mo(N_2) (150 mg, 0.31 mmol) was dissolved in 5 mL of toluene and cooled to -20 °C. ^{t}BuNC (39 mg, 0.47 mmol) was added to the solution which was allowed to stir overnight. The solvent was removed in vacuo to give an orange residue. The product was obtained as rust needles by crystallization from diethyl ether; yield 160 mg (96%). ^{1}H NMR(C_6D_6) δ 13.37 (CH_2), 3.76 (^{t}Bu), 0.12 (TMS), -39.00 (CH_2). IR(Nujol, cm^{-1}) 1838 (br, C-N). μ = 1.74 μ_B.

{[N_3N]Mo(CN^{t}Bu)}OTf (5). [N_3N]Mo(CN^{t}Bu) (110 mg, 0.20 mmol) was dissolved in 4 mL of THF and cooled to -20 °C. FcOTf (68 mg, 0.20 mmol) was added to the solution and the reaction was stirred for 25 min. The solvent was removed in vacuo and the residue was washed with 20 mL of pentane to remove ferrocene. The residue was dried to give the product as a burnt orange powder; yield 129 mg (92%). ^{1}H NMR(THF-d_8) δ 12.83 (TMS), 9.28 (^{t}Bu), -29.38 (CH_2), -98.14 (CH_2). ^{19}F NMR(THF-d_8) δ -78.64 (CF_3SO_3). IR(THF, cm^{-1}) 2147 (C-N). μ = 2.71 μ_B. Efforts to crystallize **5** were unsuccessful and so elemental analyses were not attempted.

[N_3N]Mo(CN) (6). [N_3N]Mo(CN^{t}Bu) (65 mg, 0.12 mmol) was dissolved in 6 mL of toluene and sealed in a bomb. The solution was heated to 86 °C for 36 h during which time the color changed from orange to yellow. The solvent was removed and the yellow solid was washed

References begin on page 137

with cold pentane; yield 51 mg (88%). ^{1}H NMR(C_6D_6) δ 7.73 (TMS), -25.7 (CH_2), -112.4 (CH_2). μ = 2.73 μ_B. Anal. Calcd. for $C_{16}H_{39}N_5Si_3Mo$: C, 39.89; H, 8.16; N, 14.54. Found: C, 39.72; H, 8.31; N, 14.55.

[N_3N]MoCNAr (7). [N_3N]Mo(N_2) (75 mg, 0.16 mmol) was dissolved in 4 mL of toluene and cooled to -20 °C. 2,6-$Me_2C_6H_3NC$ (25 mg, 0.19 mmol) was dissolved in 1 mL of toluene and added to the stirred solution of [N_3N]Mo(N_2). After 1 h the toluene was removed in vacuo and the residue extracted with 7 mL of hexamethyldisiloxane. After filtering, the solution was cooled to -20 °C to afford the product as red plates; yield 56 mg (62%, not optimized). ^{1}H NMR(C_6D_6) δ 61.90 (NCH_2CH_2N, $\Delta\nu_{1/2}$ = 509 Hz), 37.15 (ArH, $\Delta\nu_{1/2}$ = 138 Hz), 1.87 (TMS, $\Delta\nu_{1/2}$ = 47 Hz), -0.66 (CH_3, $\Delta\nu_{1/2}$ = 156 Hz)), -29.81 (NCH_2CH_2N, $\Delta\nu_{1/2}$ = 276 Hz), -68.85 (ArH, $\Delta\nu_{1/2}$ = 882 Hz). IR(Nujol, cm^{-1}) 1740 (C-N). Anal. Calcd. for $C_{24}H_{48}N_5Si_3Mo$: C, 49.12; H, 8.24; N, 11.93. Found: C, 48.93; H, 8.31; N, 11.82.

[bitN_3N]Mo (8). [N_3N]MoCl (500 mg, 1.02 mmol) was dissolved in 13 mL THF and placed in a bomb. Magnesium powder (30 mg, 1.23 mmol) was added and the bomb was sealed. The vessel was subjected to three freeze-pump-thaw cycles to remove any dinitrogen present and the solution was stirred under vacuum. After 7 days the solvent was removed in vacuo and the residue extracted with 15 mL of pentane and filtered to give a blood-red solution. The pentane was removed to give the crude product as a red solid (420 mg) that was (according to its ^{1}H NMR spectrum) a 1:4 mixture of [N_3N]MoH and [bitN_3N]Mo. The crude yield of [bitN_3N]Mo (in the mixture) therefore is 72%. Pure [bitN_3N]Mo was obtained by recrystallization of the crude product from hexamethyldisiloxane. ^{1}H NMR(C_6D_6) δ 18.58 (CH_2), 14.81 (TMS), 1.10 ($SiMe_2$), -18.95 (CH_2), -20.26 (CH_2), -98.65 (CH_2), -103.55 (CH_2), -125.06 (CH_2). μ = 2.87 μ_B. Anal. Calcd. for $C_{15}H_{38}N_4Si_3Mo$: C, 39.62; H, 8.42; N, 12.32. Found: C, 39.74; H, 8.73; N, 12.39.

[d_1-N_3N]MoD (9). [bitN_3N]Mo (95 mg, 0.21 mmol) was dissolved in 5 mL THF and placed in a glass bomb with a stirring bar. The vessel was sealed and subjected to two freeze-pump-thaw cycles. D_2 (1 atm) was introduced and the solution stirred for 2 days during which

References begin on page 137

time the color of the solution changed from blood-red to yellow. The solvent was removed and the solid recrystallized from pentane as yellow needles; the yield was quantitative: ^{2}D NMR (C_6H_6) δ 16.48 ($Si(CH_3)_2CH_2D$, $\Delta\nu_{1/2}$ = 6 Hz). μ = 2.83 μ_B.

Reaction of [bitN$_3$N]Mo with ^{t}BuNC to give 10. [bitN$_3$N]Mo (96 mg, 0.21 mmol) was dissolved in 3 mL toluene and cooled to -20 °C. ^{t}BuNC (36 μL, 0.32 mmol) was added to the stirred solution of [bitN$_3$N]Mo. After 2.5 h the toluene was removed in vacuo to give an orange oil. The oil was extracted with 2 mL of hexamethyldisiloxane, filtered and cooled to -20 °C to afford the product as orange crystals; yield 75 mg (58%, not optimized). ^{1}H NMR(C_6D_6) δ 4.21 (t, 2H, NCH_2CH_2N), 3.55-3.30 (m, 4H, NCH_2CH_2N), 2.73 (s, 2H, CH_2), 2.25 (t, 2H, NCH_2CH_2N), 2.21-2.01 (m, 4H, NCH_2CH_2N), 1.50 (s, 9H, ^{t}Bu), 1.45 (s, 9H, ^{t}Bu), 0.50 (s, 18H, TMS), 0.45 (s, 6H, $Si(CH_3)_2$). ^{13}C NMR(C_6D_6) δ 247.35 (s, Mo*C*NC$(CH_3)_3$), 167.21 (s, Mo(C(N^{t}Bu)*C*(N^{t}Bu)CH_2), 58.71 (s, MoCN*C*$(CH_3)_3$), 53.40 (t, NCH_2CH_2N), 53.35 (t, NCH_2CH_2N), 52.80 (s, MoCN*C*$(CH_3)_3$), 52.54 (t, NCH_2CH_2N), 51.43 (t, NCH_2CH_2N), 33.02 (q, C(*C*H$_3)_3$), 32.34 (q, C(*C*H$_3)_3$), 29.50 (t, Mo*C*H$_2$Si), 5.01 (q, $Si(CH_3)_3$), 3.08 (q, $Si(CH_3)_2$). IR(Nujol, cm^{-1}) 1586 (C-N). Anal. Calcd. for $C_{25}H_{56}N_6Si_3Mo$: C, 48.36; H, 9.09; N, 13.53. Found: C, 48.18; H, 9.52; N, 13.36.

REFERENCES

(1) Schrock, R. R. *Acc. Chem. Res.* **1997**, *30*, 9.

(2) Cummins, C. C.; Lee, J.; Schrock, R. R.; Davis, W. M. *Angew. Chem., Int. Ed. Engl.* **1992**, *31*, 1501.

(3) Cummins, C. C.; Schrock, R. R.; Davis, W. M. *Angew. Chem.* **1993**, *115*, 758.

(4) Mösch-Zanetti, N. C.; Schrock, R. R.; Davis, W. M.; Wanninger, K.; Seidel, S. W.; O'Donoghue, M. B. *J. Am. Chem. Soc.* **1997**, *119*, 11037.

(5) Schrock, R. R.; Shih, K. -Y.; Dobbs, D.; Davis, W. M. *J. Am. Chem. Soc.* **1995**, *117*, 6609.

(6) Dobbs, D. A.; Schrock, R. R.; Davis, W. M. *Inorg. Chem. Acta.* **1997**, *263*, 171.

(7) Kol, M.; Schrock, R. R.; Kempe, R.; Davis, W. M. *J. Am. Chem. Soc.* **1994**, *116*, 4382.

(8) Schrock, R. R.; Seidel, S. W.; Mösch-Zanetti, N. C.; Shih, K. -Y.; O'Donoghue, M. B.; Davis, W. M.; Reiff, W. M. *J. Am. Chem. Soc.* **1997**, *119*, 11876.

(9) Freundlich, J.; Schrock, R. R.; Cummins, C. C.; Davis, W. M. *J. Am. Chem. Soc.* **1994**, *116*, 6476.

(10) Freundlich, J. S.; Schrock, R. R.; Davis, W. M. *Organometallics* **1996**, *15*, 2777.

(11) Seidel, S. W., Ph.D. Thesis, MIT, 1998.

(12) Neuner, B.; Schrock, R. R. *Organometallics* **1996**, *15*, 5.

(13) O'Connor, C. J. *Prog. Inorg. Chem.* **1982**, *29*, 203.

(14) K. -Y. Shih, unpublished observations.

(15) Collman, J. P.; Hegedus, L. S.; Norton, J. R.; Finke, R. G. *Principles and Applications of Organotransition Metal Chemistry*; 2nd ed.; University Science Books: Mill Valley, CA, 1987.

(16) D. A. Dobbs, unpublished observations.

(17) Protasiewicz, J. D.; Lippard, S. J. *J. Am. Chem. Soc.* **1991**, *113*, 6564.

(18) Vrtis, R. N.; Liu, S.; Rao, C. P.; Bott, S. G.; Lippard, S. J. *Organometallics* **1991**, *10*, 275.

(19) Protasiewicz, J. D.; Bronk, B. S.; Masschelein, A.; Lippard, S. J. *Organometallics* **1994**, *13*, 1300.

(20) Giandomenico, C. M.; Hanau, L. H.; Lippard, S. J. *Organometallics* **1982**, *1*, 142.

(21) Dewan, J. C.; Giandomenico, C. M.; Lippard, S. J. *Inorg. Chem.* **1981**, *20*, 4069.

(22) Adachi, T.; Nobuyoshi, S.; Ueda, T.; Kaminaka, M.; Yoshida, T. *J. Chem. Soc., Chem. Commun.* **1989**, 1320.

(23) Duan, Z.; Verkade, J. G. *Inorg. Chem.* **1995**, *34*, 1576.

(24) Figgis, B. N.; Lewis, J. *Prog. Inorg. Chem.* **1964**, *6*, 37.

(25) Turner, H. W.; Simpson, S. J.; Andersen, R. A. *J. Am. Chem. Soc.* **1979**, *101*, 2782.

(26) Simpson, S. J.; Andersen, R. A. *Inorg. Chem.* **1981**, *20*, 2991.

(27) Simpson, S. J.; Andersen, R. A. *Inorg. Chem.* **1981**, *20*, 3627.

(28) Cummins, C. C.; Schrock, R. R.; Davis, W. M. *Organometallics* **1992**, *11*, 1452.

(29) Planalp, R. P.; Andersen, R. A. *Organometallics* **1983**, *2*, 1675.

(30) Berno, P.; Minhas, R.; Hao, S.; Gambarotta, S. *Organometallics* **1994**, *13*, 1052.

(31) Putzer, M. A.; Magull, J.; Goesmann, H.; Neumüller, B.; Dehnicke, K. *Chem. Ber.* **1996**, *129*, 1401.

(32) Simpson, S. J.; Andersen, R. A. *J. Am. Chem. Soc.* **1981**, *103*, 4063.

(33) Yamamoto, Y.; Yamazaki, H. *Coord. Chem. Rev.* **1972**, *8*, 225.

(34) Singleton, E.; Oosthuizen, H. E. *Adv. Organomet. Chem.* **1983**, *22*, 209.

(35) Durfee, L. D.; Rothwell, I. P. *Chem. Rev.* **1988**, *88*, 1059.

(36) Filippou, A. C.; Grünleitner, W.; Völkl, C.; Kiprof, P. *J. Organomet. Chem.* **1991**, *413*, 181.

(37) Filippou, A. C.; Völkl, C.; Kiprof, P. *J. Organomet. Chem.* **1991**, *415*, 375.

(38) Carnahan, E. M.; Protasiewicz, J. D.; Lippard, S. J. *Acc. Chem. Res.* **1993**, *26*, 90.

(39) Berg, F. J.; Petersen, J. L. *Organometallics* **1989**, *8*, 2461.

(40) Berg, F. J.; Petersen, J. L. *Organometallics* **1993**, *12*, 3890.

(41) Shih, K. -Y.; Schrock, R. R.; Kempe, R. *J. Am. Chem. Soc.* **1994**, *116*, 8804.

(42) Laplaza, C. E.; Johnson, M. J. A.; Peters, J. C.; Odom, A. L.; Kim, E.; Cummins, C. C.; George, G. N.; Pickering, I. J. *J. Am. Chem. Soc.* **1996**, *118*, 8623.

(43) Pangborn, A. B.; Giardello, M. A.; Grubbs, R. H.; Rosen, R. K.; Timmers, F. J. *Organometallics* **1996**, *15*, 1518.

(44) Schrock, R. R.; Sturgeoff, L. G.; Sharp, P. R. *Inorg. Chem.* **1983**, *22*, 2801.

(45) Rosenberger, C.; Schrock, R. R.; Davis, W. M. *Inorg. Chem.* **1997**, *36*, 123.

CHAPTER 4

Living ROMP of Norbornadienes Employing Tungsten Oxo Alkylidene Complexes

A portion of the material covered in this chapter has appeared in print:

O'Donoghue, M. B., Schrock, R. R., LaPointe, A. M., Davis, W. M. *Organometallics* **1996**, *15*, 1334.

INTRODUCTION

The ring-opening metathesis polymerization (ROMP) of strained cyclic olefins is an important application of the olefin metathesis reaction.[1,2] Previous work in our group[3-5] and others[6] has shown that well-defined molybdenum imido alkylidene complexes of the general type $Mo(CHR)(NAr)(OR')_2$ (Ar = 2,6-$^{i}Pr_2C_6H_3$; R = CMe_2Ph, ^{t}Bu; OR' = $O^{t}Bu$, $OC(CF_3)_2CH_3$, $OC(CF_3)_3$) are effective catalysts for the ROMP of norbornadienes. Key findings of these extensive studies include observations that $Mo(CH^{t}Bu)(NAr)(O^{t}Bu)_2$ will effect the polymerization of 2,3-bis(trifluoromethyl)norbornadiene (NBDF6) yielding all trans, highly tactic polymers whereas employment of $Mo(CHCMe_2Ph)(NAr)[OCCH_3(CF_3)_2]_2$ yields all cis polymers with a bias toward one tacticity.[3,6] Furthermore, the cis/trans content of polymers produced employing $Mo(CHCMe_2Ph)(N\text{-}2\text{-}^{t}BuC_6H_4)(BiphenoBu_4)$ ($BiphenoBu_4$ = 2,2'-[4,4',6,6'-$^{t}Bu_4$]$(C_6H_2)_2O_2$) was found to be highly temperature dependent, with the cis content increasing with decreasing temperature.[7] Studies on the interconversion of *syn* and *anti* rotamers in these systems and their relative rates of reactivity with norbornadienes led to the proposal that *syn* propagating alkylidene species give rise to cis double bonds in the polymer whereas *anti* propagating species yield trans double bonds.[8] The tacticity in these systems does not appear to be linked to the formation of cis or trans double bonds but is controlled by the chirality of the β carbon in the growing polymer in a process known as chain end control. If sequential monomer units add to the same CNO face of the catalyst then an isotactic polymer results whereas if sequential monomer units approach alternate CNO faces then a syndiotactic polymer results. In an elegant study utilizing enantiomerically pure monomers,[5] it has been shown that cis polymers produced employing $Mo(CHCMe_2Ph)(NAr)[OC(CF_3)_3]_2$ are isotactic whereas trans polymers produced employing $Mo(CHCMe_2Ph)(NAr)(O^{t}Bu)_2$ are syndiotactic. Chiral molybdenum imido alkylidene complexes have also been synthesized[9,10] and complexes such as $Mo(CHCMe_2Ph)(NAr')[(\pm)BINO(SiMe_2Ph)_2]$[9] (Ar' = N-2,6-$Me_2C_6H_3$) polymerize norbornadienes presumably via enantiomorphic site control to give polymers that are all cis and isotactic.

References begin on page 174

In the development of new ROMP catalysts, symmetrically-substituted norbornadienes are particularly useful as probe monomers for several reasons. First, a wide variety may be readily prepared via a Diels-Alder reaction of cyclopentadiene with substituted acetylenes. Second, the substituted double bond is not attacked for steric reasons. Third, the symmetric substitution avoids head/tail, head/head and tail/tail regiochemistries thereby simplifying characterization of the polymer by ^{13}C NMR spectroscopy. Therefore, the four most likely regular structures of 2,3-disubstituted norbornadienes are as shown in Figure 4.1.

Figure 4.1. The four most likely regular structures of 2,3-disubstituted norbornadienes.

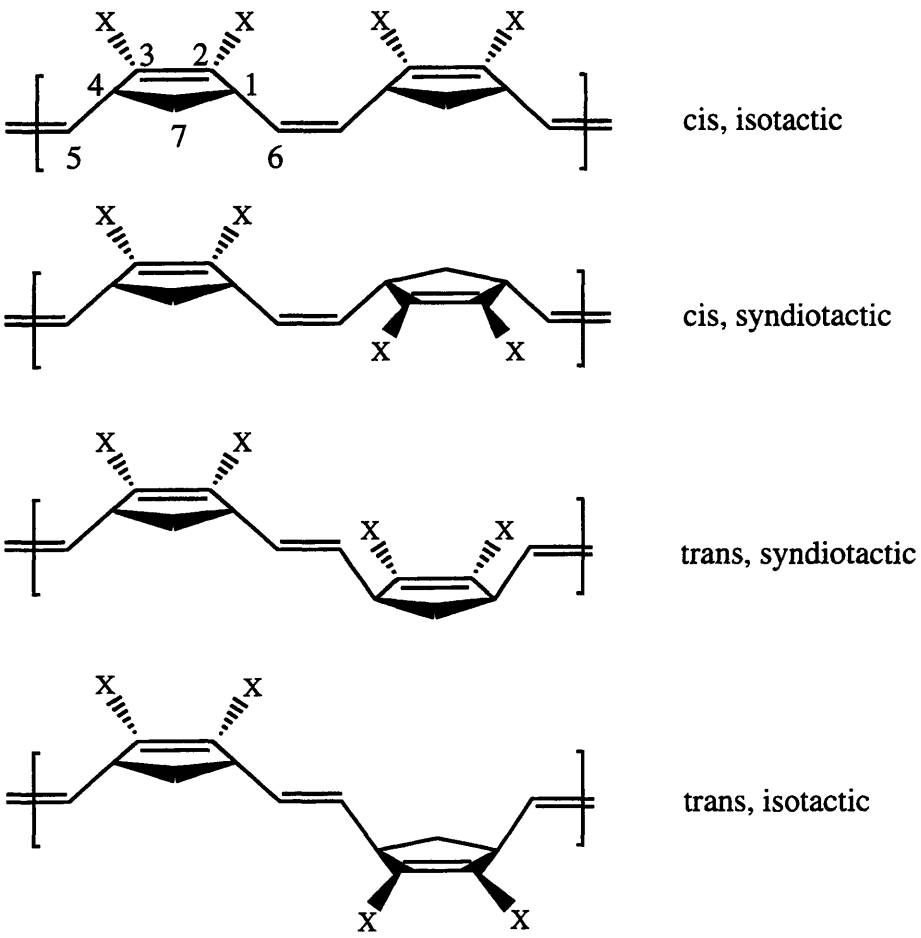

Although imido alkylidene complexes are efficient ROMP catalysts, a study of related oxo alkylidene complexes is warranted since there is a good possibility that many classical olefin

metathesis catalysts[11] are oxo alkylidene complexes (e.g. $M(CHR)(O)X_2$; X = Cl, OR, etc.). If oxo ligands are not initially present in these systems, they could be formed readily from traces of water, and at low catalyst concentrations bimolecular decomposition of oxo alkylidene complexes could be slow relative to metathesis activity. Support for this suggestion comes from the observation that WCl_6 in combination with various alkyl metal complexes such as $Zn(CH_3)_2$ is inactive as an olefin metathesis catalyst when air and water are rigorously excluded but active in the presence of trace amounts of air and water.[12] Oxo alkylidene complexes have also been implicated in the ring-closing metathesis of nonconjugated dienes.[13]

Oxo alkylidene complexes are expected to be more reactive toward norbornadienes than the analogous imido alkylidene complexes as a consequence of the smaller size and more electronegative nature of the oxo ligand compared to imido ligands. These complexes are also expected to be less prone to tautomerization to give hydroxo alkylidyne complexes. However, a potential drawback of the smaller size of the oxo ligand is that the resulting complexes may be more susceptible to decomposition via bimolecular pathways.

In contrast to imido alkylidene complexes, stable, well-defined, metathetically active tungsten oxo alkylidene complexes are rare. Oxo alkylidene complexes of the type $W(CH^tBu)(O)(PR_3)_2Cl_2$ and $W(CH^tBu)(O)(PR_3)Cl_2$ actually were the first well-defined Group 6 alkylidene complexes to be prepared but their metathesis activity was found to be short-lived, and complexes such as "$W(CH^tBu)(O)(O^tBu)_2$" were unstable.[14-17] Tungsten oxo vinyl alkylidene complexes have been reported but their behavior as ROMP catalysts has not been described in detail.[18,19] Air stable tungsten oxo alkylidene complexes incorporating a trispyrazolylborate ligand are known but are metathetically active only in the presence of a cocatalyst such as $AlCl_3$.[20] The preparation of a new family of tungsten oxo alkylidene complexes is reported in this chapter. Stable, metathetically active five coordinate complexes are accessed by replacement of the halide ligands of precursor complexes of the general type $W(CH^tBu)(O)(PR_3)_2X_2$ with bulky aryloxide ligands. These complexes are potent catalysts for the living ROMP of norbornadienes and the resulting polymers are highly cis and isotactic.

References begin on page 174

RESULTS

Synthesis of Tungsten Oxo Alkylidene Dihalide Phosphine Complexes

$WO(CH^tBu)Cl_2(PR_3)_2$ complexes (P = PMe_3, PEt_3) can be synthesized in high yield (71-83%) by reaction of $Ta(CH^tBu)Cl_3(PR_3)_2$ with $WO(O^tBu)_4$ in pentane.[17] The tantalum side-product, $ClTa(O^tBu)_4$, is more soluble in pentane than the tungsten species and this allows for easy separation. The syntheses of analogous diphenylmethylphosphine complexes proceed in moderate yields (50-60%) and the products are a mixture of the mono- and bisphosphine complexes as indicated by the presence of two alkylidene signals, a doublet and a triplet, in ^1H NMR spectra (equation 1). The ratio of mono:bis phosphine complex varies from batch to batch but generally is 1:4. The complexes are yellow powders and can be used without further

$$WO(O^tBu)_4 + Ta(CH^tBu)X_3(PPh_2Me)_2 \xrightarrow[-30\ °C]{Et_2O/C_5} \begin{matrix} WO(CH^tBu)X_2(PPh_2Me)_y \\ + \\ XTa(O^tBu)_4 \end{matrix}$$

X = Cl (**1**), Br (**2**)
y=1 or 2

(1)

purification. Analogous neophylidene complexes such as $WO(CHCMe_2Ph)Br_2(PPh_2Me)_y$ (**3**) are synthesized by employing the appropriate tantalum neophylidene precursor and are isolated in moderate yields. A second product of the reaction that yields **3** can be isolated by refrigeration of the mother liquor. A new alkylidene species (**4**) crystallizes along with $BrTa(O^tBu)_4$ and washing the mixture with pentane yields **4** cleanly (according to ^1H NMR spectroscopy). The alkylidene functionality of **4** is characterized by a resonance at 11.14 ppm in the ^1H NMR spectrum ($^2J_{HW}$ = 12 Hz) and by a resonance at 295.2 ppm in the ^{13}C NMR spectrum. **4** does not contain a phosphine ligand (according to ^{31}P NMR spectroscopy) and a W-O stretch could not be assigned in the IR spectrum. Single crystals of **4** were grown from pentane at -20 °C and an X-ray crystallographic study was carried out to determine the molecular structure of **4**. Crystallographic

data, collection parameters and refinement parameters for **4** are given in Table 4.1 while selected bond lengths and bond angles are given in Table 4.2. The molecular structure of **4** along with the atom-labeling scheme is shown in Figure 4.2. **4** is a tungsten alkylidene dihalide bisalkoxide complex that is related to a family of tungsten neopentylidene complexes synthesized by Osborn.[21,22] On the basis of ^{1}H, ^{13}C and IR data, Osborn originally proposed a trigonal bipyramidal structure for the neopentylidene complexes,[21] but the coordination environment of the tungsten atom in **4** is clearly closer to square pyramidal with C(4) lying at the apex. The O-W-C(4) and Br-W-C(4) bond angles are all close to 102° and the O(2)-W-O(1) and Br(3)-W-Br(2) angles open to 154° and 157°, respectively. The O-W-Br angles are equivalent at ~87° and the W-C(4) bond length is similar to that found in other tungsten alkylidene complexes (see **6a** below). **4** is stable at -20 °C in the solid state for extended periods of time but decomposes over the course of several hours in solution. In the presence of $GaBr_3$ or $AlBr_3$, complexes such as $W(CH^tBu)(OCH_2{}^tBu)_2Br_2$ are active metathesis catalysts,[23,24] but studies of the metathesis activity of **4** were not embarked upon, in part due to the low yield (<10%).

Synthesis of Five Coordinate Tungsten Oxo Alkylidene Complexes

As a general synthetic approach to tungsten oxo alkylidene complexes, potassium salts of alkoxides and aryloxides are reacted with a variety of tungsten oxo alkylidene dihalide bisphosphine complexes. This type of salt elimination reaction has been extensively utilized in the synthesis of tungsten and molybdenum imido alkylidene complexes.[1,25] By employing bulky aryloxides such as 2,6-diphenylphenoxide it was hoped that isolable four coordinate complexes would be formed. However, as will be discussed, all isolated tungsten oxo alkylidene complexes are five coordinate in which one phosphine ligand remains bound to the metal center. NMR data for these complexes is summarized in Table 4.3.

References begin on page 174

Table 4.1. Crystallographic data, collection parameters and refinement parameters for $W(CHCMe_2Ph)Br_2(O^tBu)_2$ (**4**) and $WO(CH^tBu)(O\text{-}2,6\text{-}Ph_2C_6H_3)_2(PPh_2Me)$ (**6a**).

	4	**6a**
Empirical Formula	$C_{18}H_{30}Br_2O_2W$	$C_{54}H_{49}O_3PW$
Formula Weight	622.09	960.80
Diffractometer	Siemens SMART/CCD	Enraf-Nonius CAD-4
Crystal Dimensions (mm)	0.33 x 0.22 x 0.18	0.38 x 0.26 x 0.24
Crystal System	Triclinic	Monoclinic
Space Group	$P\bar{1}$	$P2_1/n$
a (Å)	8.3567(7)	12.027(2)
b (Å)	10.8744(9)	19.446(3)
c (Å)	12.5453(11)	19.442(3)
α (°)	99.6130(10)	90
β (°)	94.3660(10)	100.12
γ (°)	99.0200(10)	90
V (Å^3), Z	1104.0(2), 2	4486(2), 4
D_{calc} (Mg/m^3)	1.871	1.432
F_{000}	596	1944
Temperature (K)	188(2)	187
Scan Type	ω	ω-2θ
Reflections collected	4439	6392
Independent Reflections	3104	6055
No. Variables	209	532
R	0.0362	0.041
R_w	0.0378	0.035
GoF	1.110	1.41

References begin on page 174

Table 4.2. Selected bond lengths and bond angles for **4**.

Bond Lengths (Å)

W-C(4)	1.868(8)	W-O(1)	1.820(5)	W-O(2)	1.812(5)
W-Br(2)	2.5613(8)	W-Br(3)	2.5503(8)	C(4)-C(44)	1.523(11)
O(1)-C(11)	1.438(9)	O(2)-C(21)	1.452(9)		

Bond Angles (deg)

W-C(4)-C(41)	139.9(5)	C(4)-W-O(1)	101.8(3)	C(4)-W-O(2)	104.0(3)
Br(2)-W-Br(3)	157.10(3)	O(1)-W-Br(2)	87.7(2)	O(1)-W-Br(3)	87.4(2)
C(4)-W-Br(2)	102.3(2)	C(4)-W-Br(3)	100.6(2)	O(1)-W-O(2)	154.2(2)
O(2)-W-Br(2)	87.7(2)	O(2)-W-Br(3)	87.0(2)		

Table 4.3. NMR data for five coordinate tungsten oxo alkylidene complexes.

Complex	δH_α	δC_α	J_{CH} (Hz)	δP	J_{PW} (Hz)
5	10.13	287.4	119	0.35	333
6a	10.37	287.2	118	11.60	305[a]
6b	10.41	284.9	121	11.40	na[b]
7(syn)	10.15	280.2	118	8.49	398
7(anti)	11.20	285.7	136	8.84	378
9	10.32	268.7	na	3.00	341
10	9.89	na[c]	na[c]	4.33	360
	9.63	na[c]	na[c]		

[a]recorded at -27 °C, [b]coupling between P and W is not observed at room temperature, [c]thermal instability of sample prevented acquisition of ^{13}C NMR data

Figure 4.2. A view of the structure of $W(CHCMe_2Ph)(O^tBu)_2Br_2$ (**4**).

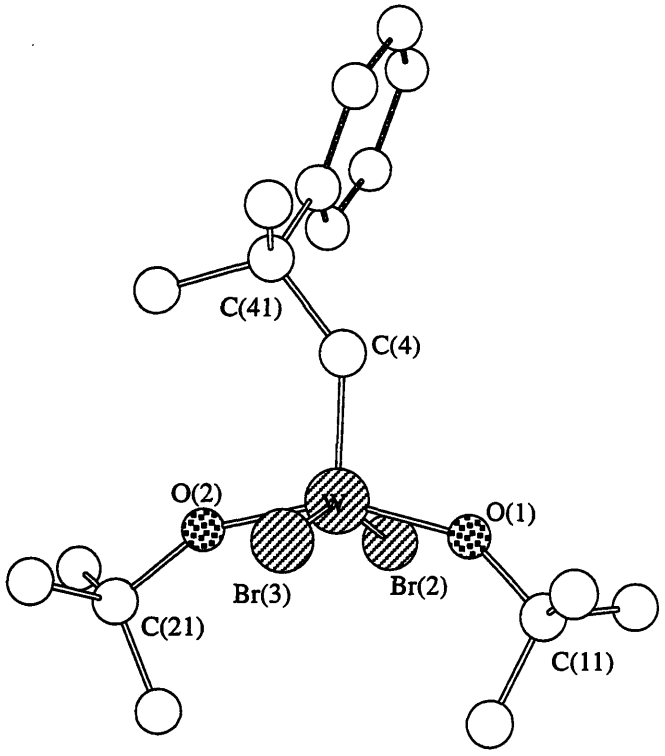

The reaction between $W(CH^tBu)(O)(PMe_3)_2Cl_2$ and two equivalents of KO-2,6-$Ph_2C_6H_3$ yields yellow, crystalline $W(CH^tBu)(O)(O\text{-}2,6\text{-}Ph_2C_6H_3)_2(PMe_3)$ (**5**) in 76% yield (equation 2). ^1H and ^{13}C NMR spectra of **5** at 23 °C exhibit sharp resonances and are indicative of only one rotamer being present in solution with the alkylidene H_α and C_α resonances appearing at 10.13 ppm ($^3J_{HP}$ = 3.5, $^2J_{HW}$ = 11 Hz) and 287.4 ppm ($^2J_{CP}$ = 11 Hz, $^1J_{CH}$ = 119 Hz), respectively. A J_{CH} value of 119 Hz suggests that the alkylidene has the *syn* orientation,[8] as shown. Only the monophosphine complex is observed presumably because the large steric bulk of the phenoxide ligands prevents the coordination of a second phosphine ligand. The observations of a single sharp resonance with coupling to tungsten in the ^{31}P NMR spectrum of **5** (0.35 ppm, $^1J_{PW}$ = 333 Hz) and a doublet resonance for H_α in the ^1H NMR spectrum suggest that the PMe_3 ligand is bound to the metal on the NMR time scale. Furthermore, in the presence of ~1 equivalent of PMe_3

at room temperature, resonances for both free and bound PMe_3 are observed in the ^1H and ^{31}P spectra, consistent with slow exchange. A strong absorbance at ~960 cm^{-1} in the IR spectrum of **5** is assigned to the metal-oxo stretch, characteristic of an oxo ligand that is triply bonded to tungsten.[26] Complex **5** is stable in solution and when stored in a sealed NMR tube for a period of years, a toluene-d_8 solution of **5** remained unchanged, according to ^1H NMR spectroscopy.

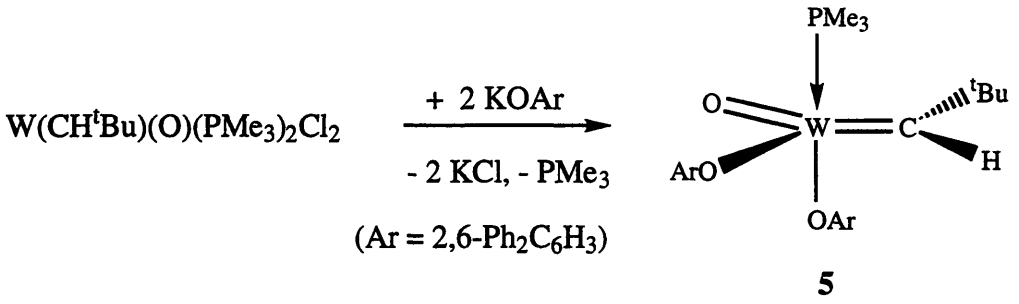

(2)

1 or **2** react with two equivalents of KO-2,6-$Ph_2C_6H_3$ in THF to give W(CH^tBu)(O)(O-2,6-$Ph_2C_6H_3$)$_2$(PPh_2Me) (**6a**) as a yellow, crystalline solid in 71% yield (equation 3).

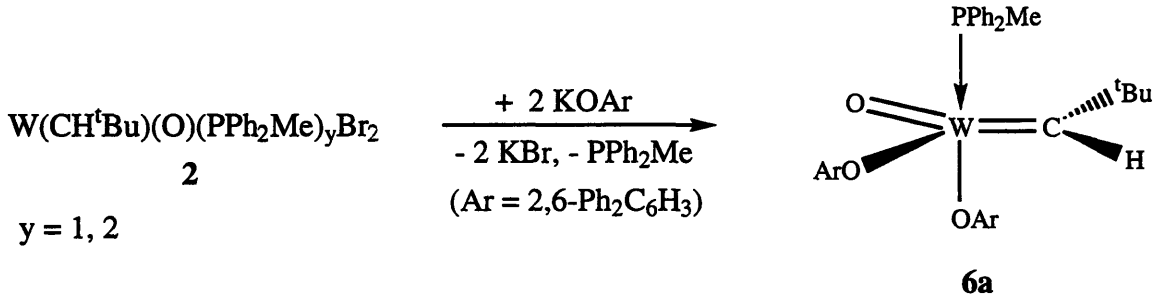

(3)

In contrast to **5**, all resonances in the ^1H NMR spectrum of **6a** are broad at 20 °C. Portions of the variable temperature ^1H NMR spectra of **6a** are shown in Figure 4.3. At 20 °C the resonance for the alkylidene proton is a broad singlet at 10.37 ppm; coupling to phosphorus is not observed. The aryl region of the spectrum exhibits a broad, rather featureless resonance between 7.8 and 6.7 ppm. At 0 °C some sharpening of the resonances is apparent although the H_α resonance remains a singlet suggesting that the phosphine ligand is still labile at this temperature. At -33 °C all resonances in the spectrum are sharp, the fine structure of the aryl region is evident

References begin on page 174

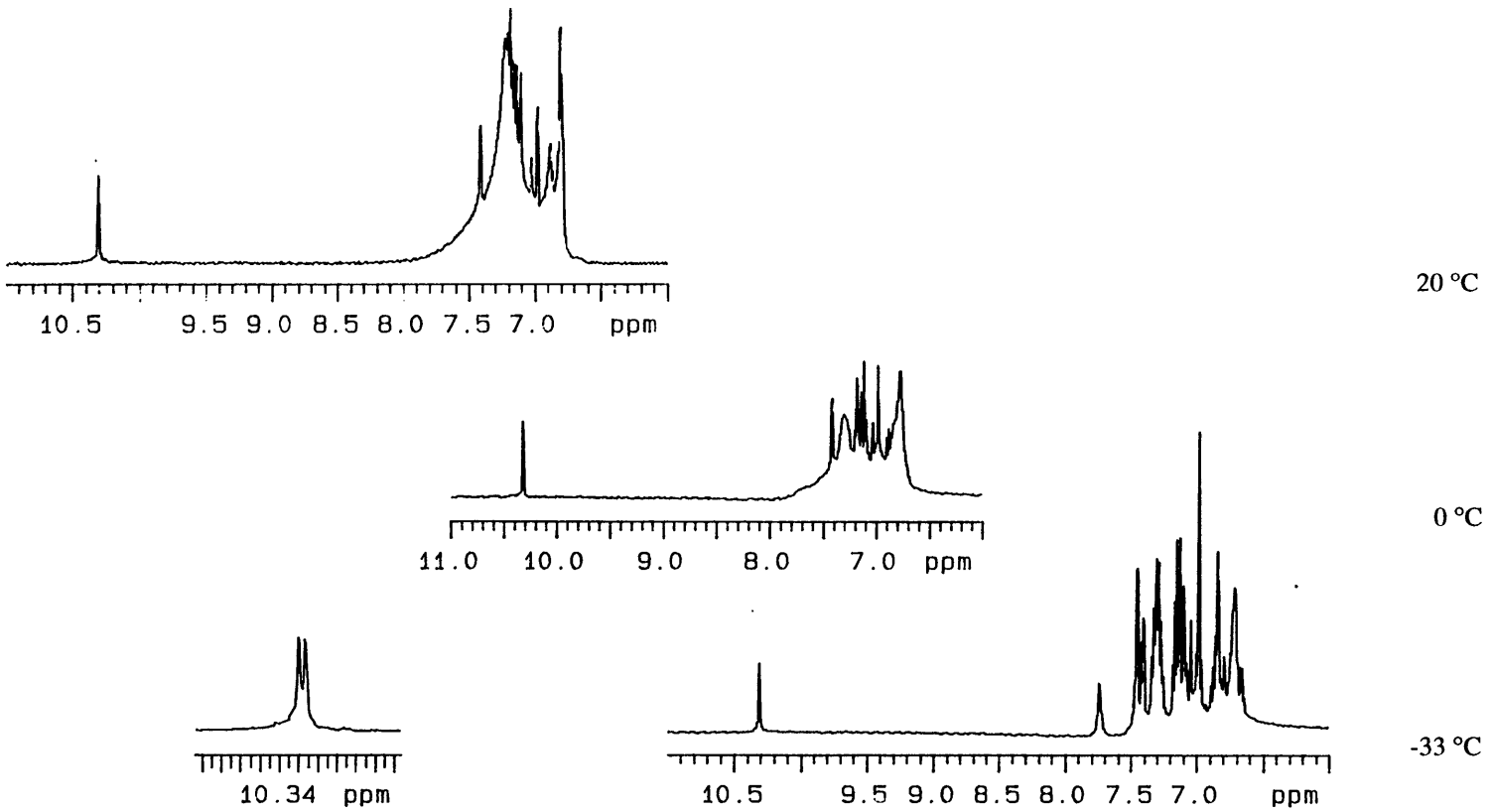

Figure 4.3. Variable Temperature ^{1}H NMR Spectra of $(DPPO)_2W(O)(CHCMe_3)(PPh_2Me)$ (**6a**).

and H_α now appears as a doublet ($^3J_{HP}$ = 3.5 Hz). A single broad resonance is observed at 11.6 ppm in the ^{31}P NMR spectrum of **6a** at 22 °C, which sharpens upon cooling the sample to -27 °C ($^1J_{PW}$ = 305 Hz). These data suggest that at or above room temperature, the PPh_2Me ligand of **6a** is labile but at low temperatures it is essentially bound to tungsten on the NMR time scale. The broadness of the resonances assigned to the aryl protons at 20 °C might also be due to hindered rotation of the ortho phenyl rings of the aryloxide ligand. However, the lability of PPh_2Me in **6a** can be demonstrated by the addition of an excess of PPh_2Me (1-2 equivalents) to toluene-d_8 solutions of **6a**. Variable temperature ^1H NMR spectra of the relevant region are shown in Figure 4.4. At low temperatures (-33 to -20 °C), resonances for both free and bound PPh_2Me are observed, consistent with slow exchange on the NMR time scale. Upon warming the sample to 20 °C, the resonances broaden and coalesce as free and bound phosphine exchange on the order of the NMR time scale while at higher temperatures (40 to 60 °C) fast exchange occurs and a single resonance is observed. Unfortunately, the exact rate of phosphine exchange has not been measured. The ^{13}C NMR spectrum of **6a**, reveals a C_α resonance at 287.2 ppm and the $^1J_{CH}$ coupling constant of 118 Hz suggests that **6a**, like **5**, exists as the *syn* rotamer. The IR spectrum of **6a** has a strong absorbance at 957 cm^{-1} which is assigned to the W-O stretch.

Crystals of **6a** suitable for an X-ray crystallographic study were grown at room temperature from a dichloromethane/pentane solution. Crystallographic data, collection parameters and refinement parameters for **6a** are given in Table 4.1 while selected bond lengths and bond angles are given in Table 4.4. The molecular structure of **6a** along with the atom-labeling scheme are shown in Figure 4.5. **6a** is a distorted trigonal bipyramid with axial and equatorial phenoxides. The oxo ligand, C_α and C_β of the neopentylidene ligand and the oxo of the equatorial phenoxide all lie in the equatorial plane. The phosphine ligand occupies an axial position, as expected on the basis of the structures of five coordinate adducts of imido alkylidene complexes[27] and the structure of $W(CH^tBu)(O)(PEt_3)Cl_2$.[28] Consistent with the NMR data, the structure is that of the *syn* rotamer with the *tert*-butyl group pointing toward the oxo ligand. The

References begin on page 174

References begin on page 174

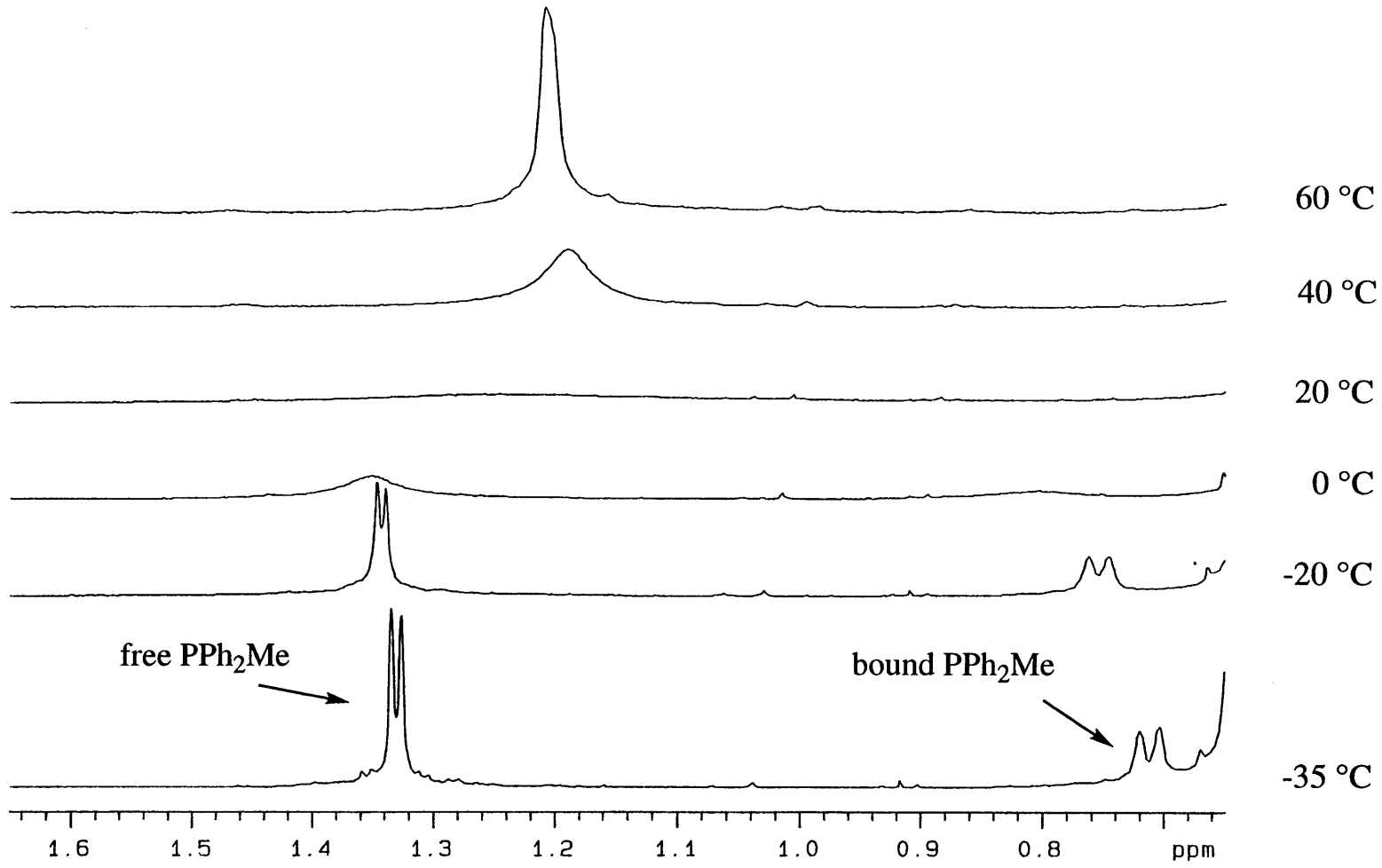

Figure 4.4. Variable temperature 500 MHz ^{1}H NMR spectra of $(DPPO)_2W(O)(CHCMe_3)(PPh_2Me)$ (**6a**) illustrating exchange between free and bound PPh_2Me.

W=O(1) (1.689(6) Å) and W=C(1) bond lengths (1.88(1) Å) and the W=C(1)-C(2) bond angle (147.8(9)°) are similar to those of $W(CH^tBu)(O)(PEt_3)Cl_2$.[28] The axial and equatorial W-O-C bond angles of 129.0° and 157.2°, respectively, result in the ortho phenyl rings of the phenoxide ligands being oriented so that they approximately encircle the neopentylidene and oxo ligands and therefore should provide a significant degree of protection against bimolecular decomposition of the base-free form of the complex.

Reaction of **3** with 2 equivalents of KO-2,6-$Ph_2C_6H_3$ in THF gives the neophylidene complex $W(CHCMe_2Ph)(O)(O\text{-}2,6\text{-}Ph_2C_6H_3)_2(PPh_2Me)$ (**6b**) as a yellow solid in 83% yield (equation 4). The ^1H NMR spectrum of **6b** at 23 °C is illustrative of the fluxional nature of the

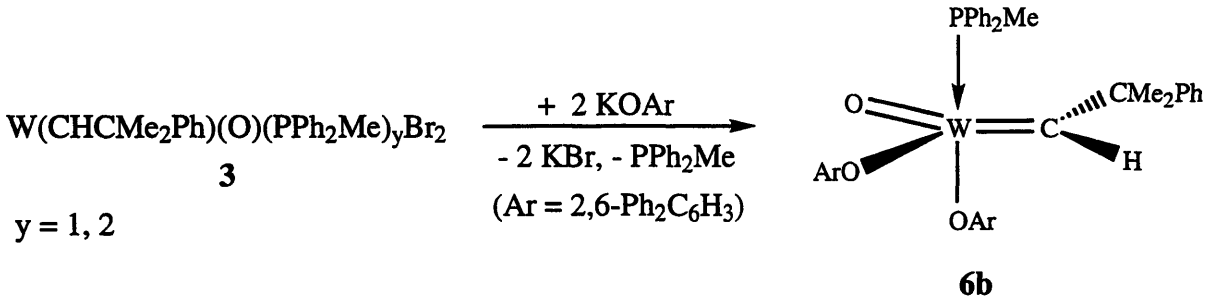

(4)

molecule; all resonances are broadened, the resonance for the alkylidene proton appearing as a singlet at 10.41 ppm and the resonance for the neophyl methyl groups appearing as a broad singlet at 1.17 ppm, suggesting that the phosphine ligand is labile at this temperature. Portions of the variable temperature ^1H NMR spectra of **6b** are shown in Figure 4.6. At -20 °C two sharp singlets are observed at 1.49 and 0.92 ppm for the inequivalent neophyl methyl groups and the signal for the alkylidene proton is a doublet ($^3J_{HP}$ = 3 Hz) consistent with the phosphine ligand being coordinated to the metal center on the NMR time scale. As the temperature is raised, the resonances attributed to the neophyl methyl groups broaden and then coalesce and at 40 °C a single resonance is observed at 1.16 ppm. These data show that, as with **6a**, phosphine exchange in **6b** is fast on the NMR time scale at or above room temperature. A single broad resonance is observed

References begin on page 174

Figure 4.5. A view of the structure of $W(CH^tBu)(O)(O\text{-}2,6\text{-}Ph_2C_6H_3)_2(PPh_2Me)$ (**6a**).

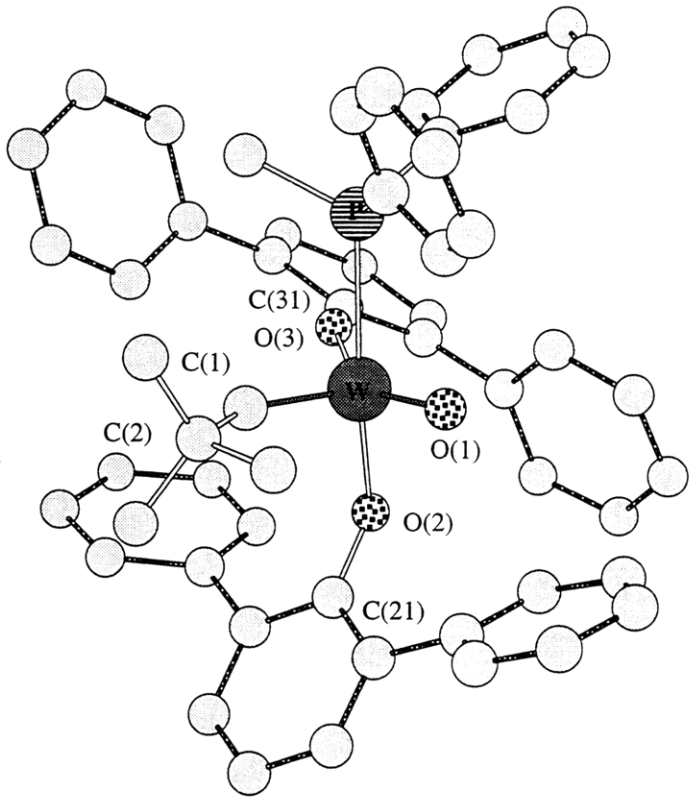

Table 4.4. Selected bond lengths and bond angles for **6a**.

Bond Lengths (Å)

W-C(1)	1.88(1)	W-O(1)	1.689(6)	W-O(3)	1.957(6)
W-P	2.590(2)	W-O(2)	1.993(5)		

Bond Angles (deg)

W-C(1)-C(2)	147.8(9)	W-O(2)-C(21)	129.0(5)	P-W-O(2)	167.2(2)
O(1)-W-O(3)	143.0(3)	O(3)-W-C(1)	109.2(4)	O(1)-W-O(2)	98.1(3)
O(3)-W-O(2)	87.7(2)	O(2)-W-C(1)	101.0(3)	P-W-O(3)	80.9(2)
W-O(3)-O(31)	157.2(6)			O(1)-W-C(1)	105.5(4)

References begin on page 174

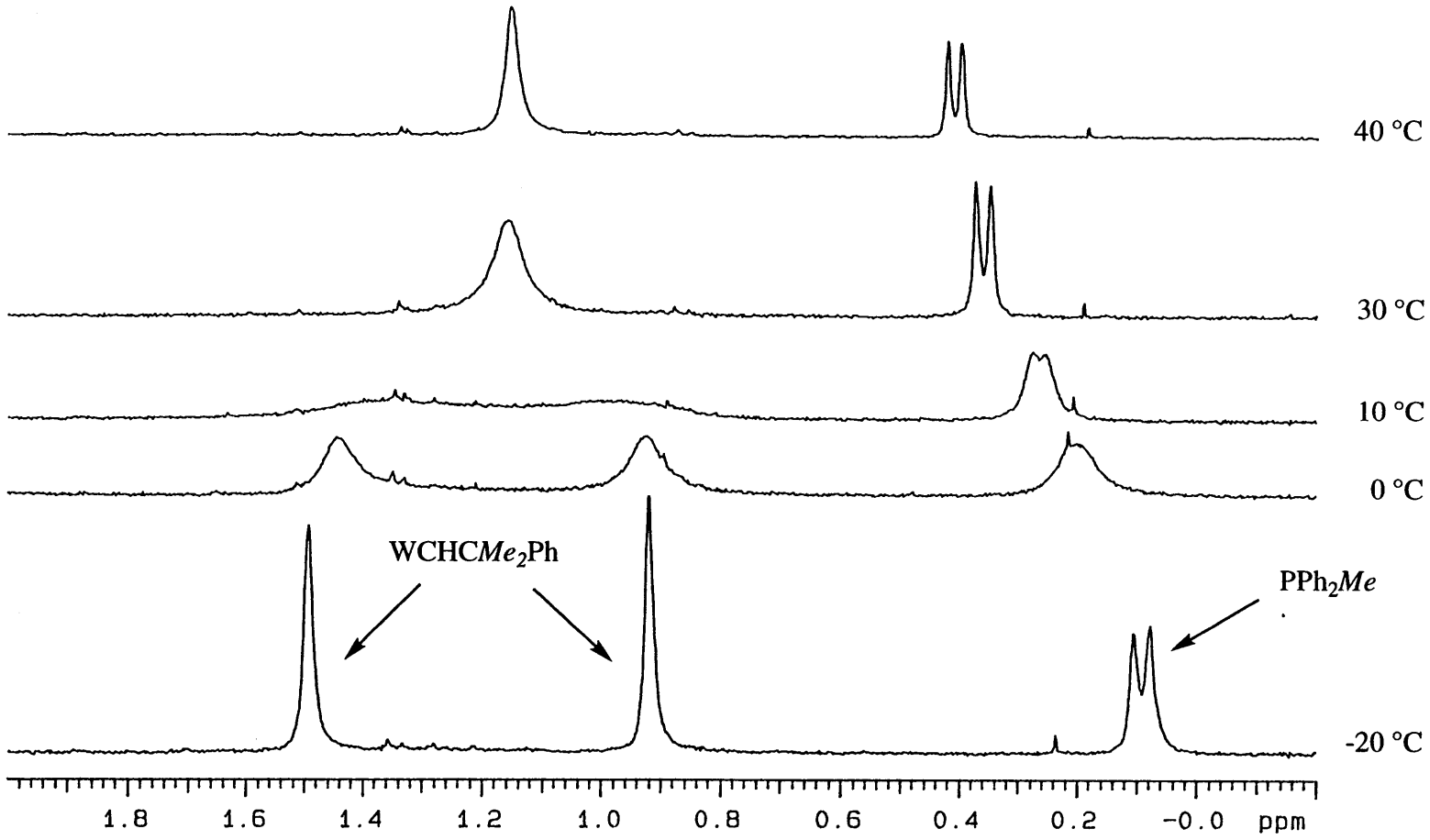

Figure 4.6. Variable temperature 500 MHz ^{1}H NMR spectra of (DPPO)$_2$W(O)(CHCMe$_2$Ph)(PPh$_2$Me) (**6b**).

in the ^{31}P NMR spectrum of **6b**, and the ^{13}C NMR spectrum reveals a C_α resonance at 284.9 ppm ($^1J_{CH}$ = 121 Hz).

$W(CH^tBu)(O)(PMe_3)_2Cl_2$ reacts with two equivalents of $(CF_3)_2CH_3COK$ to give green crystalline $W(CH^tBu)(O)(OCCH_3(CF_3)_2)_2(PMe_3)$ (**7**) as a mixture of *syn* and *anti* rotamers (equation 5). The ^1H NMR spectrum of **7** has two alkylidene signals at 11.20 ppm ($^3J_{HP}$ = 5 Hz, $^2J_{HW}$ = 8 Hz) and 10.15 ppm ($^3J_{HP}$ = 3 Hz, $^2J_{HW}$ = 10.7 Hz) and the rotamers are present in a ratio of 1:9, respectively. The ^{31}P NMR spectrum of **7** has two resonances with the major one appearing at 8.49 ppm ($^1J_{PW}$ = 398 Hz) and the minor one at 8.84 ppm ($^1J_{PW}$ = 378 Hz). The C_α resonance for the major rotamer is located at 280.2 ppm ($^1J_{CH}$ = 118 Hz) in the ^{13}C NMR spectrum and the magnitude of the coupling constant indicates that it is the *syn* rotamer. The C_α resonance for the anti rotamer is found at 285.7 ppm ($^1J_{CH}$ = 136 Hz). It should be noted that *syn* and *anti* rotamers are also observed in the related vinyl alkylidene complex $W(CHCHCPh_2)(O)(OCCH_3(CF_3)_2)_2(PPh_2Me)$.[18]

$$W(CH^tBu)(O)(PMe_3)_2Cl_2 + 2\,ROK \xrightarrow[-\,PMe_3]{-\,2\,KCl} W(CH^tBu)(O)(PMe_3)(OR)_2$$

7

syn and *anti* rotamers

$R = (CF_3)_2CH_3C$

(5)

Photolytic studies of **7** were undertaken to determine if interconversion of *syn* and *anti* rotamers would occur. (Photolysis has been found to effect interconversion of rotamers in rhenium[29] and molybdenum[8] alkylidene complexes.) Samples of **7** in toluene-d_8 were photolyzed at -45 °C for 24 h. Photolysis was carried out at low temperature in order to retard any thermal back reaction and to minimize the possibility of sample decomposition. After photolysis no change in the ratio of *syn* to *anti* rotamers was observed nor was any significant decomposition evident (according to ^1H NMR spectroscopy). This result is perhaps not surprising if phosphine dissociation is a requirement for rotamer rotation. In **7**, the metal center is rendered highly

References begin on page 174

electrophilic as a consequence of the electron-withdrawing nature of the $(CF_3)_2CH_3CO$ ligand, resulting in the PMe_3 ligand being tightly bound, even at room temperature.

Reasoning that a more bulky phenoxide such as 2,6-di-*tert*-butyl-4-methylphenoxide might allow isolation of a four coordinate tungsten oxo alkylidene complex, **3** was reacted with two equivalents of the potassium salt of 2,6-di-*tert*-butyl-4-methylphenol. The product, **8**, is isolated as rust-red crystals in low yield (39%). **8** does not contain a phosphine ligand (according to ^{31}P NMR spectroscopy) and ^{1}H and ^{13}C NMR spectra of **8** do not contain resonances characteristic of an alkylidene functionality. However, the ^{1}H NMR spectrum of **8** does exhibit four sets of multiplets between 2.80 and 2.18 ppm which integrate as 4 protons. On the basis of these data and elemental analyses, **8** is formulated as the metallacycle shown in equation 6. It appears that

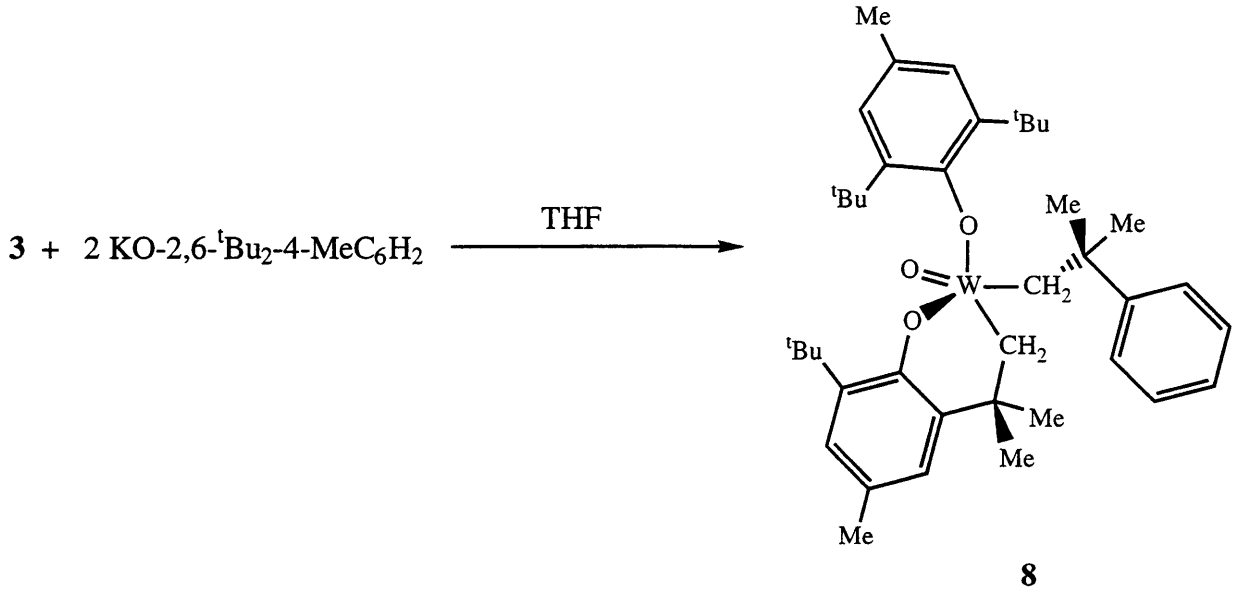

8

(6)

replacement of the bromide ligands of **3** with the bulky aryloxide ligands results in loss of PPh_2Me from the coordination sphere and generation of the coordinatively unsaturated species $W(CHCMe_2Ph)(O)(OAr')_2$ (Ar' = 2,6-$^{t}Bu_2$-4-MeC_6H_2). C-H activation of the ortho *tert*-butyl group then generates **8**. We have seen no evidence of CH activation in an ortho phenyl ring of the

O-2,6-$Ph_2C_6H_3$ ligand related to what has been found in tungsten systems discovered by Basset.[30]

Stoichiometric Olefin Metathesis Reactions of W(CH^{t}Bu)(O)(O-2,6-$Ph_2C_6H_3)_2(PMe_3)$ (5)

Complex **5** reacts with styrene or ethylene (1-2 equivalents) in less than 1 h to yield the corresponding benzylidene and methylidene complexes according to equations 7 and 8. The benzylidene product, W(CHPh)(O)(O-2,6-$Ph_2C_6H_3)_2(PMe_3)$ (**9**) can be recrystallized from toluene or dichloromethane/pentane to afford yellow cubes. The alkylidene H_α resonance for **9** is found at 10.32 ppm ($^3J_{HP}$ = 4, $^2J_{HW}$ = 7 Hz) and the C_α resonance at 268.7 ppm ($^2J_{CP}$ = 12 Hz). ^{31}P NMR data (3.00 ppm, $^1J_{PW}$ = 341 Hz) suggest that the PMe_3 ligand is bound to the metal on the NMR time scale.

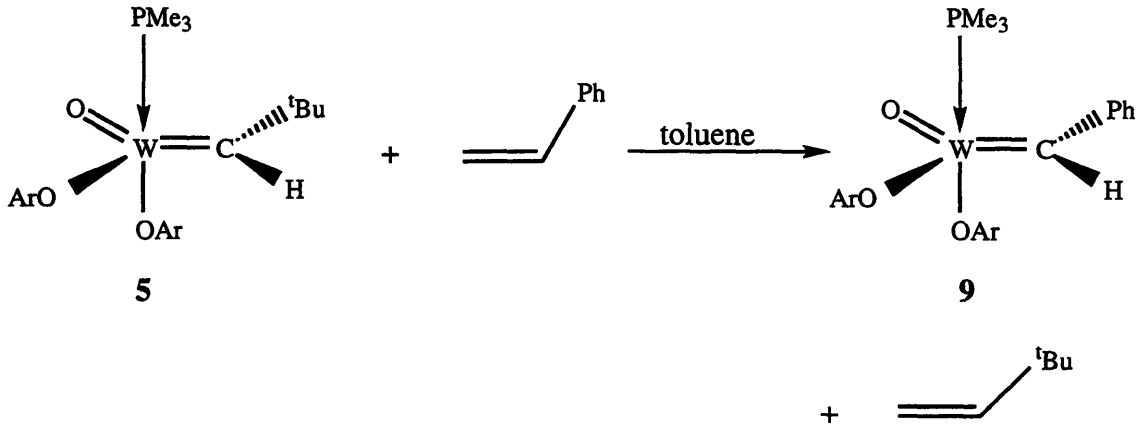

(7)

In the ^1H NMR spectrum of the methylidene complex, **10**, the H_A and H_B resonances are found at 9.89 and 9.63 ppm as two doublets of doublets ($^3J_{HP}$ = 5.5 Hz, $^2J_{HH}$ = 9 Hz and $^3J_{HP}$ = 4.5 Hz, $^2J_{HH}$ = 9 Hz, respectively). A similar pattern is observed for W(CH_2)(NAr)[$OC(CF_3)_2(CF_2CF_2CF_3)]_2(PMe_3)$[31] (Ar = 2,6-$^i Pr_2C_6H_3$) and is expected on the basis of the assumed trigonal bipyramidal geometry of

$W(CH_2)(NAr)[OC(CF_3)_2(CF_2CF_2CF_3)]_2(PMe_3)$ and **10**. In such a geometry H_A and H_B are inequivalent and hence are coupled to each other as well as to phosphorus. The ^{31}P NMR spectrum of **10** exhibits a single sharp resonance at 4.33 ppm ($^1J_{PW}$ = 360 Hz), consistent with the PMe_3 ligand being bound to the metal on the NMR time scale. Values for J_{CH} are not available, as **10** decomposes in solution during data acquisition. This decomposition is accompanied by a color change from yellow to blood red and the appearance of a resonance in the ^1H NMR spectrum that is attributable to ethylene, data which is suggestive of a bimolecular decomposition pathway. However, no products of this decomposition have been isolated.

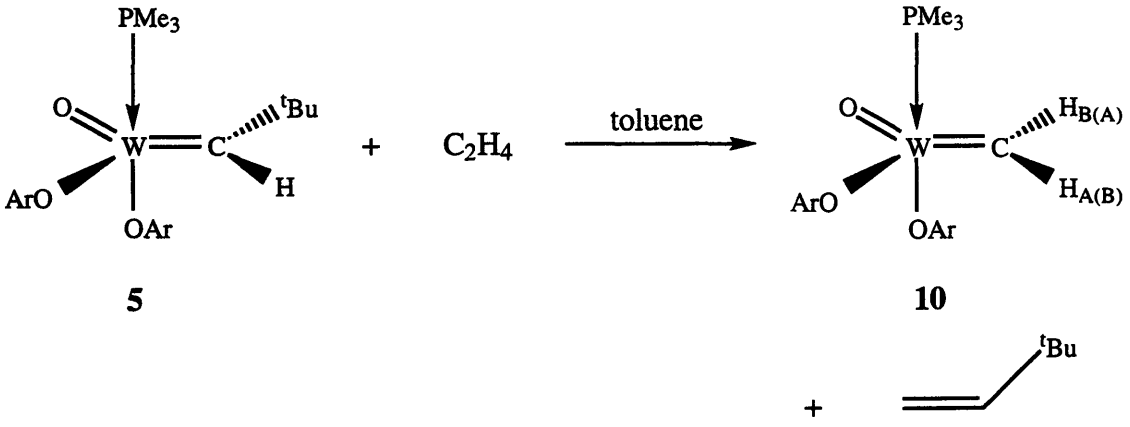

5 **10**

(8)

ROMP of 2,3-Disubstituted Norbornadienes Utilizing Tungsten Oxo Alkylidene Catalysts

To determine if complexes **5**, **6a**, **6b** and **7** could be employed as catalysts for ROMP, a study of their reactivity toward norbornadienes was undertaken. Both **6a** and **6b** react readily with 2,3-dicarbomethoxynorbornadiene (DCMNBD) in dichloromethane and the resulting polymers can be cleaved off the metal center by addition of benzaldehyde. The polymerizations are rapid being complete in 15 min and the polymers are isolated from the reaction mixtures as white powders by precipitation from methanol, followed by centrifugation with yields typically being >80%. ^1H

References begin on page 174

NMR spectra of the polymers, exhibit resonances at 5.42 and 3.95 ppm which are assigned to the olefinic and allylic protons, respectively, and are consistent with a polymer that contains >95% cis double bonds (for comparison, the allylic protons of all trans poly(DCMNBD) resonate at 3.52 ppm[3]). The observation of a single resonance at 44.4 ppm in the ^{13}C NMR spectrum that is assigned to the allylic carbon atoms in the polymer is also indicative of a highly cis polymer.[9] Furthermore, all polymers were found to be isotactic with ^{13}C NMR spectra exhibiting a single resonance for C_7 at 39.0 ppm (see Figure 4.8 for numbering scheme and peak assignments).[5] **6a** and **6b** also polymerize 2,3-bis(trifluoromethyl)norbornadiene (NBDF6) in toluene. The ^{13}C NMR spectra of the resulting poly(NBDF6) exhibit single resonances at 44.9 and 38.5 ppm ($C_{1,4}$ and C_7, respectively), data that are consistent with polymers that are >95% cis and >95% isotactic.[6]

Gel permeation chromatographic (GPC) analyses of poly(DCMNBD) produced employing **6a** and **6b** show the polymers to have polydispersities of ~1.2 (Tables 4.5 and 4.6). Furthermore, the molecular weights of the polymers are consistently higher than expected, suggesting that k_p/k_i is large although k_p/k_i has not been measured directly (k_i = rate of initiation, k_p = rate of propagation). No significant change in the polydispersities of the polymers is observed upon

Table 4.5. GPC characterization of all cis, isotactic poly(DCMNBD) prepared using **6a**.

Equiv.	Time (h)	M_n(calcd)	M_n(found)	PDI	Yield(%)
18	4	3908	7643	1.16	100
51	0.25	10779	19030	1.11	82
59	1.00	12445	20960	1.19	78[a]
89	4	18691	43440	1.27[b]	na

[a]all of polymer was not weighed, [b]low molecular weight shoulder present.

References begin on page 174

increasing the reaction time, a result that is consistent with negligible secondary metathesis. When the polymerization of DCMNBD employing **6b** is carried out at -30 °C, the yield of polymer decreases significantly. Assuming phosphine dissociation is required for reaction of the oxo alkylidene complex with an olefin, the low yield might be attributable to a slowing of the rate of polymerization due to stronger binding of the phosphine ligand at low temperatures. In related work,[7] the competitive binding of THF at low temperatures was proposed to account for the low yield of polymers obtained when molybdenum imido alkylidene catalysts were employed. Due to its insolubility in dichloromethane, poly(NBDF6) was not characterized by GPC analysis.

Table 4.6. GPC characterization of all cis, isotactic poly(DCMNBD) prepared using **6b**.

Equiv	Time (h)	M_n(calcd)	M_n(found)	PDI	Yield(%)
95	0.25	20003	51940	1.25	87
98	0.50	20627	59530	1.18	92
108	1.00	22709	57820	1.18	93
100	2.50	21043	54910	1.30	63[a]

[a]polymerization carried out at -30 °C

As with any polymerization, a living system is highly desirable and so a more detailed study of the metathesis activity of **5** was undertaken. **5** reacts smoothly with DCMNBD in dichloromethane, allowing the preparation of a series of polymers of increasing molecular weight and poly(DCMNBD) is isolated from the reactions in moderate to good yields (Table 4.7). The relatively low yield of the 22 mer polymer is believed to arise from incomplete precipitation from methanol rather than premature termination of the polymerization as higher molecular weight polymers are isolated in high yield.

References begin on page 174

GPC analyses of the polymers indicate that they are essentially monodisperse (in contrast to those obtained using **6a** and **6b**). A plot of M_n as a function of the number of equivalents of monomer added reveals a linear dependence (Figure 4.7). The low polydispersities of the polymers and the fact that their molecular weights are directly proportional to the number of monomer units added, are consistent with **5** polymerizing DCMNBD in a living manner.

Table 4.7. GPC characterization of all cis, isotactic poly(DCMNBD) prepared using **5**.

equiv	Time(h)	M_n(calcd)	M_n(found)	PDI	Yield(%)
22	4	4741	7934	1.03	56
43	4	9113	14280 (14590)	1.02 (1.01)	82
65	4	13694	19240	1.02	76
86	4	18067	27430 (27070)	1.01 (1.02)	76
129	4	27020	37530	1.03	90
166	4	34724	49050 (47160)	1.04 (1.04)	80
256	4	53463	63350 (53860)	1.05 (1.11)	90

[a]Number in parentheses are duplicate runs on the same sample.

However, the molecular weights of the polymers, as determined by GPC, are consistently higher than the theoretical molecular weights by a factor of 1.2 to 1.6. ^{1}H and ^{13}C NMR data are compatible with the polymers being >95% cis and >95% isotactic. The ^{13}C NMR spectrum of a representative polymer, along with the numbering scheme and peak assignments is shown in Figure 4.8. **5** also polymerizes NBDF6 yielding polymers that are all cis and isotactic (according to ^{1}H and ^{13}C NMR data).

The metathesis activity of **7** has been explored briefly and in contrast to **5**, **6a** and **6b**, **7** reacts slowly with DCMNBD. For example, in the polymerization of 120 equivalents of

References begin on page 174

DCMNBD, after 22 h all of the monomer is not consumed (according to ^1H NMR spectroscopy). Although the polymer was not isolated, ^1H and ^{13}C NMR spectra of the crude reaction mixture suggest that the polymer contains both cis and trans double bonds. These observations imply that **7** is not a practical catalyst for the ROMP of norbornadienes and further studies were not pursued.

Figure 4.7. Number average molecular weight (M_n) of poly(DCMNBD) versus equivalents of DCMNBD added to **5** in CH_2Cl_2.

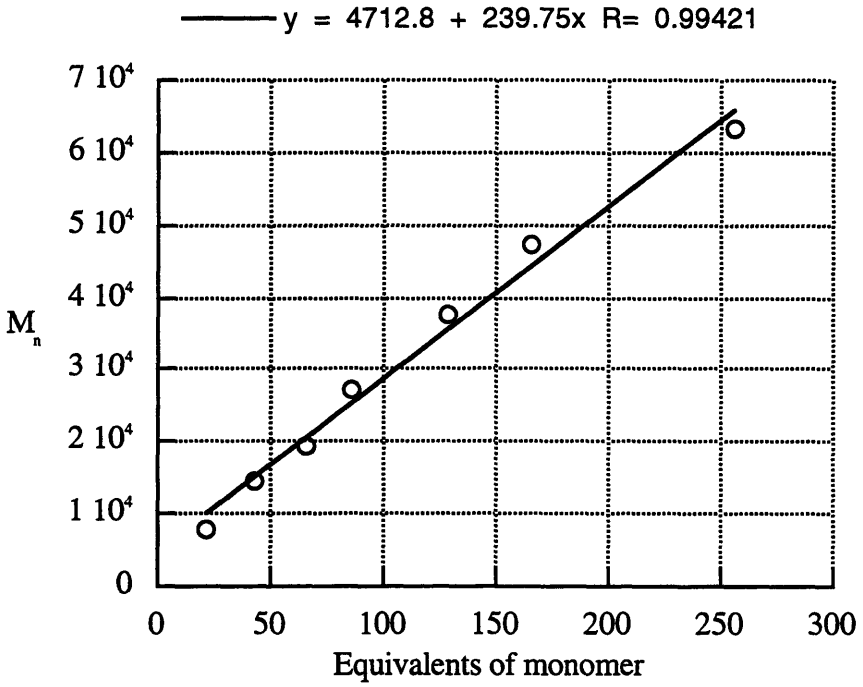

References begin on page 174

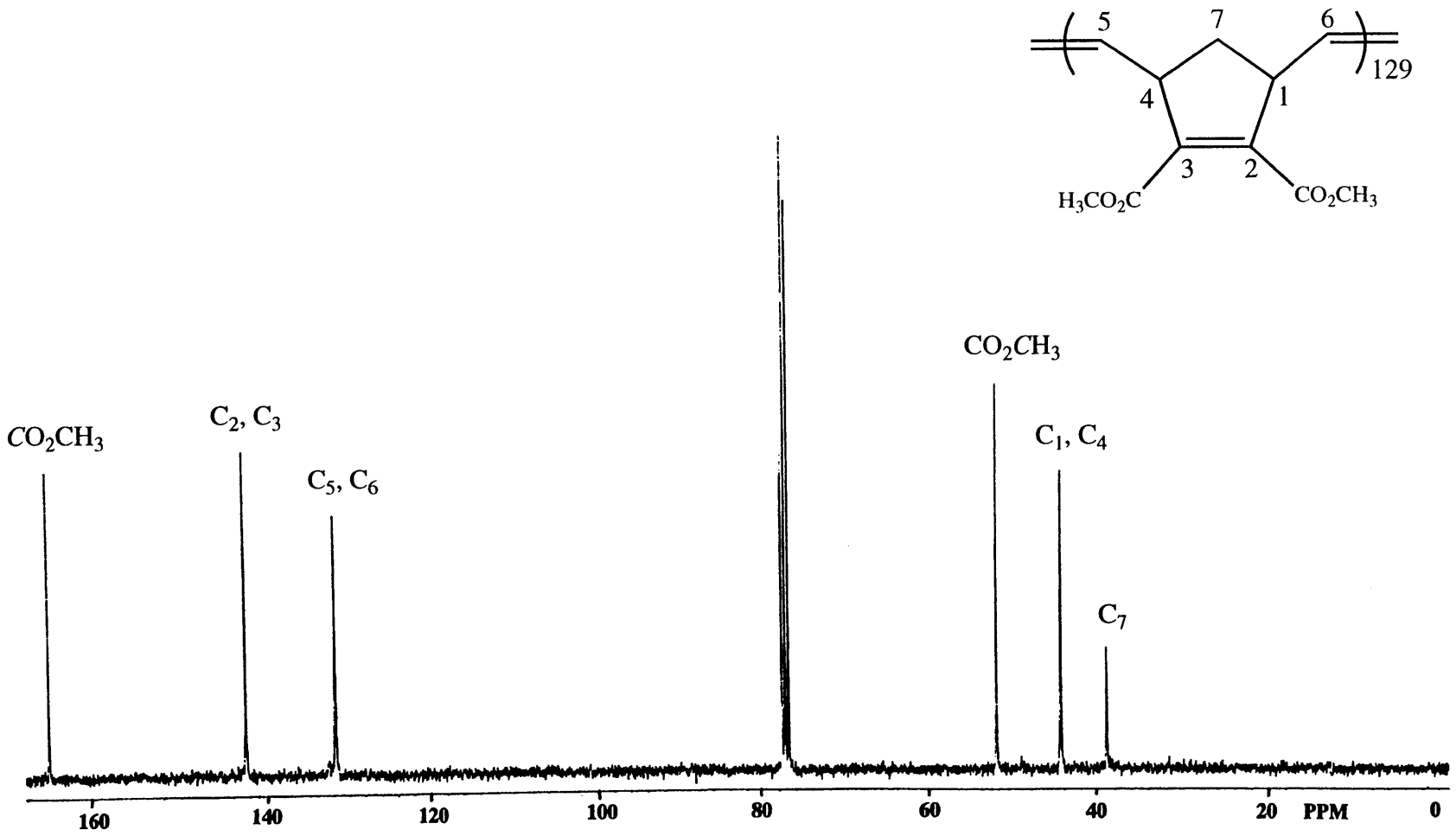

Figure 4.8. ^{13}C NMR spectrum of poly(DCMNBD) produced using $(DPPO)_2W(O)(CHCMe_3)(PMe_3)$ (**5**).

DISCUSSION

The major goals of this work were the preparation and characterization of well-defined tungsten oxo alkylidene complexes and an investigation of their utility as catalysts for the ROMP of norbornadienes. Five coordinate complexes of the general type $W(O)(CH^tBu)(OAr)_2(PR_3)$ are isolable as crystalline solids that are stable indefinitely in solution when stored under dinitrogen. It has been shown by ^1H NMR spectroscopy that large phosphines such as PPh_2Me are labile on the NMR time scale at room temperature whereas PMe_3 appears bound to the metal center. By varying the steric and electronic properties of the alkoxides employed, it is possible to observe *syn* and *anti* rotamers in solution as in the case of **7**.

Catalysts **5**, **6a** and **6b** rapidly polymerize DCMNBD to give polymers that are highly cis and isotactic. The apparent high reactivity of the oxo complexes might be expected in view of the small size and high electronegativity of the oxo ligand. Presumably, phosphine dissociation is a requirement for reaction of the oxo alkylidene complex with an olefin and therefore the phosphine ligand of **5** must be labile on the polymerization time scale. In imido alkylidene catalyst systems, cis polymers are proposed to arise from *syn* propagating species as a consequence of addition of the monomer (through the exo face) to the CNO face of the four-coordinate catalyst with C_7 of the monomer extending over the arylimido ring.[8] The high cis content found in poly(DCMNBD) prepared from **5**, **6a** and **6b** is consistent with a similar proposal in which the oxo ligand presents minimal steric hindrance toward approach of the monomer (equation 9).

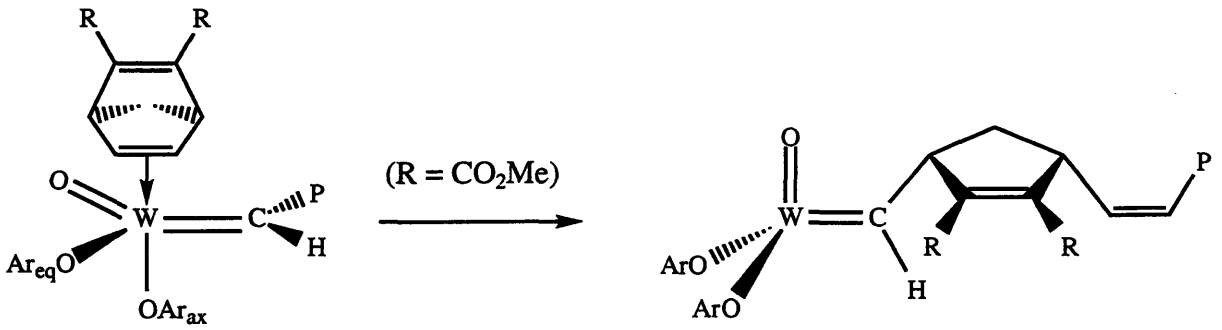

(9)

References begin on page 174

The finding that these polymers are >95% isotactic is surprising since tacticity in the oxo alkylidene systems described here can arise solely by chain end control. In chain end control, the tacticity of the polymer is dictated by the chirality of the β carbon in the growing polymer chain. If sequential monomer units add to the same COO face of the four coordinate oxo alkylidene catalyst then an isotactic polymer will result. One disadvantage of chain end control is that if a monomer adds to the "wrong" COO face, then the mistake will be propagated in the polymer chain. As a result, stereoregular polymers rarely result when achiral catalysts are employed. In fact, cis, isotactic polymers of the type described herein, previously have been prepared only through enantiomorphic site control using molybdenum imido alkylidene catalysts that contain chiral chelating dialkoxide ligands,[9,10] a process that presumably is inherently more efficient than chain end control.

Complex **7** was found to be a poor catalyst for the ROMP of norbornadienes, a result that suggests that the phosphine ligand in this complex is not labile on the time scale of the polymerization. Presumably, the strongly electron-withdrawing nature of the $(CF_3)_2CH_3CO$ ligand, renders the metal center highly electrophilic, resulting in the phosphine ligand being tightly bound. In related work, $W(CHSiMe_3)(NAr)[OCCH_3(CF_3)_2]_2(PMe_3)$[31] was also found to be virtually inactive as a metathesis catalyst as a consequence of the phosphine ligand being nonlabile.

GPC analysis of poly(DCMNBD) reveals that polymers produced using **6a** or **6b** have somewhat broadened PDI's of approximately 1.2 whereas employment of **5** as the catalyst yields essentially monodisperse polymers (PDI = 1.02). In comparing the neopentylidene catalysts, **5** and **6a**, the key difference is the size of the phosphine ligand which may play an important role in the polymerization reactions. For example, in the living ROMP of cyclobutene by $W(CH^tBu)(NAr)(O^tBu)_2$ (Ar = 2,6-diisopropylphenyl), it has been shown that PMe_3 binds more strongly to the propagating species than to the initiating species.[32] This difference results in the rate of propagation being slowed compared to the rate of initiation, allowing the preparation of monodisperse polymers. In contrast, in the absence of PMe_3, the polydispersity of the polybutadiene produced is much broader (PDI > 2). Since four coordinate analogs of **5** and **6a**

References begin on page 174

have not been isolated, we cannot compare the polymerization activity of tungsten oxo alkylidene complexes in the presence and absence of phosphine ligands. However, a comparison of poly(DCMNBD) produced using **5** and **6a** does allow us to develop a qualitative picture of the role of the phosphine ligand as a competitive inhibitor. In both **5** and **6a** we would expect that the phosphine ligand would bind more strongly to the propagating alkylidene complex than to the sterically bulkier initiating neopentylidene complex. As noted in the case of $W(CH^tBu)(NAr)(O^tBu)_2$, such binding would slow the rate of propagation compared to the rate of initiation. By ^1H NMR spectroscopy, we have shown qualitatively that the PMe_3 ligand of **5** is bound more tightly to the tungsten center than the PPh_2Me ligand of **6a** and it follows that the smaller PMe_3 ligand may also bind more tightly to the propagating species. This tighter binding of PMe_3 may result in k_p/k_i being smaller for **5** than **6a**, thereby explaining the narrower polydispersities of the polymers produced using **5**. A smaller k_p/k_i for **5** would also explain the observation that the molecular weights of polymers produced using **5** are closer to the theoretical molecular weights than polymers produced using **6a** as the catalyst (see Tables 4.5 and 4.7).

EXPERIMENTAL PROCEDURES

General Procedures. All experiments were performed under a nitrogen atmosphere in a Vacuum Atmospheres drybox or by standard Schlenk techniques unless otherwise specified. Pentane was washed with sulfuric acid/nitric acid (95/5 v/v), sodium bicarbonate, and water, stored over calcium chloride, and distilled from sodium benzophenone ketyl under nitrogen. Reagent grade diethyl ether and tetrahydrofuran were distilled from sodium benzophenone ketyl under nitrogen. Toluene was distilled from sodium, and CH_2Cl_2 was distilled from CaH_2. Polymerization grade solvents were stored over activated molecular sieves and a small amount tested with a THF solution of sodium benzophenone ketyl prior to use. Benzene-d_6 and toluene-d_8 were pre-dried on CaH_2, vacuum transferred onto sodium and benzophenone, stirred under vacuum for two days and then vacuum transferred into small storage flasks.

References begin on page 174

NMR data were obtained at 300 MHz and 500 MHz (^{1}H), 75.4 MHz (^{13}C) and 121.8 MHz (^{31}P) and are listed in parts per million downfield from tetramethylsilane for proton and carbon and in parts per million downfield from 85% H_3PO_4 for phosphorus. Coupling constants are listed in Hertz. Spectra were obtained at 25 °C unless otherwise noted. IR spectra were recorded as Nujol mulls between NaCl plates on a Perkin-Elmer 1600 FT-IR spectrometer. Elemental analyses were performed on a Perkin-Elmer PE2400 microanalyzer in our laboratories.

GPC analyses were effected using a system equipped with two Alltech columns (Jordi-Gell DVB mixed bed - 250 mm x 10 mm (i.d.)). The solvent was supplied to the columns at a flow rate of 1.0 mL/min. with a Knauer HPLC pump 64. HPLC grade CH_2Cl_2 was continuously dried over and distilled from CaH_2. Detection was effected using a Wyatt Technology miniDawn™ light scattering detector coupled to a Knauer differential refractometer. The differential refractive index increment, dn/dc, is a constant for homopolymers of identical structure. The total mass method was used to determine dn/dc which was found to be 0.096±0.005 for cis, isotactic poly(DCMNBD) in the molecular weight range studied.

W(O)(CH^{t}Bu)$Cl_2(PMe_3)$,[17] 2,3-bis(trifluoromethyl)norbornadiene,[33] and 2,3-dicarbomethoxynorbornadiene[34] were prepared as described in the literature. Potassium hydride was purchased from Aldrich as a suspension in oil and was washed with pentane prior to use. 2,6 diphenylphenol was purchased from Aldrich and used as received.

W(O)(CH^{t}Bu)$Cl_2(PPh_2Me)_y$ (1). y=1(20%), 2(80%). A solution of W(O)(O^{t}Bu)$_4$ (996 mg, 2 mmol) in 10 mL of pentane (or ether) was cooled to -30 °C. Ta(CH^{t}Bu)$Cl_3(PPh_2Me)_2$ (1534 mg, 2 mmol) was added as a solid and a yellow precipitate formed. The mixture was stirred for 1 h and allowed to sit overnight. The product was collected by filtration, washed with pentane and dried in vacuo; yield 701 mg (50%). ^{1}H NMR($CDCl_3$) for the bisphosphine complex, δ 12.07 (t, 1, WC*H*^{t}Bu, $^3J_{HP}$ = 4), 7.82, 7.68, 7.47, 7.38 (m, 20, P*Ph*$_2$Me,) 2.54 (t, 6, PPh$_2$*Me*, $^2J_{HP}$ = 5), 0.69 (s, 9, CH^t*Bu*); for the monophosphine complex, δ 10.26 (d,1, WC*H*^{t}Bu, $^3J_{HP}$ = 4), 2.40 (d, 3, PPh$_2$*Me*, $^2J_{HP}$ = 10), 1.07 (s, 9, WCH^t*Bu*). ^{31}P NMR($CDCl_3$) for the

bisphosphine complex, δ 14.16 (s, $^1J_{PW}$ = 331); for the monophosphine complex, δ 25.80 (s). ^{13}C NMR($CDCl_3$) for the bisphosphine complex, δ 323.7 (t 1, W*C*H^{t}Bu, $^2J_{HP}$ = 10), 135.4 (t, C_{ipso}, J_{CP} = 24), 133.7 (t, J_{CP} = 5), 132.5 (t, J_{CP} = 5), 131.1 (s), 130.7 (s), 130.3 (t, C_{ipso}, J_{CP} = 24), 128.7 (t, J_{CP} = 5), 128.6 (t, J_{CP} = 5). As the product is a mixture of two compounds elemental analyses were not attempted.

W(O)(CH^{t}Bu)Br$_2$(PPh$_2$Me)$_y$ (2). y=1(20%), 2(80%). A solution of W(O)(O^{t}Bu)$_4$ (552 mg, 1.12 mmol) in 7 mL pentane (or ether) was cooled to -30 °C. Ta(CH^{t}Bu)Br$_3$(PPh$_2$Me)$_2$ (1000 mg, 1.12 mmol) was added as a solid to this solution. The solution turned green in color and then yellow. Within minutes a yellow precipitate had formed. The mixture was stirred for 9 h and the product was collected by filtration, washed with pentane and dried in vacuo; yield 531 mg (60%). ^1H NMR($CDCl_3$) for the bisphosphine complex, δ 12.25 (t, 1, WCH^{t}Bu, $^3J_{HP}$ = 4), 7.81, 7.73, 7.46, 7.39 (m, 20, P*Ph* $_2$Me), 2.71 (t, 6, PPh$_2$*Me*, $^2J_{HP}$ = 5), 0.68 (s, 9, CH^t*Bu*); for the monophosphine complex, δ 9.87 (d, 1, WC*H*^{t}Bu, $^2J_{HP}$ = 3), 2.47 (d, 3, PPh$_2$*Me*, $^2J_{HP}$ = 10), 1.07 (s, 9, WCH^t*Bu*). Due to the product mixture elemental analyses were not attempted.

W(O)(CHCMe$_2$Ph)Br$_2$(PPh$_2$Me)$_x$ (3). y=1(20%), 2(80%). A solution of W(O)(O^{t}Bu)$_4$ (1136 mg, 2.31 mmol) in 10 mL of pentane (or ether) was cooled to -30 °C. Ta(CHCMe$_2$Ph)Br$_3$(PPh$_2$Me)$_2$ (2200 mg, 2.31 mmol) was added as a solid to this solution and the yellow mixture was stirred for 16 h. The yellow product was collected by filtration, washed with pentane and dried in vacuo; yield 1004 mg (51%). ^1H NMR($CDCl_3$) for the bisphosphine complex, δ 12.12 (t, 1, WC*H*CMe$_2$Ph, $^3J_{HP}$ = 4), 7.68, 7.40, 7.22, 7.03, 6.90 (m, 25, Ar*H*), 2.40 (t, 6, PPh$_2$*Me*, $^2J_{HP}$ = 5), 1.14 (s, 6, CHC*Me*$_2$Ph); for the monophosphine complex, δ 9.92 (d, 1, WC*H*CMe$_2$Ph, $^3J_{HP}$ = 4), 2.25 (d, 3, PPh$_2$*Me*, $^2J_{HP}$ = 10), 1.57 (s, 6, CHC*Me*$_2$Ph). Due to the product mixture elemental analyses were not attempted.

W(CHCMe$_2$Ph)Br$_2$(OCMe$_3$)$_2$ (4). Having isolated **3**, the mother liquor was cooled to -20 °C to yield yellow crystals which were washed with pentane; yield 122 mg (9%). ^1H NMR(C_6D_6) δ 11.14 (s, 1, WC*H*CMe$_2$Ph, $^2J_{HW}$ = 12 Hz), 7.50 (d, 2, H_o), 7.16 (t, 2, H_m), 6.98 (t, 1, H_p), 1.61 (s, 6, WCC*Me*$_2$Ph), 1.40 (s, 9, O*Me*$_3$), 1.38 (s, 9, O*Me*$_3$). $^{13}C\{^1H\}$

NMR(C_6D_6) δ 295.2 (W*C*HCMe$_2$Ph), 151.3 (C_{ipso}), 129.1, 127.3, 127.0, 93.8 (O*C*^{t}Bu), 92.3 (O*C*^{t}Bu), 50.5 (*C*Me$_2$Ph), 32.0 (CHC*Me*$_2$Ph), 30.0 (OC^t*Bu*), 29.9 (OC^t*Bu*).

W(O)(CH^{t}Bu)(2,6-Ph$_2$C$_6$H$_3$O)$_2$(PMe$_3$) (5). WO(CH^{t}Bu)(PMe$_3$)Cl$_2$ (200 mg, 0.41 mmol) were dissolved in 5 mL THF. 2,6-Ph$_2$C$_6$H$_3$OK (242 mg, 0.85 mmol) were added as a solid and the reaction mixture was allowed to stir for 5 h. The solvent was removed in vacuo to give a yellow film. The product was extracted into toluene and KCl removed by filtration through a bed of Celite. The toluene was removed in vacuo to give a yellow solid. An analytical sample was obtained by double recrystallization from dichloromethane/pentane; yield 258 mg (76%). ^{1}H NMR($CDCl_3$) δ 10.13 (d, 1, WC*H*^{t}Bu, $^3J_{HP}$ = 3.5, $^2J_{HW}$ = 11), 7.79 - 7.65 (m), 7.61 (d), 7.37 (d), 7.30 (d), 7.26 (s), 7.24(s) 7.22 - 7.03 (m), 6.88 (t), 6.63 (d) (26, Ar*H*), 0.77 (d, 9, P*Me*$_3$, $^2J_{HP}$ = 9), 0.73 (s, 9, CH-*t-Bu*). ^{31}P NMR($CDCl_3$) δ 0.35 (s, $^1J_{PW}$ = 333); ^{13}C NMR ($CDCl_3$) δ 287.4 (W*C*H^{t}Bu, $^1J_{CH}$ = 119, $^2J_{CP}$ = 11), 164.2 (C_{ipso}), 157.7 (C_{ipso}), 140.7, 130.5, 130.0, 127.8, 126.2, 119.9, 119.8, 43.6, 31.9, 15.52 (d, $^1J_{CP}$ = 26). IR(Nujol, cm^{-1}) 966 (W=0). Anal. Calcd for $C_{44}H_{45}WOP$: C, 63.17; H, 5.42. Found C, 63.24; H, 5.60.

W(O)(CH^{t}Bu)(2,6-Ph$_2$C$_6$H$_3$O)$_2$(PPh$_2$Me) (6a). W(O)(CH^{t}Bu)Cl$_2$(PPh$_2$Me)$_y$ (393 mg, 0.56 mmol) was dissolved in 10 mL THF. 2,6-Ph$_2$C$_6$H$_3$OK (375 mg, 1.32 mmol) was added as a solid and the cloudy, amber solution was stirred for 12 h. The solvent was removed in vacuo to give an oily solid. The product was extracted into 10 mL toluene and KCl was removed by filtration through a bed of Celite. The toluene was removed in vacuo to give a foam. Upon addition of pentane, a yellow solid precipitated. The solid was washed with pentane until washings were colorless and dried in vacuo; yield 383 mg (71%). An analytical sample was obtained by recrystallization from dichloromethane/pentane. ^{1}H NMR(C_6D_6) δ 10.37 (s, 1, WC*H*^{t}Bu, $^2J_{WH}$ = 9), 7.60 - 6.75 (br, m, 36, Ar*H*), 0.87 (d, 3, PPh$_2$*Me* , $^2J_{PH}$ = 7), 0.68 (s, 9, *t-Bu*). ^{31}P NMR(C_6D_6) δ 11.6 (br, s). ^{13}C NMR(C_6D_6) δ 287.2 (W*C*H^{t}Bu, $^1J_{CH}$ = 118), 141.2, 132.9, 132.3, 130.9, 130.2, 128.6, 128.5, 127.4, 126.6, 120.3 (Ar, two peaks not observed, C_{ipso} are expected to be weak), 43.9 (*C*Me$_3$), 31.9 (C*Me*$_3$), 11.2 (PPh$_2$*Me*, $^1J_{CP}$ =

25). IR(Nujol, cm^{-1}) 957 (W=O). Anal. Calcd. for $C_{54}H_{49}O_3PW$: C, 67.51; H, 5.14. Found C, 67.78; H, 5.31.

W(O)(CHCMe$_2$Ph)(2,6-Ph$_2$C$_6$H$_3$O)$_2$(PPh$_2$Me) (6b). W(O)(CHCMe$_2$Ph)Br$_2$(PPh$_2$Me)$_x$ (350 mg, 0.41 mmol) was dissolved in 10 mL of THF. 2,6-Ph$_2$C$_6$H$_3$OK (239 mg, 0.84 mmol) was added as a solid and the cloudy, amber solution was stirred for 8 h. The solvent was removed in vacuo to give an oily solid. The product was extracted into 10 mL toluene and KCl was removed by filtration through a bed of Celite. The toluene was removed in vacuo to give a foam. Upon addition of pentane, a yellow solid precipitated. The solid was washed with pentane until washings were colorless and dried in vacuo; yield 350 mg (83%). ^{1}H NMR(C_6D_6) δ 10.41 (s, 1, C*H*CMe$_2$Ph), 7.53-6.96 (br, m, Ar*H*), 6.93 (s, Ar*H*), 6.92-6.85 (br, m, Ar*H*), 6.81-6.72 (br, m, Ar*H*), 6.72-6.66 (br, m, Ar*H*), 1.39-1.05 (br, s, 6, CHC*Me*$_2$Ph), 0.38 (d, 3, PPh$_2$*Me*, J_{HP} = 8). ^{31}P NMR(C_6D_6) δ 11.4 (br, s). ^{13}C NMR(tol-*d*$_8$) δ 284.9 (*C*HMe$_2$Ph, $^1J_{CH}$ = 121).

WO(CH^{t}Bu)((CF$_3$)$_2$CH$_3$CO)$_2$(PMe$_3$) (7). WO(CH^{t}Bu)(PMe$_3$)Cl$_2$ (100 mg, 0.20 mmol) was dissolved in 5 mL of THF. (CF$_3$)$_2$CH$_3$COK (98 mg, 0.45 mmol) was added as a solid. The solution changed from green/yellow to amber in color and was allowed to stir overnight. The solution was filtered through Celite to remove KCL and the solvent removed in vacuo. Upon addition of pentane a brown/pink solid was filtered off. The product was recrystallized from pentane at -20 °C as green needles; yield 55 mg (48%). ^{1}H NMR(C_6D_6): Syn rotamer δ 10.15 (d, 1H, WC*H*^{t}Bu, $^3J_{HP}$ = 3, $^1J_{PW}$ = 11), 1.92 (s, 3H, (CF$_3$)$_2$(C*H*$_3$)CO), 1.76 (s, 3H, (CF$_3$)$_2$(C*H*$_3$)CO), 1.09 (s, 9H, WCH^t*Bu*), 0.95 (d, 9H, $^2J_{HP}$ = 12, P*Me*$_3$). Anti rotamer δ 11.20 (d, 1H, $^3J_{HP}$ = 5, $^2J_{HW}$ = 8, WC*H*^{t}Bu), 1.87 (s, 3H, (CF$_3$)$_2$(C*H*$_3$)CO), 1.81 (s, 3H, (CF$_3$)$_2$(C*H*$_3$)CO), 1.01 (half of doublet, other half is obscured by resonance at 0.97, d, 9H, P*Me*$_3$), 0.99 (s, 9H, WCH^t*Bu*). ^{31}P NMR(C_6D_6): Syn rotamer δ 8.49 ($^1J_{PW}$ = 398). Anti rotamer δ 8.84 ($^1J_{PW}$ = 378). ^{13}C NMR(C_6D_6): Syn rotamer δ 280.2 (W*C*H^{t}Bu, $^1J_{CH}$ = 118, $^2J_{CP}$ = 90, $^1J_{CW}$ = 181), 127.6, 123.8 (OC(*C*F$_3$)$_2$CH$_3$), 82.7, 80.9 (O*C*(CF$_3$)$_2$CH$_3$, 43.9 (*C*Me$_3$), 32.6 (C*Me*$_3$), 19.2, 17.6 (OC(CF$_3$)$_2$*C*H$_3$), 14.9 (P*Me*$_3$, $^1J_{CP}$ = 30). Anti rotamer δ

285.7 (W*C*H^{t}Bu, $^1J_{CH}$ = 136, $^2J_{CP}$ = 12), 131.5, 120.0 (OC(*C*F$_3$)$_2$CH$_3$), 43.1 (*C*Me$_3$), 33.4 (C*Me$_3$*), 19.7, 17.6 (OC(CF$_3$)$_2$*C*H$_3$), 15.4 (P*Me$_3$*, $^1J_{CP}$ = 30). Anal. Calcd. for $C_{16}H_{25}F_{12}O_3PW$: C, 27.14; H, 3.56. Found C, 27.07; H, 3.70.

W(O)(CH$_2$Me$_2$Ph)[O-2,6-C$_6$H$_2$(CMe$_2$CH$_2$)(^{t}Bu)-4-Me][O-2,6-C$_6$H$_2$-(^{t}Bu)$_2$-4-Me] (8). W(O)(CHCMe$_2$Ph)Br$_2$(PPh$_2$Me)$_x$ (100 mg, 0.12 mmol) was dissolved in 5 mL of THF. 2,6-(^{t}Bu)$_2$-4-Me-C$_6$H$_2$OK (63 mg, 0.24 mmol) was added as a solid and the amber solution was stirred for 16 h. Precipitated KCl was removed by filtration and the solvent was removed in vacuo. The product was extracted into pentane and refrigerated at -30 °C to give rust red crystals; yield 30 mg (39%). ^{1}H NMR (C_6D_6) δ 7.57 (d, 2, *H$_o$*, $^3J_{HH}$ = 8), 7.22 (t, 2, *H$_m$*, $^3J_{HH}$ = 8), 7.15-7.05 (overlapping resonances, 5H, *H$_p$* + Ar*H*), 2.80 (d, 1,$^2J_{HH}$ = 16), 2.70 (d, 1, $^2J_{HH}$ = 13), 2.42 (d, 1, $^2J_{HH}$ = 13), 2.21 (s, 3, C$_6$H$_2$-4-*Me*), 2.18 (d, 1, $^2J_{HH}$ = 16), 2.13 (s, 3, C$_6$H$_2$-4-*Me*), 1.92 (s, 3, CH$_2$*Me$_2$*Ph), 1.70 (s, 9, C*Me$_3$*), 1.61 (s, 3, CH$_2$*Me$_2$*Ph), 1.41 (s, 3, OC*Me$_2$*CH$_2$), 1.38 (s, 9, C*Me$_3$*), 1.31 (s, 3, OC*Me$_2$*CH$_2$), 1.25 (s, 9, C*Me$_3$*). ^{13}C{H} NMR(C_6D_6) δ 152.3 (C_{ipso}), 151.7 (C_{ipso}), 142.2, 139.9, 137.7, 134.2, 131.3, 127.3, 126.9, 126.2, 125.7, 124.2, 90.73 (W*C*H$_2$CMe$_2$Ph), 83.1 (W*C*H$_2$, $^1J_{CW}$ = 83), 43.0, 36.7, 35.6, 35.4, 34.7, 33.5, 33.4, 32.0, 31.2, 30.5, 21.8, 21.7. Anal. Calcd. for $C_{30}H_{45}WO_3$: C, 62.33; H, 7.58. Found: C, 62.78; H, 7.51.

WO(CHPh)(2,6-Ph$_2$C$_6$H$_3$O)$_2$(PMe$_3$) (9). W(O)(CH^{t}Bu)(2,6-Ph$_2$C$_6$H$_3$O)$_2$(PMe$_3$) (140 mg, 0.167 mmol) was dissolved in 5 mL of toluene. Styrene (21 μL, 0.184 mmol) was added by syringe. The reaction mixture immediately darkened in color and was allowed to stir for 0.5 h. The toluene was reduced in volume and the product obtained by crystallization at -20 °C; yield 93 mg (65%). ^{1}H NMR($CDCl_3$) δ 10.32 (d, 1, WC*H*Ph, $^3J_{HP}$ = 4, $^2J_{HW}$ = 11), 7.56 - 7.27(m), 7.32 - 7.27 (m), 7.23 - 7.13 (m), 7.10 - 7.01 (m), 6.97 - 6.87 (m), 6.68 - 6.61 (d) (31, Ar*H*), 0.47 (d, 9, P*Me$_3$* $^2J_{HP}$ = 9.5). ^{31}P NMR($CDCl_3$) δ 3.00 (s, $^1J_{PW}$ = 341). ^{13}C{^{1}H} NMR($CDCL_3$) δ 268.7 (d, W*C*HPh, $^2J_{CP}$ = 12), 163.0, 157.5, 140.7, 140.0, 139.0, 133.5, 130.5, 130.0, 129.9, 129.3, 127.9, 126.9, 126.3, 120.3, 120.7, 14.0 (d, P*Me$_3$*, $^1J_{CP}$ = 26).

References begin on page 174

$WO(CH_2)(2,6\text{-}Ph_2C_6H_3O)_2(PMe_3)$ (10). $W(O)(CH^tBu)(2,6\text{-}Ph_2C_6H_3O)_2(PMe_3)$ (200 mg, 0.24 mmol) was dissolved in 20 mL toluene and placed in a glass bomb. Ethylene (46.9 mmHg, 0.26 mmol) was added and the reaction mixture allowed to stir overnight. The toluene and volatiles were removed in vacuo to give a brown/yellow solid. The solid was recrystallized from methylene chloride/pentane as yellow cubes. ^1H NMR($CDCl_3$) δ 9.89 (dd, 1, WCH_2), 9.63 (dd, 1, WCH_2), 7.58 - 7.50, 7.48 - 7.34, 7.34 - 7.13, 7.11 - 6.96, (m, 26, Ar*H*), 0.65 (d, 9, PMe_3, $^2J_{HP}$ = 10). ^{31}P NMR($CDCl_3$) δ 4.33 (s, $^1J_{PW}$ = 360). Thermal instability of this complex prevented ^{13}C NMR and elemental analyses data from being acquired.

Polymerization Reactions. The following is a typical procedure. A solution of DCMNBD (60 mg, 0.29 mmol) in 1 mL dichloromethane was added to a solution of **5** (5 mg, 6.0 μmol) in 3 mL dichloromethane and the mixture stirred for 4 h. After said time benzaldehyde (30 mg, 0.28 mmol) was added to the mixture to react with any alkylidene present. The mixture was stirred for 12 h and the polymer precipitated from methanol and dried in vacuo. Polymerizations of 2,3-bis(trifluoromethyl)norbornadiene were carried out in toluene and the polymer precipitated from pentane. Typically, yields were >80%.

Poly - 2,3,-dicarbomethoxynorbornadiene. ^1H NMR($CDCl_3$) δ 5.42 (br, m, H_a), 3.95 (br, m, H_b, *cis*), 3.75 (s, $COCH_3$), 2.51 (br, m, H_c), 1.45 (br, m, H_c); $^{13}C\{^1H\}$ NMR($CDCl_3$) δ 165.4 (CO_2CH_3), 142.5 ($C_{2,3}$), 131.6 ($C_{5,6}$), 52.3 ($COCH_3$), 44.4 ($C_{1,4}$), 38.9 (C_7).

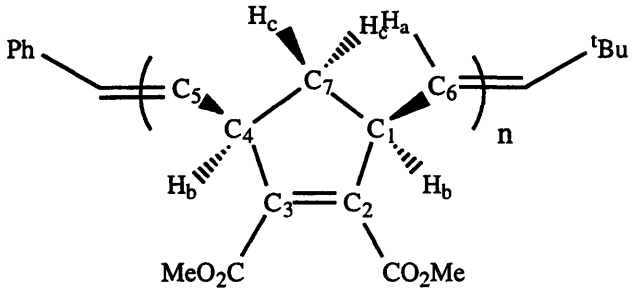

References begin on page 174

Poly - 2,3-bis(trifluoromethyl)norbornadiene. ^{1}H NMR(acetone-d_6) δ 5.62 (br, m, H_a), 4.20 (br, H_b, *cis*), 2.82 (H_c), 1.56 (H_c). $^{13}C\{^1H\}$NMR(acetone-d_6) δ 140.4 ($C_{2,3}$), 132.1 ($C_{5,6}$), 122.0 (CF_3), 44.9 ($C_{1,4}$), 38.5 (C_7).

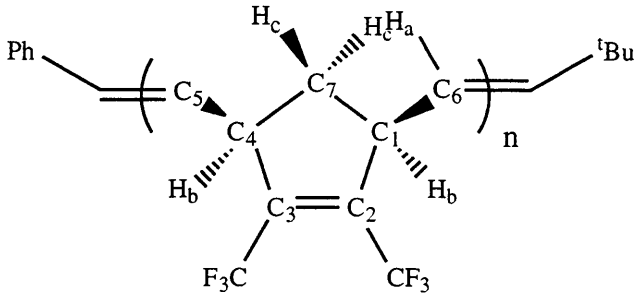

REFERENCES

(1) Schrock, R. R. *Ring-Opening Metathesis Polymerization*; Brunelle, D. J., Ed.; Hanser: Munich, 1993, pp 129.

(2) Grubbs, R. H.; Tumas, W. *Science* **1989**, *243*, 907.

(3) Bazan, G. C.; Khosravi, E.; Schrock, R. R.; Feast, W. J.; Gibson, V. C.; O'Regan, M. B.; Thomas, J. K.; Davis, W. M. *J. Am. Chem. Soc.* **1990**, *112*, 8378.

(4) Bazan, G. C.; Oskam, J. H.; Cho, H. -N.; Park, L. Y.; Schrock, R. R. *J. Am. Chem. Soc.* **1991**, *113*, 6899.

(5) O'Dell, R.; McConville, D. H.; Hofmeister, G. E.; Schrock, R. R. *J. Am. Chem. Soc.* **1994**, *116*, 3414.

(6) Feast, W. J.; Gibson, V. C.; Marshall, E. L. *J. Chem. Soc., Chem. Commun.* **1992**, 1157.

(7) Schrock, R. R.; Lee, J. -K.; O'Dell, R.; Oskam, J. H. *Macromolecules* **1995**, *28*, 5933.

(8) Oskam, J. H.; Schrock, R. R. *J. Am. Chem. Soc.* **1993**, *115*, 11831.

(9) McConville, D. H.; Wolf, J. R.; Schrock, R. R. *J. Am. Chem. Soc.* **1993**, *115*, 4413.

(10) Totland, K. M.; Boyd, T. J.; Lavoie, G. G.; Davis, W. M.; Schrock, R. R. *Macromolecules* **1996**, *29*, 6114.

(11) Ivin, K. J. *Olefin Metathesis*; Academic: New York, 1983.

(12) Mocella, M. T.; Rovner, R.; Muetterties, E. L. *J. Am. Chem. Soc.* **1976**, *98*, 4689.

(13) Nugent, W. A.; Feldman, J.; Calabrese, J. C. *J. Am. Chem. Soc.* **1995**, *117*, 8992.

(14) Wengrovius, J. H.; Schrock, R. R.; Churchill, M. R.; Missert, J. R.; Youngs, W. J. *J. Am. Chem. Soc.* **1980**, *102*, 4515.

(15) Schrock, R. R.; Rocklage, S. M.; Wengrovius, J. H.; Rupprecht, G.; Fellmann, J. *J. Molec. Catal.* **1980**, *8*, 73.

(16) Churchill, M. R.; Rheingold, A. L.; Youngs, W. J.; Schrock, R. R. *J. Organomet. Chem.* **1981**, *204*, C17.

(17) Wengrovius, J. H.; Schrock, R. R. *Organometallics* **1982**, *1*, 148.

(18) de la Mata, F. J.; Grubbs, R. H. *Organometallics* **1996**, *15*, 577.

(19) de la Mata, F. J. *J. Organomet. Chem.* **1996**, *525*, 183.

(20) Blosch, L. L.; Abboud, K.; Boncella, J. M. *J. Am. Chem. Soc.* **1991**, *113*, 7066.

(21) Kress, J.; Wesolek, M.; Osborn, J. A. *J. Chem. Soc., Chem. Commun.* **1982**, 514.

(22) Aguero, A.; Kress, J.; Osborn, J. A. *J. Chem. Soc., Chem. Commun.* **1985**, 793.

(23) Kress, J.; Osborn, J. A. *J. Am. Chem. Soc.* **1983**, *105*, 6346.

(24) Kress, J.; Osborn, J. A.; Greene, R. M. E.; Ivin, K. J.; Rooney, J. J. *J. Chem. Soc., Chem. Commun.* **1985**, 874.

(25) Schrock, R. R. *Acc. Chem. Res.* **1990**, *23*, 158.

(26) Nugent, W. A.; Mayer, J. M. *Metal-Ligand Multiple Bonds*; Wiley: New York, 1988.

(27) Feldman, J.; Schrock, R. R. *Prog. Inorg. Chem.* **1991**, *39*, 1.

(28) Churchill, M. R.; Missert, J. R.; Youngs, W. J. *Inorg. Chem.* **1981**, *20*, 3388.

(29) Toreki, R.; Schrock, R. R. *J. Am. Chem. Soc.* **1992**, *114*, 3367.

(30) Lefebvre, F.; Leconte, M.; Pagano, S.; Mutch, A.; Basset, J. -M. *Polyhedron* **1995**, *14*, 3209.

(31) Schrock, R. R.; DePue, R.; Feldman, J.; Schaverien, C. J.; Dewan, J. C.; Liu, A. H. *J. Am. Chem. Soc.* **1988**, *110*, 1423.

(32) Wu, Z.; Wheeler, D. R.; Grubbs, R. H. *J. Am. Chem. Soc.* **1992**, *114*, 146.

(33) bin Alimuniar, A.; Blackmore, P. M.; Edwards, J. H.; Feast, W. J.; Wilson, B. *Polymer* **1986**, *27*, 1281.

(34) Tabor, D. C.; White, F. H.; Collier, L. W.; Evans, S. A. *J. Org. Chem.* **1983**, *48*, 1638.

Acknowledgments

IT IS DONE! The best decision I made regarding my Ph.D. work was my choice of advisor. Working for Dick has been a tremendous experience both personally and professionally and I think I have had the perfect graduate school experience. Thank you for always letting me speak my mind and for allowing me to "play" in lab even when I did not know what I was doing. I think the key to my success has been your ability to know when to push me hard and when to gentle steer me in the right direction. Thank you.

The Chemistry Department at MIT is full of characters and the first two that I met were Kit Cummins and Alan Davison. After I applied to MIT, Kit called me up and asked me to come and speak with him and Alan. I guess I did something right because they gave me the opportunity to come to MIT for which I am very grateful. Alan, my fellow Celt from across the pond, is a great person and I have shared many a laugh with him. Along with supportive words at key moments, he also kept me informed on the progress or lack thereof of the Irish and Welsh rugby teams. I also wish to thank Kit whose support during my job search opened many doors for me. Steve Lippard also spoke up for me and signed off on the Women in Chemistry Retreat which I am glad to see is to be repeated this year.

Shortly after joining the Schrock group I crossed paths with Karen Totland, a Canadian post-doc and soul mate. Karen took me under her wing, answered my incessant questions with endless patience and was always willing to head out for a pint. Karen is one of the "biggest" people I know, big in the sense of the ease with which she gives to others. The year we shared 6-429 was the most enjoyable of my years at MIT and I suspect that the bond we forged will be one of the more enduring results of my time spent at MIT. Thank you for proofreading my story and for all the love, support and encouragement you have given me this last year. I look forward to your visits to Geneva.

After Karen's departure I was blessed with the arrival of Yann Schrodi. Yann is another big person and life holds much for him. I will especially miss our hugs and our biscotti breaks. Though Yann and I have argued fiercely on occasion, we have always agreed to differ and I think we have learned much from each other. However, I did not learn a significant amount of French from him despite our best efforts - I will be a quiet woman in Geneva, an unnatural state for me!

Collectively, I must thank the other members of the Schrock group, past and present, who have made the fourth floor an enjoyable place to work. The job search was a huge learning experience in itself and I had great company in Michael Aizenberg, David Graf and Steven Reid. Good luck on your new adventures. Thanks also to John Alexander for proofreading duties. My final labmate is another Canadian, Jennifer Jamieson who has the uniquely Canadian habit of playing a CD until you never want to hear it again :). Jenn has graciously dealt with my occasional foul mouth and in these final weeks, my commandeering of the box. Thanks for your patience.

As with most theses, mine has it's origins in the labor of others. I was fortunate to inherit two great projects from Drs. Anne LaPointe and Nadia Zanetti who I thank wholeheartedly.

Outside of lab many a fine evening was spent with the "wine tasting" group of Deryn Fogg, Dan Dobbs, Scott Seidel, Mike Fickes, Fred, Gretchen and Tot. I didn't learn much about wine but I have developed quite a lip for port, the responsibility for which lies with Fickes. Special thanks to Scotty for proofreading and for encouraging e-mails during the final months. Gretchen also deserves huge credit for keeping the Schrock group running smoothly.

Chris Morse had the misfortune to be in the lab next door to mine and so he has had to endure many an hour of my complaining. He has always listened graciously and somehow managed to bolster my confidence every time. Thanks for the parties and the chocolate chip cookies and good luck with finishing up.

Another social outlet was the First Thursday Group who provided a haven during the hell prior to Orals. They helped put everything in perspective and kept me conscious of the fact that there was plenty of life outside MIT. Finally, the Northeastern "Crew" were also a wonderful source of support and will be sorely missed. Special thanks goes to Denise Messinese who convinced me that I was good enough to apply to MIT, supported me in so many ways, and who refused to let me quit my first semester.

Finally, I am deeply indebted to my parents and six siblings, Pod, Clare, Lynn, Tim, Dan and Paul, who have supported all of my decisions in life. I am very proud of my family and all that they have achieved and I love them dearly. When I graduated college in 1988, I felt a little one-dimensional so I decided not to enter a Ph.D. program and instead I came to Boston for the summer with a view to heading on to Australia for a year (that summer turned into a decade!). Not all of my family understood my decision and I think they were worried that I would not return to school. It took me five years to feel "rounded out" enough to contemplate graduate school and MIT was the first place that came to mind. MIT was first brought into my field of vision by Pod, the night before I left Ireland for the US and strangely enough, I think that my graduation from MIT means more to him then it does to me. I was very fortunate to have Clare living in Boston while I was at school and there was many a night that she and Jackie either fed me and/or gave me a bed. Thank you. Growing up in a large family is great and it certainly knocks the corners off you! As several years separate Paul and I from the others, we are particularly close. Paul has a huge heart and he has been there for me in good times and in bad times. I hope that with my move to Geneva I will get to spend more time with him. Lastly, I am indebted to my mother who has always encouraged me to aim high and to plough my own field, so to speak. How am I doing, Mum?